Altered Cellular Signalling and Metabolism in Cisplatin Cytotoxicity and Chemoresistance

Aleck William Evan Gregory Jones

University College London

Thesis submitted for the degree of Doctor of Philosophy

2011

I, Aleck William Evan Gregory Jones confirm that the work presented in this thesis is my own. Where information has been derived from other sources, I confirm that this has been indicated in the thesis.

.....

Acknowledgements

It is with great pleasure that I finally put the finishing touches to this immense undertaking. My thanks go firstly to my supervisor Dr. Gyorgy Szabadkai, for always providing an open door to his knowledge and advice. I am further grateful for the valuable contributions of Dr. Zhi Yao to this project. It has been a genuine pleasure working with you both. Thanks also go to all members of the Szabadkai and Duchen labs, both past and present, for the enjoyable working environment and the background of helpful discussions present throughout my time in the lab.

I would like to express my gratitude for the long term support and encouragement of my family, both during my PhD. and over the many years leading up to it, without which it would not have been possible for me to reach this point. Digna deserves no small amount of credit for the understanding and support shown to me all through my PhD. work, it has been appreciated!

The work in this project was made possible through helpful collaborations with the research groups of Dr. Takehiro Yasukawa (UCL), Dr. Shamima Rahman (UCL), Dr. Mariusz Wieckowski (Nencki Institute of Experimental Biology), Dr. Iain Hargreaves (UCL), Dr. Guido Kroemer (INSERM) and Dr. Catherine Brenner (INSERM).

Abstract

Cisplatin (cDDP) is a potent chemotherapeutic agent used in the management of a range of tumours, however its clinical efficacy is limited by tumour cell chemoresistance. Whilst the major target of the drug is considered to be nuclear DNA, cDDP has been shown to interact with other organelles, notably the ER and mitochondria, although the importance of these interactions is not fully understood. The contribution of such extranuclear effects is here addressed through comparative studies of two lung adenocarcinoma cell lines with differing sensitivity towards cDDP. Exposure to cDDP induced proliferative arrest and caspase-dependent apoptosis in A549-WT cells, without requirement for caspase-8, calpains, ROS or Ca^{2+}. Two-fold resistance towards cDDP-induced apoptosis was measured in A549-CR cells, generated through long term exposure to the drug. A549-CR cells showed marked inhibition of Ca^{2+} signalling from the ER due to a 50% reduction of IP_3R function. However, cDDP treatment did not alter cytosolic Ca^{2+} levels nor deplete the ER Ca^{2+} store. Further, neither chelation of intracellular Ca^{2+} nor pharmacological inhibition of IP_3R Ca^{2+} channel opening inhibited cDDP-induced A549-WT cell death, thus under the present experimental conditions Ca^{2+} flux through the IP_3R does not modulate cDDP sensitivity. Basal and maximal cellular O_2 consumption in A549-WT cells significantly increased following cDDP treatment, but was unaltered in A549-CR cells. Sequencing of mtDNA identified a novel point mutation in A549-CR mtDNA causing a 50% reduction of complex I activity. Mutations of mtDNA and reduced respiratory chain activity might inhibit apoptosis. The abundance of complex I was increased by 50%, potentially an example of pro-survival mitochondrial-nucleus compensatory retrograde signalling. Thus, key differences in mitochondrial function and response to cDDP which may alter A549 cell sensitivity to cDDP have been identified for further investigation.

Table of Contents

Table of Contents

Table of Contents

Table of Contents

Table of Contents

Table of Contents

Table of Contents

Tables and Figures

List of Figures

Tables and Figures

Tables and Figures

Tables and Figures

List of Tables

Abbreviations

Abbreviations:

The following abbreviations are used throughout this manuscript:

ΔΨ – Mitochondrial transmembrane potential

$[Ca^{2+}]_{cyt}$ – Cytosolic Ca^{2+} concentration

$[Ca^{2+}]_{ER}$ – ER intra-lumenal Ca^{2+} concentration

2-APB – 2-Aminoethoxydiphenyl borate

AIF – Apoptosis inducing factor

AMPK – 5'-AMP activated protein kinase

ANT – Adenine nucleotide transporter

APAF-1 – Apoptotic protease activating factor-1

BAK – BCL-2 antagonist killer-1

BAPTA-AM – 1,2-Bis(2-aminophenoxy)ethane-N,N,N',N'-tetraacetic acid tetrakis acetoxymethylester

BAX – BCL-2 associated x protein

BCL-2 – B-cell lymphoma-2

BH domain – BCL-2 homology domain

BIK – BCL-2 interacting killer

BSA – Bovine serum albumin

CaMKIV – Ca^{2+}/ calmodulin-dependent kinase IV

cDDP – cis-Diamminedichloroplatinum II/ cisplatin

CFP – Cyan fluorescent protein

CICR – Ca^{2+}-induced Ca^{2+} release

CsA – Cyclosporin A

Abbreviations

Cyp D – Cyclophilin D

DCA – Dichloroacetate

DDC – Deleted in colorectal cancer

DEM – Diethylmaleate

DHE – Dihydroethidium

DISC – Death-inducing signalling complex

DMEM – Dulbecco's Modified Eagle Medium

Drp-1 – Dynamin-related protein-1

ER – Endoplasmic reticulum

ETC – Mitochondrial electron transport chain

FADD – Fas-associated death domain containing protein

FDG-PET – 18Fluorodeoxyglucose-positron emission topography

FRET – Förster resonance energy transfer

Grp75 – Glucose-regulated protein 75

GSH – Glutathione

HIF – Hypoxia-inducible factor

HMG proteins – High mobility group proteins

IP_3 – Inositol 1,4,5-triphosphate

IP_3R – Inositol 1,4,5-triphosphate receptor

KRB – Kreb Ringer buffer

MCB – Monochlorobimane

MCU – Mitochondrial Ca^{2+} uniporter

MDR proteins – Multidrug resistance proteins

Abbreviations

MEF – Mouse embryonic fibroblast

Mfn2 – Mitofusin-2

MMR pathway – Mismatch repair pathway

MOMP – Mitochondrial outer membrane permeabilisation

mPT – Mitochondrial permeability transition

mPTP – Mitochondrial permeability transition pore

mtDNA – Mitochondrial DNA

NAD+ – Oxidised nicotinamide adenine dinucleotide

NADH – Reduced nicotinamide adenine dinucleotide

NADPH – Reduced nicotinamide adenine dinucleotide phosphate

NER pathway – Nucleotide excision repair pathway

NSCLC – Non-small cell lung cancer

PACS2 – Phosphofurin acidic cluster sorting protein-2

PARP-1 – Poly(ADP ribose) polymerase-1

PBST – PBS + 0.05% Tween-20

PDH – Pyruvate dehydrogenase

PDK – Pyruvate dehydrogenase kinase

PFK-1 – Phosphofructokinase-1

PFK2/ F2,6BP – 6-phosphfructo-2-kinase/ fructose-2,6-bisphosphatase

PGC-1 – Peroxisome proliferator-activated receptor α co-activator-1

PI – Propidium iodide

PI3K – Phosphatidylinositol-3-kinase

PI3P – Phosphatidylinositol-3-phosphate

Abbreviations

rCRS – Revised Cambridge mtDNA reference sequence

RIP-1 – Receptor interacting protein-1

ROS – Reactive oxygen species

RYR – Ryanodine receptor

SCO2 – Synthesis of cytochrome oxidase 2

SERCA – Sarcoplasmic/ endoplasmic reticulum Ca^{2+} ATPase

SOC – Store-operated Ca^{2+} channel

SOCE – Store-operated Ca^{2+} entry

STIM-1 – Stromal interaction molecule-1

TCA cycle – Tricarboxylic acid cycle

TFAM – Mitochondrial transcription factor A

Tg – Thapsigargin

TIGAR – TP53-induced glycolysis regulator

TNFR – Tumour necrosis factor

UCP2 – Mitochondrial uncoupling protein-2

VDAC – Voltage-dependent anion channel

YFP – Yellow fluorescent protein

1.1 Cancer

1.1.1 What is Cancer?

The term 'cancer' refers to a collection of clinically diverse diseases affecting multicellular organisms which may manifest in a multiplicity of phenotypes. Such diseases are caused by the accumulation of a number of genetic alterations within a cell, leading to altered patterns of gene expression. Ultimately these changes give rise to an imbalance of cell proliferation over cell death processes, producing a proliferating mass of cells, or tumour. Should these cells acquire the capability to invade local tissue(s) and metastasise to, or colonise, remote sites within the host organism to establish secondary sites of growth, the tumour is termed *malignant*, whilst those which remain localised to the initial site of tumour growth are categorised as *benign* (Ruddon, 2007a). In comparison to the benign form, malignant tumours contain cells less differentiated than the tissue from which they arose and frequently, although not invariably, show a faster rate of growth. Left untreated such neoplasms are of significant detriment, and may lead to the death of the host. Cancer remains the leading cause of death in humans, responsible for approximately 7.4 million deaths in 2004, a figure predicted to rise to 12 million by 2030 (World Health Organisation, 2009). Coupled with the increasing cost of new anti-cancer therapies, the rise in cases of cancer represents a serious social and economic burden for both patients and health care providers (Bosanquet & Sikora, 2006).

Cancer incidence increases dramatically with age (DePinho, 2000), reflecting the requirement of cancerous cells to accrue multiple genetic changes. The number of mutational events required varies depending upon the cell type and genes involved, from as little as one or two in the case of chronic myeloid leukaemia and retinoblastoma respectively (Paget & London, 2006), to more than six for solid tumours such as colon cancer (Ruddon, 2007b). The nature of these genetic changes may be broadly classified into two areas as those affecting *oncogenes* and those affecting *tumour suppressor genes*. Oncogenes are genes in which an increase in the activity of the gene product promotes cellular transformation to the cancer cell phenotype; the non-mutated form of such genes, *proto-oncogenes*, often encode proteins involved in proliferation, growth and signalling. Activation of oncogenes may occur either by increased expression of the gene product through gene amplification or mutation of regulatory sequences, as is the case for the *myc* oncogene in Burkitt's lymphoma, or through

producing a product with dysregulated activity, exemplified by constitutive activation of the Ras GTPase in numerous cancers (R. J. B. King & Robins, 2006a; Ruddon, 2007c). Tumour suppressor genes often encode regulatory proteins which act to restrain cellular growth and proliferation and promote differentiation, in which a loss of function contributes to tumourigenicity by allowing these processes to proceed unchecked. This loss of function may occur through mutation of both normal alleles or of a single allele leading to haploinsufficiency, or through inactivation by increased inhibitory modifications, such as phosphorylation or binding of inhibitory proteins. The retinoblastoma and p53 tumour suppressor proteins variably demonstrate such alterations in multiple tumour contexts (R. J. B. King & Robins, 2006a; Ruddon, 2007c)(Ruddon, 2007c)(Ruddon, 2007c)(Ruddon, 2007c)(Ruddon, 2007c)(Ruddon, 2007c)(Ruddon, 2007c). Most commonly cancers result from synergistic mutations in oncogenes, driving a proliferative transformation, and in tumour suppressors, allowing these changes to occur in an unrestrained manner (R. J. B. King & Robins, 2006a).

The sources of mutations leading to cancer are varied, and reflect a complex interplay of genetic and environmental risk factors balanced by processes repairing and removing damaged cells. Spontaneous mutation of DNA during the cell cycle may contribute to, but alone cannot explain, the incidence of human cancers (Ruddon, 2007c). The ability to effectively repair damage once it has occurred is key to preventing carcinogenesis, thus individuals carrying heritable deficiencies in DNA repair associated pathways experience earlier and more frequent cancer onset (Paget & London, 2006; Su & Lenardo, 2010). Exposure to conditions which directly or indirectly alter the structure of DNA and/ or its constituent bases, including a wide range of chemical carcinogens and both UV and ionising radiation, may drastically increase cancer risk. It is notable however that these mutations need not directly affect the structure or sequence of a given protein. Changes in the level of gene expression by mutations altering transcriptional activity, mRNA and protein half-life, transcription of regulatory miRNA and heritable epigenetic modifications including DNA methylation and histone acetylation may aid cellular transformation (Esteller, 2008; Lujambio et al., 2007; Ruddon, 2007b). Viral infection may also drive carcinogenesis through direct provision of a viral-oncogene (v-onc), disruption of key regulatory or protein coding sequences by viral genome insertion into the host cell DNA or indirectly by interfering with the function of endogenous cellular proteins (R. J. B. King & Robins, 2006a; Ruddon, 2007c).

Overall, cancer is a multifaceted disease with both genetic and environmental components. The increasing longevity and changing lifestyles of individuals within many populations makes cancer a growing problem in both the developed and developing world.

1.1.2 Strategies for Cancer Treatment

The goal of cancer treatment varies depending upon the type and stage of cancer at the time of presentation, the location of the tumour(s) and both the physical condition and wishes of the patient. For early stage and localised cancers, radical treatment attempts to be fully curative. Cases in which tumours are highly advanced and/ or have metastasised often require a palliative approach, aiming to prolong the period of time in which symptoms may be controlled and quality of life for the patient maintained. In both cases three major routes of treatment exist; *surgery*, *radiotherapy* and *chemotherapy*. Often the best results are achieved through the combined use of two or more of these strategies (Watson, Barrett, Spence, & Twelves, 2006).

Surgical intervention with a curative intent aims to completely remove the tumour along with a surrounding border of histologically normal tissue and nearby structures such as lymph nodes into which tumour cell invasion may have occurred (Stephens & Aigner, 2009). Surgery may be applied to a range of cancers, including those of the lung and breast. Whilst surgical resection is potentially curative, it is not possible for all tumour types, such as those occurring deeply within the brain or spine, and carries a risk of disfigurement or loss of function of the affected area.

Radiotherapy uses irradiation of tumour cells with directed beams of high-intensity x-rays or γ-radiation to induce DNA damage. Such treatment is effective only in cells actively progressing through the cell cycle, thus requires multiple administrations attempting to destroy previously quiescent cells, and is most effective when tumour burden is low and a greater proportion of cells are actively dividing (R. J. B. King & Robins, 2006b). Combined with improved imaging techniques to precisely locate neoplasms, radiotherapy may be used to treat deep-seated tumours and those not suitable for surgery, but carries risks for surrounding healthy tissue which also receives doses of radiation.

Chemotherapy attempts to kill cells using cytotoxic drugs to inhibit processes vital to cellular function or by engaging cell death pathways (Kaufmann & Vaux, 2003). Some cancers may be cured in this manner, but more commonly chemotherapy is used in combination with other modes of treatment, either before (neoadjuvant chemotherapy) or after (adjuvant chemotherapy) surgery and radiotherapy (R. J. B. King & Robins, 2006b). Chemotherapy may also be used in a palliative context. However, unlike surgery and radiotherapy, chemotherapy may achieve systemic delivery, thus is used to combat metastases, particularly in patients where such secondary growths are thought likely but are not yet clinically apparent. Such systemic delivery may be associated with notable adverse side effects such as alopecia, cardiotoxicity, myelosuppression, nausea and renal toxicity, depending upon the drug in question (Watson et al., 2006).

Most frequently several drugs with different activities are used in combination, the dose and treatment regime subject to the particular combination. Using combination therapy allows for lower effective concentrations of each drug to be administered, and whilst a given cell in the heterogeneous tumour cell population may acquire resistance to one compound, it is likely to remain susceptible to the others. Antimetabolites such as methotrexate and 5-fluorouracil are drugs which inhibit the synthesis of nucleic acid either through enzyme inhibition or direct incorporation. Cisplatin (cDDP) and cyclophosphamide exemplify a class of drugs known as alkylating (or alkylating-like) agents, which form direct adducts with the existing bases of nucleic acids, interfering with replication and cell division (R. J. B. King & Robins, 2006b; Stephens & Aigner, 2009). Vinca alkyloids and taxanes act upon the cellular microtubule network, whilst others inhibit enzymes including targeting of topioisomerase II by etoposide or of a cancer specific Bcr/Abl fusion kinase by Gleevec (Ruddon, 2007b). Specific cancers may show hormone dependent proliferation, thus ablating circulating hormone levels can be used to inhibit cancer growth, as is the case for breast and prostate cancers derived from sex hormone-sensitive progenitor cells (Stephens & Aigner, 2009).

1.1.3 Lung Cancer and the A549 Cell Line

Lung cancer is the most common form of the disease in males and, after cancers of the breast, cervix and colon, the fourth most frequent in females (Ferlay J, Shin HR, Bray F, Forman D, Mathers C, 2010); globally approximately 1.61 million new diagnoses of lung cancer were

made in 2008, 39750 of these in the United Kingdom (Cancer Research UK, 2010). Cancers of the lung account for the greatest number of cancer-related deaths worldwide, responsible for more than 1.3 million deaths annually (Cancer Research UK, 2010; World Health Organisation, 2009), and are predicted to remain the leading cause of cancer deaths in Western countries (Jemal, Siegel, Xu, & Ward, 2010). Such high mortality rates are due in part to the late stage at which diagnosis is made (Wistuba & Gazdar, 2006), evidenced by a five year survival rate of less than 10% for patients diagnosed in England between 2001 and 2006 (Cancer Research UK, 2010).

By far the most common cause of lung cancer is long term exposure to tobacco smoke, and the epidemiology linking the uptake of cigarette smoking with increased deaths from lung cancer is well established (Doll, Peto, Boreham, & Sutherland, 2004, 2005). The relative risk of lung cancer is increased in regular tobacco smokers up to 22 times in comparison to non-smokers (Doll et al., 2004; Ruddon, 2007b), however it is estimated that 90% of this smoking-related risk may be avoided by cessation of smoking before middle age (Jha, 2009). Other contributing factors include exposure to natural radon gas, industrial carcinogens such as asbestos and air pollution and particulate matter (Cancer Research UK, 2010). Lung cancer is classified into four major histological types: squamous cell carcinomas, arising from epithelial cell layers; adenocarcinomas, arising from glandular epithelium; large-cell carcinomas, a heterogenous group of undifferentiated tumours; and small-cell carcinomas, a highly metastatic form (Stephens & Aigner, 2009). Clinically, treatment for the first three of these histological types is similar, thus they are together classed non-small cell lung cancer (NSCLC). Treatment for lung cancer may involve surgical resection, chemotherapy and radiotherapy, depending upon tumour type and progression, however the late stage disease with which many patients present leads ultimately to a poor prognosis.

The A549 cell line was established from a lung tumour explant derived from basal epithelial cells, thus falls into the squamous cell carcinoma subdivision of NSCLC (American Type Culture Collection (ATTC), 2010; Giard, Aaronson, & Todaro, 1973; Lieber, Smith, Szakal, Nelson-Rees, & Todaro, 1976). The cell line is well characterised, and commonly used as an *in vitro* model for both lung cancer and cDDP treatment (Beleford, Rattan, Chien, & Shridhar, 2010; Dasgupta et al., 2006; Guo et al., 2010).

1.2 Cell Death and Cellular Ca^{2+} Signalling

1.2.1 Apoptosis

Apoptosis is the most studied form of cell death, and is best defined through a set of morphological criteria (Galluzzi et al., 2007; Kroemer et al., 2009). Originally described by Kerr *et al.* in 1972 with regard to hepatocytes (Kerr, Wyllie, & Currie, 1972), the apoptotic morphology consists of pyknosis (reduced cellular volume) accompanied by a 'rounding up' of the cell, blebbing of the plasma membrane, chromatin condensation, nuclear fragmentation (karyorrhexis) and disintegration of the cell into 'apoptotic bodies', small membrane bound structures which often contain intact cellular organelles (Galluzzi et al., 2007; Kroemer et al., 2009). Plasma membrane integrity is maintained until the final stages of this process. *In vivo* the resulting apoptotic bodies are subsequently engulfed by neighbouring phagocytes, usually without an immune response. That apoptosis lacks a tight biochemical definition belies the fact that it is a broad process encompassing a number of distinct signalling pathways, yet certain biochemical observations may still be used in conjunction with morphology as an aid in identifying apoptotic cell death (Kroemer et al., 2009).

The best characterised signalling cascades leading to apoptosis are the *receptor-mediated* (or 'extrinsic') pathway and the *mitochondrial* (or 'intrinsic') pathway, although other routes are known to exist (Rao et al., 2002). Both pathways converge upon a class of cysteine-dependent aspartate specific proteases known as *caspases* (I. Chowdhury, Tharakan, & Bhat, 2008; Kroemer, Galluzzi, & Brenner, 2007), the activation of which seems to be required for full manifestation of apoptotic morphology. However, many caspases may also fulfil roles in normal physiology aside from cell death (Feinstein-Rotkopf & Arama, 2009; Lamkanfi, Festjens, Declercq, Vanden Berghe, & Vandenabeele, 2007), whilst caspase inhibition does not always prevent cell death signalled through apoptotic pathways, thus caspase activation may not alone be considered a marker of apoptosis (Galluzzi et al., 2007; Kroemer et al., 2009).

All caspases are synthesised as zymogens (inactive pro-enzymes) which may be divided according to substrate specificity and structural considerations (Chowdhury et al., 2008; Pop & Salvesen, 2009). The *executioner caspases* contain a short pro-domain, and are responsible for the cleavage of many proteins which lead directly or indirectly to destruction of cellular architecture, including disassembly of the cytoskeleton, nucleus and Golgi (Fischer, Jänicke,

& Schulze-Osthoff, 2003; Timmer & Salvesen, 2007). Activation of these executioners occurs through cleavage mediated by a second subset of caspases, the long pro-domain *initiator caspases*, themselves activated by recruitment to multi-protein complexes and autoproteolysis (Pop & Salvesen, 2009). Apoptosis is thus initiated by a minimally two step proteolytic cascade, the heterogeneity of the apoptotic response due to differences in the particular enzymes which become activated and the manner in which they are recruited.

Signalling through the receptor-mediated apoptotic pathway begins at the plasma membrane. Initiation classically occurs through ligand binding to the extracellular face of receptors belonging to the tumour necrosis factor receptor (TNFR) superfamily, such as CD95 (Fas/APO-1), TNFR1 and TRAIL receptors 1 and 2 (Debatin & Krammer, 2004). Ligand binding causes receptor clustering and recruitment of the adaptor molecule 'Fas-associated death domain containing protein' (FADD), which may in turn recruit and oligomerise initiator caspases -8 and -10 (Kroemer et al., 2007; Walczak & Krammer, 2000). Collectively termed the death-inducing signalling complex (DISC), these multimers of receptors, adaptor proteins and initiator caspases stimulate apoptosis through cleavage of executioner caspases -3, -6 and -7. The receptor mediated pathway may conversely be engaged by a group of plasma membrane receptors upon the absence of ligand. The so-called 'dependence receptors', typified by 'deleted in colorectal cancer' (DDC), require constitutive ligand binding for cell survival, whilst ligand withdrawal induces apoptosis through direct activation of caspases (Goldschneider & Mehlen, 2010).

The mitochondrial pathway of apoptosis may be initiated by a variety of stimuli, including DNA damage, ER stress, growth factor deprivation and viral infection (Youle & Strasser, 2008). Mitochondrial outer membrane permeabilisation (MOMP) driving the release of cytochrome *c* along with other pro-apoptotic factors from the mitochondrial inter-membrane space into the cytosol is the defining event in this pathway, and is considered to be the 'point of no return' in the cell death program. This permeabilisation is regulated by members of the B-cell lymphoma-2 (BCL-2) family (see Section 1.2.2). Once released, cytochrome *c* and the nucleotide dATP interact with monomeric apoptotic protease activating factor-1 (APAF-1), promoting its oligomerisation. This large protein complex, the apoptosome, acts as an activation platform for the initiator caspase of the pathway, caspase-9. Caspase-9 is thus activated and may mediate cleavage of executioner caspases -3, -6 and -7. Other factors released from the inter-membrane space after MOMP include SMAC/ DIABLO and OMI/

HTRA2, antagonists of X-linked inhibitor of apoptosis (XIAP), an endogenous caspase inhibitor, and apoptosis inducing factor (AIF) and endonuclease G, which may contribute to genomic fragmentation (Tait & Green, 2010).

1.2.2 The BCL-2 Family in Apoptosis

During the mitochondrial pathway of apoptosis the integrity of the mitochondrial outer membrane is regulated by interactions between members of the *BCL-2 family* of proteins (Chipuk, Moldoveanu, Llambi, Parsons, & Green, 2010; Tait & Green, 2010; Youle & Strasser, 2008). BCL-2 family members show opposing activities during apoptosis, and are therefore functionally divided into *anti-apoptotic* and *pro-apoptotic* groups, the latter of which may be further subdivided into pro-apoptotic *effectors* and *BH3-only* proteins. Anti-apoptotic proteins maintain mitochondrial outer membrane integrity through direct inhibition of the pro-apoptotic effectors (Chipuk et al., 2010). Members of this group include BCL-2, BCL-xL and MCL-1 proteins, and characteristically contain four BCL-2 homology (BH) domains (BH 1-4). Pro-apoptotic effector proteins BCL-2-associated x protein (BAX) and BCL-2 antagonist killer 1 (BAK) contain three BH domains (BH 1-3) and are responsible for the release of apoptogenic factors from the inter-membrane space. Apoptotic signalling causes translocation of monomeric effector proteins from the cytosol to the mitochondrial outer membrane where BAX and BAK form homo-oligomeric pores (Chipuk et al., 2010; Tait & Green, 2010; Youle & Strasser, 2008). Whilst this oligomerisation event is known to coincide with MOMP, the biochemical nature of these pores remains elusive (Tait & Green, 2010). BH 3-only proteins contain just one BH domain (BH 3), and are induced by specific cellular stresses. They act to stimulate apoptosis through inhibitory interactions with anti-apoptotic BCL-2 proteins and/ or synergistic interactions with BCL-2 effectors. BH 3-only proteins tBID and BIM may directly promote effector polymerisation and MOMP (‘direct activation’), whilst others such as BAD, BIK, NOXA and PUMA act to sequester anti-apoptotic members or relieve inhibition of direct activator proteins (Tait & Green, 2010).

1.2.3 Non-Apoptotic Modes of Cell Death

Macroautophagy, or simply 'autophagy', is a conserved catabolic process for the bulk degradation of cellular organelles and turnover of long-lived proteins. Portions of the cytosol are sequestered into double membrane bound autophagosome structures, which subsequently fuse with lysosomes. The contents of the resulting autolysosome lumen are then subject to degradation and/ or recycling. Such autophagy occurs under basal growth conditions, and is well documented as a pro-survival stress response, particularly during nutrient and growth factor deprivation (Duprez, Wirawan, Vanden Berghe, & Vandenabeele, 2009; Gozuacik & Kimchi, 2007). A 'Janus-like' nature has been ascribed to this process however, and under certain circumstances autophagy has been proposed to be causative in cell death (Gozuacik & Kimchi, 2007; Shintani & Klionsky, 2004). *Autophagic cell death*, that is death occurring with massive vacuolarisation of the cytosol but without chromatin condensation (Galluzzi et al., 2007; Kroemer et al., 2009), might conceptually occur through destruction of a proportion of the cytosol past a 'point of no return' and subsequent cellular atrophy, or by selective degradation of organelles vital for viability. This causative role in cell death has been brought into question however, and the model systems which show an indispensable requirement for autophagy in cell death are limited, thus it may be more appropriate to term this pathway 'death with autophagy' (Berry & Baehrecke, 2007; Kroemer & Levine, 2008; Kroemer et al., 2009). The multiple links between the apoptotic and autophagic machinery and shared activating stimuli might be explained as a means of ensuring efficient clearance of apoptotic bodies (Duprez et al., 2009; Kroemer & Levine, 2008).

Necrosis is generally defined as a gain in cellular volume leading to swelling of organelles and loss of plasma membrane integrity, in the absence of apoptotic or autophagic morphologies (Galluzzi et al., 2007; Kroemer et al., 2009). Membrane rupture occurs early during this mode of cell death, and the release of intracellular contents may stimulate an inflammatory immune response (Galluzzi et al., 2007; Kroemer et al., 2007). For these reasons necrosis has traditionally been viewed as an accidental form of cell death, yet observations of common signalling patterns in necrotic cells have challenged this idea. Indeed, the term *necroptosis* has been spawned to differentiate 'accidental' and 'programmed' necrosis (Galluzzi et al., 2007; Tait & Green, 2008). Whilst it remains an open question as to which organelles and mediators may be directly involved in executing

necroptosis, the receptor interacting protein-1 (RIP-1), an adaptor protein in TNFR signalling, appears to play a key role (Degterev et al., 2008; Tait & Green, 2008).

Mitotic catastrophe is cell death occurring during or following a dysfunctional or abnormal mitosis, and requires deficiencies in cell cycle and DNA damage checkpoints as well as a damaging stimulus (Kroemer et al., 2009; Vakifahmetoglu, Olsson, & Zhivotovsky, 2008). Whilst this process can lead to formation of micronuclei or multinucleate cells, death may occur with either apoptotic or necrotic phenotypes, and mitotic catastrophe itself may be better considered as a route to these modalities (Vakifahmetoglu, Olsson, & Zhivotovsky, 2008). Failure to undergo mitotic catastrophe can lead to asymmetric segregation of chromosomes to daughter cells, and contribute to tumourigenesis (Kroemer et al., 2007).

1.2.4 Intracellular Ca^{2+} Homeostasis and Signalling

The pivotal role played by Ca^{2+} as an intracellular signalling molecule is well documented in processes as diverse as fertilisation, muscle contraction, secretion, metabolism and cell death (Alberts, 2008a). The distribution of this almost ubiquitous signalling molecule is highly compartmentalised, the concentration within each compartment reflecting a balance between uptake and extrusion processes. At rest the concentration of free Ca^{2+} in the cytosol ($[Ca^{2+}]_{cyt}$) is low (~0.1 μM in most cases) compared to the intracellular Ca^{2+} storage organelles and the extracellular fluid, thus a concentration gradient exists to readily permit increases in $[Ca^{2+}]_{cyt}$. Cellular Ca^{2+} signalling occurs through oscillatory rises in $[Ca^{2+}]_{cyt}$, integrating both the amplitude and frequency of the resulting Ca^{2+} spikes (Alberts, 2008a; Berridge, Bootman, & Roderick, 2003).

Ca^{2+} flux across the plasma membrane is vital in cellular Ca^{2+} homeostasis. In mammalian cells two types of pump expel Ca^{2+} to maintain the low $[Ca^{2+}]_{cyt}$. Ca^{2+} is transported out of the cell by isoforms of the plasma membrane Ca^{2+} ATPase via active transport, or by ion exchangers which exploit the Na^+ and K^+ concentration gradients also existing across the membrane. Re-entry of Ca^{2+} in the context of signalling may occur through cation channels of varying selectivity, including the transient receptor potential channels, or through voltage gated Ca^{2+} channels in response to plasma membrane depolarisation (Hancock, 2010; Marks, Klingmüller, & Müller-Decker, 2009).

1.2 Introduction – Cell Death and Cellular Ca^{2+} Signalling

The greatest concentration of Ca^{2+} within the cell is found in the lumen of the *endoplasmic reticulum* (ER) (~300-500 μM). Maintenance of a high intra-lumenal ER Ca^{2+} concentration ($[Ca^{2+}]_{ER}$) is important both for the role of the ER as a major site of protein and lipid biosynthesis, and as a store from which intracellular Ca^{2+} signalling may be initiated (Hancock, 2010). The ER membrane contains a Ca^{2+} pump similar in function to that at the plasma membrane, the sarcoplasmic/ endoplasmic reticulum Ca^{2+} ATPase (SERCA), capable of active transport to sequester Ca^{2+} within the ER. This ATPase is responsible for generating the Ca^{2+} gradient across the ER membrane, although its function is inhibited by high $[Ca^{2+}]_{ER}$, and may form up to 90% of the membrane protein content of specialised muscle sarcoplasmic reticulum (Brini & Carafoli, 2009; J. Hancock, 2010).

Release of ER Ca^{2+} occurs through two separate processes, that of poorly characterised basal 'leak' and stimulated Ca^{2+} release occurring via the *inositol triphosphate receptor* (IP_3R) and the *ryanodine receptor* (RYR). The IP_3R exists in three isoforms (IP_3R-1, IP_3R-2 and IP_3R-3) which form homo- and hetero-tetramers ~1200 kDa in size. Each subunit contains six transmembrane helices with a short cytosolic C-terminus involved in channel function and a large cytosolic N-terminus responsible for ligand binding, regulatory modifications and capable of multiple protein interactions (Devogelaere, Verbert, Parys, & Missiaen, 2008; Hancock, 2010). Binding of the ligand inositol 1,4,5-triphosphate (IP_3), generated during cellular signal transduction, causes opening of the IP_3R channel to allow Ca^{2+} efflux into the cytosol. Ca^{2+} itself is a co-activator of the IP_3R in a biphasic manner; low concentrations stimulate channel opening (peaking ~0.2-0.3 μM) whilst high concentrations are inhibitory. Regulation of the receptor occurs through a complex interaction of protein binding and post-translational modifications (Ando, Mizutani, Kiefer, & Tsuzurugi, 2006; Devogelaere et al., 2008). The RYR is a second tetrameric channel in the ER membrane whose endogenous ligand has not yet been fully identified. The channel exhibits similar biphasic modulation by Ca^{2+} to the IP_3R, and the combined Ca^{2+} sensitivity of these channels means a small release of Ca^{2+} in one cellular locale may be propagated across the entire cell in the process of Ca^{2+}-induced Ca^{2+} release (CICR). Interestingly, the RYR contains two key cysteine residues within its channel domain, indicating the receptor may be redox sensitive (Hancock, 2010).

Depletion of the ER Ca^{2+} store stimulates the opening of a set of plasma membrane *store-operated Ca^{2+} channels* (SOCs), allowing Ca^{2+} influx into the cytosol to aid store refilling, a process known as *store-operated Ca^{2+} entry* (SOCE) (Marks et al., 2009). SOCE is mediated

by the integral ER membrane protein stromal interaction molecule-1 (STIM-1) which acts as a Ca^{2+} sensor of the ER lumen. Decreases in store Ca^{2+} leads to clustering of STIM-1 in juxtaposition with Orai plasma membrane Ca^{2+} channels, the opening of which raise $[Ca^{2+}]_{cyt}$ (Cahalan, 2009; Marks et al., 2009).

Mitochondria make important contributions to cellular Ca^{2+} signalling, and their capacity to accumulate Ca^{2+} is capable of boosting oxidative metabolism, altering the spatiotemporal properties of Ca^{2+} signals and inducing cell death (Duchen, Verkhratsky, & Muallem, 2008; McCormack, Halestrap, & Denton, 1990; Szabadkai & Duchen, 2008). Ca^{2+} uptake occurs through the relatively low affinity *mitochondrial Ca^{2+} uniporter* (MCU) whose molecular identity has eluded researchers for decades, but the identification of which (or a component thereof) has recently been made (Baughman et al., 2011; De Stefani, Raffaello, Teardo, Szabò, & Rizzuto, 2011; Perocchi et al., 2010). Extrusion occurs through a Na^{+}/ Ca^{2+} ion exchanger. Ca^{2+} may also be stored and released from acidic compartments such as lysosomes, gated by NAADP (Patel, 2004).

The A549 cell line has previously been demonstrated to express an L-type voltage gated Ca^{2+} channel and both P2X and P2Y purinergic receptors, which generate intracellular Ca^{2+} signals upon ATP or UTP stimulation, at the plasma membrane. All three isoforms of the IP_3R and the type-1 RYR are also present (H. Xue, Zhao, Suda, & Uchida, 2000).

1.2.5 Functional Coupling Between the ER and Mitochondria

Crosstalk between the ER and mitochondria plays an important role in cellular physiology and pathology. The association of the ER and mitochondrial networks has long been suggested by co-sedimentation studies and fluorescence microscopy (Montisano, Cascarano, Pickett, & James, 1982; R Rizzuto, Pinton, Carrington, Fay, & Fogarty, 1998; Shore & Tata, 1977), and indeed electron micrographs have revealed these local contacts to represent areas of tight physical coupling between the two membranes (Csordás et al., 2006). Although the exact molecular nature of the tethers connecting the two organelle membranes has not been fully determined, evidence suggests they are likely to be proteinacious complexes. Mitofusin-2 (Mfn2), a dynamin-related GTPase involved in mitochondrial fusion, has been demonstrated to localise to both the outer mitochondrial membrane and the ER membrane,

and Mfn2 ablation in mouse embryonic fibroblasts (MEFs) caused mitochondrial fragmentation and a decrease in the number of ER-mitochondria contact sites. Whilst recombinant expression of Mfn2 targeted to the outer mitochondrial membrane restored elongation of the mitochondrial network in Mfn2 deficient MEFs, additional Mfn2 expression at the ER membrane was required to re-establish inter-organelle contacts (de Brito & Scorrano, 2008). The IP_3R and voltage dependant anion channel (VDAC), a major protein component of the mitochondrial outer membrane, have also been shown to form a direct physical complex, an interaction mediated by the molecular chaperone glucose-regulated protein 75 (Grp75) (Szabadkai et al., 2006). This tight coupling of organelles has functional consequences, notably so in Ca^{2+} homeostasis, where, after release from the ER, the formation of so called high *Ca^{2+} 'microdomains'* allow rapid mitochondrial accumulation of Ca^{2+} to concentrations far above global cytosolic levels (R Rizzuto, Brini, Murgia, & Pozzan, 1993). Contacts between the ER and mitochondria have also long been recognised as important in the process of phospholipid biosynthesis, since many synthetic enzymes catalysing these pathways may be found at either the ER or mitochondrial membranes. Phosphatidylcholine, for example, is synthesised in sequential stages by enzymes present in the ER membrane and mitochondrial intermembrane space (Lebiedzinska, Szabadkai, Jones, Duszynski, & Wieckowski, 2009). Complexes mediating ER-mitochondria contacts may also directly impact upon cell fate. Disruption of complexes containing the multifunctional ER sorting protein phoshofurin acidic cluster sorting protein-2 (PACS2) caused dynamin-related protein-1 (Drp-1) dependent fragmentation of the mitochondrial network, whilst PACS2 was shown to translocate pro-apoptotic BH3-only protein t-Bid to the outer mitochondrial membrane in response to apoptotic stimuli, promoting oligomerisation of pro-apoptotic effector BCL-2 proteins and cell death (Simmen et al., 2005).

1.2.6 Ca^{2+} Mediated Cell Death Pathways

Ca^{2+} signalling plays a central role in both the life and death of the cell. Dysregulation of previously tightly controlled Ca^{2+} homeostasis (see Section 1.2.4) may generate prolonged rises in intracellular Ca^{2+} unlike the oscillations characteristic of intracellular signalling, and promote cell death.

1.2 Introduction – Cell Death and Cellular Ca^{2+} Signalling

In many cases apoptotic Ca^{2+} signals are initiated by release of Ca^{2+} from the ER. Indeed, the BCL-2 proteins, which so crucially regulate the integrity of the mitochondrial outer membrane (see Section 1.2.2), also control Ca^{2+} retention in the ER store (Rong & Distelhorst, 2008). Anti-apoptotic BCL-2 inhibits Ca^{2+} release from the ER by inhibiting IP_3R function. This effect may be due to direct binding, since BCL-2 is able to inhibit IP_3R opening in an *in vitro* membrane-reconstituted system (R. Chen et al., 2004), or by promoting inhibitory phosphorylation of the receptor. BCL-2 also causes a decrease in $[Ca^{2+}]_{ER}$, thereby lowering its apoptogenic potential, possibly by increasing basal Ca^{2+} leak from the IP_3R (R Rizzuto et al., 2003; Rong & Distelhorst, 2008). BCL-2 also inhibits Ca^{2+} transfer along the ER-mitochondrial axis, the importance of which is outlined below. Conversely, pro-apoptotic BAX and BAK promote redistribution of Ca^{2+} from the ER to mitochondria, and the BH3-only protein tBid increases mitochondrial Ca^{2+} uptake (Csordás, Madesh, Antonsson, & Hajnóczky, 2002; Rong & Distelhorst, 2008). ER Ca^{2+} release is also enhanced during the apoptotic cascade. Cytochrome c released from mitochondria in the mitochondrial pathway of apoptosis may bind directly to the IP_3R to potentiate Ca^{2+} release, whilst the IP_3R is also a caspase-3 substrate, the cleavage of which increases Ca^{2+} release (Boehning et al., 2003; Rong & Distelhorst, 2008). Pro-apoptotic Ca^{2+} transfer from the ER to mitochondria may also occur during prolonged periods of ER-stress (Chami et al., 2008).

Cytochrome *c* resides in the cristae of mitochondria, where it fulfils a vital function in ferrying electrons between complexes III and IV of the respiratory chain. During apoptosis a widening of cristae junctions, termed *cristae remodelling*, and fragmentation of the mitochondrial network promoted by Drp-1 has been proposed to aid cytochrome *c* egress into the cytosol in a process which may be mediated by Ca^{2+} (Cereghetti & Scorrano, 2006; Scorrano et al., 2002). The pro-apoptotic BH3-only protein BCL-2 interacting killer (BIK) localises to the ER (Chinnadurai, Vijayalingam, & Rashmi, 2008). Under conditions of cellular stress BIK activation promotes the release of Ca^{2+} from the ER store to mitochondria and leads to Drp-1 regulated cristae remodelling (Mathai, Germain, & Shore, 2005). Cristae remodelling by Drp-1 may both induce BAX/ BAK-dependent cytochrome *c* release via the intrinsic pathway of apoptosis and cooperatively sensitise cells to death induced by the action of other pro-apoptotic molecules such as NOXA (Germain, Mathai, McBride, & Shore, 2005).

1.2 Introduction – Cell Death and Cellular Ca^{2+} Signalling

The *calpain* family of proteases provide a direct link between Ca^{2+} and apoptosis. Calpains are expressed in both tissue specific and ubiquitous isoforms, which may be activated proteolytically by increased Ca^{2+} in the micromolar (μ-calpain/ calpain I) to millimolar (m-calpain/ calpain II) range, and are localised to multiple subcellular organelles (Kar et al., 2010; R Rizzuto et al., 2003). Calpains have been shown to cleave many proteins involved in apoptosis, including p53, BAX, Bid, XIAP and initiator caspase-12, thus may engage the cell death pathway at multiple entry points (G. Gao & Dou, 2000; Kobayashi et al., 2002; Kubbutat & Vousden, 1997; Mandic et al., 2002; Orrenius, Zhivotovsky, & Nicotera, 2003; Wood et al., 1998). Processing by calpains has also been shown to be important in releasing AIF from mitochondria after MOMP. Whilst it appears AIF is not required for most forms of apoptosis, calpain-mediated AIF cleavage does seem to play a role in staurosporine-induced cell death in a NSCLC cell line (Gallego et al., 2004; Norberg et al., 2008; Norberg, Orrenius, & Zhivotovsky, 2010).

Ca^{2+}-sensitive protein kinases and phospholipases have been assigned both pro-apoptotic and anti-apoptotic roles. Notably, the phosholipase calcineurin may exert pro-apoptotic effects by removing inhibitory phosphate groups from the BH3-only protein BAD (Orrenius et al., 2003; R Rizzuto et al., 2003).

Intracellular rises in Ca^{2+} may also activate the necrotic pathway of cell death. Phospholipase A2 activation through increased $[Ca^{2+}]_{cyt}$ destabilises the cellular membrane system by liberating arachidonic acid, aiding necrotic membrane rupture (Declercq, Van Herreweghe, Vanden Berghe, & Vandenabeele, 2010). The most prominent route leading to necrosis however occurs through *mitochondrial permeability transition* (mPT). mPT is the abrupt permeabilisation of the inner mitochondrial membrane caused by the opening of a large non-selective pore with a maximum conductance of approximately 1.5 kDa, the *mitochondrial permeability transition pore* (mPTP) (Halestrap, 2009; Kroemer et al., 2007; Lemasters, Theruvath, Zhong, & Nieminen, 2009). The strongest inducer of opening of this pore is mitochondrial Ca^{2+} overload, again highlighting the importance of Ca^{2+} communication along the ER-mitochondrial axis, although the concentration of Ca^{2+} at which opening occurs is highly dependent upon both cell type and prevailing local conditions within the mitochondrion. Oxidative stress, increased inorganic phosphate concentration and depletion of adenine nucleotides are also strong inducers, whilst high mitochondrial transmembrane potential ($\Delta\Psi$) inhibits mPT (Halestrap, 2009). Pore opening may be transient ('flickering')

or permanent, and leads to dissipation of $\Delta\Psi$, switching of ATP synthase into reverse mode, equilibration of solutes across the inner mitochondrial membrane and osmotic swelling of mitochondria accompanied by subsequent rupture of the outer membrane (Halestrap, 2009; Kroemer et al., 2007). Since these changes cause depletion of ATP required for caspase activity, mPT is considered a necrotic mechanism, although it has been shown to promote cyt *c* release through swelling-induced rupture of the outer mitochondrial membrane. The molecular components of the pore have been hotly debated. Cyclophilin D (Cyp D), a matrix peptidyl-prolyl cis-trans isomerase, remains the only confirmed component, and Cyp D knock-out massively reduces the ability of Ca^{2+} to induce mPT. The adenine nucleotide transporter (ANT) is generally considered to play a regulatory role, whilst VDAC isoforms and the benzodiazepine receptor have largely been discounted (Halestrap, 2009; Kroemer et al., 2007). It has also been suggested the mPTP may in fact be a pathological accumulation of misfolded inner-membrane proteins (Lemasters et al., 2009).

In summary, pathological intracellular Ca^{2+} signals may lead to both apoptosis and necrosis through a variety of mechanisms.

1.2.7 Cell Death and Cancer

The ability to remove cells through programmed cell death pathways is vital for multicellular organisms. An estimated 60 billion new cells are produced by the adult human body each day, with an approximately equal number required to die to counterbalance this increase (Cotter, 2009). The comparative infrequency with which errors occur and remain unfixed is of great testament to the fidelity of both processes. When such errors do occur however, cancer may result. The idea that inhibition of cell death may contribute to tumour formation was initially proposed nearly 40 years ago, and is now considered a defining feature of cancer cells (Hanahan & Weinberg, 2000; Kerr et al., 1972; Luo, Solimini, & Elledge, 2009). In discovering that BCL-2 mutations could drive carcinogenesis not by increasing proliferation as an oncogene but by protecting cells from normal cell death pathways, the first molecular link with the apoptotic machinery was made. Immortalised mouse cell lines harbouring mutant BCL-2 form tumours when injected into mice only after the acquisition of secondary mutation(s), demonstrating the synergy between increased proliferation and apoptosis resistance in tumourigenesis (Cotter, 2009; Paget & London, 2006; Vaux, Cory, & Adams,

1988). Indeed, overactivation of some oncogenes such as *Myc* cause a concomitant increase in both cellular proliferation and apoptosis, a type of cellular 'safety valve', whilst the resulting hyperplasia becomes neoplasia only when deficiencies in the death pathway are acquired (Cotter, 2009; Evan et al., 1992). Dysregulation of cell death not only contributes to tumour initiation, but may also negatively impact upon chemotherapy treatments, many of which aim to engage apoptotic signalling (Kaufmann & Vaux, 2003; Yip & Reed, 2008; Zhivotovsky & Orrenius, 2010).

Resistance to cell death may be caused by the overactivation of an anti-apoptotic protein or by invalidation of an apoptotic activator or effector (Deng et al., 2007). The importance of BCL-2 overexpression in increasing cell survival has already been discussed. It should be noted however that this overexpression often occurs alongside overexpression of pro-apoptotic proteins such as BAX and caspases, indicating the integrated activity of the apoptotic machinery as a whole, rather than the absolute levels of individual proteins, is the important factor in tipping the balance of life and death (Zhivotovsky & Orrenius, 2010). Inactivation of BAX has been observed in human cancers, and loss of caspases may promote oncogenic transformation (Yip & Reed, 2008; Zhivotovsky & Orrenius, 2010). Tumour suppressor protein *p53* is mutated in over half of human cancers. A transcription factor involved in cell cycle arrest after DNA damage, p53 may upregulate many pro-apoptotic genes such as PUMA, BAX and NOXA, and act in a transcription-independent manner to activate BAX (Wolyniec, Haupt, & Haupt, 2010). Loss of p53 may, amongst other effects, induce resistance to cell death.

1.3 Cellular Metabolism and Cancer

1.3.1 Cellular Energy Metabolism – Glycolysis to the TCA Cycle, a Brief Overview

Metabolism is the total set of reactions occurring within a cell to support its viability and function. Animal cells contain many thousands of these enzymatically catalysed reactions working in anabolic and catabolic pathways, which may both converge upon and diverge from common substrates and intermediates. The ATP demands of human cells are met by two well characterised pathways, *glycolysis* and the *tricarboxylic acid (TCA) cycle* followed by *oxidative phosphorylation*, both of which shall be briefly discussed.

Glycolysis is a catabolic pathway occurring in the cytosol, and consists of ten enzyme catalysed reactions which result in the stepwise oxidation of one molecule of glucose into two molecules of pyruvate. Key enzymes and substrates of the glycolytic pathway are outlined in Figure 1. Glucose enters the cell through facilitated diffusion via different isoforms of the GLUT glucose transporter, expression of which is tissue and cell specific (Thorens & Mueckler, 2009). During the first three steps of the pathway glucose undergoes two phosphorylation events to generate fructose-1,6-bisphosphate, thus the early stages utilise two molecules of ATP. The resulting hexose is cleaved, producing two phosphoryl-containing triose sugars, which undergo oxidation and phosphorylation, each reducing one molecule of the co-factor *nicotinamide adenine dinucleotide* from the oxidised form (NAD^+) to the reduced form (NADH) in the process. NADH may be used as an electron-donor by the *mitochondrial electron transport chain* (ETC, see Section 1.3.2). The final steps of the pathway produce pyruvate through isomerisation reactions and hydrolysis of both phosphoryl bonds; the Gibbs free energy release associated with this hydrolysis is used to synthesise two molecules of ATP (Alberts, 2008b; Stryer, Berg, & Tymoczko, 2002; D. Voet & Voet, 2004a). Glycolysis therefore is biochemical pathway producing ATP, in which input of one glucose molecule results in the *net output* of two molecules of pyruvate, two molecules of ATP and two molecules of NADH. Alternatively, after the initial phosphorylation reaction of glycolysis, glucose (as glucose-6-phosphate) may be diverted for use in the *pentose-phosphate pathway*. The major products of this pathway are *reduced nicotinamide adenine dinucleotide phosphate* (NADPH), a co-factor used in the reductive biosynthesis of molecules such as lipids and endogenous antioxidants, and ribose-5-phosphate, a precursor of nucleotide biosynthesis (D. Voet & Voet, 2004a).

1.3 Introduction – Cellular Metabolism and Cancer

NADH produced during glycolysis must be oxidised to avoid depleting cellular NAD^+, and to allow glycolysis to continue. To this end, cellular energy metabolism may follow one of two routes. Under anaerobic conditions, as may be encountered in skeletal muscle during vigorous exercise, pyruvate is reduced to lactate using NADH by the enzyme lactate dehydrogenase, regenerating NAD^+ for use in glycolysis. Under aerobic conditions NADH is re-oxidised by the mitochondrial respiratory chain, accompanied by further ATP production. In this case pyruvate is imported into the mitochondrial matrix, where it undergoes oxidative decarboxylation to produce acetyl-CoA for entry into the TCA cycle. The TCA cycle (also known as the Krebs cycle or citric acid cycle) is a set of eight enzymatic reactions occurring in the mitochondrial matrix, leading to the oxidation of the acetyl group of acetyl-CoA. One complete 'revolution' of the cycle generates three molecules of NADH, one molecule of *reduced flavin adenine dinucleotide* ($FADH_2$), two molecules of CO_2 and one molecule of GTP (Alberts, 2008b; Stryer et al., 2002; D. Voet & Voet, 2004a). Numerous metabolic pathways converge upon the TCA cycle. β-Oxidation of fatty acids provides another source of acetyl-CoA, whilst catabolism of amino acids may yield intermediates of the TCA cycle. Replenishing of the citric acid cycle in this way is termed *anaplerosis.* TCA cycle intermediates may also enter into other interconnected pathways in *cataplerotic* reactions, including gluconeogenesis and biosynthesis of lipids and amino acids (D. Voet & Voet, 2004a).

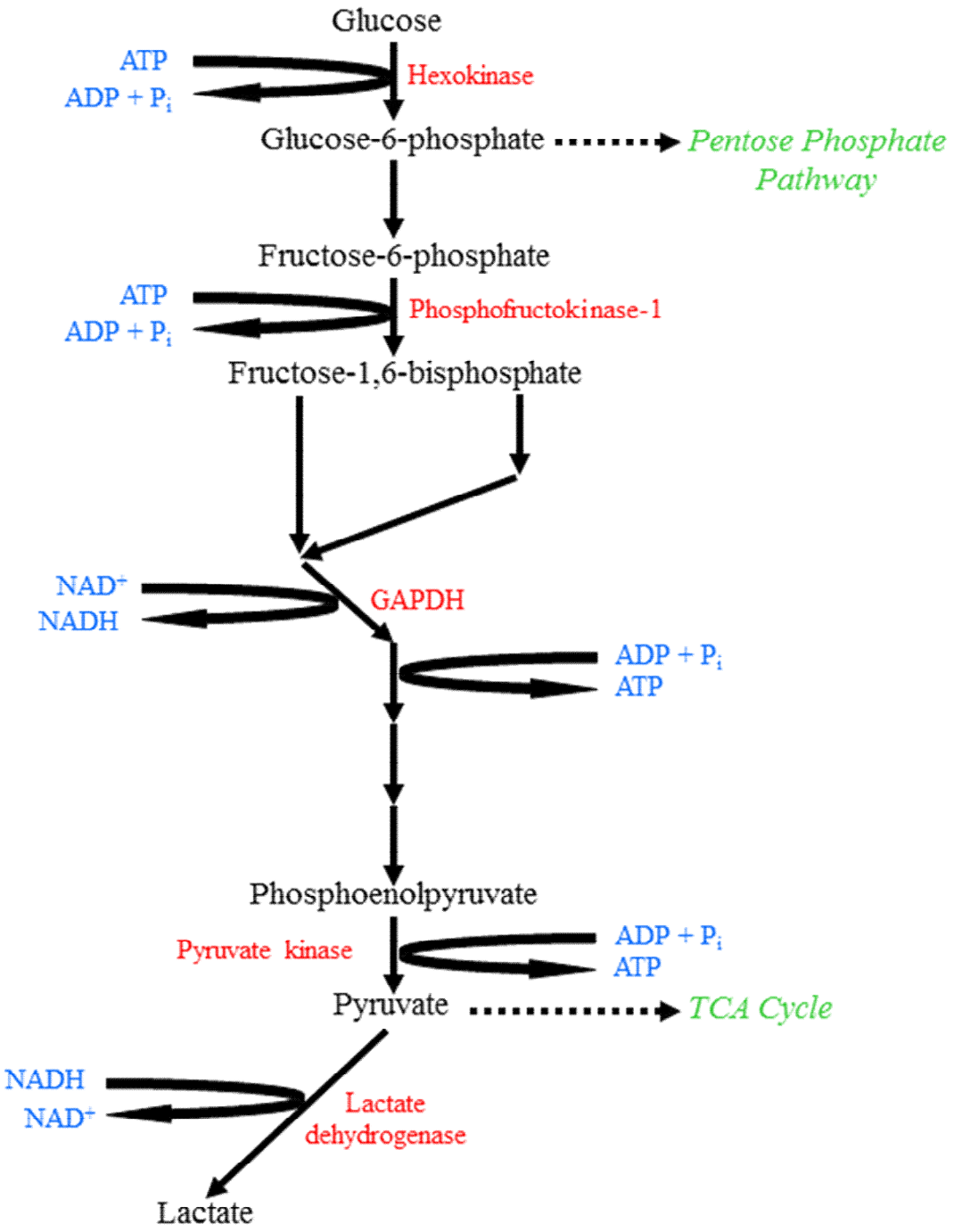

Figure 1: Key enzymes and substrates of the glycolytic pathway. For each molecule of glucose passing through the ten enzyme catalysed reactions of glycolysis, the usage of two molecules of ATP during the initial steps of the pathway results in net production of two molecules of pyruvate, two molecules of ATP and two molecules of the cellular redox intermediate NADH. In turn, pyruvate may be imported into the mitochondrial matrix as a

substrate for the TCA cycle, or may be reduced to lactate by cytosolic lactate dehydrogenase, oxidising NADH without the requirement of molecular oxygen. The two initial phosphorylation reactions of glycolysis, catalysed by hexokinase and phosphofructokinase-1 respectively, represent key rate limiting steps regulating the flux of substrate through the pathway. Following the initial phosphorylation of glucose, glucose-6-phosphate may be diverted away from glycolysis and cellular energy production into the biosynthetic pentose phosphate pathway.

1.3.2 Chemiosmotic Theory and Oxidative Phosphorylation

Under aerobic conditions the bulk of cellular ATP generation in many cells occurs through oxidative phosphorylation in mitochondria. The *chemiosmotic theory*, proposed by Peter Mitchell in 1961 (Mitchell, 1961), explains the underlying concept of oxidative phosphorylation, in which the electrochemical proton gradient established by the ETC across the inner mitochondrial membrane is directly harnessed to drive ATP synthesis.

The ETC consists of four multi-protein *respiratory complexes* of increasing redox potential (complexes I, II, III and IV), the soluble haem protein cytochrome *c* and the lipid soluble co-factor ubiquinone (Alberts, 2008b; Nicholls & Ferguson, 2002; D. Voet & Voet, 2004b). Transfer of electrons between redox centres within the ETC components is associated with the release of Gibbs free energy, used at complexes I, III and IV to pump protons from the mitochondrial matrix into the inter-membrane space. Thus transfer of electrons along the ETC is coupled to proton transport across the inner mitochondrial membrane, and is the source of the proton electrochemical gradient (Nicholls & Ferguson, 2002; D. Voet & Voet, 2004b). The major sources of electrons for the ETC are the reduced pyrimidine and flavoprotein co-factors, NADH and $FADH_2$ respectively, generated by glycolysis and the TCA cycle. By transferring electrons from the soluble dehydrogenases of these pathways to the membrane bound ETC, NADH and $FADH_2$ act as ‘high-energy’ intermediates to couple energy released by metabolic oxidation of organic molecules to ATP synthesis (Nicholls & Ferguson, 2002). After transport through complex IV, electrons are passed to molecular oxygen, the final electron acceptor, which is reduced using four electrons and recombined with protons to produce water (Alberts, 2008b). Figure 2 summarises this process. Electrons may be inappropriately transferred to oxygen from complexes other than complex IV,

producing *reactive oxygen species* (ROS), oxygen free radicals which may react with and damage cellular components.

The action of the ETC in generating a proton electrochemical gradient means translocation of protons back into the mitochondrial matrix is thermodynamically favoured, and acts as a 'store' of energy; this is the *proton-motive force*. Since the inner mitochondrial membrane is impermeable to protons, this movement may only occur through specific proton pores and channels such as *ATP synthase*, which may couple this energetically favoured process with a second process requiring energy input (Nicholls & Ferguson, 2002; D. Voet & Voet, 2004b). The ATP synthase consists of two major multi-subunit functional domains. F_o is a membrane bound complex which forms a proton channel. F_1 is a soluble ATPase associated with F_o on the matrix side of the inner membrane, capable of operating in reverse to synthesise ATP from ADP and inorganic phosphate. Proton flow through F_o causes rotary conformational changes in F_1, promoting phosphorylation of ADP (D. Voet & Voet, 2004b).

Oxidative phosphorylation driven by the oxidation of co-factors reduced by the passage of one molecule of glucose through glycolysis and the TCA cycle produces a theoretical maximum of between 30 and 36 ATP molecules. Oxidative phosphorylation is therefore a high energy yield process in comparison to the net production of two molecules of ATP by glycolysis coupled to lactate production (D. Voet & Voet, 2004b).

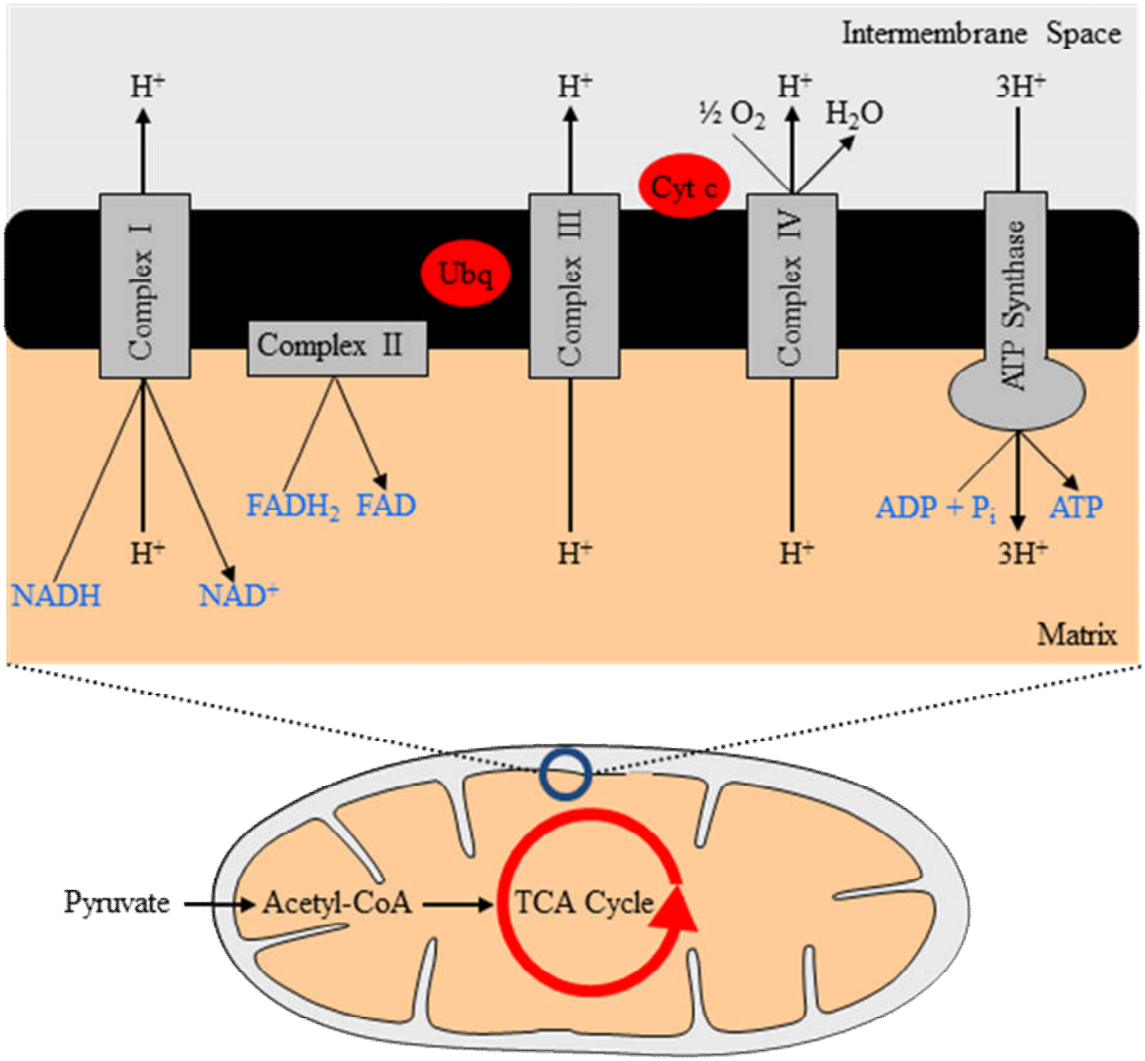

Figure 2: The TCA cycle and oxidative phosphorylation. During aerobic respiration, pyruvate produced by glycolysis undergoes oxidative decarboxylation upon import into the mitochondrial matrix, generating acetyl-CoA for entry into the TCA cycle. Passage of acetyl-CoA through the eight enzymatic reactions of the TCA cycle results in oxidation of the acetyl group and production of the 'high energy intermediate' redox carrier molecules NADH and FADH which, along with NADH generated by glycolysis, may be oxidised by the mitochondrial electron transport chain (ETC) during oxidative phosphorylation. The ETC couples the transfer of electrons from NADH and FADH to molecular oxygen with concomitant pumping of H^+ across the inner mitochondrial membrane. Following oxidation of NADH at complex I and FADH at complex II, electrons are passed from the respective complexes to the membrane soluble cofactor ubiquinone (Ubq), which in turn ferries

electrons to complex III. Electrons are subsequently transferred between complex III and complex IV by membrane associated cytochrome *c* (Cyt *c*), and finally used along with H^+ from the intermembrane space in reduction of oxygen to H_2O. The Gibb's free energy release associated with passage of electrons through complexes I, III and IV is utilised to pump into the intermembrane space against its electrochemical gradient, generating the mitochondrial transmembrane potential ($\Delta\Psi$). Translocation of H^+ back along this electrochemical gradient drives phosphorylation of ADP by ATP synthase.

1.3.3 Metabolic Adaptation in Cancer Cells

By necessity, rapidly proliferating cells must match their proliferative rates with increased production of ATP and biochemical components such as amino acids and lipids required for cell growth and division. During cellular transformation, cancer cells undergo *metabolic reprogramming* in which intracellular metabolism is altered to cope both with rapid division and the unique challenges of the tumour microenvironment (DeBerardinis, Lum, Hatzivassiliou, & Thompson, 2008; Kroemer & Pouyssegur, 2008; Tennant, Durán, Boulahbel, & Gottlieb, 2009). Amongst the most prominent of these changes is an increased use of glycolysis for ATP production, even under adequate oxygen tension ('*aerobic glycolysis*'), and a relative decrease in oxidative phosphorylation, a phenomenon known as the *Warburg effect* (Kroemer & Pouyssegur, 2008; Warburg, 1956; Zhivotovsky & Orrenius, 2009). At first sight the use of glycolysis, a pathway with a relatively poor ATP yield per molecule of glucose, to meet cellular energy demands is counter-intuitive. However, a vast increase in *glycolytic flux* ensures ample provision of ATP and a rate of production which may outstrip oxidative phosphorylation. As an additional benefit, pools of glycolytic intermediates are syphoned off for use in biosynthetic pathways (DeBerardinis et al., 2008; Kroemer & Pouyssegur, 2008; Shlomi, Benyamini, Gottlieb, Sharan, & Ruppin, 2011; Vander Heiden, Cantley, & Thompson, 2009).

Increased glycolytic flux calls for a greater provision of substrate for the pathway. Tumours do indeed exhibit greatly increased glucose uptake, a property exploited in medical imaging of tumours and metastases by ^{18}fluorodeoxyglucose-positron emission topography (FDG-PET). This augmentation of glucose uptake is achieved through a variety of mechanisms. The insufficient vasculature of many tumours means cancer cells, especially those in the central

tumour region, experience low oxygen tension. Such conditions lead to the stabilisation of *hypoxia-inducible factor* (HIF) transcription factor subunits, usually targeted for degradation under normoxia. HIF target genes promote glycolysis over oxidative phosphorylation, limiting oxygen usage under hypoxic conditions. In terms of substrate provision, HIF induces greater expression of the Glut I glucose transporter (Kroemer & Pouyssegur, 2008). *Phosphatidylinositol-3-kinases* (PI_3Ks) are a key class of enzymes activated by growth factor signalling. Lipid phosphorylation by PI_3K can produce phosphatidylinositol-3-phosphate (PI_3P) and directly lead to activation of *Akt protein kinase*, an enzyme capable of enhancing cell growth and survival. Mutations causing increased activity of the PI_3K/ Akt pathway are common in human cancer, and proliferation independent of growth factors is a hallmark of cancer cells (Hanahan & Weinberg, 2000; Shaw & Cantley, 2006). Akt activation may stimulate Glut I expression and Glut IV translocation to the plasma membrane.

The first step in glycolysis, phosphorylation of glucose to glucose-6-phosphate by *hexokinase* (Figure 1), is also the first rate-limiting step. Hexokinase has been shown to associate with VDAC-1 on the mitochondrial outer membrane, enhancing its activity by allowing direct access to mitochondrially-derived ATP. This association is promoted by Akt activity, and occurs much more frequently in tumour cells to increase glucose entry into glycolysis (Kroemer & Pouyssegur, 2008; Pastorino & Hoek, 2008). VDAC-1 may also act as a direct activator of BAX, whilst formation of the VDAC-1/ hexokinase complex appears to inhibit this pro-apoptotic interaction, protecting against MOMP (Gottlob et al., 2001; Kroemer & Pouyssegur, 2008; Pastorino, Shulga, & Hoek, 2002). Glucose-6-phosphate may either continue into glycolysis or be diverted into the pentose-phosphate pathway (see Section 1.3.3). Increased glucose phosphorylation allows for greater activity of this pathway for biosynthesis of nucleotide precursors, antioxidants and lipids.

Phosphofructokinase-1 (PFK-1) catalyses the second phosphorylation event of glycolysis (Figure 1), and is the major rate-limiting step. The enzyme may be allosterically activated by binding of fructose-2,6-bisphosphate, a regulatory molecule formed from its substrate by the bifunctional enzyme 6-phosphfructo-2-kinase/ fructose-2,6-bisphosphatase (PFK-2/ F2,6BP) (D. Voet & Voet, 2004c). Akt activation promotes the PFK-2 activity, and thus boosts glycolysis. Regulation by p53 also occurs through transcriptional activation of TP53-induced glycolysis regulator (TIGAR). TIGAR inhibits PFK-1 by degrading fructose-2,6-

bisphosphate, thus loss of p53 function promotes glycolysis by relieving PFK-1 inhibition (R. G. Jones & Thompson, 2009; Vousden & Ryan, 2009).

More than 90% of pyruvate produced by glycolytic cancers is reduced to lactate (R. G. Jones & Thompson, 2009). *Lactate dehydrogenase*, the enzyme responsible for this reduction (Figure 1), may be upregulated by aberrant c-myc and HIF signalling, whilst HIF may additionally inhibit *pyruvate dehydrogenase*, decreasing production of acetyl-CoA from pyruvate, thereby favouring aerobic glycolysis (Kroemer & Pouyssegur, 2008; Shim et al., 1997; Tennant et al., 2009). Active transport of this lactate out of the cell causes a decrease in the pH of tissue surrounding the tumour, which may suppress the host immune response and promote an invasive phenotype (Kroemer & Pouyssegur, 2008; Shim et al., 1997). Such a high rate of lactate production and export might reflect an excess production of pyruvate over the capacity for entry into the TCA cycle (DeBerardinis et al., 2008), but may also provide some protection from apoptosis. Evidence suggests ROS may play a key role both in activating BAX and BAK, and in efficient caspase activation by promoting cytochrome c release (Borutaite & Brown, 2007; Tomiyama et al., 2006). By inhibiting mitochondrial oxidative activity and bolstering antioxidant defences cancer cells may therefore gain a survival advantage. It seems that activity of the respiratory chain is required for apoptosis under certain circumstances, and *mitochondrial DNA* (mtDNA) mutations affecting respiratory complex function have been found to associate with some types of cancer (Chatterjee, Mambo, & Sidransky, 2006; Kwong, Henning, Starkov, & Manfredi, 2007). Loss of p53 may also inhibit oxidative phosphorylation by repressing the expression of synthesis of cytochrome oxidase 2 (SCO2), a respiratory chain assembly factor (Kroemer & Pouyssegur, 2008; Vousden & Ryan, 2009).

The function of the TCA cycle is also altered to take on more of a biosynthetic role. The intermediates of the cycle may be used in anaplerosis as precursors for amino acid and lipid synthesis. It is notable that some oncogenes, particularly c-myc, may cause upregulation of enzymes involved in glutamine import and catabolism (Wise et al., 2008). This allows for glutamine metabolism to yield significant amounts of *α-ketoglutarate*, replenishing cycle intermediates lost through *de novo* synthesis of lipids. Interestingly, mutations in the enzymes *fumarate hydrolase* and *succinate dehydrogenase* can lead to accumulation of TCA cycle intermediates, a *pseudohypoxic* state which causes HIF activation and the accompanying shift

towards glycolysis (Frezza & Gottlieb, 2009; A. King & Gottlieb, 2009; Sudarshan, Pinto, Neckers, & Linehan, 2007).

Metabolism in tumour cells is thus altered to support cell division and survival, representing an attractive target for cancer therapy (Michelakis, Webster, & Mackey, 2008; Rodríguez-Enríquez, Marín-Hernández, Gallardo-Pérez, Carreño-Fuentes, & Moreno-Sánchez, 2009; Tennant, Durán, & Gottlieb, 2010).

1.4 *Cis*-Diamminedichloroplatinum II

1.4.1 Chemistry and Biochemistry of cDDP

The serendipitous discovery of the anti-proliferative effects of *cis*-diamminedichloroplatinum II (cDDP), more commonly known as *cisplatin*, by Rosenberg and co-workers in 1965 remains a landmark in cancer treatment (Rosenberg, Van Camp, & Krigas, 1965). Within eight years of this finding the anti-tumour properties of the drug had been demonstrated and clinical trials begun. Curative as a single agent in testicular cancer, cDDP is widely used as a first-line treatment for lung, head and neck and ovarian tumours (O'Dwyer, Stevenson, & Johnson, 1999; Watson et al., 2006). However, whilst undoubtedly potent, cDDP treatment is limited in the clinic by two major factors; chemoresistance (see Section 1.4.2) and adverse side effects. The latter of these considerations is characterised by pronounced toxicity in the kidney and inner ear, peripheral neuropathy and severe nausea, with limited myelosuppression (O'Dwyer et al., 1999). Nephrotoxicity may be largely overcome by aggressive pre-hydration and diuresis systems, whilst ototoxicity is both cumulative and irreversible, thus requires careful monitoring of patients. Likewise, neural damage is monitored throughout the course of treatment, whilst anti-emetics and the use of 'rescue agents' to prevent off-target effects serve to limit other unfavourable consequences.

At the molecular level cDDP consists of two amine and two chloride groups in *cis*-configuration, bound into a square planar complex by a single atom of platinum. Four decades of research have yielded more than 3000 platinum drug derivatives, replacing these side groups with increasingly complex structures in an effort to reduce toxicity and improve efficacy, yet just three are registered as marketable drugs, and only two (*carboplatin* and *oxaliplatin*) find common use (Jung & Lippard, 2007; O'Dwyer et al., 1999). Administered by intravenous injection, the process by which cDDP enters cells remains unclear. Considering the neutral charge of the molecule and that rate of uptake is not inhibited by structurally similar molecules but is limited only by cDDP concentration, a model of passive diffusion across the membrane has traditionally been favoured (Jung & Lippard, 2007; Kelland, 2007). Recent evidence has demonstrated facilitated diffusion through copper transporters may also occur (Holzer et al., 2004; Ishida, Lee, Thiele, & Herskowitz, 2002; Kelland, 2007; Safaei, 2006).

1.4 Introduction – *Cis*-Diamminedichloroplatinum

After entry into the cytoplasm, the relatively low intracellular concentration of chloride (~4-20 mM compared to ~100 mM in the extracellular fluid) promotes hydrolysis of one chloride group of cDDP (Figure 3). Mono-aquated cDDP is a highly reactive electrophile, the formation of which is rate-limiting in intracellular reactions (Knox, Friedlos, Lydall, & Roberts, 1986; Siddik, 2003). The major target is considered to be nuclear DNA, where cDDP may covalently bond with the N7 residue of purine bases; this overwhelmingly occurs at guanine sites (Ahmad, 2010). Hydrolysis of the second chloride group allows reaction with either a second purine or a protein. Both intra-strand and inter-strand crosslinks are formed, although intra-strand 1,2-guanine-guanine are most common (~65 %), followed by 1,2-adenine-guanine (~25 %), with inter-strand links accounting for just 1% of total adducts (Ahmad, 2010; Eastman, 1999; Siddik, 2003). It is the intra-strand links which are postulated to be the toxic lesions. Aquated cDDP is also highly reactive towards thiol groups, and a significant proportion of the drug reacts with S-donor ligands including microfilaments and the abundant tripeptide glutathione (GSH). Reaction with other amino acids is also possible (Appleton, 1999). Indeed, less than 5% of the total cDDP within a cell may associate with DNA (Fuertes, Alonso, & Pérez, 2003; Mandic, Hansson, Linder, & Shoshan, 2003). That cDDP does not fully react with these ligands before reaching DNA is by virtue that interactions are kinetically slow, and the reaction with guanine bases thermodynamically favourable (Jung & Lippard, 2007; Reedijk, 1999). In some cases, transfer of platinum from protein to DNA may occur (Reedijk, 1999).

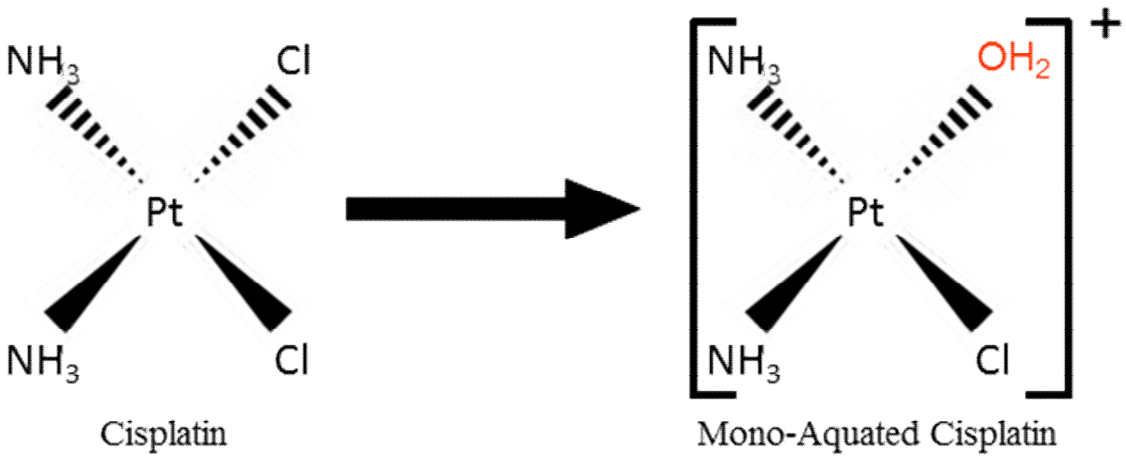

Figure 3: Intracellular activation of cDDP through aquation reactions. Upon uptake of cDDP into the cytoplasm, the relatively low intracellular concentration of chloride ions promotes hydrolysis of a single chloride group, generating mono-aquated cDDP, a reactive electrophile. Reaction of this electrophile with cellular nucleophiles, most commonly purine nucleotides or protein thiol groups, promotes subsequent hydrolysis of the remaining chloride group of cDDP, again generating a nucelophile which reacts with cellular electrophillic sites. Thus, cDDP forms the bulky adducts with DNA and/ or proteins which underlie its cytotoxic activity, interfering with normal cellular function and resulting in activation of DNA repair pathways, stress signalling and, eventually, apoptosis.

1.4.2 Cellular Response to cDDP – Cytotoxicity and Resistance

The response of cells treated with cDDP is complex, and may involve cell death by the mitochondrial or receptor-mediated pathways of apoptosis, necrosis, senescence or survival (Ahmad, 2010; L. Liu et al., 2008; Mandic et al., 2002; Puig et al., 2008). The way a cell processes cDDP and the damage it causes ultimately determines cell fate. This is a key point since resistance to cDDP, both intrinsic and acquired, is a major limiting factor in clinical use of the drug; the relapse rate due to acquired resistance may be as high as 95% in small cell lung cancer patients (Giaccone G., 2000). Classically such resistance mechanisms occur by decreasing cDDP-DNA interactions, or by increasing damage tolerance or repair once it has

occurred (Fuertes et al., 2003; Kelland, 2007). Resistance to cDDP is in most cases multi-factorial, and involves changes in distinct cellular pathways. A two-fold level of resistance has been estimated using patient samples, although *in vitro* studies suggest resistant cells may require more than fifty times greater drug concentrations for significant toxicity to occur (Siddik, 2003).

Binding of cDDP to DNA introduces bulky adducts which significantly distort the structure of the double helix (Eastman, 1999; Jung & Lippard, 2007). These lesions may be recognised with varying specificity by numerous proteins, and such DNA-damage recognition has been reviewed in detail (Jung & Lippard, 2007; Siddik, 2003; D. Wang & Lippard, 2005). Platinated DNA adducts are mostly repaired by the *nucleotide excision repair* (NER) pathway, by which whole damaged oligonucleotides may be removed from DNA. Upregulation and inhibition of NER proteins is associated with decreased and increased cDDP sensitivity respectively, whilst the hypersensitivity of testicular cancers to cDDP treatment has been explained by low levels of NER in these tumours (Ahmad, 2010; Jung & Lippard, 2007; Siddik, 2003; D. Wang & Lippard, 2005). On the other hand, the *mismatch repair* (MMR) pathway has been shown to contribute to cytotoxicity. It is hypothesised that MMR proteins bind DNA on strands opposite platinum adducts and undergo several futile repair cycles, eventually resulting in apoptosis, and loss of MMR may aid resistance (Ahmad, 2010; Jung & Lippard, 2007; Kelland, 2007; Siddik, 2003). Recognition of cDDP-DNA adducts may also lead to cell death by more indirect mechanisms. *High mobility group* (HMG) proteins show specificity in binding cDDP damaged DNA, and may prevent enzymes involved in NER accessing the lesions. Alternatively, large protein complexes at abundant sites of DNA damage may titrate proteins such as HMGs away from endogenous sites of action (Ahmad, 2010; Siddik, 2003). Whilst p53 and other related proteins such as p73 have been shown to be induced by cDDP, no clear link between p53 status and sensitivity has been established, highlighting that cellular responses may be cell and condition specific (Ahmad, 2010; Jung & Lippard, 2007; Siddik, 2003; D. Wang & Lippard, 2005). *Translesion synthesis* of DNA past cDDP adducts during DNA replication may also be increased to improve tolerance of DNA damage in cDDP resistant cells (Köberle, Tomicic, Usanova, & Kaina, 2010).

Cell death may occur through either apoptosis or necrosis, and indeed cDDP may induce both in a population of cells in a non-mutually exclusive manner. The apoptotic program may be

engaged through multiple pathways converging upon caspases and/ or calpains, the exact route appears to be context-dependent (Jung & Lippard, 2007; Mandic et al., 2002; Siddik, 2003). *Poly(ADP ribose) polymerase-1* (PARP-1) attaches poly(ADP ribose) polymers to specific targets in response to DNA damage, utilising NAD^+ and ATP. Overactivation of PARP-1 upon cDDP treatment may deplete cellular stores of NAD^+ and ATP, resulting in necrotic cell death (Jung & Lippard, 2007).

DNA damage may halt the cell cycle by engaging cell cycle checkpoints to allow for DNA repair. Treatment with cDDP may result in a transient S-phase arrest, yet the majority of cells arrest at the *G_2/ M-phase transition* (Eastman, 1999; Siddik, 2003). Cells arrested at this stage attempt repair of platinated DNA, and eventually undergo an aberrant mitosis leading to cell death (Eastman, 1999). In rare cases these aberrant mitoses may generate viable cells, promoting clonogenic outgrowth with a cDDP resistant phenotype (Puig et al., 2008).

The intracellular concentration of cDDP is an important factor in determining the extent of DNA modification. Decreased accumulation may occur either through as yet obscure changes in the passive uptake process or by decreased expression of copper transporters (Holzer et al., 2004; Kelland, 2007; Siddik, 2003). Increased drug efflux appears to be a less common mode of resistance, and cDDP itself is not a substrate for the multidrug resistance (MDR) proteins, although increased expression of copper transporting ATPases has been shown to reduce intracellular drug concentration (Kelland, 2007; R. J. B. King & Robins, 2006b; Siddik, 2003).

The interactions of cDDP with biomolecules other than DNA are also important in understanding its mode of action. The most influential of these may by binding of cDDP by the abundant endogenous antioxidant GSH. The high reactivity of aquated cDDP with thiol groups allows the drug to be sequestered before reaction with DNA, and increased expression of this tripeptide is a confirmed means of resistance in some cell types. GSH-cDDP conjugates may also be actively transported out of the cell (Fuertes et al., 2003; Kelland, 2007; R. J. B. King & Robins, 2006b; Siddik, 2003). Consideration of this mechanism must be tempered by understanding that binding of GSH by cDDP may deplete the intracellular antioxidant pool and promote cell death, especially since ROS production may be stimulated by cDDP treatment (Martins, Santos, Curti, Bianchi, & Santos, 2008). Furthermore, it has been proposed that these proteins may also act as a 'drug reservoir' for prolonged platination of DNA (Reedijk, 1999). The activity of other proteins may be negatively affected by cDDP

binding. The *Hsp90 chaperones* may be inhibited by cDDP treatment, as may several glycolytic enzymes and ETC respiratory complexes (Aull et al., 1979; Donnelly & Blagg, 2008; Rodríguez-Enríquez et al., 2009; R. Zhou, Vander Heiden, & Rudin, 2002).

The extensive modification of cellular protein has been shown to induce *ER stress* and cell death signalling in enucleated cells, a death pathway independent of nuclear effects (Mandic et al., 2003). Furthermore, the ER has been directly implicated in mediating cellular sensitivity to cDDP through the level of expression of IP_3R-1, and ER Ca^{2+} release is an early response to cDDP in some cell types (Kawai, Nakao, Kunimura, Kohda, & Gemba, 2006; Tsunoda et al., 2005). However, the degree to which effects at the ER contribute to the efficacy of cDDP and whether this effect is generally applicable remains unknown.

1.5 Aims of Thesis

1.5.1 Summary and Aims of Thesis

Cancer is a disease affecting millions worldwide, and future incidence is set to increase with changing lifestyles and increasing longevity in the global population. Section 1.1 of this introductory chapter has outlined both the scale of the problem and the strategies which may be used in attempts to overcome it. Chemotherapy remains a key player in both the management and treatment of this disease. In Section 1.4 greater detail is given on the properties and activity of the well studied chemotherapy drug cDDP. An alkylating-like agent, the antineoplastic effects of cDDP are considered to be mediated through DNA damage. Less well characterised effects of cDDP may also occur through direct damage to cellular proteins. Despite its widespread usage, the clinical efficacy of cDDP is limited by cancer cell chemoresistance, both intrinsic and acquired. Current strategies to augment cDDP cytotoxicity target common resistance mechanisms (see Section 1.4.2), and aim to maximise drug accumulation, prevent cDDP detoxification, increase tumour cell DNA damage and inhibit damage repair (Fuertes et al., 2003; Köberle et al., 2010). It is not known whether changes in effects not directly mediated by DNA damage, such as ER stress induction or alterations in cellular metabolism, contribute to the efficacy of cDDP treatment, and this is the issue this thesis seeks to address, with particular focus on the ER and mitochondria. The aims of the thesis may be broadly divided into three categories:

- *Use a NSCLC cell line to model cDDP resistance* – Exposure to cDDP has been reported to induce cell death through multiple pathways, with varying requirements for cell death effectors such as caspases, calpains, ROS and Ca^{2+}. Two sub-types of the A549 cell line with differing propensity to undergo cDDP-induced cell death will be investigated throughout this work. The A549-CR cell line was derived and selected for survival and growth in the presence of cDDP through prolonged culture of the parental wild type A549-WT cell line, which retains sensitivity to cDDP treatment, in the presence of a low concentration of cDDP. The difference in cDDP sensitivity between the two cell lines will be demonstrated, and the mode of cell death induced by cDDP will be determined with reference to previous literature, to establish whether the system is appropriate for investigating factors modulating cDDP cytotoxicity. Such work will contribute to the understanding of how cDDP causes cell death in

cancer cells. Variations in the response of the two A549 cell lines to cDDP treatment shall be used further in the investigation to identify properties of the ER and mitochondria which may modulate cDDP sensitivity.

- *Investigate the role of the ER in cDDP-induced cell death* – The ER is recognised as an organelle capable of inducing cell death through multiple pathways. The intracellular ER Ca^{2+} store is targeted during cell death induction by ER stress and apoptosis, both of which may result from cDDP treatment. ER Ca^{2+} handling will be compared in A549-WT cells and A549-CR cells to elucidate the contribution of Ca^{2+} and the ER in modulating cDDP sensitivity.

- *Examine mitochondrial response to cDDP treatment* – Mitochondria are key regulators in both the life and death of a cell. Changes in mitochondrial activity may promote cell survival or sensitise to cell death. The response of mitochondria to cDDP treatment, and the mechanism of any dissimilarities observed, will be investigated in A549-WT cells and A549-CR cells. The contribution of differences in this response to altered cDDP sensitivity will be explored.

Identification of novel cellular responses to cDDP treatment may provide alternative targets to improve the efficacy of cDDP based chemotherapy, and potentially circumvent chemoresistance. Greater understanding of how cDDP affects cellular physiology as a whole, and how these effects outside of the nucleus may contribute to cell death, may allow for targeted sensitisation of tumour cells to cDDP chemotherapy, reduce the acquisition of drug resistance and allow for the use of decreased drug concentrations, potentially limiting the occurrence of undesirable side effects associated with the drug. Conversely, modulation of extranuclear targets of cDDP may provide a unique strategy to protect non-tumour cells from cDDP-induced cell death whilst maintaining the anti-tumour activity of the drug.

2. Materials and Methods

2.1 Drugs and Reagents

Thapsigargin (Tg), cDDP, EGTA, ascorbic acid, TEMPOL, N-acetyl cysteine (NAC), 2-aminoethoxydiphenyl borate (2-APB), BAPTA-AM, ionomycin, diethylmaleate (DEM) and cyclosporine A (CsA) were purchased from Sigma-Aldrich. Hoechst 33342 (Hoechst), z-VAD-FMK and IETD-FMK were purchased from Enzo Life Sciences. D-2,3-O-Isopropylidene-6-O-(2-Nitro-4,5-Dimethoxy)benzyl-myo-Inositol 1,4,5 TrisphosphateHexakis(Propionoxymethyl) Ester (caged IP_3) was purchased from SiChem. Fluo-4-AM, Fura-2-AM, monochlorobimane (MCB) and tetramethylrhodamine methyl ester (TMRM) were purchased from Invitrogen. Calpain inhibitor ALLN was purchased from Calbiochem.

2.2 Cell Culture and Manipulation

A549-WT and A549-CR cell lines were maintained in Dulbecco's Modified Eagle Medium (DMEM)/ F12 1:1 + GlutaMAX (Invitrogen) supplemented with 10% foetal bovine serum, 100 units/ ml penicillin and 100 µg/ ml streptomycin (Invitrogen) ('normal cell culture medium') at 37 ^{o}C in 5% CO_2. Unless otherwise indicated, A549-WT and A549-CR cells treated with cDDP were maintained in normal cell culture medium supplemented with 75 µM cDDP at 37 ^{o}C in 5% CO_2 for the indicated time period. A549 Rho-0 cells were maintained in Dulbecco's Modified Eagle Medium (DMEM)/ F12 1:1 + GlutaMAX (Invitrogen) supplemented with 10% foetal bovine serum, 100 units/ ml penicillin, 100 µg/ ml streptomycin (Invitrogen) and 50 µg/ ml uridine at 37 ^{o}C in 5% CO_2. HeLa cells were maintained in DMEM + GlutaMAX (Invitrogen) supplemented with 10% foetal bovine serum, 100 units/ ml penicillin and 100 µg/ ml streptomycin (Invitrogen) at 37 ^{o}C in 5% CO_2. Cells were passaged every 3-4 days upon reaching 90% confluence.

During cell imaging procedures, fluorescent dye loading, drug pre-treatment for imaging procedures and measurement of aequorin bioluminescence cells were bathed in Krebs-Ringer buffer (KRB; 125 mM NaCl, 5 mM KCl, 1 mM Na_3PO_4, 1 mM $MgSO_4$, 1 g/ l glucose, 20

mM HEPES, 1 mM $CaCl_2$, pH 7.4) with the indicated supplements, unless otherwise indicated. During 'Ca^{2+} free' experiments cells were bathed in nominally 'Ca^{2+} free' KRB (125 mM NaCl, 5 mM KCl, 1 mM Na_3PO_4, 1 mM $MgSO_4$, 1 g/ l glucose, 20 mM HEPES, pH 7.4) with indicated the supplements. During overnight imaging of A549 cell morphology, cells were loaded with fluorescent dyes and imaged in normal cell culture medium at 37 ^oC in a heated imaging chamber perfused with 5% CO_2 for the entire duration of the experiment.

For transfection of cDNA constructs A549-WT or A549-CR cells were seeded in 6-well tissue culture plates (Falcon) or onto 22 mm diameter glass coverslips in 6-well tissue culture plates 24 hours before transfection at 40-60% confluence. Cells contained in individual wells of the culture plate were transfected with a total of 4 µg cDNA using Lipofectamine 2000 (Invitrogen) according to the manufacturer's instructions, and incubated at 37 ^oC for 48 hours before experimental procedures began.

2.3 Imaging Apparatus

Confocal images were acquired using a Zeiss 510 LSM Meta confocal microscope system (Carl Zeiss Ltd.) with a 40x oil immersion objective lens (N.A. 1.3) or a 63x oil immersion objective lens (N.A. 1.4), and cells maintained at 37 ^oC throughout the experimental time course. Excitation illumination was provided by emission lines from a helium/ neon laser, an argon laser, a 405 nm laser diode or a Coherent Enterprise UV laser. Where indicated, linear unmixing of fluorescence emission was performed using Zeiss LSM 4.0 software (Carl Zeiss Ltd.), using reference spectra previously obtained from A549-WT cells singly expressing the relevant recombinant fluorophore(s).

Measurements of SOCE Ca^{2+} signals using Fura-2-AM were made using an Axiovert inverted epifluorescence microscope (Carl Zeiss Ltd.) with a 20x fluorite objective lens (N.A. 0.45). Images were collected using a Hamamatsu 4880 cooled charge-coupled device camera (Hamamatsu Corporation), and recorded and analysed using Kinetic Imaging software (Kinetic Imaging Ltd.). Excitation illumination was provided by light from a xenon arc lamp passing through a computer controlled filter wheel (Cairn Research). Coverslips were maintained at 37 ^oC throughout the experimental time course.

Overnight timelapse images of A549-WT and A549-CR cells, determination of cellular GSH and Fura-2-AM measurements of A549-WT cell response to ATP were made using an Olympus IX71 inverted epifluorescence microscope (Olympus) fitted with a computer controlled motorised stage (Applied Scientific Instrumentation) with a 40x fluorite objective lens (N.A. 0.6). Images were collected using a Hamamatsu C10600-10B cooled charge-coupled device camera (Hamamatsu Corporation), and recorded and analysed using Simple PCI 6.6.0.0 software (Hamamatsu Corporation). Excitation illumination was provided by light from a metal halide arc lamp passing through a computer controlled filter wheel (Prior Scientific).

2.4 Estimation of Cell Viability by Flow Cytometry

A549 cells were cultured in 6-well tissue culture plates (Falcon) for 24 hours following cell seeding before intervention. For caspase inhibitor experiments, A549-WT cells were incubated in normal cell culture medium + 20 µM z-VAD-FMK or in normal cell culture medium + 20 µM z-VAD-FMK + 75 µM cDDP for 24 hours before assay. For calpain inhibitor experiments, A549-WT cells were incubated in normal cell culture medium + 50 µM ALLN or in normal cell culture medium + 50 µM ALLN + 75 µM cDDP for 24 hours before assay. For CsA experiments A549-WT cells were incubated in normal cell culture medium + 5 µM CsA or in normal cell culture medium + 5 µM CsA + 75 µM cDDP for 24 hours before assay. For antioxidant experiments A549-WT cells were incubated in normal cell culture medium + 1 mM ascorbic acid or in normal cell culture medium + 1 mM ascorbic acid + 75 µM cDDP, in normal cell culture medium + 200 µM TEMPOL or in normal cell culture medium + 200 µM TEMPOL + 75 µM cDDP or in normal cell culture medium + 5 mM NAC or in normal cell culture medium + 5 mM NAC + 75 µM cDDP for 24 hours before assay. Cells transfected with IP_3R-1 cDNA constructs (Miyawaki et al., 1999) were incubated for 48 hours after transfection before the culture medium was changed either to fresh normal cell culture medium or normal cell culture medium + 75 µM cDDP and cells were incubated for a further 24 hours before assay. For Ca^{2+} chelation experiments with BAPTA-AM, A549-WT cells were incubated in normal cell culture medium + BAPTA-AM at 1 µM, 3 µM or 10 µM or pretreated with BAPTA-AM at 1 µM, 3 µM or 10 µM for 30 minutes before addition of 75 µM cDDP for 24 hours before assay. For Ca^{2+} chelation experiments with EGTA, A549-WT cells were incubated in normal cell culture medium + 1.4

mM EGTA or in normal cell culture medium + 1.4 mM EGTA + 75 µM cDDP for 24 hours before assay. For cell viability experiments with 2-APB, A549-WT cells were incubated in normal cell culture medium + 10 µM 2-APB or pretreated with + 10 µM 2-APB for 30 minutes before addition of 75 µM cDDP for 24 hours before assay.

Following the indicated cell treatment periods, culture medium was collected from each well in which cell viability was to be assayed. Adherent cells were removed by partial digestion with trypsin, resuspended in normal cell culture medium and combined with the original culture medium. The resulting cell suspension was centrifuged at 500 G for 5 minutes and the cell pellet resuspended in PBS containing 5 µg/ ml Hoechst 33342 at a density of approximately 1 million cells/ ml. The cell suspensions were incubated at 37 ^{o}C for 10 minutes before storage on ice until the start of the assay. 1 µg/ ml PI was added to cell suspensions immediately before measurement. Fluorescence was measured using a CyAN ADP flow cytometer (Beckman-Coulter) using 405 nm and 488 nm excitation wavelengths. A minimum population size of 50,000 cells was assayed under each experimental condition. Data were analysed using Summit 4.3 software (Beckman-Coulter) using threshold PI fluorescence set according to non-treated control A549-WT and A549-CR cells to discriminate between live ('low PI') and dead ('PI positive') cells.

2.5 Timelapse Imaging of A549 Cell Morphology

A549 cells were cultured in 24 well cell culture plates (Falcon) for 24 hours. Prior to imaging, cells were incubated in normal cell culture medium + 5 µg/ ml Hoechst 33342 for 15 minutes at 37 ^{o}C, washed twice with PBS and returned to normal cell culture medium in a custom built heated imaging chamber at 37 ^{o}C perfused with 5% CO_2. Image acquisition occurred every 20 minutes with excitation illumination provided by light from a metal halide arc lamp passing through a Chroma D-350/50x excitation filter (Chroma Technology). After 1 hour of image acquisition, 75 µM cDDP was added to the appropriate wells, and images acquired for a further 24 hours. A minimum of 10 individual image fields of at least 20 cells were studied under each experimental condition in each individual experiment. Cell divisions were counted manually according to the morphological criteria outlined in Figure 6 A. Divisions were judged to have been successfully completed once both daughter cells

generated by the division returned to a morphology indistinguishable from surrounding cells which were not undergoing division or cell death.

2.6 Aequorin Measurements

A549-WT and A549-CR cells seeded onto 22 mm diameter glass coverslips and transiently transfected with cytoplasmic aequorin cDNA constructs (Chiesa et al., 2001) were incubated in KRB + 1 mM Ca^{2+} + 5 µM coelenterazine at 37 ^{o}C for 90 minutes before transfer to a thermostated perfusion chamber. Coverslips were maintained at 37 ^{o}C under continuous perfusion throughout the experimental procedure. A custom built luminometer was used to for measurement of bioluminescence (Cairn Research), and photon counts calibrated to [Ca^{2+}] according to Brini M. *et al* (Brini et al., 1995).

For ATP stimulation experiments, aequorin transfected cells were perfused with KRB + 1 mM Ca^{2+} + 100 µM ATP before the experiment was terminated by perfusion with KRB + 10 mM Ca^{2+} + 100 µM digitonin until no further photon count signal was detected.

For Ca^{2+} influx experiments, A549-WT and A549-CR cells transiently transfected with cytoplasmic aequorin were perfused with KRB + 1 mM Ca^{2+} for 60 s before the following changes in perfusate were made: (i) nominally 'Ca^{2+} free' KRB for 60-90 s; (ii) nominally 'Ca^{2+} free' KRB + 500 nM Tg for 40 s before perfusion was halted for approximately 300 s; (iii) KRB + 1 mM Ca^{2+} until the photon count signal returned to a stable value and (iv) KRB + 10 mM Ca^{2+} + 100 µM digitonin until no further photon count signal was detected.

2.7 IP_3R Stimulation Using Cell Permeable Caged IP_3

A549-WT and A549-CR cells were seeded onto 22 mm diameter glass coverslips 24 hours before imaging. Cells were incubated at room temperature in KRB + 1 mM Ca^{2+} + 1 µM cell permeable photolabile caged IP_3 (SiChem) for 45 minutes before the addition of 5 µM Fluo-4-AM to the buffer solution and incubation at room temperature for a further 20 minutes. Both the buffer solution and coverslips were protected from light during the entire period of

incubation at room temperature. After this incubation, coverslips were washed twice with KRB + 1 mM Ca^{2+} and imaged immediately.

Image acquisition occurred every 1 second, with excitation illumination provided by the 488 nm emission line of an argon laser, and emitted fluorescence collected above 505 nm using a long pass emission filter. Uncaging of IP_3 occurred after acquisition of the initial 5 images through 1 second of illumination of the entire image field with the 351 nm and 364 nm emission lines of a Coherent Enterprise UV laser at maximum output, and images acquired for a further 195 s. Fluorescence signals from individual cells were normalised to the mean fluorescence signal of the initial 5 images of that cell. The mean normalised fluorescence signal measured in A549-WT and A549-CR cells was divided by the mean normalised fluorescence signal measured in control A549-WT cells not subjected to the period of UV illumination was at corresponding time points to correct for the effects of Fluo-4 bleaching due to the imaging process.

2.8 Measurement of $[Ca^{2+}]_{cyt}$ and SOCE Using Fura-2

A549-WT and A549-CR cells were seeded onto 22 mm diameter glass coverslips 24 hours before measurement. Prior to imaging, cells were incubated in KRB + 1 mM Ca^{2+} + 1 μM Fura-2-AM at 37 ^{o}C for 20 minutes. Following incubation, coverslips were washed twice with KRB + 1 mM Ca^{2+}, transferred to nominally 'Ca^{2+} free' KRB and imaged immediately.

Image acquisition occurred every 10 s. Basal cytosolic Fura-2 fluorescence was measured for 120 s preceding the addition of 500 nM Tg, and images acquired for a further 300 s before the addition of 1 mM Ca^{2+} directly to the KRB bathing solution. Images were recorded until the fluorescence signal returned to a stable value. Control cells were imaged in nominally 'Ca^{2+} free' KRB for 420 s before the addition of 1 mM Ca^{2+} directly to the KRB bathing solution, and images acquired for a further 180 s. Background fluorescence was calculated from a region in each image not occupied by cells, and subtracted from each time point individually.

2.9 Western Blotting

For immunodetection of endogenous protein expression, A549-WT and A549-CR cells were cultured in 6-well tissue culture plates for 24 hours, before further incubation in either normal cell culture medium or normal cell culture medium + 75 μM cDDP for 24 hours prior to harvesting samples. For immunodetection of transient IP_3R overexpression, A549-WT transiently transfected with IP_3R-1 cDNA constructs were incubated in either normal cell culture medium or normal cell culture medium + 75 μM cDDP for 24 hours before harvesting samples. Control cells were cultured under the same conditions without transfection.

Cells were washed with PBS on ice and lysed directly in lysis buffer consisting of 4% SDS (w/v), 20% glycerol and 125 mM Tris-HCl, pH 6.8. Total cellular protein concentration was quantified using the Pierce BCA protein assay kit (G. E. Healthcare) according to the manufacturer's instructions, and 30 μg of sample protein diluted in loading buffer consisting of 1% SDS (w/v), 50% sucrose (w/v), bromophenol blue, 10% β-mercaptoethanol and 0.625 mM Tris-base, pH 6.6. Samples were separated by electrophoresis on NuPAGE 4-12% polyacrylamide gels (Invitrogen) and electroblotted onto PVDF membranes (Millipore). Membranes were incubated in PBS + 0.05% Tween-20 (PBST) + 5% fat-free milk or PBST + 5% bovine serum albumin (BSA) for 1 hour at room temperature before the addition of primary antibody.

Primary antibody specific for IP_3R-1 (rabbit anti-IP_3R-1 (Abcam)) was diluted 1:500 in PBST + 5% BSA and incubated with membranes overnight at 4 ^{o}C. Primary antibody specific for p53 (mouse-anti p53 DO-1 (Santa Cruz)) was diluted 1:1000 in PBST + 5% fat-free milk and incubated with membranes for 2 hours at room temperature. Primary antibody specific for β-actin (mouse anti-β-actin (Sigma-Aldrich)) was diluted 1:4000 in PBST + 5% fat-free milk and incubated with membranes for 2 hours at room temperature. MitoProfile® Total OXPHOS Human antibody cocktail (raised in mouse (MitoSciences)) was diluted 1:250 in PBST + 5% fat-free milk and incubated with membranes overnight at 4 ^{o}C.

For immunodetection of Akt, membranes were stained with Ponceau-S (Sigma Aldrich) and imaged immediately following electroblotting. Membranes were incubated in PBS + 0.05% Tween-20 (PBST) + 5% fat-free milk for 1 hour at room temperature, before incubation with primary antibody specific for Akt (rabbit anti-pan Akt (Cell Signalling)) or Ser473 phospho-

Akt (rabbit anti-Ser473 phospho Akt (Cell Signalling) diluted 1:1000 in PBST + 5% fat-free milk for 2 hours.

Membranes were incubated with goat anti-rabbit horseradish peroxidase conjugated secondary antibody (Thermo Scientific) diluted 1:4000 in PBST + 5% BSA or goat anti-mouse horseradish peroxidase conjugated secondary antibody (Thermo Scientific) 1:4000 in PBST + 5% fat-free milk, as appropriate, for 1 hour at room temperature, and visualised using the ECL Plus Western Blotting Detection System (G. E. Healthcare). Quantification of protein band intensity was performed using ImageJ software.

2.10 Oxidative Stress Induced by TMRM Photoactivation

A549-WT and A549-CR cells were seeded onto 22 mm diameter glass coverslips 24 hours before measurement. Cells were incubated in KRB + 1 mM Ca^{2+} + 200 nM TMRM for 20 minutes at 37 ^{o}C. Where indicated, cells were further incubated in either KRB + 1 mM Ca^{2+} + 200 nM TMRM + 1mM ascorbic acid, KRB + 1 mM Ca^{2+} + 200 nM TMRM + 1 μM CsA or KRB + 1 mM Ca^{2+} + 200 nM TMRM + 10 μM CsA for 30 minutes before imaging, or further incubated in nominally 'Ca^{2+} free' KRB + 500 nM Tg + 2 mM EGTA or nominally 'Ca^{2+} free' KRB + 1 μM BAPTA-AM + 2 mM EGTA for 20 minutes before imaging. All drugs added were present throughout the entire experimental protocol.

Image acquisition occurred every 1 second using a confocal microscope, with excitation illumination provided by the 543 nm emission line of a helium/ neon laser at 10% of maximal output. Fluorescence emission was collected at wavelengths above 560 nm using a long pass emission filter. Data were analysed using Zeiss LSM 510 software. Briefly, after applying an intensity threshold to remove background fluorescence, the mean fluorescence intensity of the illuminated field of cells was calculated for each frame of the image series, and normalised relative to the initial mean fluorescence of the illuminated field. Statistical significance was assessed through comparison of the mean normalised fluorescence intensity of the final 5 frames of the image series using a paired Student's t-test.

2.11 $[Ca^{2+}]_{ER}$ Measurements Using Recombinant D1ER Cameleon Probe

A549-WT and A549-CR cells seeded onto 22 mm diameter glass coverslips and transiently transfected with D1ER cameleon cDNA constructs were incubated in normal cell culture medium or normal cell culture medium + 75 μM cDDP for 24 hours at 37 ^{o}C before measurement. Images were acquired using a confocal microscope. The D1ER probe contains two recombinant fluorophores, cyan fluorescent protein (CFP) and yellow fluorescent protein (YFP) (Palmer, Jin, Reed, & Tsien, 2004). Control A549-WT cells were incubated in KRB + 500 nM Tg + 1.4 mM EGTA for 10 minutes to deplete ER store Ca^{2+} before measurement. Excitation illumination was provided by the 405 nm emission of a laser diode, and fluorescence emission collected between 456 nm and 756 nm using the Zeiss Meta detector. Linear unmixing was used to separate CFP and YFP emission, and images were analysed using Zeiss LSM 510 4.0 software. The proportion of probe in the Ca^{2+} bound form undergoing Förster resonance energy transfer (FRET) was estimated using the acceptor photobleaching method (Karpova et al., 2003). Five sequential images of transfected cells were acquired prior to and immediately following a 40 iteration period of YFP photobleaching using the 488 nm and 514 nm emission lines of an argon laser at maximum output. The fluorescence emission intensities of CFP and YFP were determined in the single images immediately preceding and immediately following the period of photobleaching, and used to determine the percentage change in CFP fluorescence emission intensity and YFP fluorescence emission intensity due to the photobleaching process. Changes are expressed as 'FRET Ratio', calculated thus:

'FRET Ratio' = Percentage Increase in CFP Intensity / Percentage Decrease in YFP Intensity

2.12 Measurement of $[Ca^{2+}]_{cyt}$ After cDDP Treatment Using Fura-2

A549-WT and A549-CR cells were cultured in 24 well tissue culture plates for 24 hours before imaging. Excitation illumination was provided by light from a metal halide arc lamp passing through a Chroma D340xV2 excitation filter (Chroma Technology) or a Chroma D380xV2 excitation filter (Chroma Technology), and images acquired every 150 s in all experiments. Background fluorescence at 340 nm and 380 nm excitation was determined using regions not occupied by cells in each field of view, and subtracted individually from

Fura-2 340 nm and 380 nm fluorescence signals respectively, before the background-corrected 340 nm : 380 nm Fura-2 fluorescence ratio was calculated. Data were normalised relative to the initial 340 nm : 380 nm Fura-2 fluorescence ratio in non-treated A549-WT cells.

For acute measurement of $[Ca^{2+}]_{cyt}$ up to 60 minutes after cDDP exposure, A549 cells were incubated in KRB + 1 mM Ca^{2+} + 1 µM Fura-2-AM + 1 mM probenecid for 15 minutes at 37 ^{o}C, washed twice with KRB + 1 mM Ca^{2+} and imaged immediately. For treatment with 2-APB, cells were further incubated in KRB + 10 µM 2-APB + 1 mM probenecid for 15 minutes at 37 ^{o}C before imaging. Following 10 minutes of image acquisition to determine baseline Fura-2 fluorescence, 75 µM cDDP was added directly to the appropriate samples, and data acquired for a further 60 minutes. Data was acquired at the same time point for each test condition from cells in adjacent wells of the tissue culture plate loaded simultaneously with Fura-2-AM. Statistical significance was assessed through comparison of the background-corrected 340 nm : 380 nm Fura-2 fluorescence ratio of the final 10 frames of the image series using a paired Student's t-test.

For measurement of $[Ca^{2+}]_{cyt}$ 24 hours after cDDP exposure, A549-WT and A549-CR cells were incubated in normal cell culture medium or normal cell culture medium + 75 µM cDDP for 24 hours at 37 ^{o}C, before 1 µM Fura-2-AM + 1 mM probenecid was added directly to the cell culture medium and incubated for 15 minutes at 37 ^{o}C. After incubation, cells were washed twice with KRB + 1 mM Ca^{2+} and imaged immediately. Images were acquired for 10 minutes. Values for R_{min} and R_{max} were determined separately for A549-WT and A549-CR cells immediately following acquisition of experimental data using A59 cells cultured and loaded with Fura-2 in adjacent wells of the same tissue culture plate. R_{min} was determined by incubation of cells in nominally 'Ca^{2+} free' KRB + 1 mM EGTA + 1 µM ionomycin, and R_{max} by incubation of cells in KRB + 10 mM Ca^{2+} + 1 µM ionomycin. Ca^{2+} concentrations were calculated from background-corrected Fura-2 fluorescence ratios using the following equation:

$$[Ca^{2+}] = K_d * (R - R_{min}) / (R_{max} - R) * S_{f2} / S_{b2}$$

Where the dissociation constant for Fura-2 binding of Ca^{2+} K_d = 225 nM, R = background-corrected Fura-2 fluorescence ratio, R_{min} = background-corrected Fura-2 fluorescence ratio in the absence of Ca^{2+}, R_{max} = background-corrected Fura-2 fluorescence ratio under saturating

Ca^{2+} binding conditions, S_{f2} = background-corrected Fura-2 380 nm fluorescence signal in the absence of Ca^{2+} and S_{b2} = background-corrected Fura-2 380 nm fluorescence signal under saturating Ca^{2+} binding conditions.

2.13 mtDNA Copy Number Quantification by RT-qPCR

A549-WT and A549-CR cells were cultured in 6 well tissue culture plates for 24 hours in normal cell culture medium or normal cell culture medium + 75 μM cDDP, before isolation of the total cellular DNA content. Cells were lysed directly in culture plates and solutions of total cellular DNA were made from individual wells of the culture plate using the DNeasy Blood and Tissue Kit (Qiagen). Quantification of mtDNA copy number in isolated DNA preparations was made by RT-qPCR with the Dynamo SYBR Green qPCR Kit (New England Biolabs). The primer set used for mtDNA amplification was 5′-CCTGACTCCTACCCCTCACA-3′ and 5′-ATCGGGTGATGATAGCCAAG-3′, and the primer set used for β-actin amplification was 5′- TCACCCACACTGTGCCCATCTACGA-3′ and 5′-CAGCGGAACCGCTCATTGCCAATGG-3′. RT-qPCR was performed using a Mastercycler ep Realplex RT-qPCR system (Eppendorf) through 40 cycles of 95 ^{o}C for 15 s, 56 ^{o}C for 15 s and 72 ^{o}C for 20 s. Quantification was made via a standard curve. β-actin was used as a nuclear gene standard, and mtDNA copy number expressed normalised to the β-actin content of that sample.

2.14 Measurement of Cellular H_20_2 and $O_2^{\bullet-}$ Production

A549-WT and A549-CR cells were cultured in 24 well tissue culture plates for 24 hours in normal cell culture medium or normal cell culture medium + 75 μM cDDP before measurement.

For measurement of cellular H_20_2 production, cells were washed twice with PBS and incubated in PBS + 5 mM glucose + 2 μM 5-(and 6)-chloromethyl-2′,7′-dichlorohydrofluorescein diacetate (DCF) for 40 minutes. Fluorescence emission was measured at 520 nm under 495 nm excitation illumination every 2 minutes during the 40 minute incubation period. The rate of change in fluorescence intensity was calculated using

time points between 10 minutes and 30 minutes following DCF addition in which the rate of change in fluorescence remained linear. Background fluorescence was measured in control A549-WT and A549-CR cells without DCF loading and subtracted from experimental values before calculation of rate of change of fluorescence.

For measurement of cytosolic $O_2^{\bullet -}$ production, cells were incubated in normal cell culture medium + 0.5 µM dihydroethidium (DHE) for 20 minutes at 37 ^{o}C, washed twice with PBS and fluorescence emission at 635 nm under 535 nm excitation illumination recorded using a microplate reader. Background fluorescence was measured in control A549-WT and A549-CR cells without DHE loading and subtracted from experimental values before calculation of mean fluorescence.

For measurement of mitochondrial $O_2^{\bullet -}$ production, cells were incubated in PBS + 1 g/ l glucose + 5 µM MitoSOX for 10 minutes at 37 ^{o}C, washed twice with PBS and fluorescence emission at 595 nm under 510 nm excitation illumination recorded using a microplate reader. Background fluorescence was measured in control A549-WT and A549-CR cells without MitoSox loading and subtracted from experimental values before calculation of mean fluorescence. Performed by Dr. M. Wieckowski.

2.15 Measurement of Cellular GSH

A549-WT and A549-CR cells were cultured in 24 well tissue culture plates for 24 hours in normal cell culture medium or normal cell culture medium + 75 µM cDDP before imaging. Cells were incubated in KRB + 1 mM Ca^{2+} + 50 µM monocholorobimane (MCB) for 1 hour and images taken immediately. Control A549-WT cells were incubated in KRB + 50 mM diethylmaleate (DEM) for 15 minutes prior to MCB loading. MCB loading time was determined empirically by measuring MCB fluorescence in A549-WT cells and A549-CR cells during the dye loading period, the point at which no further change in fluorescence was detected representing the point of GSH saturation. Excitation illumination was provided by light from a metal halide arc lamp passing through a Chroma D-350/50x excitation filter (Chroma Technology). Ten images containing a minimum of twenty cells per image field were collected under each individual condition, and mean MCB fluorescence calculated using

MetaMorph 6.1 software (Molecular Devices). Fluorescence intensities were normalised relative to non-treated A549-WT cells.

2.16 Measurement of ΔΨ

A549-WT and A549-CR cells were cultured in 6 well tissue culture plates for 24 hours in normal cell culture medium or normal cell culture medium + 75 μM cDDP before imaging. Cells were incubated in KRB + 1 mM Ca^{2+} + 10 nM TMRM for 20 minutes at 37 ^{o}C and images taken immediately. Serial z-sections were acquired throughout the image field using a Zeiss LSM 510 confocal microscope. Excitation illumination was provided by the 543 nm emission line of a helium/ neon laser, and fluorescence emission was collected at wavelengths above 560 nm using a long pass emission filter. Mean TMRM fluorescence was calculated from at least ten images containing a minimum of twenty cells under each individual condition after maximal projection and thresholding of images to remove background fluorescence using MetaMorph 6.1 software. Fluorescence intensities were normalised relative to non-treated A549-WT cells.

2.17 Mitochondrial Respiratory Complex I Activity Assays

A549-WT cells, A549-CR cells and A549 Rho-0 were cultured in 6 well tissue culture plates for 24 hours in normal cell culture medium or normal cell culture medium prior to assay. Measurement of either rotenone-insensitive or rotenone-sensitive activity of mitochondrial respiratory complex I was made using two separate protocols.

For measurement of rotenone-insensitive complex I activity, enzyme activity was assessed using MitoSciences Microplate Assay for Human Complex I Activity (MitoSciences) according to the manufacturer's instructions. Proteins were extracted from the cell pellets by incubation in non-ionic lauryl maltoside detergent + protease inhibitors for 30 minutes on ice and centrifuged at 1600 g at 4 ^{o}C for 20 minutes. 200 μg of sample protein was loaded into each well of a microplate and incubated for 3 hours at room temperature for immunocapture of complex I. Microplate wells containting buffer without sample addition were used as controls to allow subtraction of background fluorescence. Following incubation, microplate

wells were rinsed with buffer solution, 200 µl assay solution added to each well and absorbance measured at 450 nm every minute for 30 minutes using a microplate reader. The linear rate of increase in absorbance at 450 nm after background subtraction was calculated for each sample, and data expressed as rate of change in absorbance at 450 nm per minute per µg loaded protein.

For measurement of rotenone-sensitive complex I activity, the oxidation of NADH to NAD^+ dependent upon passage of electrons through complex I to ubiquinone was monitored by spectrophometry before and after the addition of rotenone. Cells were harvested by manual scraping into phosphate buffer (25 mM KH_2PO_4 + 10 mM $MgCl_2$, pH 7.2), centrifuged at 500 g for 5 minutes and lysed through three sequential freeze-thaw cycles. Assays were performed at 30 ^oC in assay solutions consisting of: 20 µl sample solution + 800 µl phosphate buffer + 10 µl 100 mM KCN + 50 µl 50 mg/ ml BSA + 80 µl H_20. Absorbance was measured at 340 nm every 20 s for 5 minutes following addition of 10 µl 5mM ubiquinone. Assay solutions were mixed for 3 minutes upon addition of 20 µl 1 mM rotenone, and absorbance measured for a further 5 minutes. Complex I activity was calculated as: Activity (nmol $minute^{-1}$ ml^{-1}) = (Change in 340 nm absorbance $minute^{-1}$ before rotenone addition/ Change in 340 nm absorbance after rotenone $minute^{-1}$ addition) x 50 x 10^6 / 6.81 x 10^3 M^{-1} cm^{-1}. Total protein concentration in the assay solution was quantified immediately following measurement, using the Pierce BCA protein assay kit (G. E. Healthcare) according to the manufacturer's instructions, and activity normalised per µg protein. Performed by Dr. Z. Yao.

2.18 Measurement of Cellular O_2 Consumption

A549-WT and A549-CR cells were cultured in 6 well tissue culture plates for 24 hours in normal cell culture medium or normal cell culture medium + 75 µM cDDP. Before measurement cells were washed twice with PBS, and adherent cells were removed by partial digestion with trypsin and resuspended in recording medium (1.38 mM NaCl, 5.6 mM KCl, 4.2 mM $NaHCO_3$, 1.2 mM NaH_2PO_4, 1.2 mM $MgCl_2$, 2.6 mM $CaCl_2$, 10 mM D-glucose, 10 mM HEPES). O_2 consumption was measured using a Clark type electrode at 37 ^oC in a population of approximately one million cells. The maximal cellular oxidative capacity was measured after addition of 2 µM FCCP to uncouple the ETC. The assay solution was collected from the electrode chamber at the end of the experimental period, and the

concentration of cells estimated. O_2 consumption rates were normalised relative to the number of cells present during measurement. Performed by Dr. G. Szabadkai.

2.19 mtDNA Sequencing by GeneChip® Resequence Analysis

The GeneChip® Human Mitochondrial Resequencing Array 2.0 (Mitochip) (Affymetrix) was used to interrogate the entire mtDNA sequence. The 16.5kb mitochondrial genome was amplified in two fragments using the Expand Template Long PCR kit from Roche Diagnostics according to the manufacturer's protocol. PCR primers were Mito1-2F ACATAGCACATTACAGTCAAATCCCTT CTCGTCCC, Mito1-2R ATTGCTAGGGTGGCGCTTCCAATTAGGTGC-9307, Mito3F TCATTTTTATTGCCACAACTAACCTCCTCGGACTC and Mito3R CGTGATGTCTTATTTAAGGGGAACGTGTGGGCTAT-7814. Cycling conditions consisted of an initial denaturation step of 3 minutes at 94°C, followed by 10 cycles of denaturation for 10 seconds at 94°C, annealing for 30 seconds at 60°C and extension for 10 minutes at 8°C; then 25 cycles of denaturation for 10 seconds at 94°C, annealing for 30 seconds at 60°C and extension for 10 minutes + an additional 20 seconds per cycle at 68°C; and a final extension step of 10 minutes at 68°C. Concentration of DNA in the long PCR products was determined using Nanodrop spectrophotometry and equimolar concentrations of the two PCR products were pooled. Performed by Mary Sweeney. These were digested with DNAseI. Prehybridization, hybridization, washing and scanning of the GeneChip® were performed according to the Affymetrix CustomSeq Resequencing protocol. Sequences were analysed using GSEQ 4.2 software. SNPs were automatically called by GSEQ and presented in a SNP viewer format. Performed by Kerra Pearce.

2.20 mtDNA PCR and sequencing

Primer sets specific to the six regions of mtDNA identified by Mitochip sequencing as containing point mutations present in the A549-CR cell line but not the A549-WT cell line were used to amplify these regions through PCR. PCR reactions were performed in a final volume of 25 µl, using BioTaq DNA Polymerase (Bioline USA Inc., Boston, MA), as

follows: one cycle at 95°C for 2 minutes, followed by 30 cycles at 95 °C for 30 s, 50 °C for 30 s, and 72 °C for 40 s, and finally one cycle at 72 °C for 5 minutes. PCR products were purified by Microclean (Microzone Limited, Haywards Heath, UK), directly sequenced using the Big Dye v3.1 Terminator System and analysed on an automated sequencer (ABI 3130, Applied Biosystems, Carlsbad, CA). Sequence data were analyzed using Sequencher (version 4.8) and sequences were compared with the human mtDNA consensus sequence, NCBI reference sequence: NC_012920.1. Performed by the group of Dr. S. Rahman.

3.1 Characterisation of cDDP-Induced Cell Death in A549 Cells

3.1.1 A549-CR Cells Have Reduced Sensitivity to cDDP Treatment

To investigate extranuclear effects which may modulate tumour cell sensitivity to cDDP, an *in vitro* model of acquired cDDP resistance was employed. A drug-resistant cell line was derived through one year of continuous culture of the parental, cisplatin-sensitive A549-WT cell line in the presense of 5 μM cDDP, generating the cDDP-resistant A549-CR cell line (Tajeddine, N., Unpublished). A549-WT and A549-CR cells were incubated in normal cell culture medium containing cDDP in the concentration range 0-100 μM for 24 hours. After this period of incubation, cell viability was assayed using the ability of live cells to exclude the plasma membrane-impermeant fluorescent dye PI. No significant increase in the percentage of PI stained cells in comparison with untreated control cells was caused by treatment with cDDP at concentrations up to and including 20 μM in either cell type (Figure 4). A significant increase in the percentage of PI positive A549-WT cells was observed using cDDP concentrations of 50 μM (46.4 ± 4.8% PI positive), 75 μM (50.0 ± 6.6% PI positive) or 100 μM (53.4 ± 6.6% PI positive), increasing more than 30% above the basal level in untreated control A549-WT cells (Figure 4). The percentage of PI positive A549-CR cells after treatment with 50 μM (19.0 ± 7.8% PI positive), 75 μM (25.0 ± 4.1% PI positive) or 100 μM (31.1 ± 5.1% PI positive) cDDP was approximately halved in comparison to A549-WT cells under the same conditions (Figure 4).

These data estimate the median lethal dose (LD_{50}) of cDDP in A549-WT cells after a 24 hour period of treatment to be 75 μM, and an approximately two-fold, statistically significant difference in cDDP sensitivity exists between A549-WT and A549-CR cells at this drug concentration ($p < 0.01$). For this reason, treatment of cells using 75 μM cDDP over a 24 hour period of exposure was selected for use in further investigations.

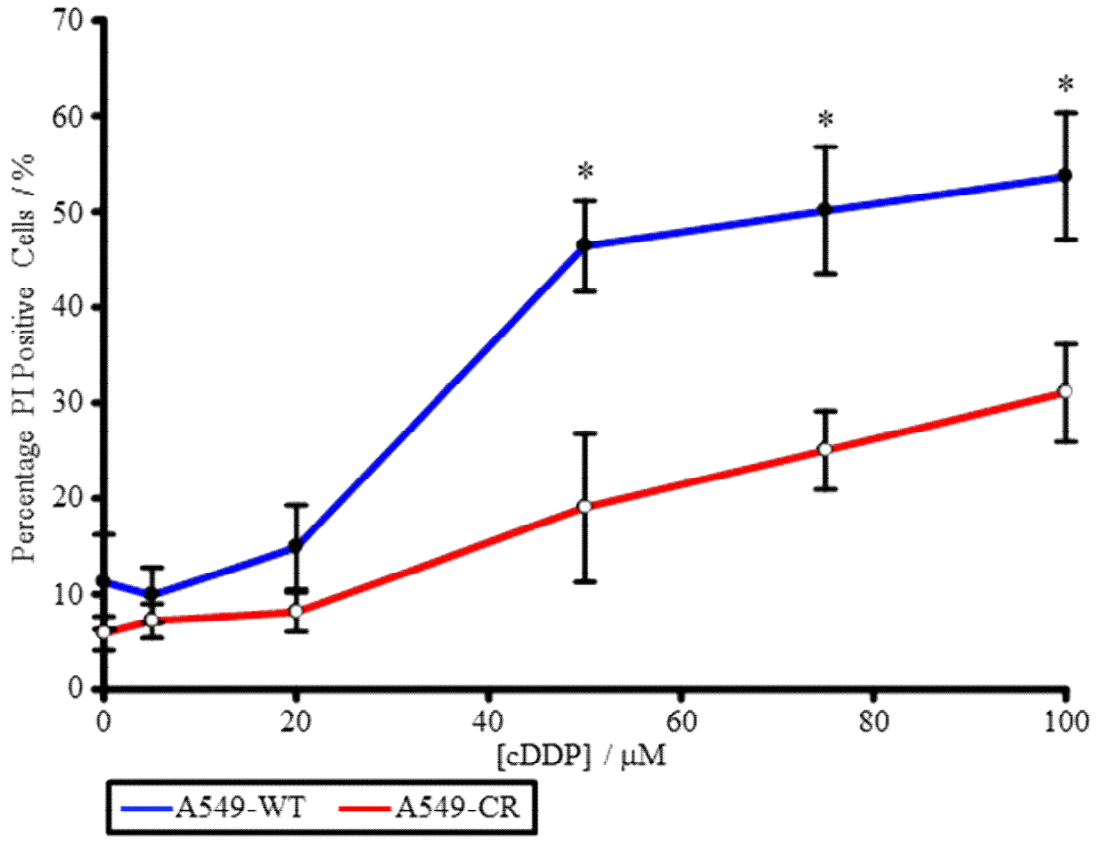

Figure 4: Cell death induced by 24 hours incubation with 75 µM cDDP is reduced in A549-CR cells relative to the A549-WT cell line. A549-WT cells and A549-CR cells were incubated in normal cell culture medium + cDDP in the concentration range 0 – 100 µM for 24 hours, and cytotoxicity assayed by PI exclusion as outlined in *'Methods 2.4'*. Data represent the mean of three independent experiments ± S.E.M. * $p < 0.05$.

3.1.2 cDDP Treatment Induces p53 Accumulation in Both A549-WT Cells and A549-CR Cells

Upon damage to DNA, activation and increased cellular levels of the tumour suppressor protein p53 may cause cell cycle arrest, activate DNA damage repair pathways and induce apoptosis. Since exposure to cDDP may result in both intra-strand and inter-strand DNA crosslinks, the relative induction of p53 was determined by western blot in A549-WT cells and A549-CR cells cultured either in normal cell culture medium or in normal cell culture medium + 75 µM cDDP for 24 hours (Figure 5 A). Treatment with cDDP increased cellular p53 protein levels by approximately seven-fold in A549-WT cells ($p < 0.05$) and nine-fold in A549-CR cells ($p < 0.05$), relative to non-treated A549-WT cells and non-treated A549-CR cells respectively (Figure 5 B). No significant difference existed in cellular p53 protein levels between A549-WT cells and A549-CR cells incubated in normal cell culture medium or following exposure to cDDP (Figure 5 B). Thus, cDDP treatment induced a comparable strong increase in p53 protein level in both A549-WT cells and A549-CR cells. However, whilst the absolute level of expression of p53 protein does not differ between A549-WT cells and A549-CR cells, differences in p53 transcription promoting activity may not be excluded by the present data, and should therefore be assessed using a suitable reporter gene assay, measuring induction of p53 target genes, or the enrichment of p53 at target promoters investigated via chromatin immunoprecipitation.

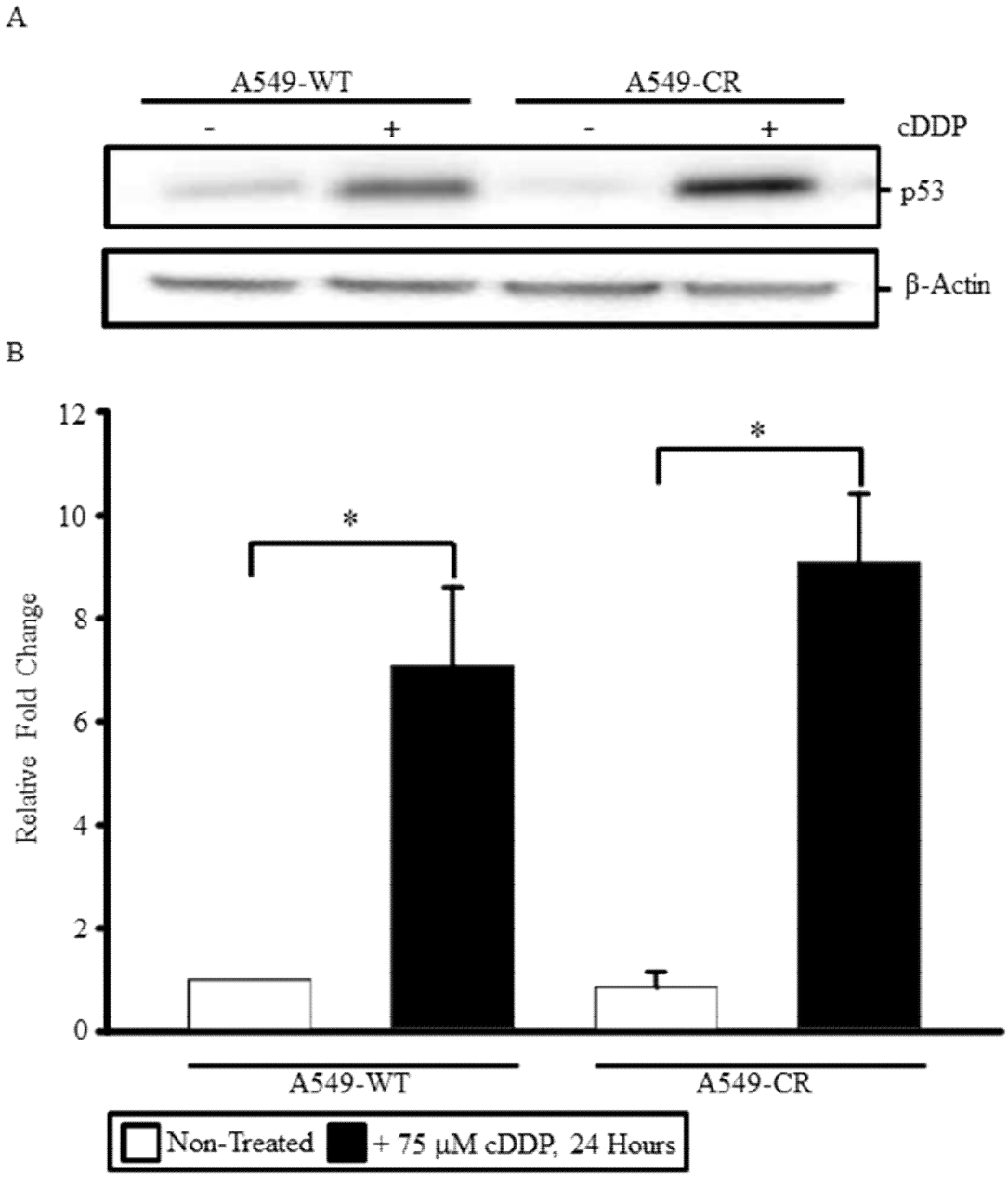

Figure 5: Exposure to cDDP causes comparable induction of p53 protein in both A549-WT cells and A549-CR cells. A549-WT cells and A549-CR cells were incubated in normal cell culture medium or normal cell culture medium + 75 µM cDDP for 24 hours, and cellular p53 protein levels measured by western blot. (A) Representative p53 western blot and (B) quantification of mean p53 band intensity. Data represents the mean of three independent experiments + S.E.M. * $p < 0.05$.

3.1.3 cDDP Inhibits Proliferation and Induces Apoptosis in A549 Cells

A549 cells treated with cDDP begin to lose plasma membrane integrity within 24 hours, as determined by PI staining. We next sought to characterise the mode of cell death induced by cDDP in this cell model. Since cell death is best defined through a set of morphological criteria (Kroemer et al., 2009), time-lapse images of A549 cells treated with 75 μM cDDP were made during the 24 hour treatment period. Few control cells of either cell type underwent morphological changes associated with cell death without cDDP treatment, indicating the imaging process itself does not cause toxicity (Figure 6 C). Incubation with cDDP induced clear morphological changes in A549-WT cells (Figure 6 D). The first morphologically altered cells appeared approximately 6 hours after drug addition, characterised by reduced cell size, a rounded cellular shape, irregular plasma membrane structure and concomitant nuclear condensation. Condensed nuclei fragmented as the cell death process continued (Figure 6 D Hoechst panel), and significant blebbing of the plasma became evident during the latter stages. Together this sequence of events is consistent with an apoptotic mode of cell death. Following 24 hours exposure to cDDP, the vast majority of A549-WT cells displayed morphological changes and abnormal nuclei. Incubation of A549-CR cells with cDDP induced morphological changes in a number of cells as described for A549-WT cells, again consistent with apoptotic cell death. These changes followed a similar time course, with the first morphologically altered cells appearing approximately 6 hours post drug addition. However, in contrast to the A549-WT cell line, most A549-CR cells did not undergo morphological changes in plasma membrane and nuclear structure during the cDDP treatment period (Figure 6 E), consistent with the cDDP resistant phenotype of this cell line. The marked decrease in Hoechst fluorescence intensity in cells not undergoing morphological changes is likely due to a combination of dye extrusion by live cells and bleaching of the fluorophore due to the imaging process (Figure 6 C, D & E).

During mitosis cells adopt a distinct morphology from both apoptotic cells and those cells not undergoing division (Figure 6 A and B). It is notable that whilst a number of cells were observed to divide up to approximately 7 hours after cDDP treatment, cell division ceased thereafter (Table 1). There was no statistically significant difference in the time at which the last successful cell division occurred after cDDP treatment between A549-WT and A549-CR cells. Dividing cells were observed throughout the 24 hour imaging period in untreated

control cells. Thus, treatment of cells with 75 μM cDDP inhibited cellular proliferation in both the A549-WT and A549-CR cell lines.

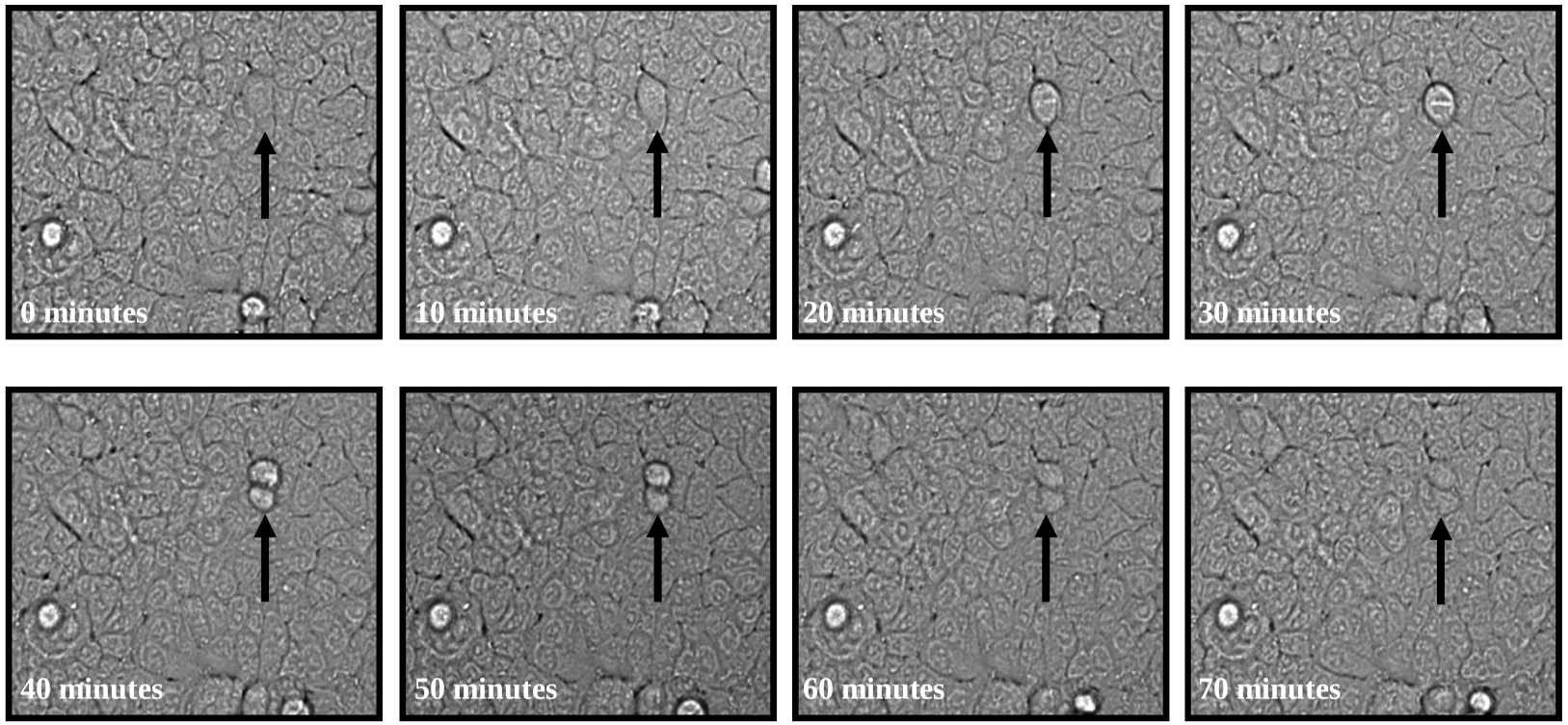

Figure 6 A: The morphology of cell division in A549 cells. A549 cells were prepared for timelapse imaging of cellular morphology as described in '*Methods 2.5*'. A representative cell undergoing morphological changes associated with division is marked by the black arrow. During mitosis A549 cells underwent changes in morphology distinct from the cell death process. Dividing cells adopted a bright, rounded plasma membrane morphology before cleavage to form two rounded daughter cells. The daughter cells further adopted an irregular plasma membrane morphology and became indistinguishable from surrounding cells not undergoing morphological changes. The process completed between 60 – 120 minutes.

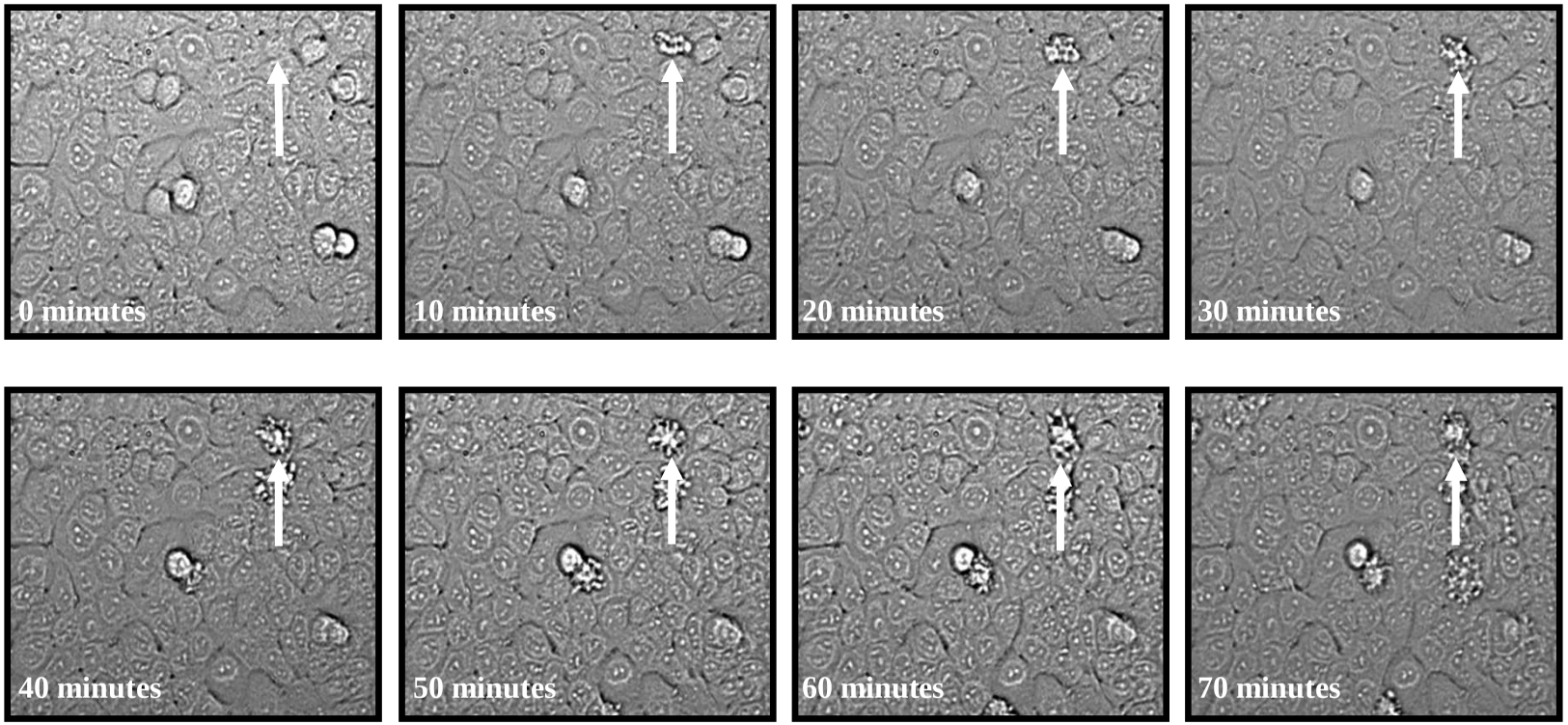

Figure 6 B: The morphology of cDDP-induced cell death in A549 cells. A549 cells were prepared for timelapse imaging of cellular morphology as described in '*Methods 2.5*'. A representative cell undergoing morphological changes associated with cell death following addition of 75 µM cDDP is marked by the white arrow. Dying A549 cells underwent changes in morphology distinct from the cell division process. Cells adopted a bright, irregular rounded plasma membrane morphology, smaller than cells undergoing division. Once changes in plasma membrane structure had begun, cells did not regain their original morphology, and persisted without further change throughout the experimental timecourse.

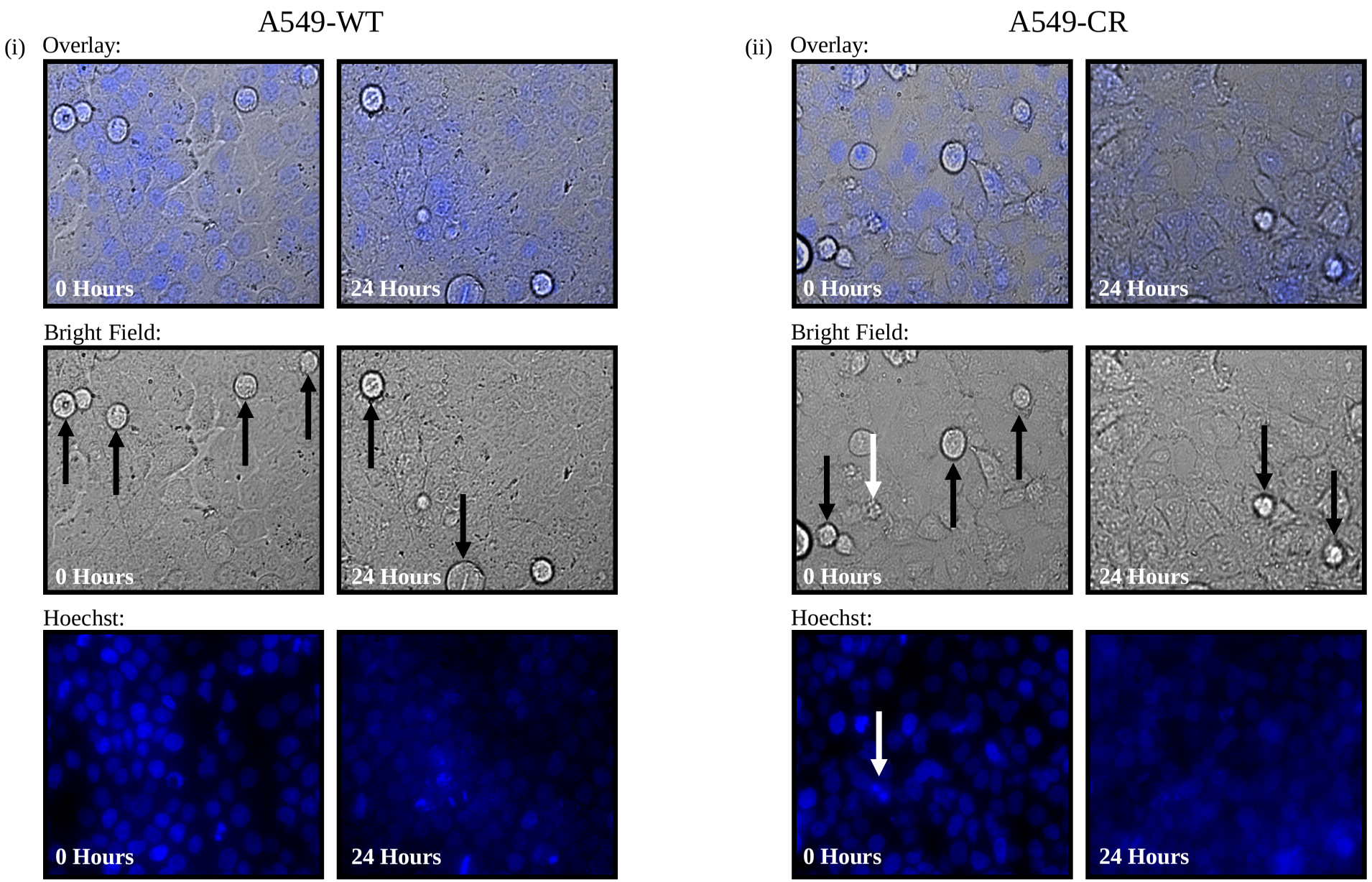

Figure 6 C: Under normal growth conditions cell death is uncommon in A549 cells. Figure legend continues p84.

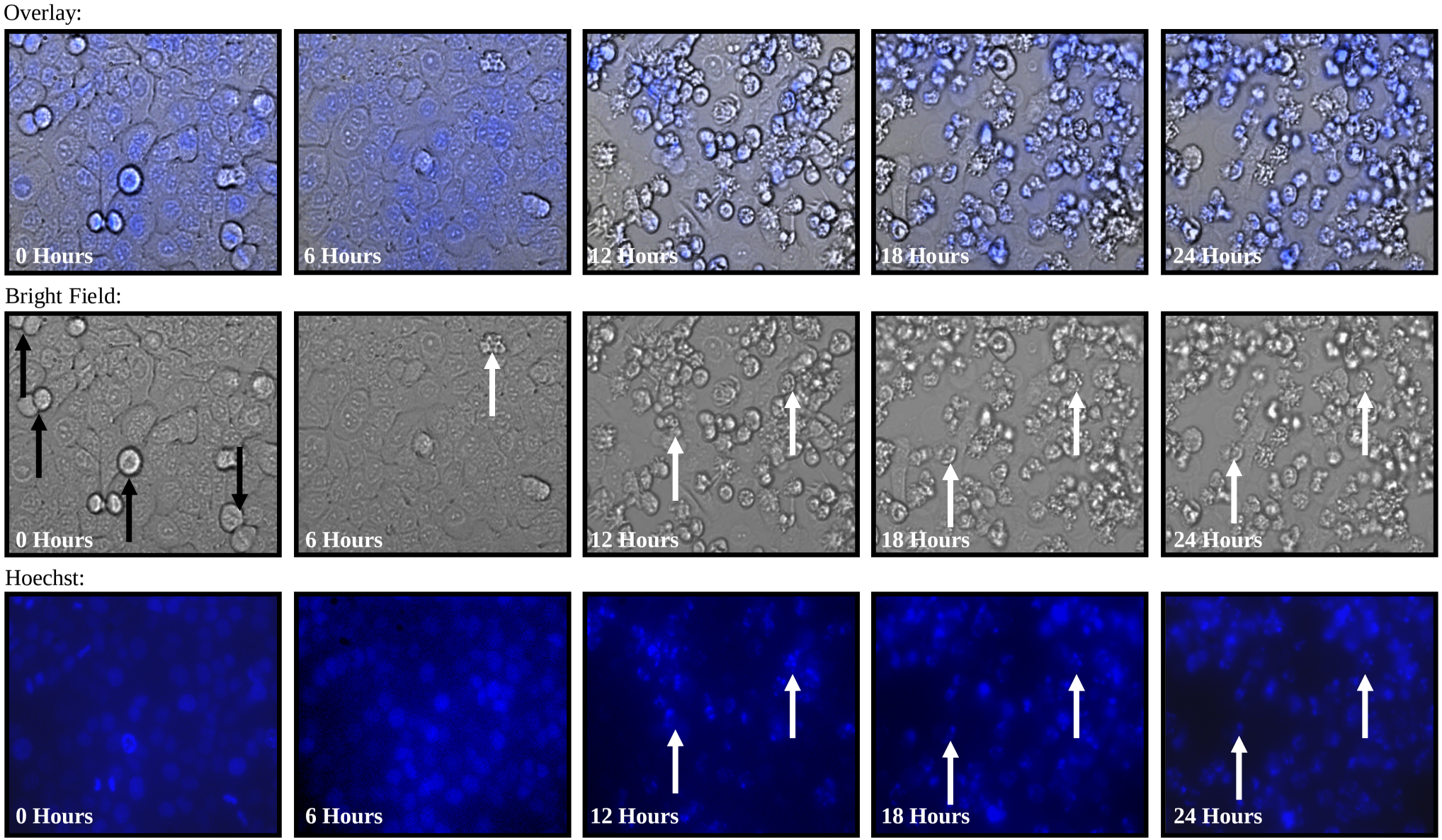

Figure 6 D: Exposure to cDDP induces apoptosis in A549-WT cells. Figure legend continues p84.

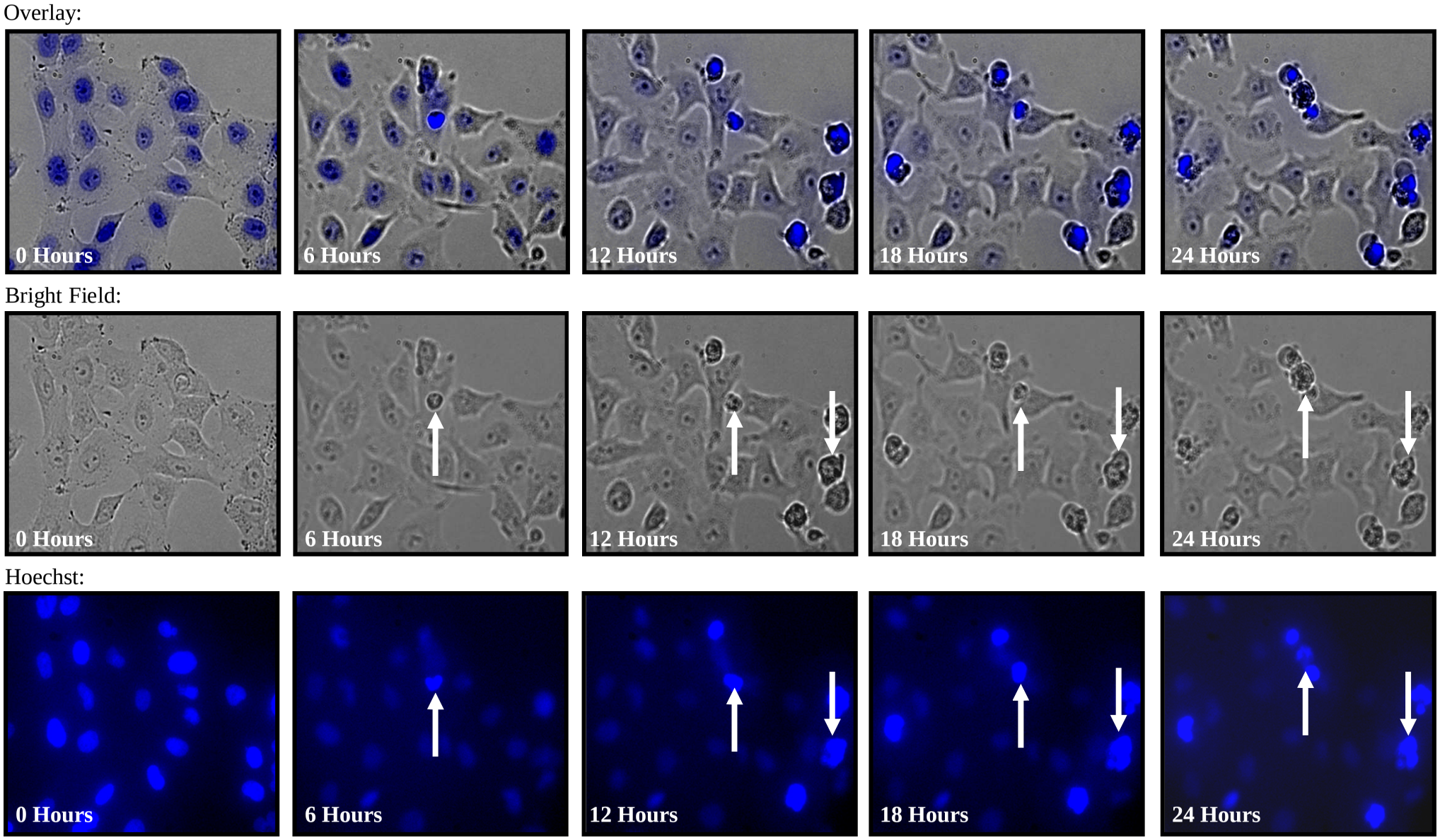

Figure 6 E: Exposure to cDDP induces apoptosis in A549-CR cells. Figure legend continues p84.

Figure 6 C: Under normal growth conditions cell death is uncommon in A549 cells. Dividing cells were commonly observed throughout the entire experimental period in both A549 cell lines incubated in normal growth medium (black arrows, Bright Field panel). Rarely, single cells adopted a small, rounded irregular plasma membrane morphology (white arrow, Bright Field panel) and condensed fragmented nuclear morphology (white arrow, Hoechst panel) characteristic of dying cells, whilst the majority of cells did not undergo morphological changes.

Figure 6 D: Exposure to cDDP induced apoptosis in A549-WT cells. A549-WT cells were prepared for time lapse imaging of cellular morphology as described in '*Methods 2.5*', and maintained in normal cell culture medium + 75 μM cDDP from the beginning of the imaging process. Morphology characteristic of cell division was observed at the start of the experimental time period before cDDP addition (black arrows mark representative cells, Bright Field panel, 0 hours). Cells adopting morphology associated with apoptosis first appeared approximately 6 hours post cDDP addition, characterised by reduced cell size, a rounded cellular shape and irregular plasma membrane structure (white arrows mark representative cells, Bright Field panel), with concomitant condensation and fragmentation of nuclei (white arrows mark representative cells, Hoechst panel). The majority of cells undergoing such morphological changes had begun to do so 12 hours post drug addition.

Figure 6 E: Exposure to cDDP induced apoptosis in A549-CR cells. A549-CR cells were prepared for time lapse imaging of cellular morphology as described in '*Methods 2.5*', and maintained in normal cell culture medium + 75 μM cDDP from the beginning of the imaging process. Cells adopting morphology associated with apoptosis first appeared approximately 6 hours post cDDP addition, characterised by reduced cell size, a rounded cellular shape and irregular plasma membrane structure (white arrows mark representative cells, Bright Field panel), with concomitant condensation and fragmentation of nuclei (white arrows mark representative cells, Hoechst panel). The majority of cells undergoing such morphological changes had begun to do so 12 hours post drug addition. The majority of cells did not undergo morphological changes during the experimental time period.

Table 1: cDDP treatment inhibits cell division in A549 cells. A549-WT and A549-CR cells were incubated in normal cell culture medium or normal cell culture medium + 75 µM cDDP in a heated imaging chamber, and images acquired throughout the 24 hour treatment period. Cell divisions were counted as outlined in *´Methods 2.5'*. There was no statistically significant difference between the time of the last successful cell division which occurred in A549-WT and A549-CR cells after cDDP addition.

	Mean Time Last Successful Cell Division Completed / minutes					
	Experiment 1	Experiment 2	Experiment 3	Mean / minutes	Standard Deviation	S.E.M.
A549-WT n = 10	1149	1440	1433	1436	166.1	95.9
A549-WT + cDDP n = 10	327	443	349	373	61.6	35.6
A549-CR n = 10	1055	1440	1435	1437	221.0	127.6
A549-CR + cDDP n = 10	341	482	458	427	75.4	43.6

3.1.4 Activation of Caspases, But Not Calpains, is Involved in cDDP Induced A549-WT Cell Death

Incubation of A549-WT cells with 75 µM cDDP leads to cell death with an apoptotic morphology. Apoptosis is mediated through the proteolytic activation of executioner caspases. The involvement of these proteases was confirmed by assessing the effect of the pan-caspase inhibitor z-VAD-FMK on cDDP induced cell death. Whilst the basal rate of cell death in control cells was unaffected by caspase inhibition, incubation of A549-WT cells with

75 μM cDDP + 20 μM z-VAD-FMK significantly decreased the percentage of PI positive cells measured after 24 hours cDDP exposure (33.3 ± 5.6% PI positive, $p < 0.05$) compared with A549-WT cells without caspase inhibition (52.8 ± 9.6% PI positive, $p < 0.05$) (Figure 7).

It has been suggested that activation of caspase-8 may be involved in mediating cDDP induced cell death (Lacour et al., 2004; Toyozumi et al., 2004). To determine whether caspase-8 activation contributed to cDDP induced cell death in this A549 cell model, A549-WT cells were incubated with caspase-8 inhibitor IETD-FMK during the cDDP treatment period. No significant difference in the percentage of PI positive cells was measured between A549-WT cells treated with both 2 μM IETD-FMK and 75 μM cDDP and A549-WT cells treated with 75 μM cDDP without caspase-8 inhibition (42.5 ± 1.23% PI positive vs. 40.3 ± 6.5% PI positive, respectively, $p < 0.05$**)** (Figure 8), suggesting caspase-8 is not required for cDDP-induced cell death in this model. IETD-FMK did not alter cell death in control A549-WT cells without exposure to cDDP.

Inhibition of caspases could not fully prevent cell death caused by cDDP. Calpain proteases are also capable of engaging the cell death pathway in a pro-apoptotic manner, and thus the effect of calpain inhibition using the pharmacological inhibitor ALLN was also studied. No significant difference in the percentage of PI positive cells was measured between A549 cells incubated in normal cell culture medium + 75 μM cDDP + 50 μM ALLN and control A549 cells treated with cDDP without calpain inhibition (Figure 9). Thus, under the present experimental conditions, calpain activation does not play a major role in cDDP induced cell death of A549-WT cells.

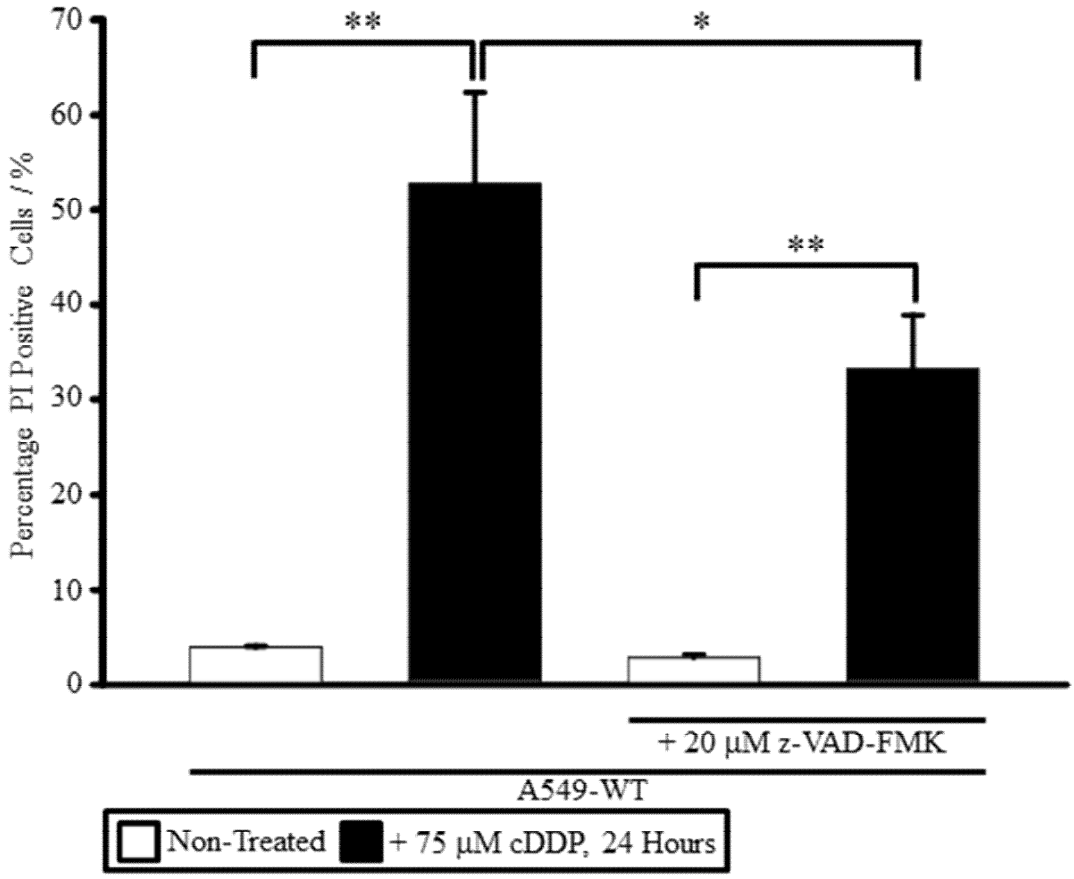

Figure 7: Pharmacological inhibition of caspases inhibits cDDP induced cell death in A549-WT cells. A549-WT cells were incubated in normal cell culture medium or normal cell culture medium + 75 µM cDDP in the absence or presence of 20 µM pan-caspase inhibitor z-VAD-FMK for 24 hours, and cytotoxicity assayed by PI exclusion as outlined in *'Methods 2.4'*. Data represent the mean of three independent experiments + S.E.M. * $p < 0.05$. ** $p < 0.01$.

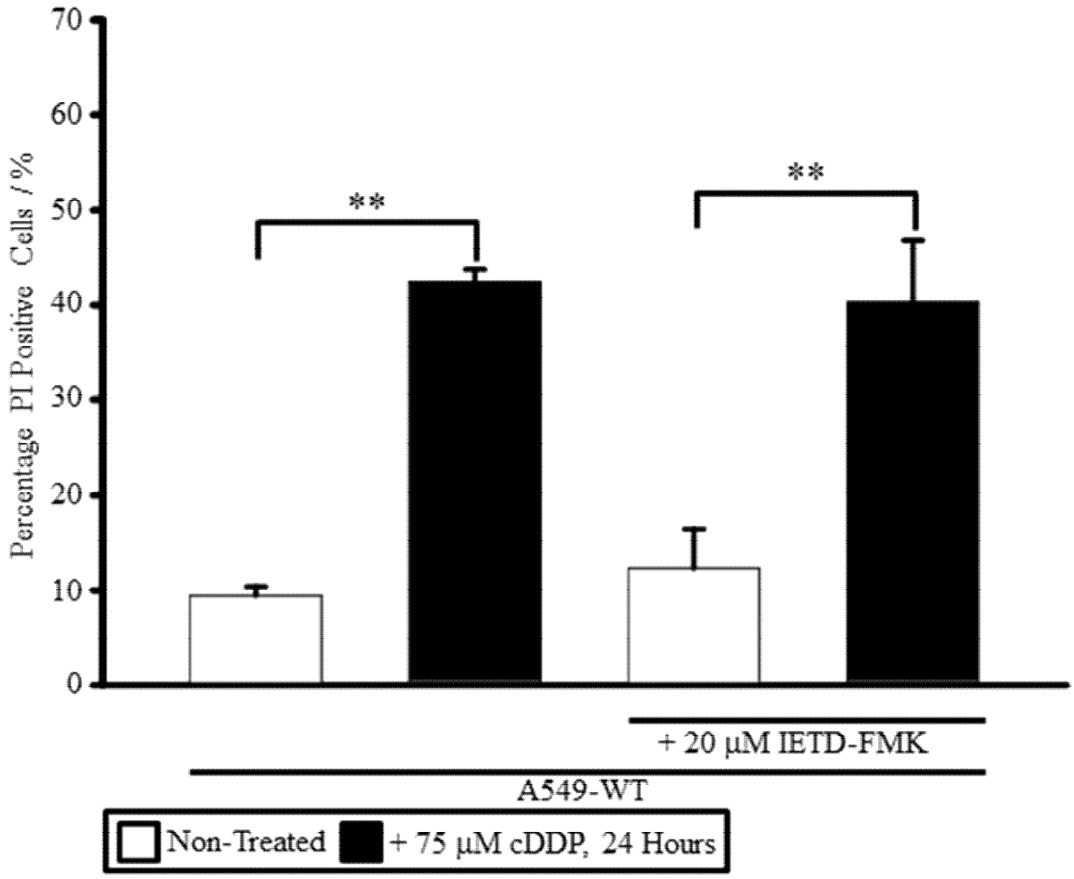

Figure 8: Pharmacological inhibition of caspase-8 does not inhibit cDDP induced cell death in A549-WT cells. A549-WT cells were incubated in normal cell culture medium or normal cell culture medium + 75 µM cDDP in the absence or presence of 2 µM caspase-8 inhibitor IETD-FMK for 24 hours, and cytotoxicity assayed by PI exclusion as outlined in *'Methods 2.4'*. Data represent the mean of three independent experiments + S.E.M. ** $p < 0.01$.

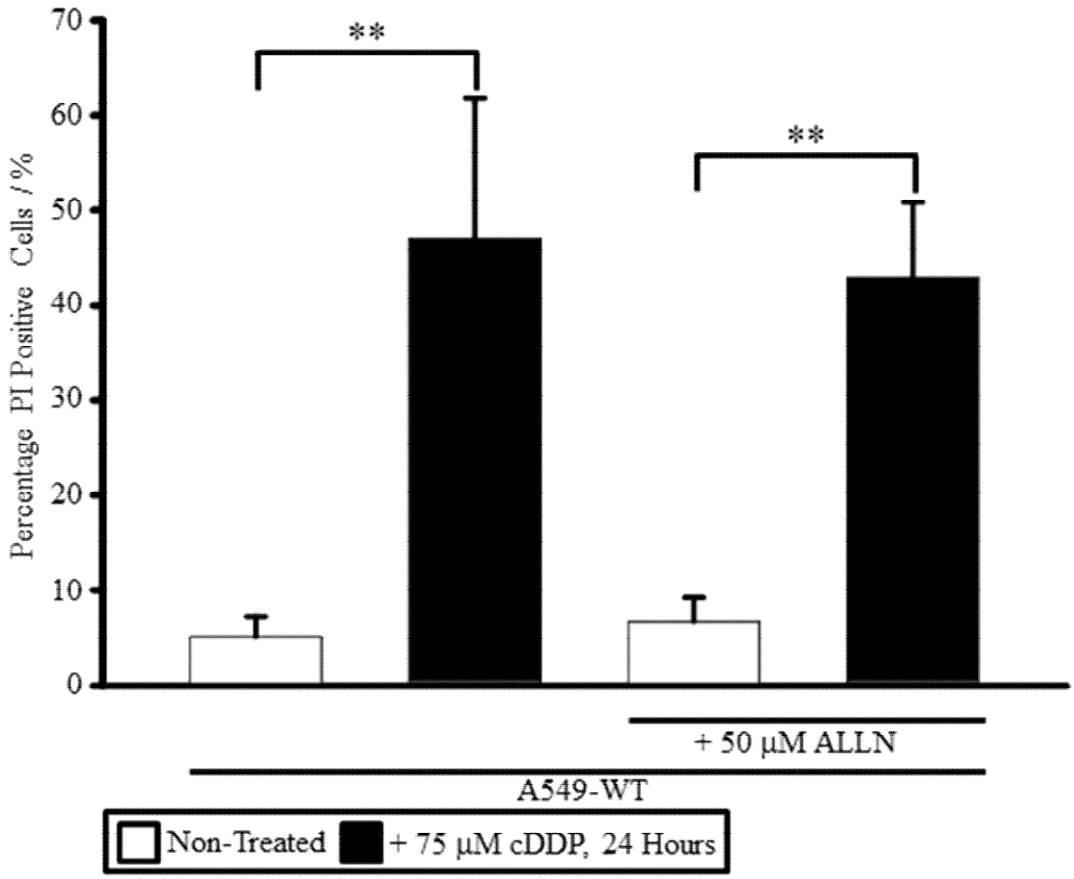

Figure 9: Pharmacological inhibition of calpains does not inhibit cDDP induced cell death in A549-WT cells. A549-WT cells were incubated in normal cell culture medium or normal cell culture medium + 75 µM cDDP in the absence or presence of 50 µM calpain inhibitor ALLN for 24 hours, and cytotoxicity assayed by PI exclusion as outlined in *'Methods 2.4'*. Data represent the mean of three independent experiments + S.E.M. ** $p < 0.01$.

3.1.5 CsA Does Not Prevent Cell Death in A549-WT Caused by cDDP

Opening of the mPTP is associated with necrotic cell death, and may mediate the cytotoxic effects of some chemotherapy drugs. Thus far, the only known component of the mPTP to be verified as playing a major role in opening of the pore is Cyp D. To determine whether necrotic cell death acting through mPT contributes to cDDP induced cell death in the present A549 cell model, A549-WT cells were incubated for 24 hours with 75 μM cDDP in the absence or presence of 5 μM CsA, an inhibitor Cyp D activity known to inhibit mPT (Griffiths & Halestrap, 1993). CsA treatment did not prevent loss of plasma membrane integrity in A549-WT cells caused by cDDP, but rather caused a significant increase in the percentage of PI positive cells measured after 24 hours exposure to 75 μM cDDP relative to A549-WT cells treated with 75 μM cDDP without CsA pre-treatment (73.2 ± 1.0% and 61.9 ± 0.6% respectively, $p < 0.05$) (Figure 10).

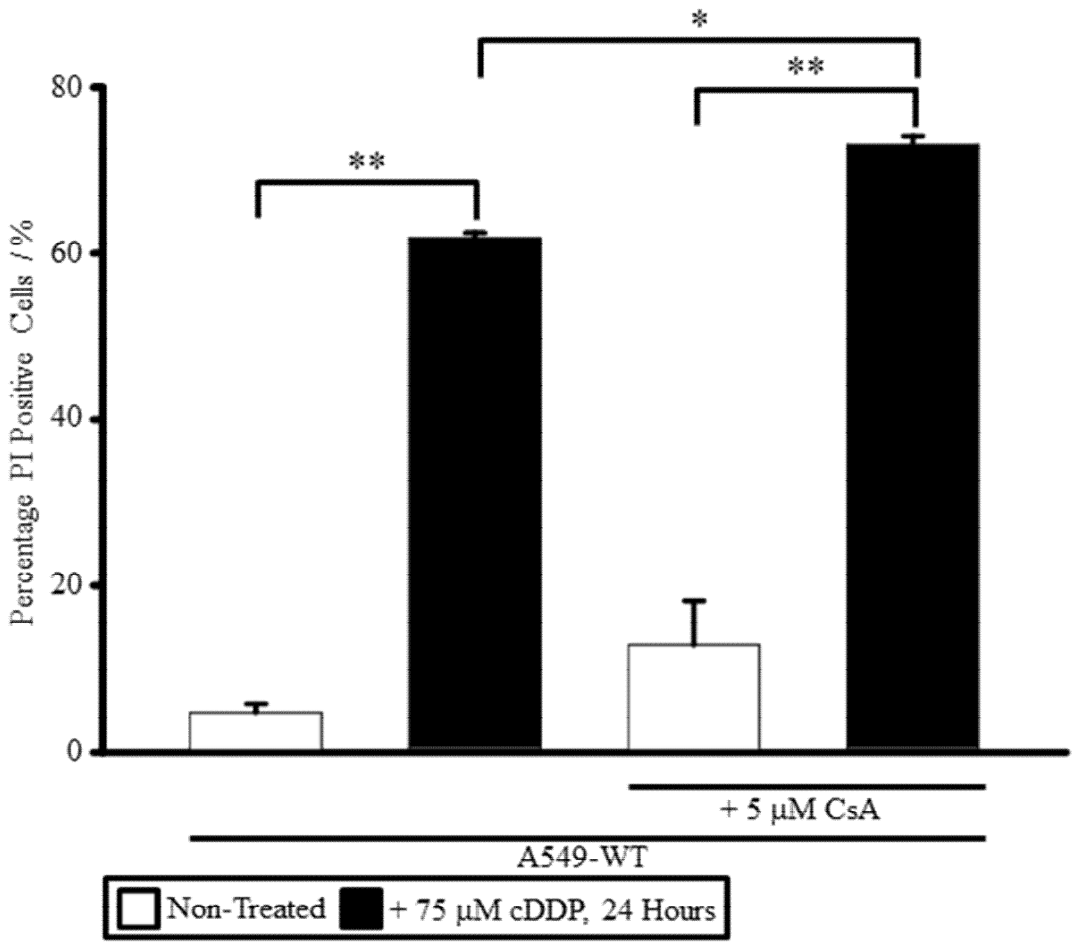

Figure 10: Pre-incubation of A549-WT cells with CsA increases cDDP induced cell death in A549-WT cells. A549-WT cells were incubated in normal cell culture medium or normal cell culture medium + 75 µM cDDP in the absence or presence of 5 µM CsA, an inhibitor of mPT, for 24 hours, and cytotoxicity assayed by PI exclusion as outlined in *'Methods 2.4'*. Data represent the mean of three independent experiments + S.E.M. * $p < 0.05$.

3.1.6 cDDP Induced ROS Production is Greater in A549-WT Cells Than in A549-CR Cells

It has been reported that cDDP treatment may cause an increase in the rate of intracellular ROS production, leading to cell death in a number of cell types (Brozovic, Ambriović-Ristov, & Osmak, 2010). Thus ROS production was measured in A549-WT cells and A549-CR cells using ROS sensitive fluorescent dyes to investigate whether incubation with cDDP altered the rate of ROS production in the present cell model. No significant difference was observed in the rate of increase in fluorescence of DCF between A549-WT cells and A549-CR cells incubated in normal cell culture medium, indicating a comparable rate of production of H_2O_2 (Figure 11). Following 24 hours incubation with 75 µM cDDP, a significant increase in the rate of change in fluorescence of DCF was observed in A549-WT cells relative to control A549-WT cells without cDDP exposure (0.46 ± 0.03 AU/ minute vs 0.90 ± 0.11 AU/ minute respectively, $p < 0.01$), however no significant change was observed in the rate of change of DCF fluorescence measured in A549-CR cells following the same cDDP treatment period, relative to control A549-CR cells without cDDP exposure (Figure 11).

ROS production was further investigated in both A549 cell lines using DHE and MitoSox to investigate cytoplasmic and mitochondrial $O_2^{\bullet -}$ production respectively. No significant difference in fluorescence intensity was measured in A549-WT cells and A549-CR cells loaded with DHE or MitoSox following incubation in normal cell culture medium. A significant increase in fluorescence intensity was observed in A549-WT cells incubated with 75 µM cDDP over 24 hours, relative to control A549-WT cells without cDDP exposure, in cells loaded with either DHE (122.0 ± 8.1 AU vs 75.1 ± 6.3 AU respectively, $p < 0.05$) (Figure 12) or MitoSox (68.5 ± 12.7 AU vs 7.9 ± 1.9 AU respectively, $p < 0.05$) (Figure 13). Similarly, fluorescence intensity measured in A549-WT cells incubated with 75 µM cDDP over 24 hours, relative to control A549-WT cells without cDDP exposure, in cells loaded with either DHE (83.0 ± 4.2 AU vs 58.9 ± 2.0 AU respectively, $p < 0.05$) (Figure 12) or MitoSox (27.2 ± 3.0 AU vs 10.3 ± 1.4 AU respectively, $p < 0.05$) (Figure 13). The change in flourescence intensity of DHE (Figure 12) and MitoSox (Figure 13) following cDDP exposure was significantly greater in A549-WT cells than in A549-CR cells.

Thus, prior to cDDP treatment, no significant difference in H_2O_2 or $O_2^{\bullet -}$ production exists between A549-WT cells and A549-CR cells. Incubation with cDDP induces a significant increase in H_2O_2 or $O_2^{\bullet -}$ production, however this effect is significantly more pronounced in A549-WT cells than in A549-CR cells.

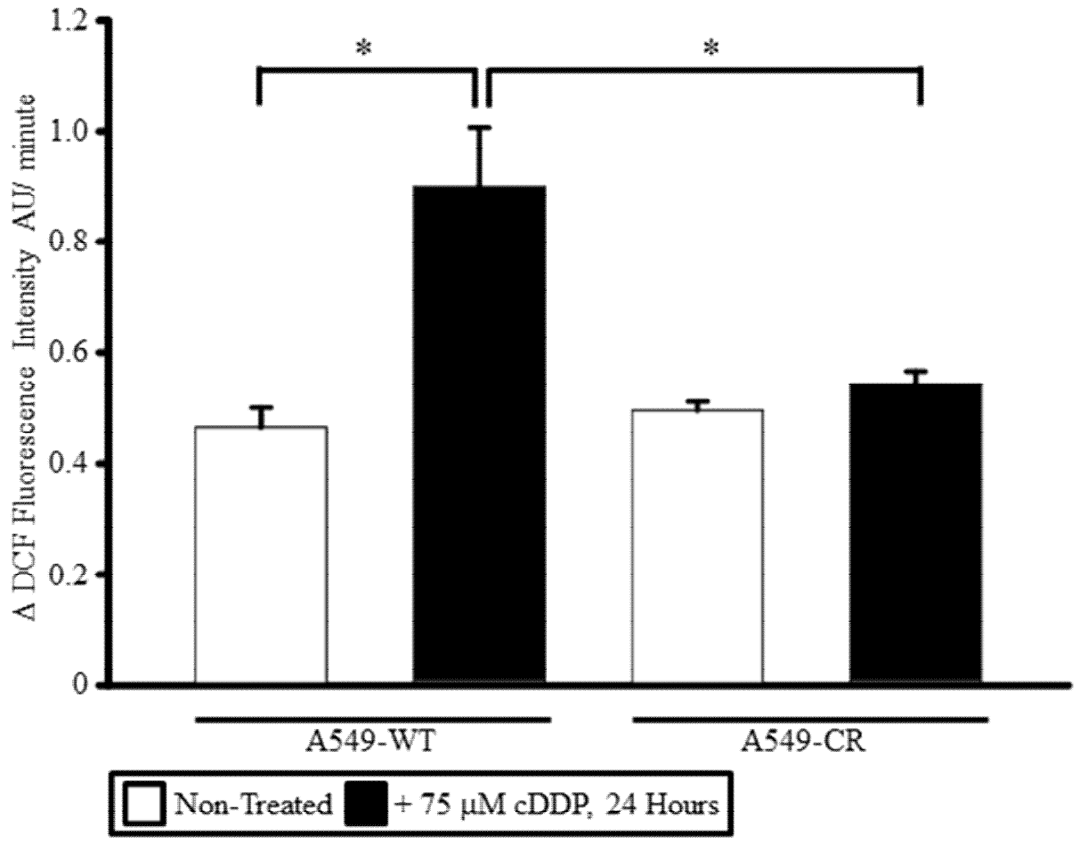

Figure 11: Exposure to cDDP increases the rate of H_20_2 production in A549-WT cells, but does not alter the rate of H_20_2 production in A549-CR cells. A549-WT cells and A549-CR cells were incubated in normal cell culture medium or normal cell culture medium + 75 µM cDDP for 24 hours, and the rate of H_20_2 production measured using a microplate reader as the rate of increase in DCF fluorescence in cells incubated in buffer solution containing 2 µM DCF over 40 minutes. Data represent the mean of three independent experiments + S.E.M. * $p < 0.05$.

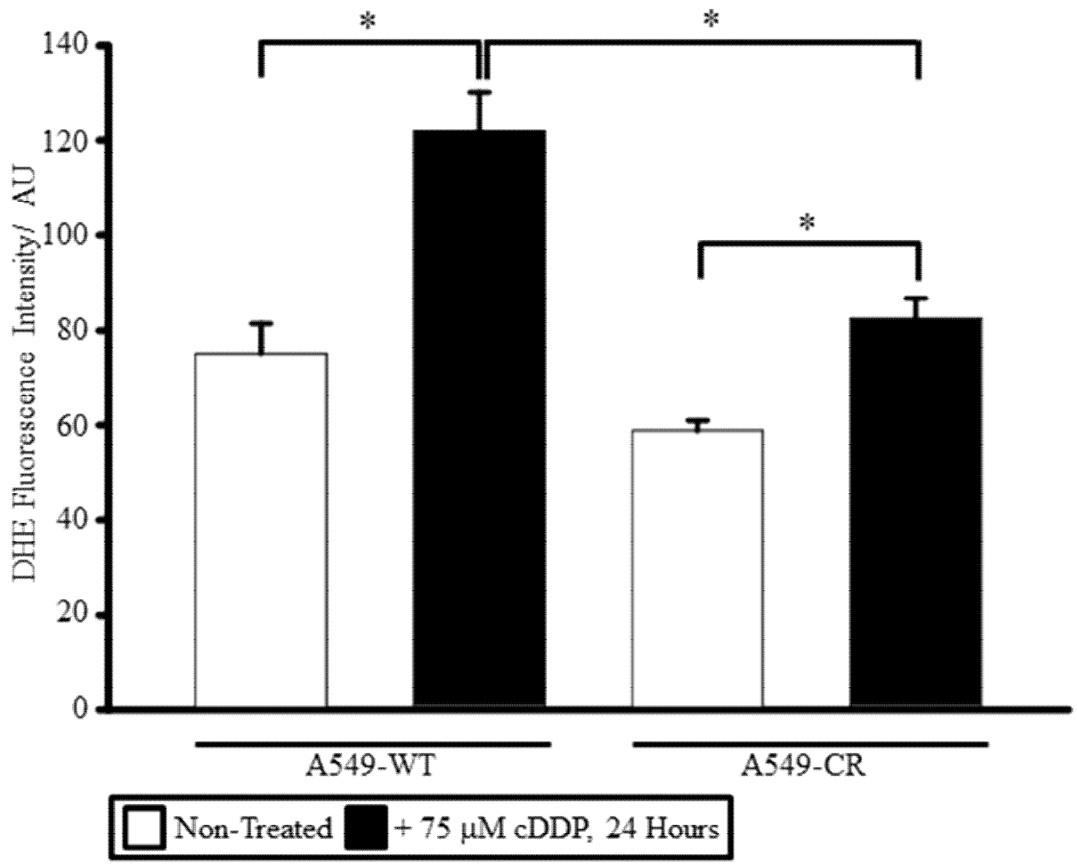

Figure 12: Exposure to cDDP increases cytosolic $O_2^{\bullet -}$ production in A549-WT cells, but does not alter cytosolic $O_2^{\bullet -}$ production in A549-CR cells. A549-WT cells and A549-CR cells were incubated in normal cell culture medium or normal cell culture medium + 75 µM cDDP for 24 hours, and cytosolic $O_2^{\bullet -}$ production measured using a microplate reader as the intensity of fluorescence in cells loaded with 0.5 µM DHE for 20 minutes following the incubation period. Data represent the mean of three independent experiments + S.E.M. * $p < 0.05$.

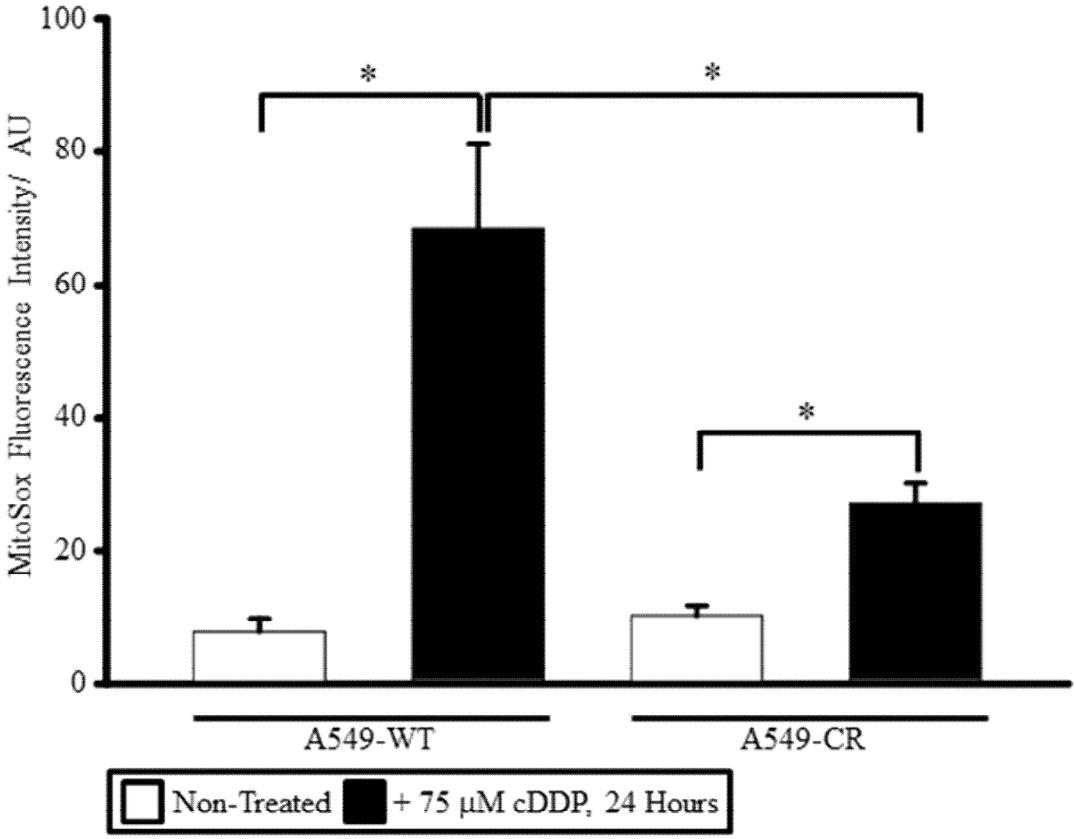

Figure 13: Exposure to cDDP increases mitochondrial $O_2^{\bullet-}$ production in A549-WT cells, but does not alter mitochondrial $O_2^{\bullet-}$ production in A549-CR cells. A549-WT cells and A549-CR cells were incubated in normal cell culture medium or normal cell culture medium + 75 µM cDDP for 24 hours, and mitochondrial $O_2^{\bullet-}$ production measured using a microplate reader as the intensity of fluorescence in cells loaded with 5 µM MitoSox for 10 minutes following the incubation period. Data represent the mean of three independent experiments + S.E.M. * $p < 0.05$.

3.1.7 Increased ROS Production is Not Required for A549-WT Cell Death Induced by cDDP

Whilst exposure to cDDP over a 24 hour treatment period caused an increase in the rate of ROS production in the cytosol and mitochondria of both A549-WT and A549-CR cells, the increase was markedly less pronounced in cDDP-resistant A549-CR cells. Given that increased ROS production may activate cell death pathways, these data suggested that changes in ROS production might play a role in promoting cell death induced by cDDP, thus the effect of incubation of A549-WT cells with antioxidants during the cDDP treatment period was investigated. Addition of 5 mM NAC almost completely abolished the increase in PI positive A549-WT cells measured after 24 hours exposure to 75 µM cDDP relative to control A549-WT cells treated with 75 µM cDDP without NAC (15.4 ± 2.8% and 45.16 ± 9.0% respectively, $p < 0.05$) (Figure 14). However, NAC contains a prominent thiol group, raising the possibility that this protective effect may have been due, at least in part, to a direct chemical interaction with cDDP. Incubation with NAC reduced DNA damage-induced phosphorylation of the H2AX histone subunit, suggesting a direct inhibition of DNA modification by cDDP (Appendix IV). Direct proof of direct interaction between NAC and cDDP would require the demonstration that incubation with NAC effectively prevents the formation of DNA platination by cDDP, which is not dependent upon ROS production. No significant difference was observed between the percentage of PI positive control A549-WT cells measured after 24 hours exposure to 75 µM cDDP and A549-WT cells exposed to 75 µM cDDP + 200 µM TEMPOL (Figure 15) or 75 µM cDDP + 1 mM ascorbic acid (Appendix I Figure 1), neither of which contain reactive thiol groups. It is notable that the dataset for the effect of TEMPOL on cDDP-induced cell death at present lacks a positive control, thus may not yet be properly interpreted. Treatment with cDDP causes an increase in cellular $O_2^{\bullet -}$ production in A549-WT cells (Figure 12), thus to exclude ROS production as a factor contributing to cell death in the present experimental system, the ability of TEMPOL to prevent changes in $O_2^{\bullet -}$ generation following cDDP treatment must also be demonstrated. Increased ROS production therefore does not appear to be required for cDDP induced cell death in A549-WT cells.

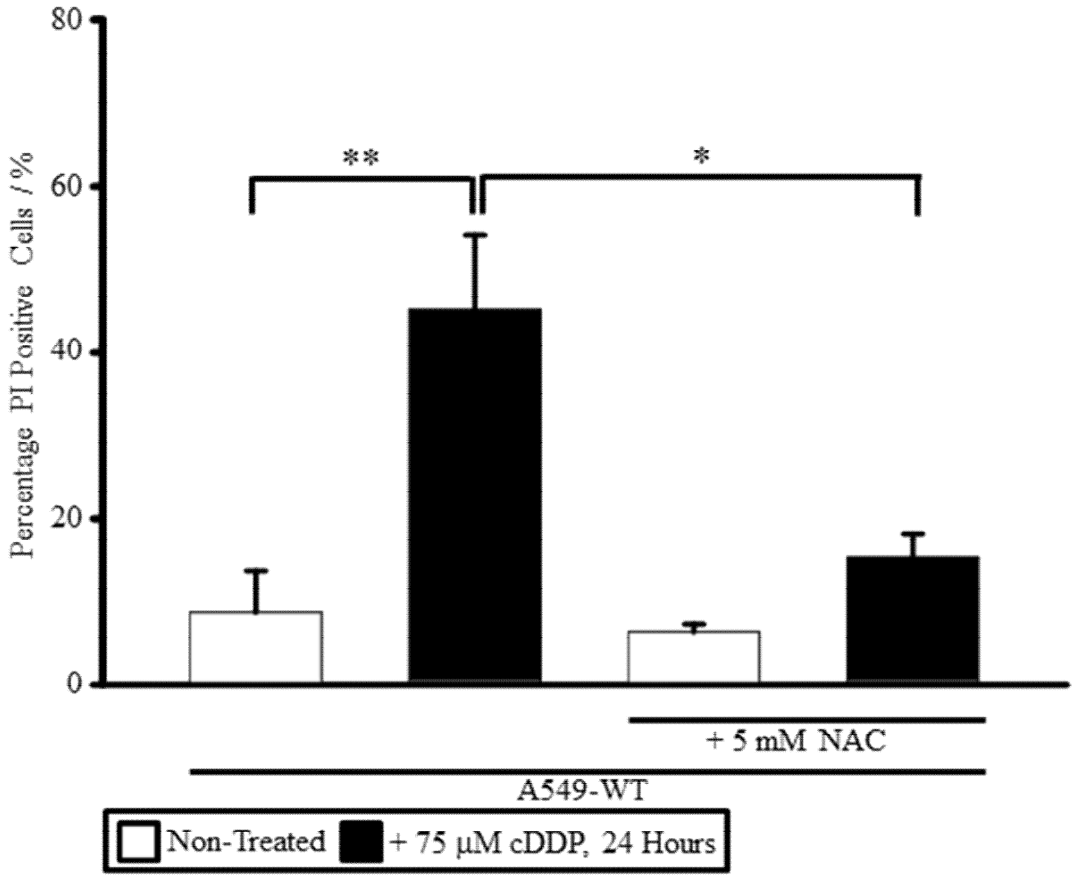

Figure 14: NAC fully prevents cDDP-induced cytotoxicity in A549-WT cells. A549-WT cells were incubated in normal cell culture medium + 5 mM NAC or in normal cell culture medium + 5 mM NAC + 75 µM cDDP for 24 hours and cytotoxicity assayed by PI exclusion as outlined in *'Methods 2.4'*. Data represent the mean of three independent experiments + S.E.M. * $p < 0.05$. ** $p < 0.01$.

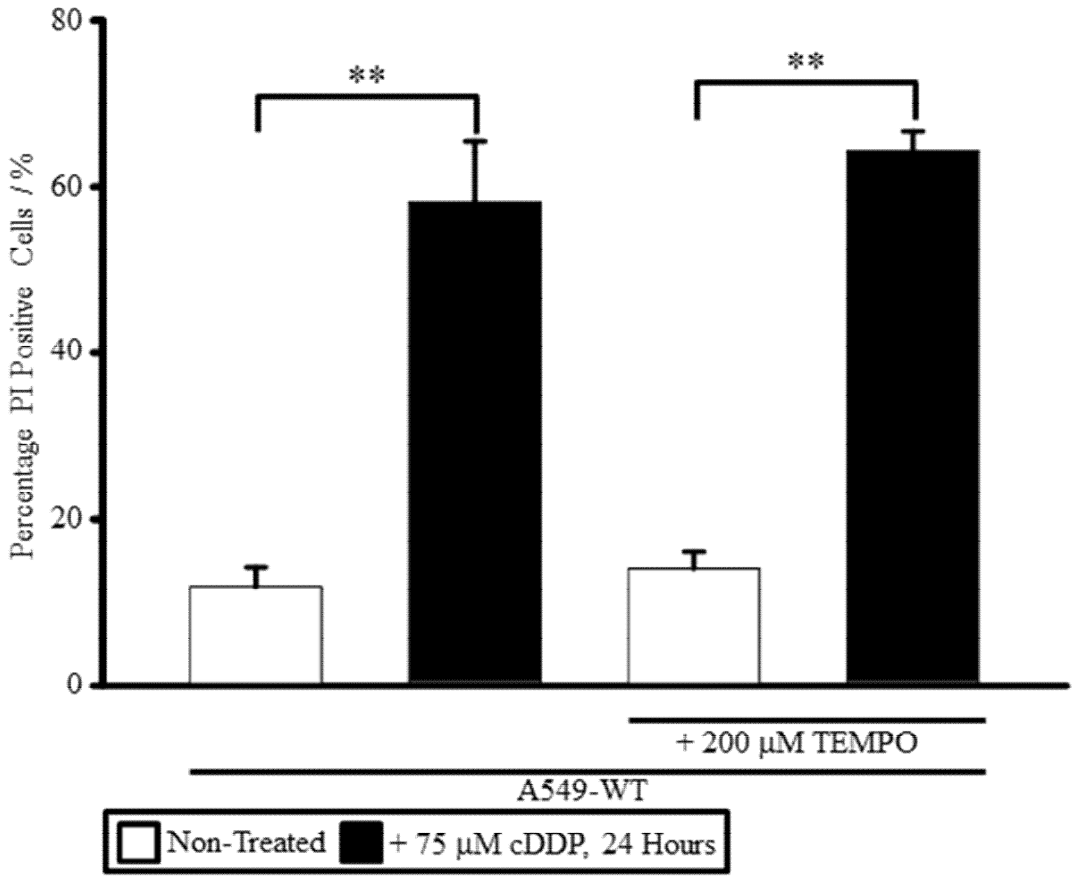

Figure 15: TEMPOL does not prevent cDDP-induced cytotoxicity in A549-WT cells. A549-WT cells were incubated in normal cell culture medium + 200 µM TEMPOL or in normal cell culture medium + 200 µM TEMPOL + 75 µM cDDP for 24 hours and cytotoxicity assayed by PI exclusion as outlined in *'Methods 2.4'*. Data represent the mean of three independent experiments + S.E.M. * $p < 0.05$.

3.1.8 Akt Phosphorylation is Reduced in A549-CR Cells Relative to A549-WT Cells

Mutations in the mtDNA of cancer cells may lead to increased activity of Akt, a change known to induce cell growth, protein translation and inhibit pro-apoptotic BCL-2 family proteins, thus the phosphorylation state of Akt at the activating Ser473 residue (hereafter 'phospho-Akt') in A549-WT cells and A549-CR cells was investigated by western blotting (Figure 16 A). The ratio of phospho-Akt to total cellular Akt detected by western blot was reduced by approximately 45% in A549-CR cells relative to A549-WT cells ($p < 0.05$), whilst 24 hours incubation with 75 µM cDDP caused an approximately 20% decrease in this ratio in A549-WT cells relative to non-treated control A549-CR cells ($p < 0.05$), but did not significantly alter this ratio in A549-CR cells (Figure 16 B). Thus, in comparison to A549-WT cells, Akt activation is reduced in A549-CR cells both prior to and following exposure to cDDP.

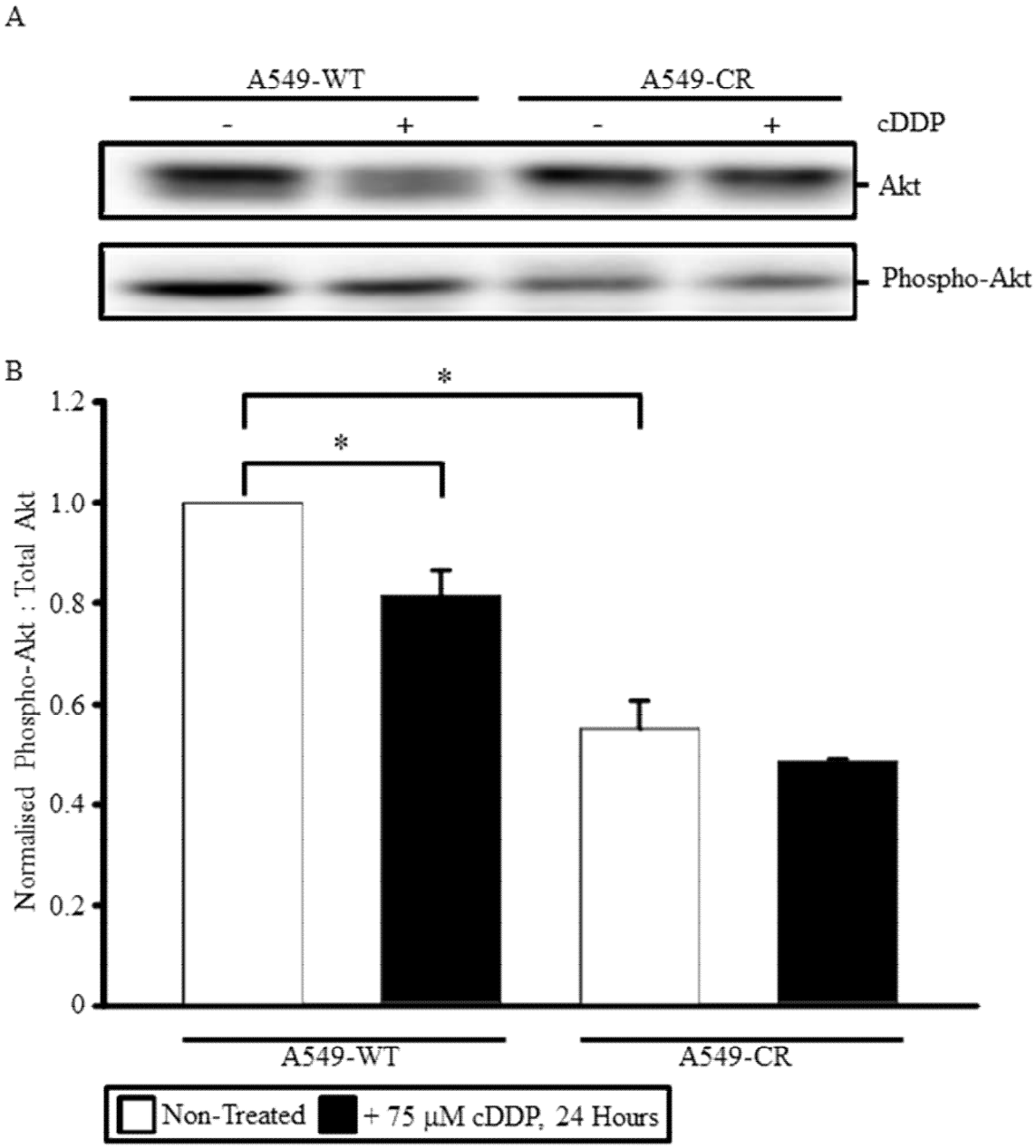

Figure 16: Akt phosphorylation is significantly decreased in A549-CR cells relative to A549-WT cells. A549-WT cells and A549-CR cells were incubated in normal cell culture medium or normal cell culture medium + 75 µM cDDP for 24 hours, and the ratio of active Ser473 phospho-Akt to total cellular Akt determined by western blot. (A) Representative total Akt and Ser 473 phospho-Akt western blots. (B) Quantification of normalised Ser473 phospho-Akt : total Akt protein band intensities. Data were normalised to non-treated A549-WT cells and represent the mean of three independent experiments + S.E.M. * $p < 0.05$.

3.2 The Contribution of ER Ca^{2+} Signalling to cDDP-Sensitivity

3.2.1 IP_3R Function is Inhibited in A549-CR Cells

Effects at the ER have been implicated in cDDP cytotoxicity, but the importance of this organelle in the cellular response to cDDP remains unknown (Kawai et al., 2006; Mandic et al., 2003). The question as to whether the ER plays a role in cDDP sensitivity in A549 cells was first explored by making comparative measurements of ER function between A549-WT and A549-CR cells. Ca^{2+} release is a central function of the ER in both a physiological and pathophysiological context, thus the Ca^{2+} release properties of the ER were investigated in A549-WT and A549-CR cells transfected with cytoplasmic aequorin cDNA constructs. Stimulation of A549 cells with extracellular ATP results in Ca^{2+} efflux from the ER mediated by IP_3 binding to IP_3Rs (Zhao et al., 2000). Addition of 100 μM ATP to A549-WT cells evoked a rapid cytosolic Ca^{2+} signal (peak $[Ca^{2+}]_{cyt}$ = 1.08 ± 0.14 μM) (Figure 17 A), whilst no detectable changes in $[Ca^{2+}]_{cyt}$ were observed in A549-CR cells (Figure 17 A). A comparable number of photons were detected in experiments with both A549-WT and A549-CR cells (Table 2), indicating equal expression of the probe. Challenge of control HeLa cells with 100 μM ATP generated a rise in intracellular Ca^{2+} similar to that in A549-WT cells (Figure 17 B).

The difference in intracellular Ca^{2+} response following application of extracellular ATP in the two A549 cell lines might be equally well explained through altered purinergic receptor expression, changes in the signalling pathway leading to IP_3 generation or inhibition of ER Ca^{2+} release. To further investigate this, the function of the IP_3R in both cell lines was directly probed using a cell permeable, photolabile caged IP_3 compound (hereafter referred to simply as 'caged IP_3'), and changes in $[Ca^{2+}]_{cyt}$ measured using Fluo-4. Uncaging of caged IP_3 through UV illumination resulted in a rapid increase of Fluo-4 fluorescence in A549-WT cells (peak = 1.18 ± 0.02 AU) and A549-CR cells (peak = 1.10 ± 0.02 AU) (Figure 18 A & B). The difference in response of the two cell types was highly statistically significant ($p < 0.01$). Imaging of cells loaded with the caged IP_3 compound without UV illumination did not result in any Fluo-4 fluorescence changes (Figure 18 C & Appendix II Figure 1). IP_3R function is therefore reduced in A549-CR cells relative to the A549-WT cell line.

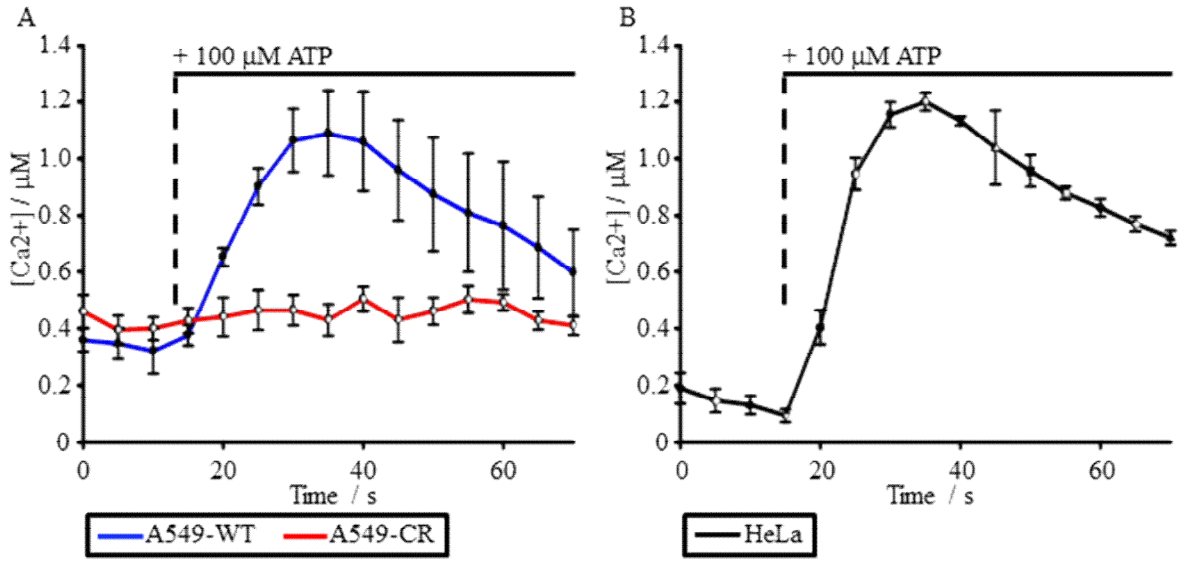

Figure 17: Cytosolic Ca^{2+} signalling invoked by extracellular ATP is inhibited in A549-CR cells, relative to A549-WT cells. A549-WT cells, A549-CR cells and HeLa cells transiently transfected with cytoplasmically targeted aequorin were stimulated by perfusion with KRB + 100 µM ATP, and bioluminescence recorded in a custom built luminometer. Photon counts were calibrated to $[Ca^{2+}]$ as outlined in *'Methods 2.5'*. (A) Mean changes in $[Ca^{2+}]_{cyt}$ measured in A549-WT cells and A549-CR cells following challenge with extracellular ATP. (B) Mean changes in $[Ca^{2+}]_{cyt}$ measured in control HeLa cells following challenge with extracellular ATP. Traces represent the mean response of a minimum of five coverslips from three independent experiments ± S.E.M. * $p < 0.05$.

Table 2: Total number of photons collected over the entire experimental time-course for ATP stimulation of aequorin transfected cells is comparable for A549-WT cells and A549-CR cells.

	Total Number of Detected Photons			
	Experiment 1	Experiment 2	Experiment 3	Experiment 4
A549-WT	510483	531447	1593459	1551850
A549-CR	340470	409805	812267	1579633
HeLa	15808570	26615256	20649907	15996487

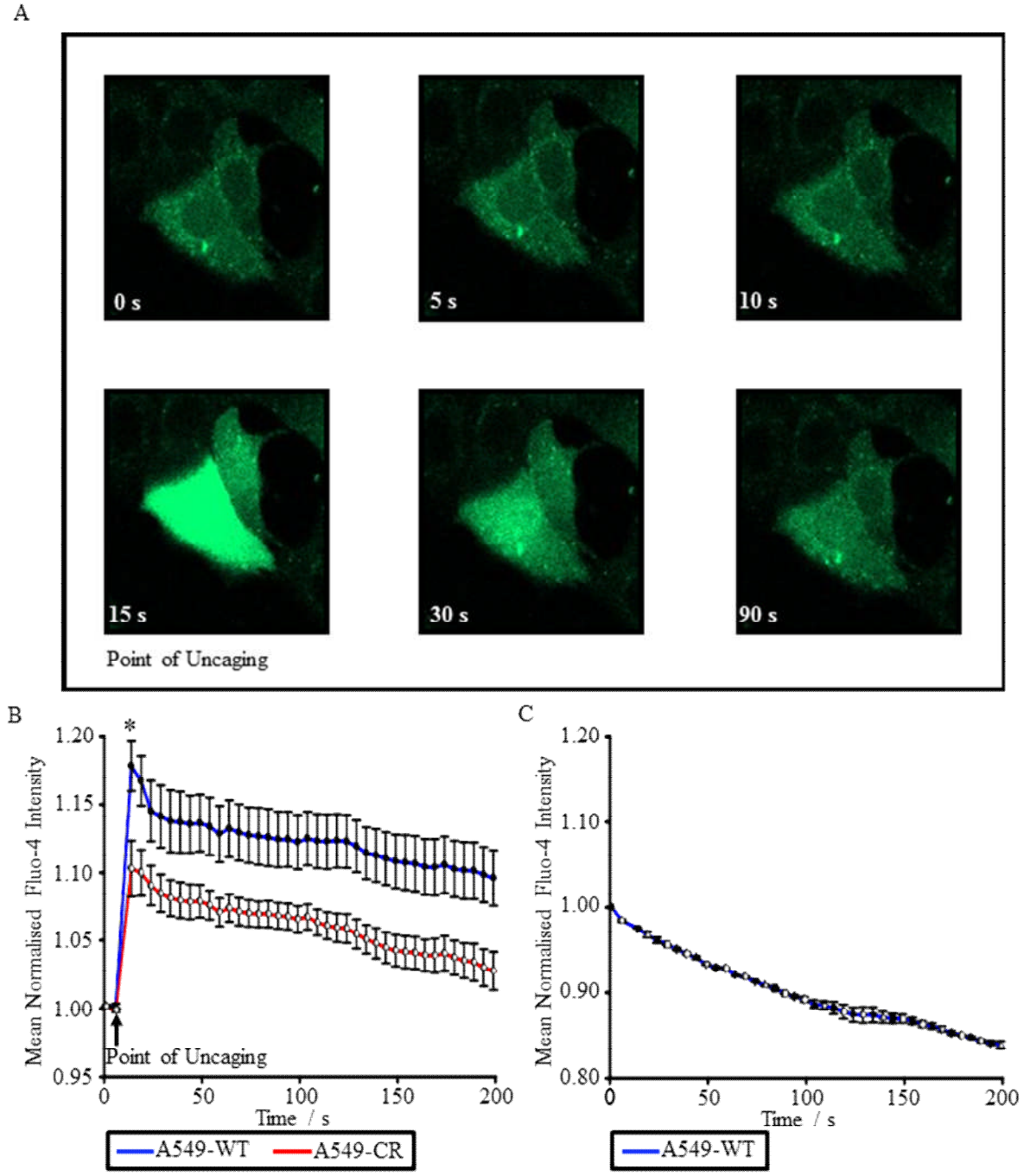

Figure 18: IP_3R function is reduced in A549-CR cells relative to A549-WT cells. Cells were loaded with photolabile caged IP_3 and 5 µM Fluo-4-AM, and fluorescence intensity recorded after IP_3 uncaging caused by a period of UV illumination, as described in *'Methods 2.6'*. (A) Representative image sequence demonstrating changes in Fluo-4 fluorescence in A549-WT cells prior to and following UV illumination. (B) Mean changes in dye bleaching corrected normalised Fluo-4 fluorescence in A549-WT and A549-CR cells loaded with caged

IP_3 following UV illumination. (C) Mean changes in normalised Fluo-4 fluorescence without dye bleaching correction in A549-WT cells loaded with caged IP_3 without the UV illumination period. Traces represent the mean response of a minimum of five coverslips from four independent experiments ± S.E.M. * $p < 0.05$.

3.2.2 Decreased SOCE Following ER Ca^{2+} Store Depletion in A549-CR Cells

Activation of the SOCE pathway upon depletion of the ER Ca^{2+} store results in a prolonged rise in $[Ca^{2+}]_{cyt}$, and allows for restoration of normal $[Ca^{2+}]_{ER}$. ER function plays a key role in activating this Ca^{2+} entry pathway through the action of the integral ER membrane protein STIM-1 activating the plasma membrane Orai Ca^{2+} channel upon a decrease in ER luminal Ca^{2+}. Given the IP_3-induced Ca^{2+} release from the ER in A549-CR cells, ER function was further studied by investigating the ability of the organelle to induce SOCE following pharmacological depletion of the ER Ca^{2+} store. Further, since prolonged rises in intracellular Ca^{2+} may activate both the apoptotic and necrotic pathways of cell death (Section 1.2.6), and reduced intracellular Ca^{2+} signalling often correlates with reduced sensitivity to apoptotic stimuli (Pinton, Giorgi, Siviero, Zecchini, & Rizzuto, 2008; R Rizzuto et al., 2003), reduced activation of SOCE may contribute to the cDDP resistant phenotype of A549-CR cells. Indeed, knockdown of Orai expression has previously been demonstrated to reduce the sensitivity of prostate cancer cells to cDDP (Flourakis et al., 2010).

$[Ca^{2+}]_{cyt}$ was measured using aequorin targeted to the cytoplasm, and depletion of Ca^{2+} from the ER induced by addition of 500 nM Tg. To differentiate between Ca^{2+} release induced by Tg and influx of extracellular Ca^{2+} into the cytoplasm, Tg treatment occurred in nominally 'Ca^{2+} free' KRB, and subsequent re-addition of Ca^{2+} to the extracellular buffer allowed examination of Ca^{2+} influx pathways. Control cells were treated with nominally 'Ca^{2+} free' KRB without Tg before re-addition of Ca^{2+}. It was not possible to identify increases in $[Ca^{2+}]_{cyt}$ attributable to emptying of Tg-sensitive Ca^{2+} stores in either A549 cell line, likely due to the low Ca^{2+} affinity of aequorin which makes the probe unsuitable for measuring the slow, low amplitude Ca^{2+} signals caused by Tg (Figure 19 B & D). Re-addition of Ca^{2+} to the external buffer solution generated a large cytosolic Ca^{2+} signal (peak $[Ca^{2+}]_{cyt}$ = 2.89 ± 0.12 μM) in A549-WT cells after treatment with Tg (Figure 19 B). Control A549-WT cells showed much smaller changes in $[Ca^{2+}]_{cyt}$, peaking at less than 1 μM, upon return to buffer

containing Ca^{2+} (Figure 19 A). Conversely, the increase in $[Ca^{2+}]_{cyt}$ in A549-CR cells upon reperfusion of buffer containing Ca^{2+} was not significantly greater in Tg treated cells (Figure 19 D) than in control A549-CR cells (Figure 19 C), and did not exceed 1 μM in either case. The total number of photons detected resulting from aequorin bioluminescence in experiments with both A549-WT and A549-CR cells were again comparable, indicating comparable aequorin expression in the cell lines. (Table 3).

SOCE following depletion of ER Ca^{2+} was further investigated using Fura-2. A549 cells loaded with the Ca^{2+} indicator dye were again treated with 500 nM Tg in nominally 'Ca^{2+} free' KRB before the reintroduction of Ca^{2+} to the extracellular buffer. Emptying of ER Ca^{2+} into the cytosol after Tg addition was evident in both cell lines as a similar prolonged low amplitude increase in the normalised Fura-2 fluorescence ratio (A549-WT peak = 1.12 ± 0.03 AU, A549-CR peak = 1.14 ± 0.02 AU) (Figure 20 A). Addition of Ca^{2+} to the buffer solution after 5 minutes Tg treatment caused a 2-fold increase in the normalised Fura-2 fluorescence ratio in A549-WT cells (peak = 1.98 ± 0.03 AU) and a 1.5-fold increase in A549-CR cells (peak = 1.57 ± 0.09 AU) (Figure 20 A). The difference in peak response after Ca^{2+} readdition is statistically significant ($p < 0.05$). Control cells did not undergo Tg treatment. No changes in normalised Fura-2 fluorescence ratio were measured upon addition of extracellular Ca^{2+} to the buffer solution in control cells of either A549 cell line (Figure 20 B). SOCE is thus diminished in A549-CR cells relative to A549-WT cells.

Table 3: Total number of photons collected over the entire experimental time-course for investigation of SOCE in aequorin transfected cells is comparable for A549-WT cells and A549-CR cells.

	Total Number of Detected Photons			
	Experiment 1	Experiment 2	Experiment 3	Experiment 4
A549-WT	153629	258119	202651	-
A549-WT + Tg	201835	408866	352746	-
A549-CR	428524	522684	979947	1254771
A549-CR + Tg	597870	443226	-	-

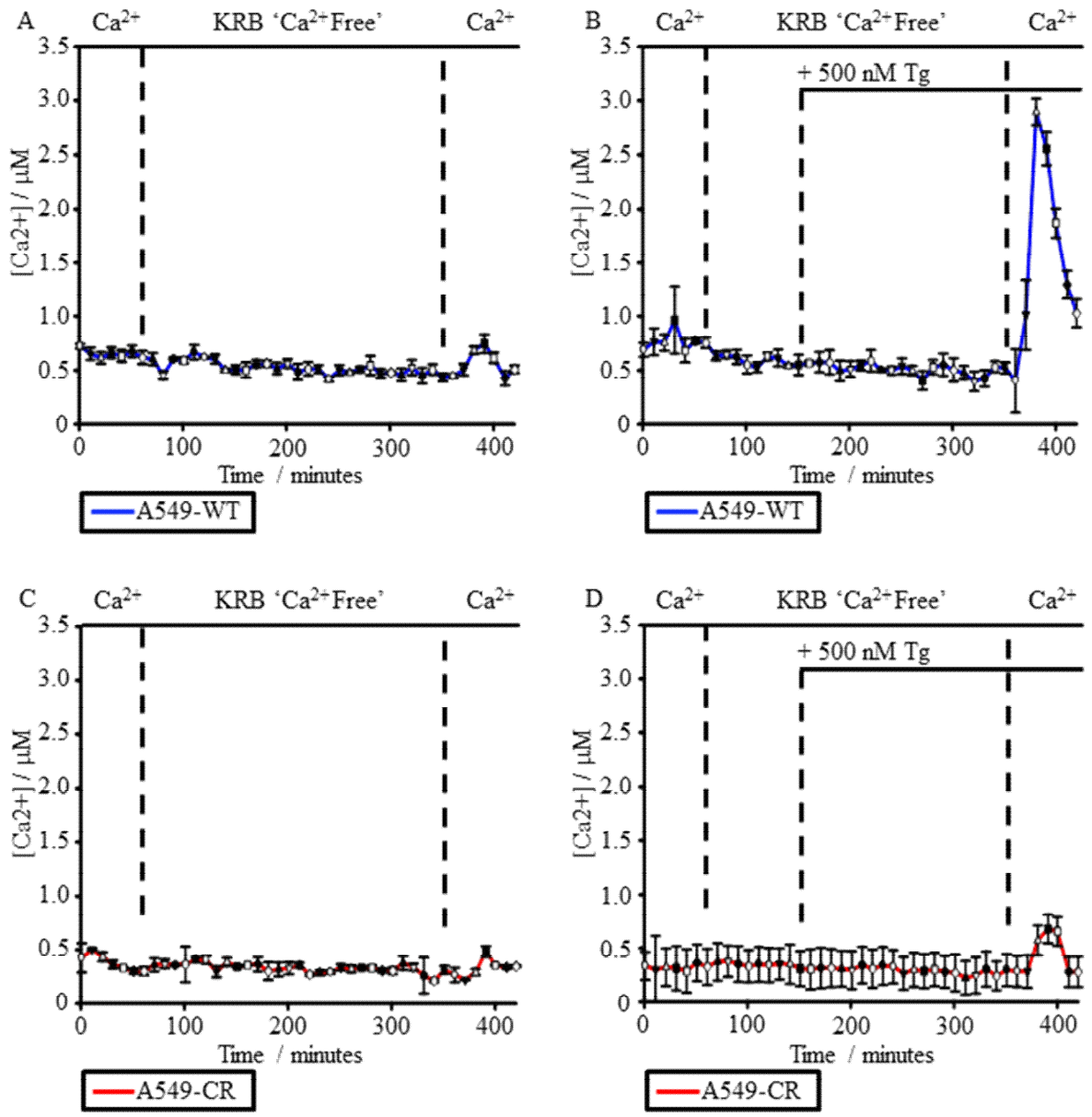

Figure 19: SOCE following pharmacological depletion of $[Ca^{2+}]_{ER}$ is reduced in A549-CR cells relative to A549-WT cells. A549-WT cells and A549-CR cells transiently transfected with cytoplasmic aequorin were incubated with 500 nM Tg in nominally 'Ca^{2+} free' KRB to deplete the ER Ca^{2+} store, before readdition of Ca^{2+} to the bathing buffer solution. Bioluminescence was recorded in a custom built luminometer and photon counts were calibrated to $[Ca^{2+}]$ as outlined in *'Methods 2.5'*. (A) Mean $[Ca^{2+}]_{cyt}$ measured in A549-WT cells and (C) mean $[Ca^{2+}]_{cyt}$ measured in A549-CR cells upon reperfusion of Ca^{2+} containing buffer following 5 minutes incubation in nominally 'Ca^{2+} free KRB'. (B) Mean $[Ca^{2+}]_{cyt}$ measured in A549-WT cells and (D) mean $[Ca^{2+}]_{cyt}$ measured in A549-CR cells

upon reperfusion of Ca^{2+} containing buffer following 5 minutes incubation in nominally 'Ca^{2+} free KRB' + 500 nM Tg. Traces represent the mean response of a minimum of five coverslips from three independent experiments ± S.E.M. * $p < 0.05$.

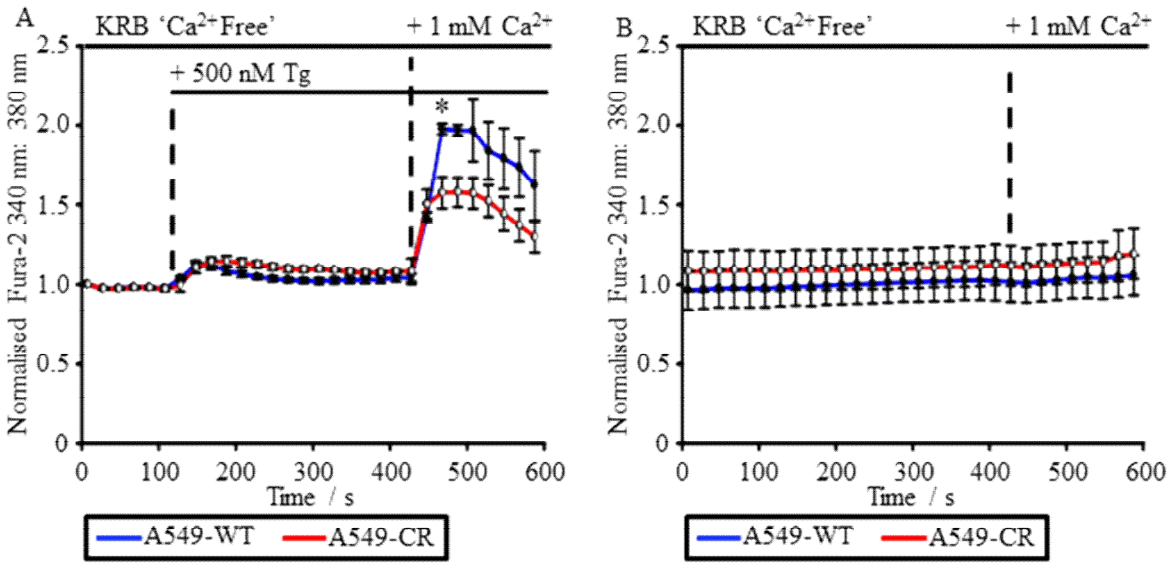

Figure 20: SOCE following pharmacological depletion of $[Ca^{2+}]_{ER}$ is reduced in A549-CR cells relative to A549-WT cells. A549-WT cells and A549-CR cells loaded with Fura-2 were incubated with 500 nM Tg in nominally 'Ca^{2+} free' KRB to deplete the ER Ca^{2+} store, before readdition of Ca^{2+} to the bathing buffer solution. (A) Mean normalised Fura-2 340 nm : 380 nm ratio measured in A549-WT cells and A549-CR cells upon reperfusion of Ca^{2+} containing buffer following incubation in nominally 'Ca^{2+} free KRB' + 500 nM Tg. (B) Mean normalised Fura-2 340 nm : 380 nm ratio measured in A549-WT cells and A549-CR cells upon reperfusion of Ca^{2+} containing buffer following incubation in nominally 'Ca^{2+} free KRB'. Traces were normalised relative to A549-WT cells and represent the mean response of a minimum of seven coverslips from three independent experiments ± S.E.M. * $p < 0.05$.

3.2.3 IP_3R-1 Expression Level Does Not Alter A549-WT cDDP Sensitivity

Reduced expression of IP_3Rs in A549-CR cells could account for the inhibition of IP_3-dependent Ca^{2+} signalling observed in this cell line. Decreased expression of IP_3R-1 relative to the parental cells in a bladder cancer cell line with acquired cDDP-resistance has previously been demonstrated to closely associate with the acquisition of drug resistance (Tsunoda et al., 2005). IP_3R-1 is highly expressed in A549 cells (H. Xue et al., 2000), and in light of the previous literature linking IP_3R-1 to cellular sensitivity to cDDP treatment, this isoform was selected for further investigation in this study. The relationship between the expression of IP_3R-1 and cDDP resistance was investigated thus in the present cell model. Western blot analysis was performed on both A549-WT and A549-CR cells without drug treatment and after 24 hours incubation with 75 μM cDDP. No difference in the level of IP_3R-1 protein expression was observed between untreated control A549-WT and A549-CR cells (Figure 21 A & B). Likewise, cDDP did not significantly alter the expression of IP_3R-1 in A549-WT or A549-CR cells, nor was there any difference in the expression of this IP_3R isoform between cDDP treated A549-WT and A549-CR cells (Figure 21 A & B).

The potential for modulating the IP_3R expression level as a means of increasing the efficacy of cDDP treatment was further investigated by overexpressing IP_3R-1 in A549-WT and A549-CR cells. Transient transfection of an IP_3R-1 construct dramatically increased the protein expression level of IP_3R-1, as measured by western blot (Figure 22 A). However, the percentage of PI positive cells after 24 hours treatment using 75 μM cDDP did not differ between untransfected A549-WT cells (45.9 ± 5.0%), A549-WT cells transfected with the IP_3R-1 construct (47.7 ± 7.8%) nor A59-WT cells transiently transfected with a control ER-targetted GFP construct (48.2 ± 6.0%) (Figure 22 B). A549-CR cells transiently transfected with ER-GFP or IP_3R-1 showed a marked basal toxicity in comparison to A549-WT cells transfected with the same cDNA constructs (Figure 21 B). No difference in the percentage of PI positive cells measured after 24 hours incubation with 75 μM cDDP was observed between A549-CR cells expressing ER-GFP (47.2 ± 6.3%) or A549-CR cells overexpressing IP_3R-1 (51.0 ± 6.3%) (Figure 22 B). The transfection efficiency of siRNA targeted towards IP_3R-1 mRNA did not prove effective enough for efficient IP_3R-1 silencing in either A549-WT cells or A549-CR cells (data not shown), thus this approach did not form part of the investigation.

Together these data show the expression level of the IP_3R-1 is not a modulator of cDDP sensitivity in this A549 cell model.

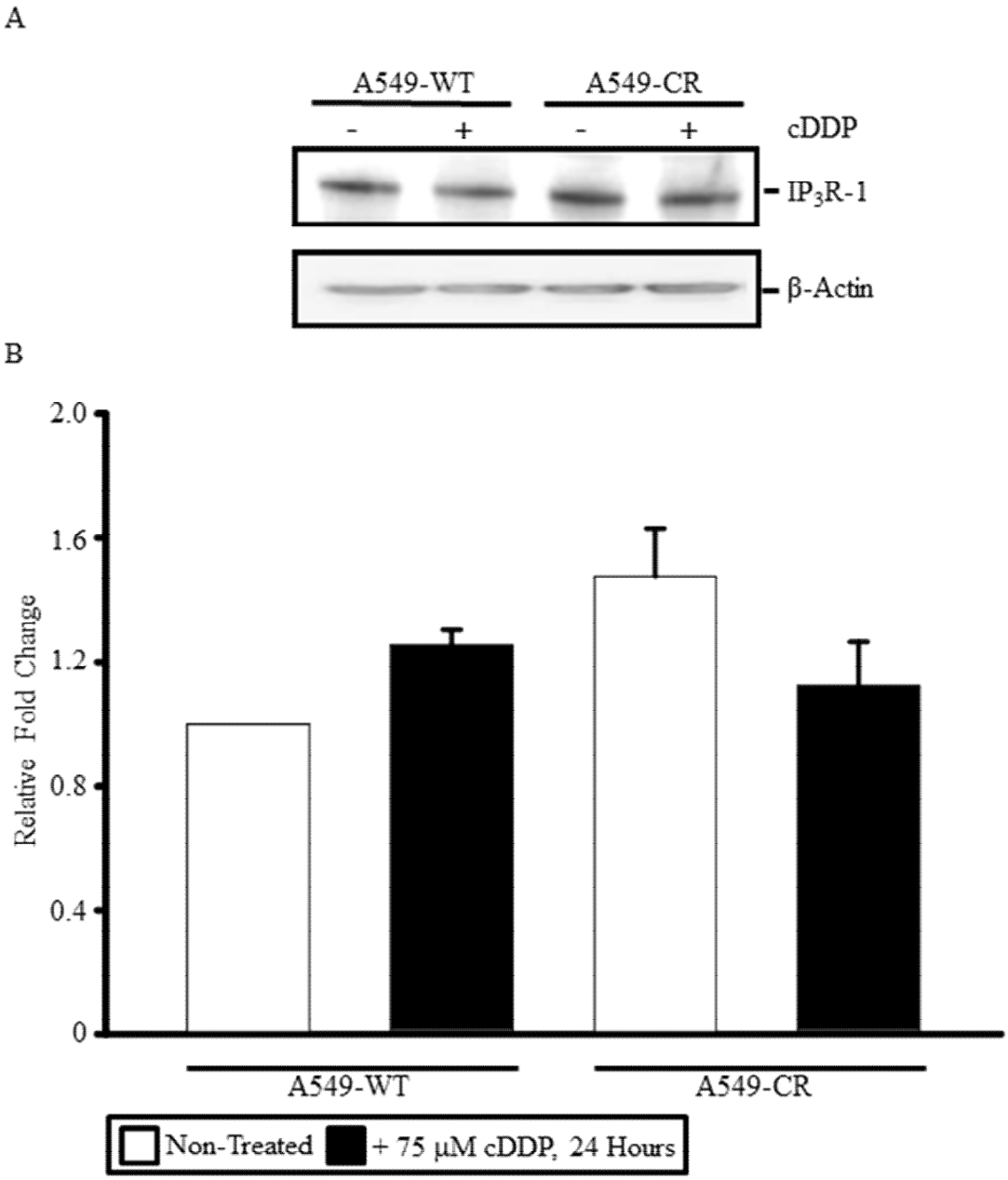

Figure 21: IP_3R-1 expression does not differ between A549-WT cells and A549-CR cells. A549-WT cells and A549-CR cells were incubated in normal cell culture medium or normal cell culture medium + 75 µM cDDP for 24 hours before immunoblotting as described in *'Methods 2.8'*. (A) Representative IP_3R-1 western blot. (B) Quantification of IP3R-1 band intensity. Data represents the mean of three independent experiments + S.E.M.

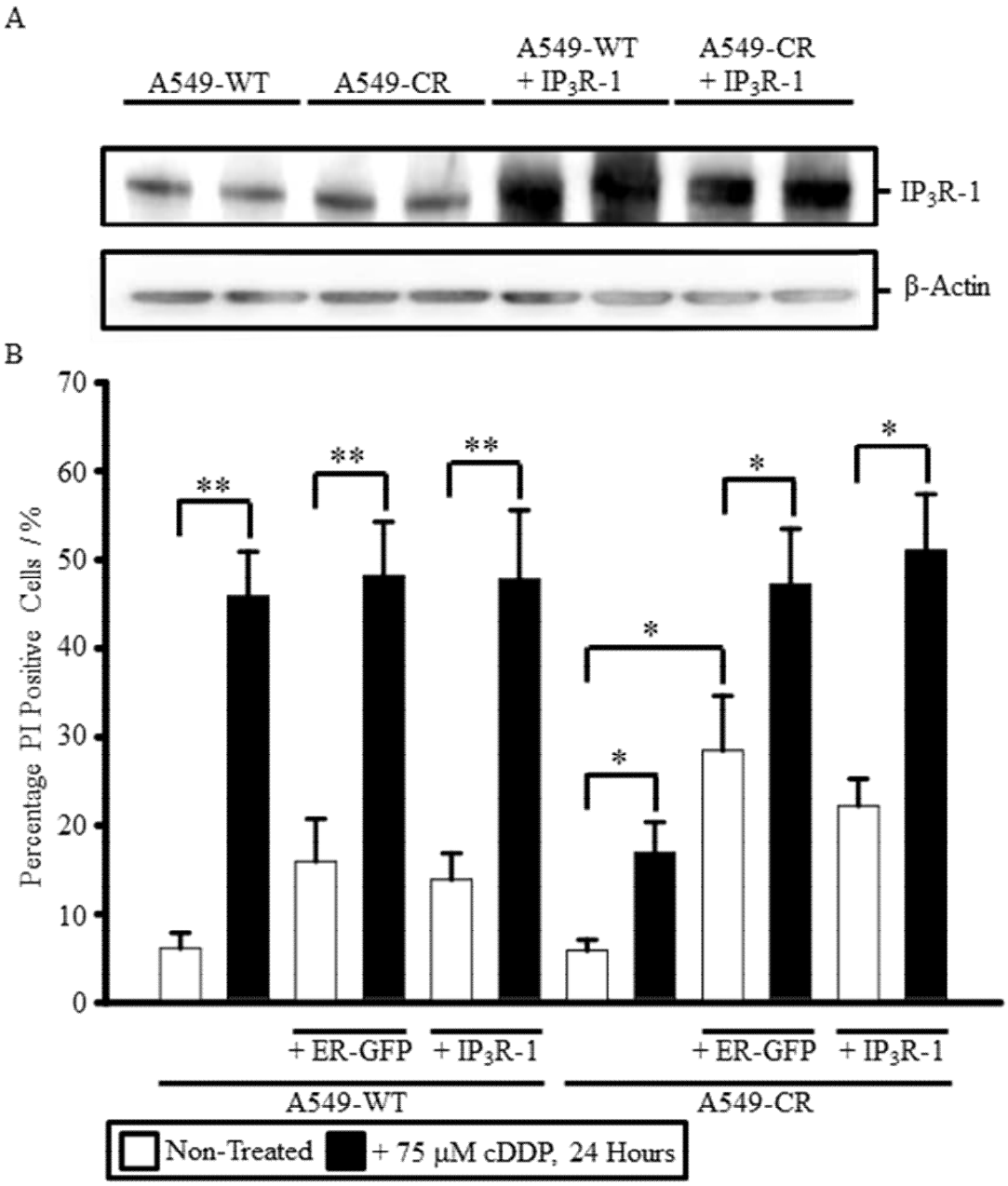

Figure 22: IP_3R-1 overexpression does not alter A549-WT cell cDDP sensitivity. A549-WT cells and A549-CR cells transfected with ER-GFP or an IP_3R-1/ GFP construct were incubated in normal cell culture medium or normal cell culture medium + 75 µM cDDP 24 hours, and cytotoxicity assayed by PI exclusion as outlined in *'Methods 2.4'*. (A) Representative IP_3R-1 western blot for untransfected control and IP3R-1/ GFP transfected A549-WT cells and A549-CR cells. (B) Percentage of PI positive cells measured following incubation of control, ER-GFP transfected and IP_3R-1/ GFP transfected A549-WT cells and A549-CR cells with cDDP. Note increased basal toxicity in A549-CR cells following

transfection. Data represent the mean of three independent experiments + S.E.M. * $p < 0.05$. ** $p < 0.01$.

3.2.4 Chelation of Intracellular Ca^{2+} Modulates A549-WT Cell Death Induced by cDDP

A549-CR cells exhibited decreased intracellular Ca^{2+} signalling in comparison with A549-WT cells. Since increases in intracellular Ca^{2+} may activate cell death pathways, the potential for modulating Ca^{2+} signalling as a means to alter A549-WT sensitivity to cDDP was investigated using the cell permeable Ca^{2+} chelator BAPTA-AM. A549-WT cells were pre-incubated with 1 μM, 3 μM or 10 μM BAPTA-AM for 30 minutes before 24 hours incubation with 75 μM cDDP. BAPTA-AM did not cause toxicity in A549-WT cells without cDDP addition over a 24 hour period at any concentration tested (Figure 23). Ca^{2+} chelation using 1 μM or 3 μM BAPTA-AM did not cause a statistically significant decrease in the percentage of cells which lost plasma membrane integrity after cDDP treatment, as measured by PI staining. Pre-treatment with 10 μM BAPTA-AM provided a 10% decrease in PI positive cells caused by cDDP compared to control A549-WT cells without Ca^{2+} chelation (41.3 ± 3.7% and 52.3 ± 2.2% respectively, $p < 0.05$) (Figure 23).

Cell death induced by cDDP in A549-WT cells is partially dependent upon Ca^{2+}, demonstrated by the protective effect of 10 μM BAPTA-AM during cDDP exposure. To determine whether this effect reflects a requirement for extracellular Ca^{2+}, A549-WT cells were pre-incubated with 1 mM EGTA for 30 minutes prior to 75 μM cDDP treatment. As the plasma membrane is impermeable to EGTA, pre-incubation of cells with EGTA can chelate extracellular Ca^{2+} but not prevent intracellular Ca^{2+} signalling. No difference in the percentage of PI positive cells caused by 24 hours cDDP treatment was observed between control cells and those pre-incubated with EGTA (Figure 25), indicating changes in intracellular Ca^{2+} homeostasis, rather than chelation of external Ca^{2+}, are responsible for the protective effects of BAPTA-AM.

It is notable that both the dataset concerning the effect of BAPTA-AM and that concerning the effect of EGTA on cDDP-induced cell death lack positive control data to demonstrate that these agents inhibit cellular Ca^{2+} signalling in the expected manner, and thus may not yet be properly interpreted. As an appropriate control experiment, the ability of each Ca^{2+} chelator

to inhibit changes in $[Ca^{2+}]_{cyt}$ in A549-WT cells upon stimulation with extracellular ATP relative to cells stimulated without Ca^{2+} chelation, following 24 hours incubation with the chelator, should be demonstrated, thus ensuring that Ca2+ signalling is effective prevented over the entire 24 hour cDDP treatment period. In the case of BAPTA-AM treatment, changes in intracellular Ca^{2+} should be expected to be greatly reduced. In the case of EGTA, the initial peak in $[Ca^{2+}]_{cyt}$, resulting from intracellular stores, should be unaffected, however the plateau in raised cytosolic Ca^{2+} levels attributable to SOCE should not occur, or be greatly reduced, as EGTA treatment is expected to reduce the extracellular free Ca^{2+} concentration to nominal levels. These effects of BAPTA-AM and EGTA have been previously extensively demonstrated in wide variety of primary cells and cancer cell lines (Berridge et al., 2003).

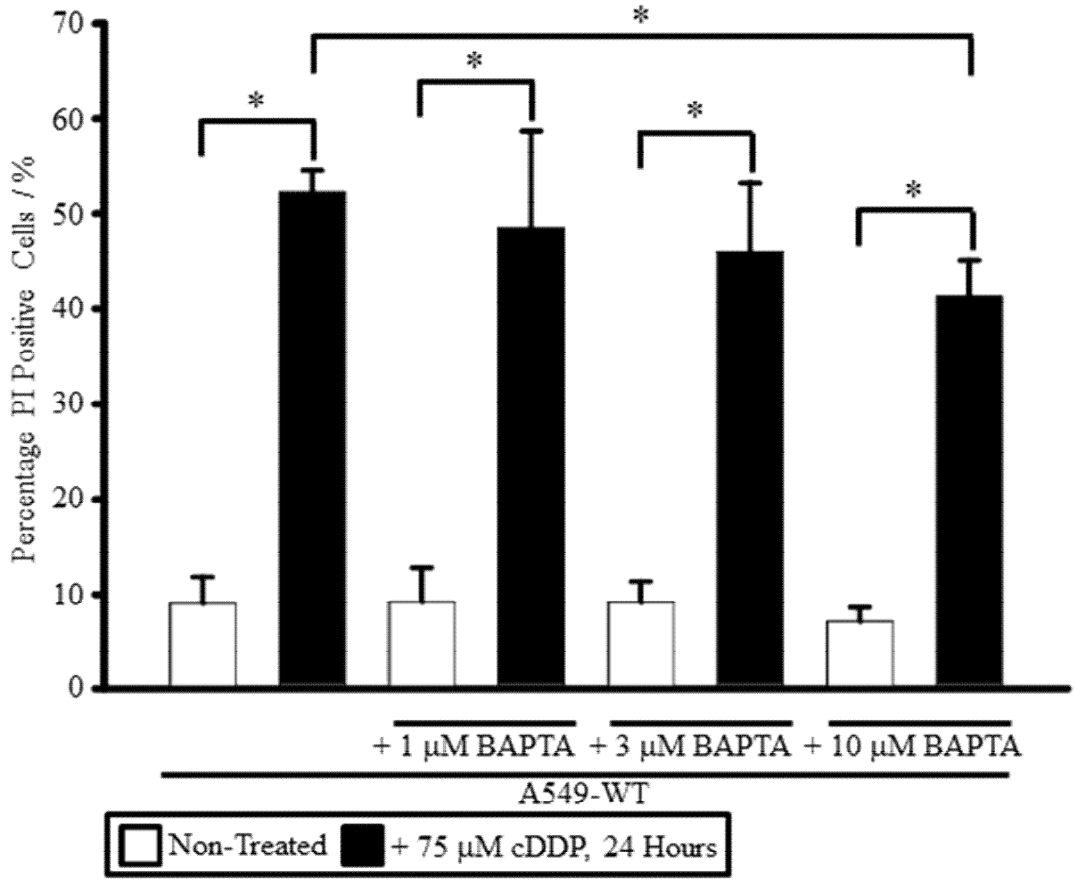

Figure 23: Ca^{2+} chelation by BAPTA-AM partially inhibits cDDP-induced cell death in A549-WT cells. A549-WT cells were incubated in normal cell culture medium or normal cell culture medium + 75 µM cDDP in the presence of BAPTA-AM in the concentration range 0 – 10 µM for 24 hours, and cytotoxicity assayed by PI exclusion as outlined in *'Methods 2.4'*. Data represent the mean of three independent experiments + S.E.M. * $p < 0.05$.

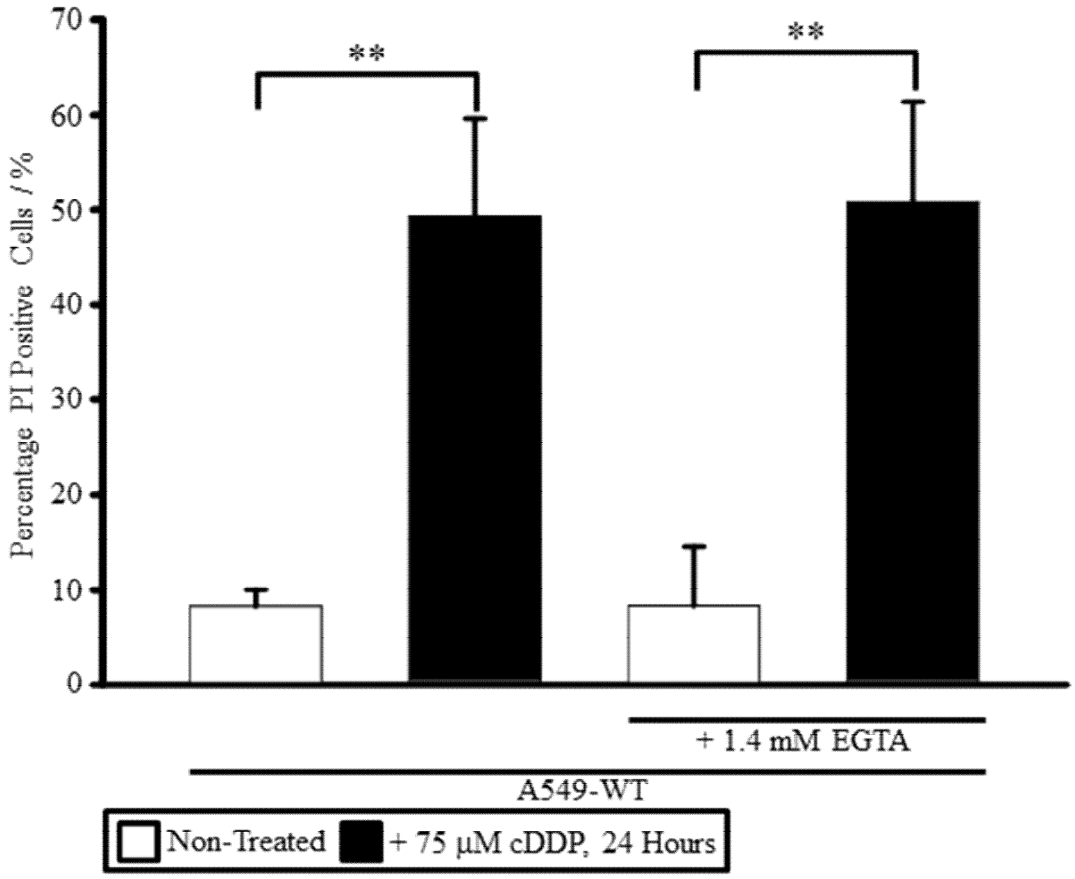

Figure 24: Ca^{2+} chelation by EGTA does not inhibit cDDP-induced cell death in A549-WT cells. A549-WT cells were incubated in normal cell culture medium or normal cell culture medium + 75 µM cDDP in the presence of 1.4 mM EGTA for 24 hours, and cytotoxicity assayed by PI exclusion as outlined in *'Methods 2.4'*. Data represent the mean of three independent experiments + S.E.M. ** $p < 0.01$.

3.2.5 Oxidative Stress Induced Through TMRM Photoactivation Does Not Model Pathophysiological ER-Mitochondria Ca^{2+} Transfer in A549 Cells

Cell death induced by cDDP in cDDP-sensitive A549-WT cells appeared to have a partial requirement for intracellular Ca^{2+}. Furthermore, cDDP-resistant A549-CR cells showed an inhibition of intracellular Ca^{2+} responses after stimulation with extracellular ATP, an IP_3 releasing ligand, or direct activation of the IP_3R. Together these data suggested that Ca^{2+} release from the ER could participate in mediating cDDP toxicity. Since the IP_3R forms part of a complex directly regulating Ca^{2+} transfer along the ER-mitochondria axis (Szabadkai et al., 2006), decreased function of this channel may render A549-CR cells less sensitive to cell death caused by mitochondrial Ca^{2+} overload. To examine this possibility, a model of phototoxicity induced by TMRM illumination was employed.

In some cell types, mitochondria loaded with rhodamine dyes have been shown to undergo store Ca^{2+} dependent depolarisation, mediated by the mPT, in response to ROS generated by dye illumination inducing Ca^{2+} release from the ER/SR, presumably through IP_3Rs and RyRs (Jacobson & Duchen, 2002). This process is characterised by transient 'flickering' depolarisations of one or more mitochondria, followed by a global collapse of $\Delta\Psi_m$. Indeed, such short lived changes in $\Delta\Psi_m$ were observed in both A549 cell lines loaded with 200 nM TMRM within approximately 15 minutes of continuous illumination (Figure 25 A). This period of transient loss and recovery of $\Delta\Psi_m$ was followed by a steady decline in $\Delta\Psi_m$ throughout the experimental time course, followed up to 50 minutes continuous illumination. No significant difference existed in either the kinetics of depolarisation of mitochondria or in the final TMRM fluorescence intensity between A549-WT and A549-CR cells (Figure 25 B). However, neither the period of transient 'flickering' nor the slow global loss of $\Delta\Psi_m$ in A549-WT cells could be prevented by store Ca^{2+} depletion prior to illumination using 500 nM Tg + 2mM EGTA nor 2mM EGTA + 1 µM BAPTA-AM (Figure 25 C). Furthermore, preincubation of A549-WT cells with 1 µM or 10 µM CsA, an inhibitor of Cyp D, did not alter this depolarisation (Figure 25 C). In contrast, addition of 1 mM ascorbic acid at the beginning of the illumination period fully prevented A549-WT mitochondrial depolarisation (Figure 25 D), whilst A549-WT cells loaded with 50 nM TMRM did not undergo any changes in $\Delta\Psi_m$ over the experimental time course (Figure 25 E). Together these data demonstrate that TMRM phototoxicity in A549-WT cells is not dependent upon interorganelle Ca^{2+} transfer but is fully mediated by the production of ROS above a certain

threshold level, thus is not an appropriate model to investigate pathophysiological ER-mitochondrial communication in the A549 cell line.

3.2 The Contribution of ER Ca^{2+} Signalling to cDDP-Sensitivity

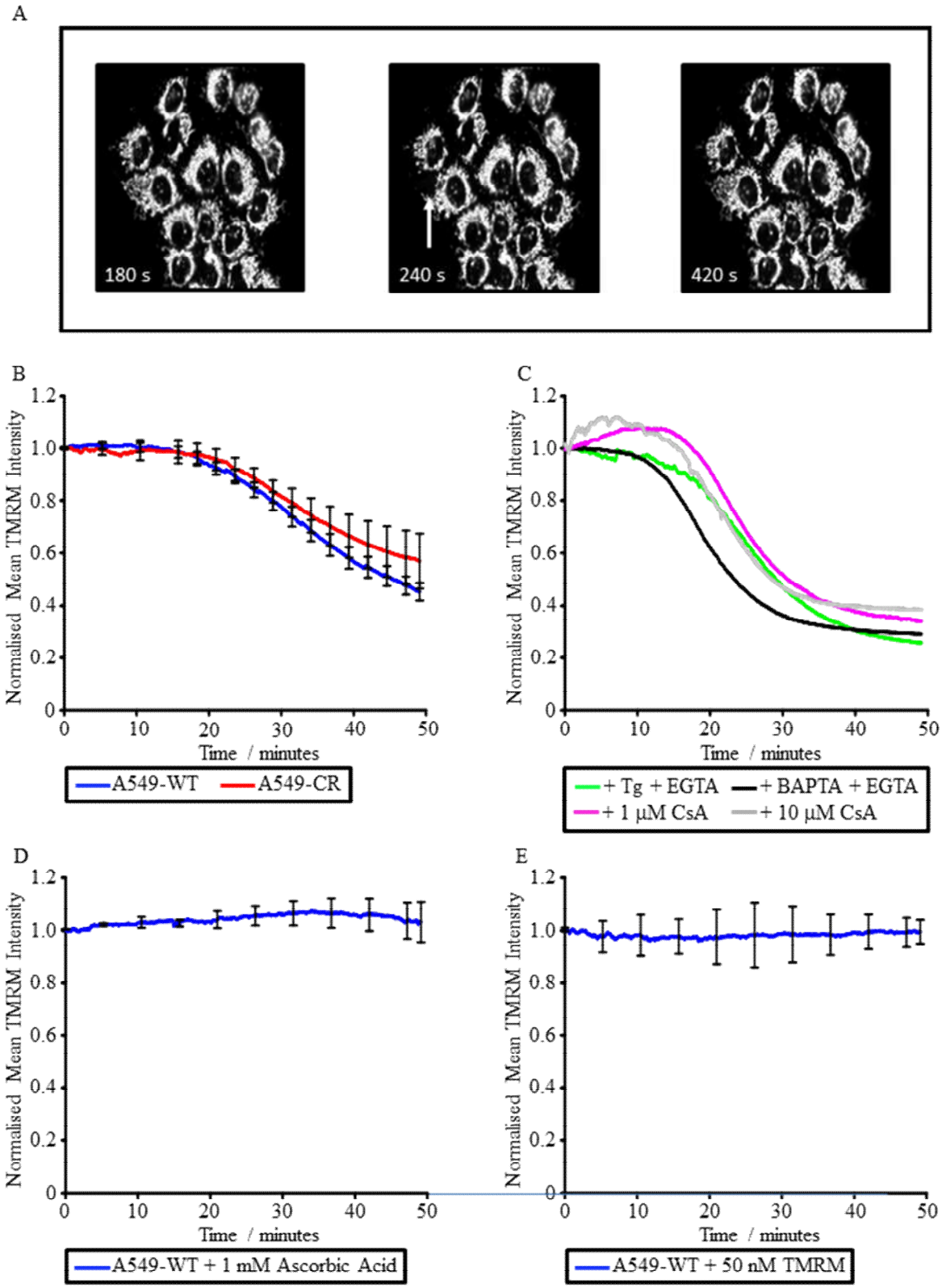

Figure 25: Loss of ΔΨ in A549 cells induced by TMRM photoactivation does not occur through Ca^{2+} dependent mPT, but is fully dependent upon ROS generation. To attempt to model pathological interorganelle Ca^{2+} transfer between the ER and mitochondria, A549-WT cells and A549-CR cells loaded with 200 nM TMRM were imaged continuously for 50 minutes, and TMRM fluorescence intensity measured to monitor changes in ΔΨ occurring in this period, as outlined in *'Methods 2.9'*. (A) Representative image sequence demonstrating transient loss of ΔΨ ('flickering') observed in both A549-WT cells and A549-CR cells within 15 minutes of continuous illumination. Depolarised mitochondria are marked by the white arrow. (B) Mean normalised TMRM fluorescence intensity measured in A549-WT cells and A549-CR cells under 50 minutes continuous illumination. Traces were normalised to the mean fluorescence of the first ten images and represent the mean of at least seven coverslips from three independent experiments ± S.E.M. (C) Representative normalised TMRM fluorescence intensity measured in A549-WT cells under 50 minutes continuous illumination following depletion of cellular Ca^{2+} using 500 nM TG + 2 mM EGTA or 1 μM BAPTA-AM + 2 mM EGTA, or pre-incubation with 1 μM or 10 μM Cyp D inhibitor CsA. (D) Mean normalised TMRM fluorescence intensity measured in A549-WT cells under 50 minutes continuous illumination in the presence of 1 mM ascorbic acid. (E) Mean normalised TMRM fluorescence intensity measured in A549-WT cells loaded with 50 nM TMRM under 50 minutes continuous illumination. Traces were normalised to the fluorescence of the first ten images and represent the mean of at least two coverslips from two independent experiments ± S.E.M.

3.2.6 cDDP Treatment Does Not Deplete ER Ca^{2+}

IP_3R function is reduced in A549-CR cells, whilst pre-incubation with 10 μM BAPTA-AM, but not 1 mM EGTA, afforded some inhibition of A549-WT cell death after cDDP treatment, suggesting Ca^{2+} release from the ER may contribute to cDDP cytotoxicity. To determine whether cDDP treatment caused depletion of the ER Ca^{2+} store, comparative measurements of $[Ca^{2+}]_{ER}$ were made in control A549-WT and A549-CR cells without cDDP treatment and in A549-WT and A549-CR cells after treatment with 75 μM cDDP over a 24 hour period, using the FRET-based, ER-targeted cameleon probe D1ER (Palmer et al., 2004). Basal $[Ca^{2+}]_{ER}$ did not significantly differ between A549-WT cells ('FRET-ratio' = 1.24 ± 0.04 AU) and A549-CR cells ('FRET-ratio' = 1.32 ± 0.07 AU) (Figure 26). Although incubation

with cDDP is associated with an increasing trend in the 'FRET-ratio' of the probe in both A549-WT cells ('FRET ratio' = 1.49 ± 0.07 AU) and A549-CR cells ('FRET ratio' = 1.64 ± 0.16 AU), there is no statistically significant difference in 'FRET-ratio' between non-treated and cDDP treated cells of either A549 cell line, nor between cDDP treated A549-WT cells and cDDP treated A549-CR cells (Figure 26). Pharmacological depletion of ER Ca^{2+} in A549-WT cells using Tg was associated with a statistically significant decrease in the 'FRET-ratio' of the probe compared with untreated A549-WT cells ('FRET-ratio' = 0.78 ± 0.02 AU, $p < 0.01$) (Figure 26). The ER is thus not depleted of Ca^{2+} by 24 hours cDDP treatment.

Exposure to cDDP has been reported to induce changes in $[Ca^{2+}]_{cyt}$ in a number of cell types (Al-Bahlani et al., 2011; Kawai et al., 2006; Splettstoesser, Florea, & Büsselberg, 2007) within one hour of drug exposure. However, no cytosolic Ca^{2+} signals were observed using Fura-2 in A549-WT cells or A549-CR cells up to one hour post addition of 75 µM cDDP to the cell bathing solution (Figure 27). No changes in $[Ca^{2+}]_{cyt}$ were observed in control A549-WT cells and A549-CR imaged under the same conditions without cDDP treatment (Figure 27).

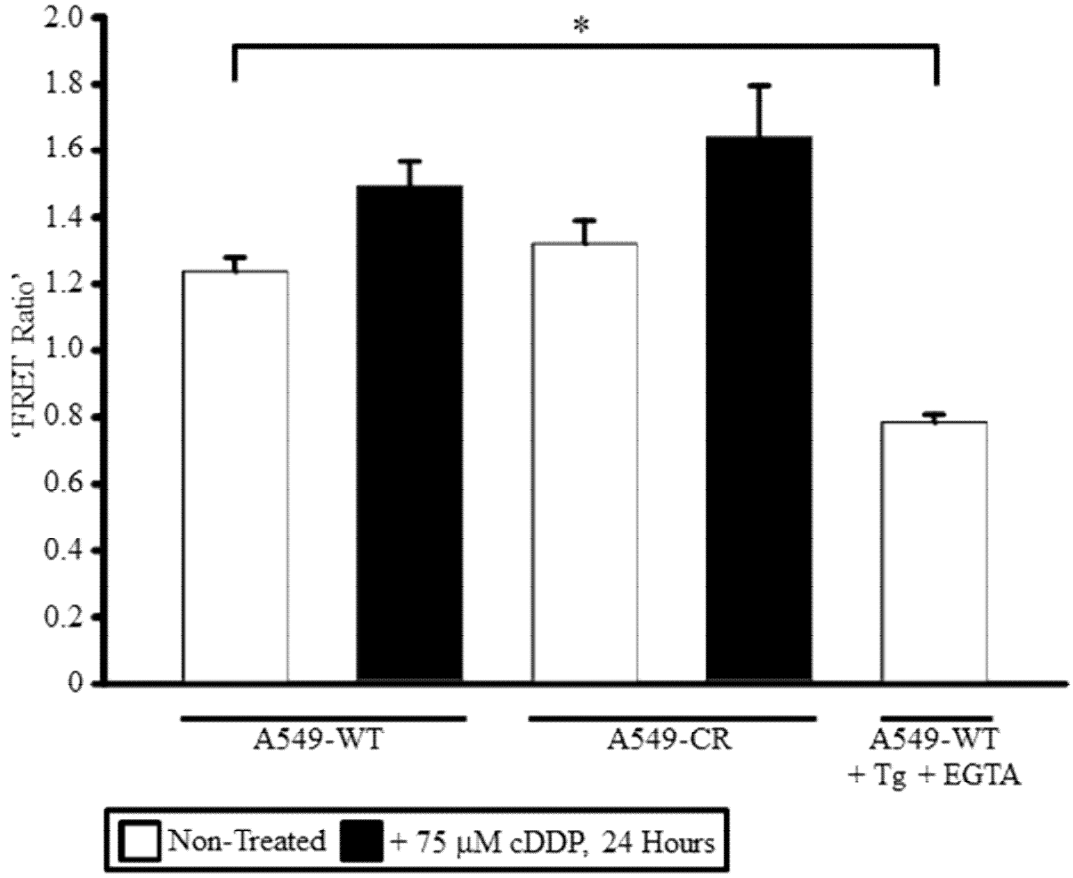

Figure 26: ER store Ca^{2+} content is not depleted by cDDP treatment in either A549-WT cells or A549-CR cells. A549-WT cells and A549-CR cells transiently transfected with the ER targeted D1ER cameleon Ca^{2+} probe were incubated in normal cell culture medium or normal cell culture medium + 75 µM cDDP for 24 hours. Control A549-WT cells were incubated in KRB + 500 nM Tg + 1.4 mM EGTA for 10 minutes to deplete ER store Ca^{2+} before measurement. D1ER 'FRET ratio' was used as an indicator of $[Ca^{2+}]_{ER}$, and estimated by acceptor photobleaching as described in *'Methods 2.10'*. Data represent the mean of three independent experiments + S.E.M. * $p < 0.05$.

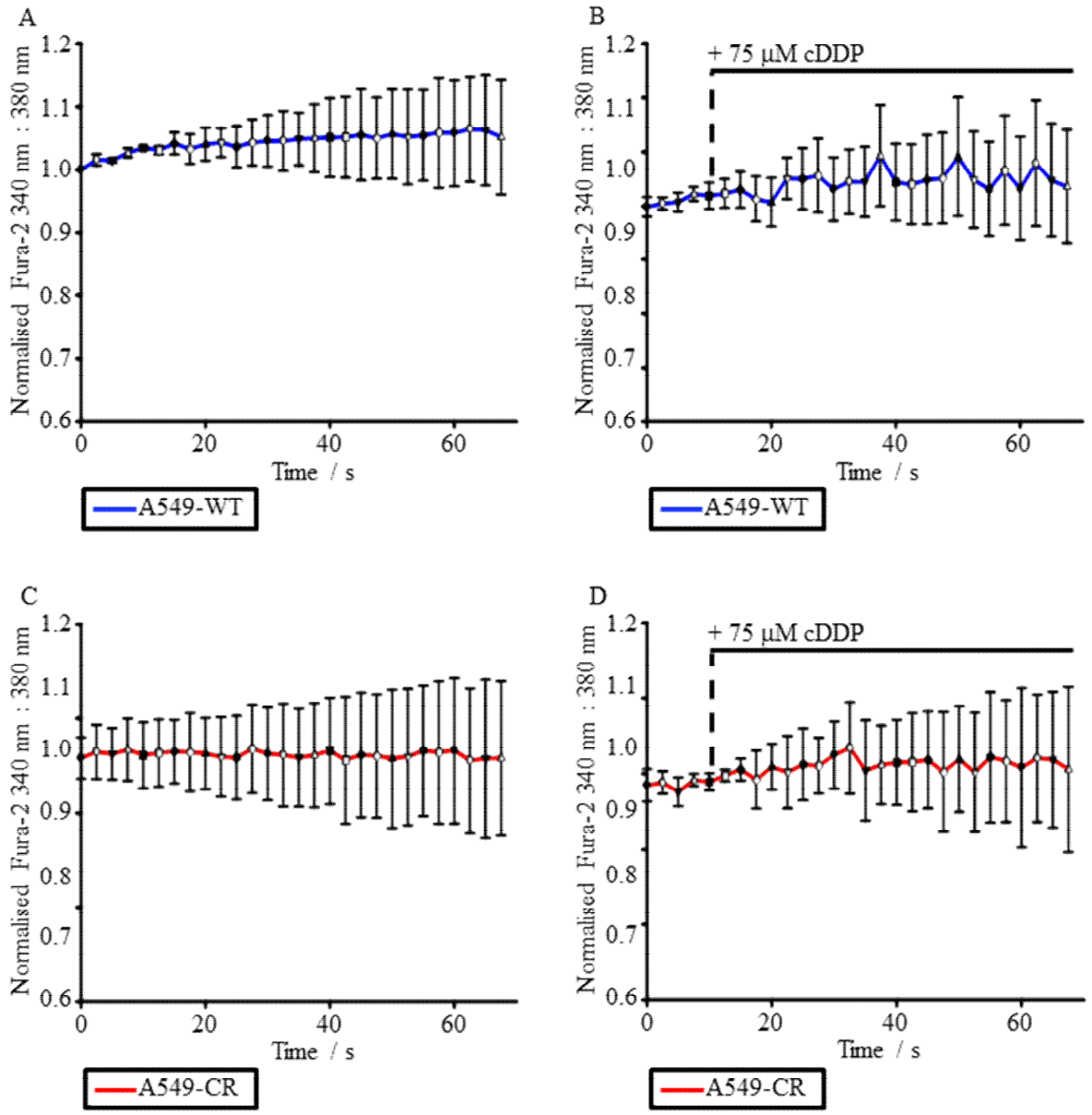

Figure 27: cDDP treatment does not cause acute changes in $[Ca^{2+}]_{cyt}$ in A549-WT cells or A549-CR cells. Flouresence in A549-WT cells and A549-CR cells loaded with Fura-2 was monitored for one hour in the absence or presence of 75 µM cDDP in a heated imaging chamber. (A) Mean normalised Fura-2 340 nm : 380 nm ratio measured in A549-WT cells and (C) A549-CR cells without cDDP exposure. (B) Mean normalised Fura-2 340 nm : 380 nm ratio measured in A549-WT cells and (D) A549-CR cells following addition of 75 µM cDDP. Traces were normalised relative to non-treated A549-WT cells and represent the mean of three independent experiments ± S.E.M.

3.2 The Contribution of ER Ca^{2+} Signalling to cDDP-Sensitivity

3.2.7 IP_3R Inhibition by 2-APB Does Not Inhibit cDDP-Induced A549-WT Cell Death

Although cDDP does not decrease the $[Ca^{2+}]_{ER}$, Ca^{2+} signalling through IP_3Rs could play a role in the induction of cell death in a manner which does not cause chronic store depletion. To test whether Ca^{2+} release through IP_3Rs is involved in cell death signalling after cDDP treatment, the effect of the addition of the cell permeable IP_3R channel blocker 2-aminoethoxydiphenyl borate (2-APB) prior to cDDP treatment was investigated. As a control experiment, pre-treatment of A549-WT cells with 10 μM 2-APB for 30 minutes completely inhibited changes in $[Ca^{2+}]_{cyt}$ in A549-WT cells induced by the addition of 100 μM ATP to the external buffer medium, as measured by Fura-2 ($p < 0.05$) (Figure 28)**,** confirming the ability of this agent to block intracellular Ca^{2+} signalling in A549-WT cells. Having validated the action of 2-APB in the present A549 cell model, the potential role of IP_3R-mediated Ca^{2+} release in cDDP-induced cell death was investigated through pharmacological inhibition of the receptor Ca^{2+} channel. A549-WT cells were incubated with 10 μM 2-APB for 30 minutes prior to, and during, treatment with 75 μM cDDP. The percentage of PI positive cells after cDDP treatment over a 24 hour period was not significantly different in control A549-WT cells exposed to cDDP in normal cell culture medium or A549-WT cells pre-treated with 10 μM 2-APB prior to drug treatment (48.6 ± 9.3% vs. 46.9 ± 0.1% respectively) (Figure 29), demonstrating IP_3R mediated Ca^{2+} release is not required for cell death induction by cDDP in the A549-WT cell line.

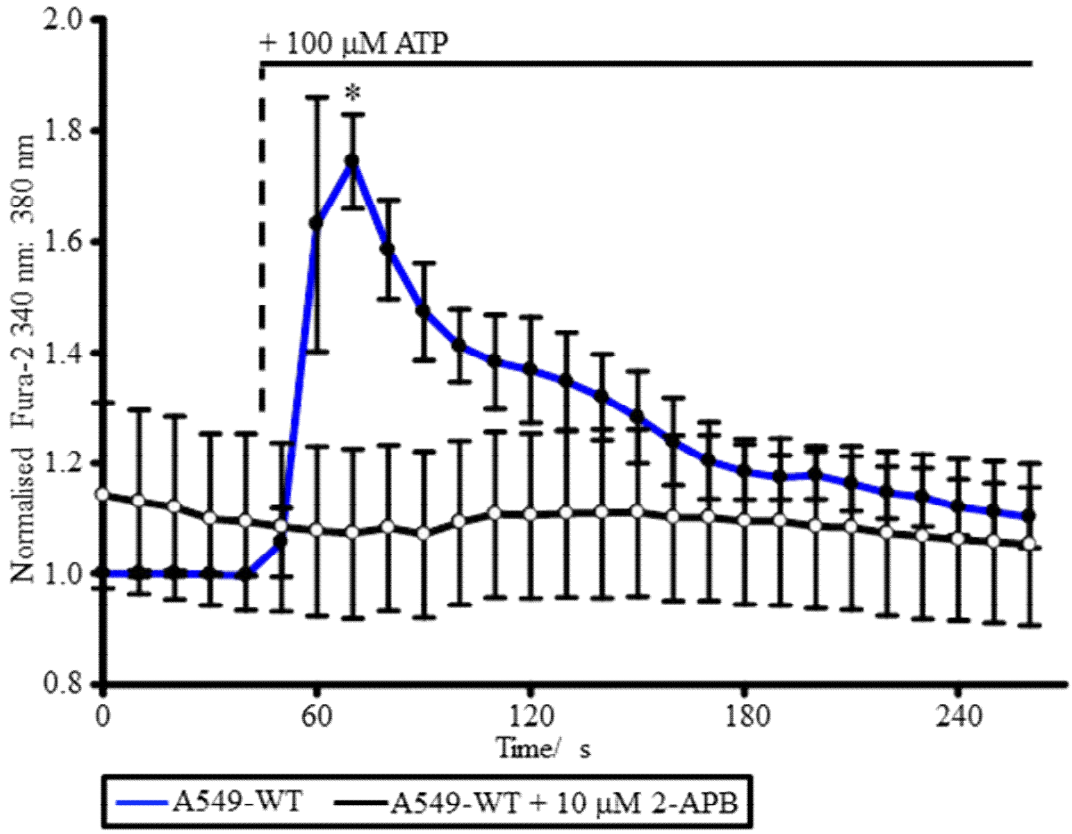

Figure 28: 2-APB prevents agonist-induced Ca^{2+} signalling in A549-WT cells. A549-WT cells loaded with Fura-2 were challenged with 100 µM ATP. Cells treated with 2-APB were pre-incubated with 10 µM 2-APB for 15 minutes prior to ATP challenge. Traces were normalised relative to non-treated A549-WT cells and represent the mean of three independent experiments ± S.E.M. * $p < 0.05$.

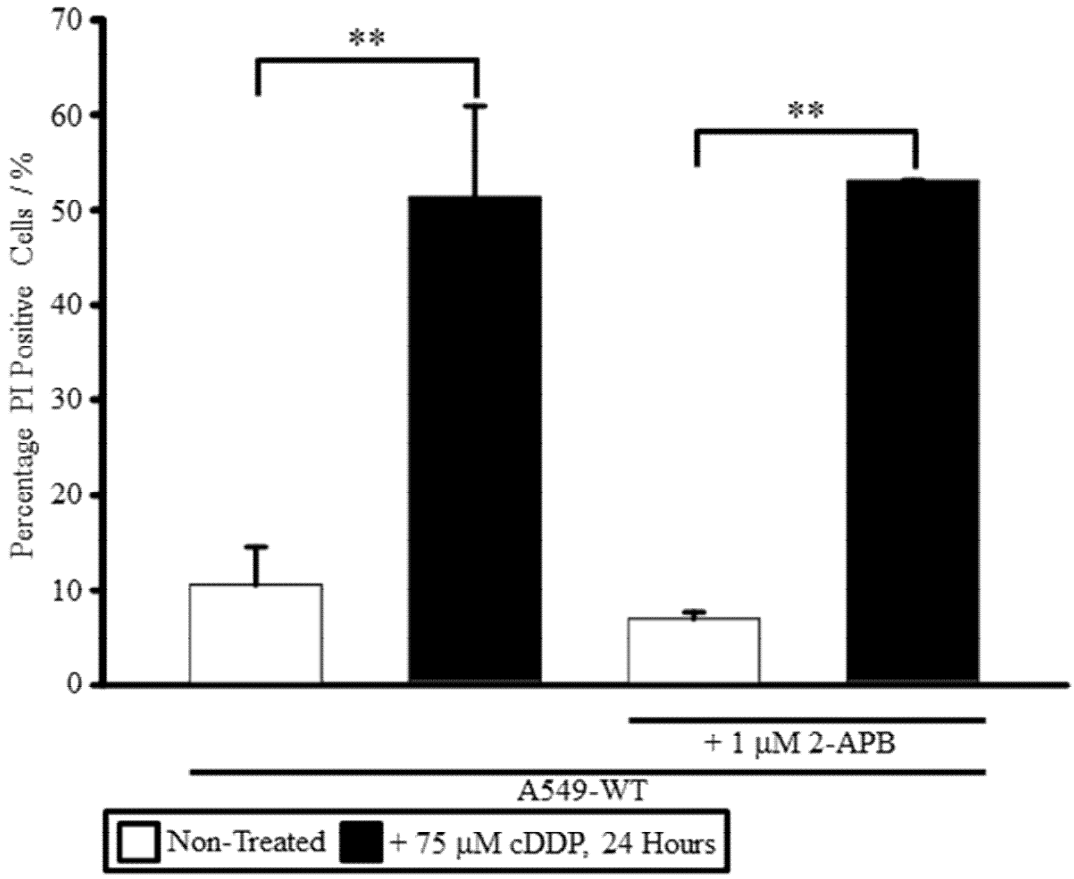

Figure 29: 2-APB does not inhibit cDDP-induced cytotoxicity in A549-WT cells. A549-WT cells were incubated in normal cell culture medium or in normal cell culture medium + 75 µM cDDP for 24 hours and cytotoxicity assayed by PI exclusion as outlined in *'Methods 2.4'*. Where indicated, cells were pre-incubated with 10 µM 2-APB for 15 minutes prior to cDDP addition. Data represent the mean of three independent experiments + S.E.M.

3.3 Mitochondrial Function and cDDP-Sensitivity

3.3.1 Cellular Level of GSH Tripeptide Does Not Differ Between A549-WT Cells and A549-CR Cells

Although cell death induced by cDDP in A549-WT cells does not depend upon increased ROS production, A549-CR cells produced ROS at a significantly reduced rate following 24 hours exposure to 75 µM cDDP compared to A549-WT cells under the same conditions, potentially indicating that decreased ROS production may be a secondary result of another adaptation in A549-CR cells. Increased cellular levels of GSH, a major cytosolic and mitochondrial antioxidant peptide which may directly bind cDDP, is a recognised mechanism of tumour cell cDDP resistance which might also explain the difference in the rate of ROS production observed between A549-WT and A549-CR cells. However, no significant difference in fluorescence intensity was measured in A549-WT and A549-CR cells loaded to saturation with 50 mM MCB (Figure 30), indicating that the basal cellular GSH pool is similar in both cell types. Furthermore, incubation of A549-WT and A549-CR cells with 75 µM cDDP for 24 hours caused a comparable small significant decrease of approximately 5% in MCB fluorescence ($p < 0.01$) (Figure 30), thus increased ROS production following cDDP treatment is not due to a greater depletion of GSH in A549-WT cells than in A549-CR cells. Control A549-WT cells pre-incubated with 50 mM DEM for 15 minutes to deplete the cellular GSH pool showed a significant decrease of approximately 40% in MCB fluorescence ($p < 0.01$) (Figure 30), demonstrating that MCB may reliably detect changes in GSH in A549 cells.

3.3 Mitochondrial Function and cDDP-Sensitivity

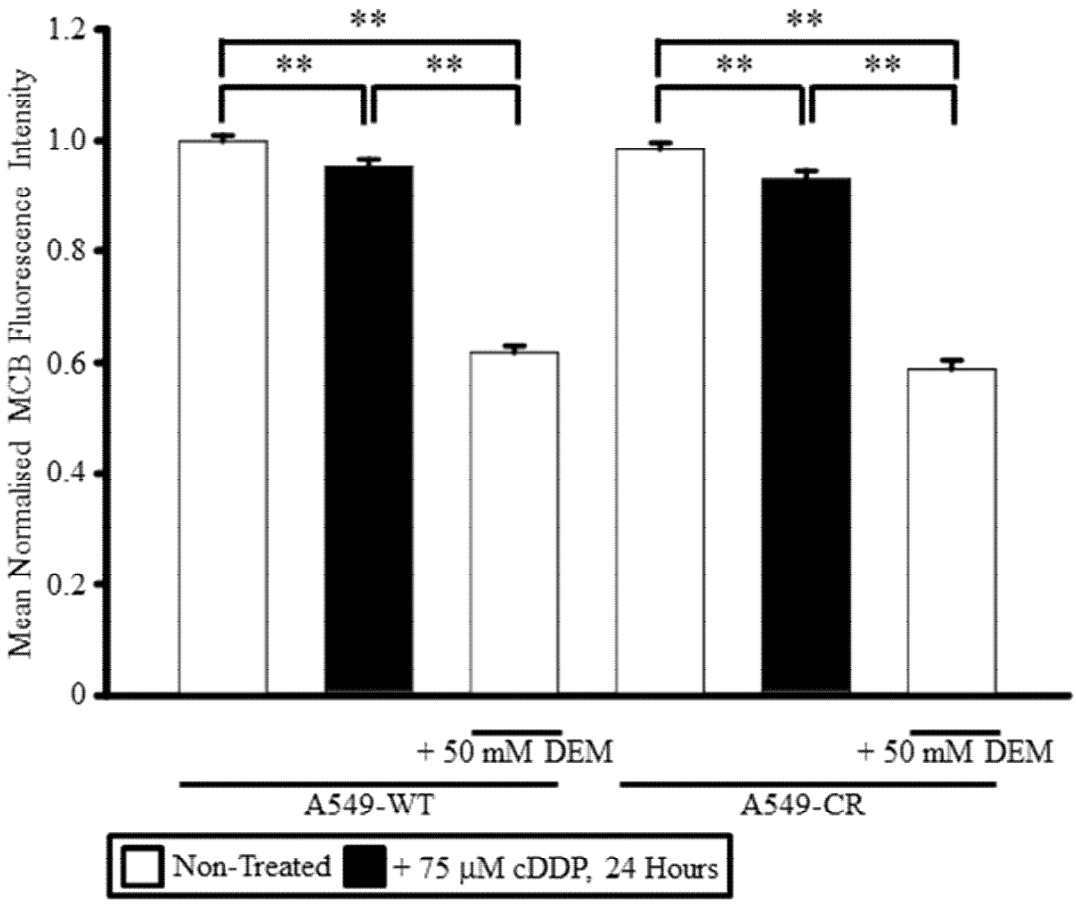

Figure 30: MCB fluorescence intensity does not differ between A549-WT cells and A549-CR cells. A549-WT cells were incubated in normal cell culture medium or in normal cell culture medium + 75 µM cDDP for 24 hours**,** and cellular GSH measured as the intensity of fluorescence in cells loaded with 50 µM MCB for one hour following the incubation period. Control A549-WT cells were incubated with 50 mM DEM for 15 minutes prior to MCB loading. Data were normalised relative to non-treated A549-WT cells and represent the mean of three independent experiments + S.E.M. * $p < 0.05$.

3.3 Mitochondrial Function and cDDP-Sensitivity

3.3.2 Mitochondrial Function Does Not Differ Between A549-WT and A549-CR Cells

Mitochondria are the major source of intracellular ROS generation, and are closely linked to cell fate, thus the difference in the rate of ROS production in A549-WT and A549-CR cells after cDDP treatment may be indicative of altered mitochondrial function. This possibility was investigated through comparison of functional state of mitochondria in A549-WT and A549-CR cells without exposure to cDDP, measuring the parameters of $\Delta\Psi$ and cellular O_2 consumption. No significant difference was observed in the mean fluorescence signal measured in A549-WT and A549-CR cells loaded with 50 nM TMRM, indicating that basal $\Delta\Psi$ before exposure to cDDP is comparable in both cell types (Figure 31). Similarly, the rate of cellular O_2 consumption and the degree of respiratory uncoupling in mitochondria measured with a Clark-type electrode did not differ significantly between A549-WT and A549-CR cells which had not been incubated with cDDP (Figure 32 & Table 4). Therefore, the basal activity of mitochondria in A549-WT and A549-CR cells is comparable before exposure to cDDP.

3.3 Mitochondrial Function and cDDP-Sensitivity

A

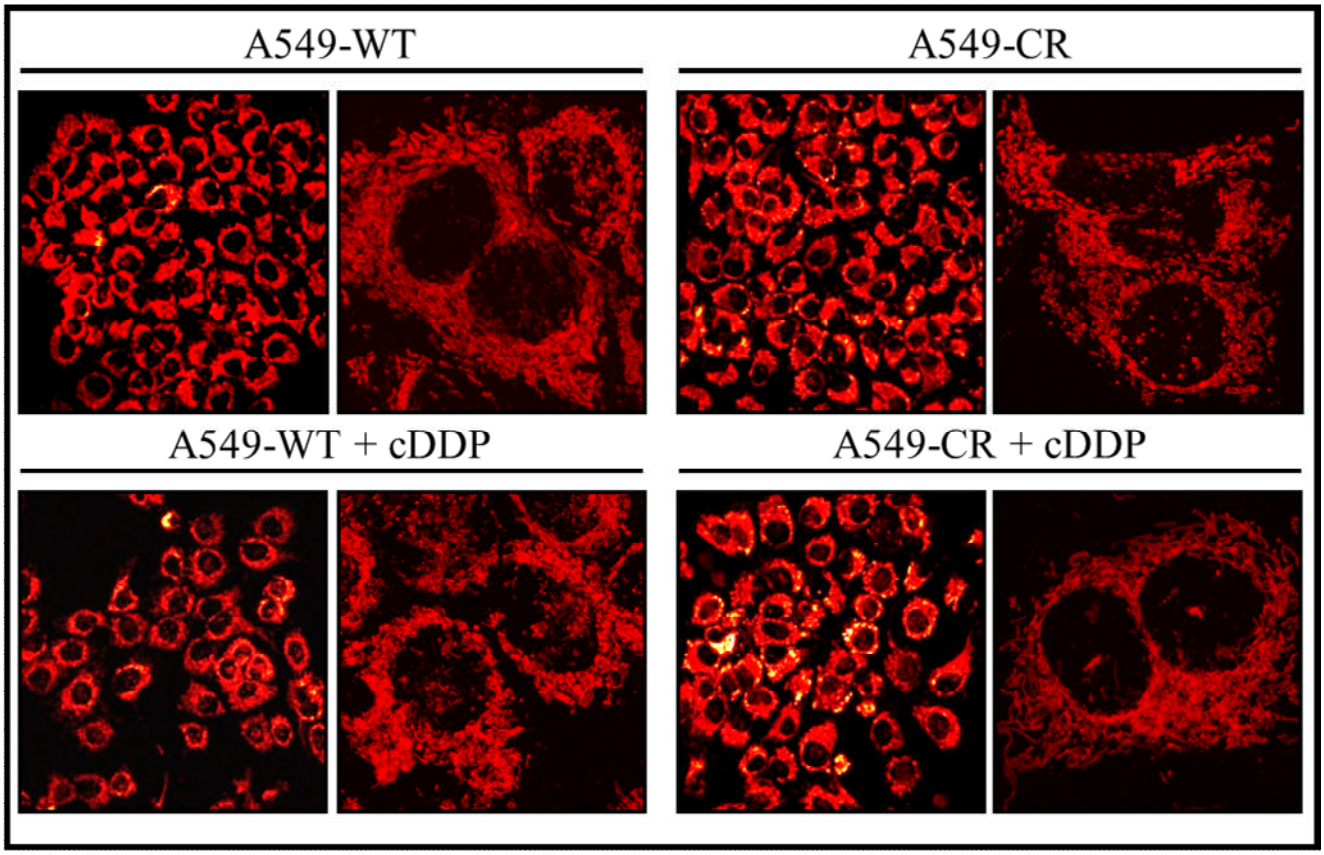

B

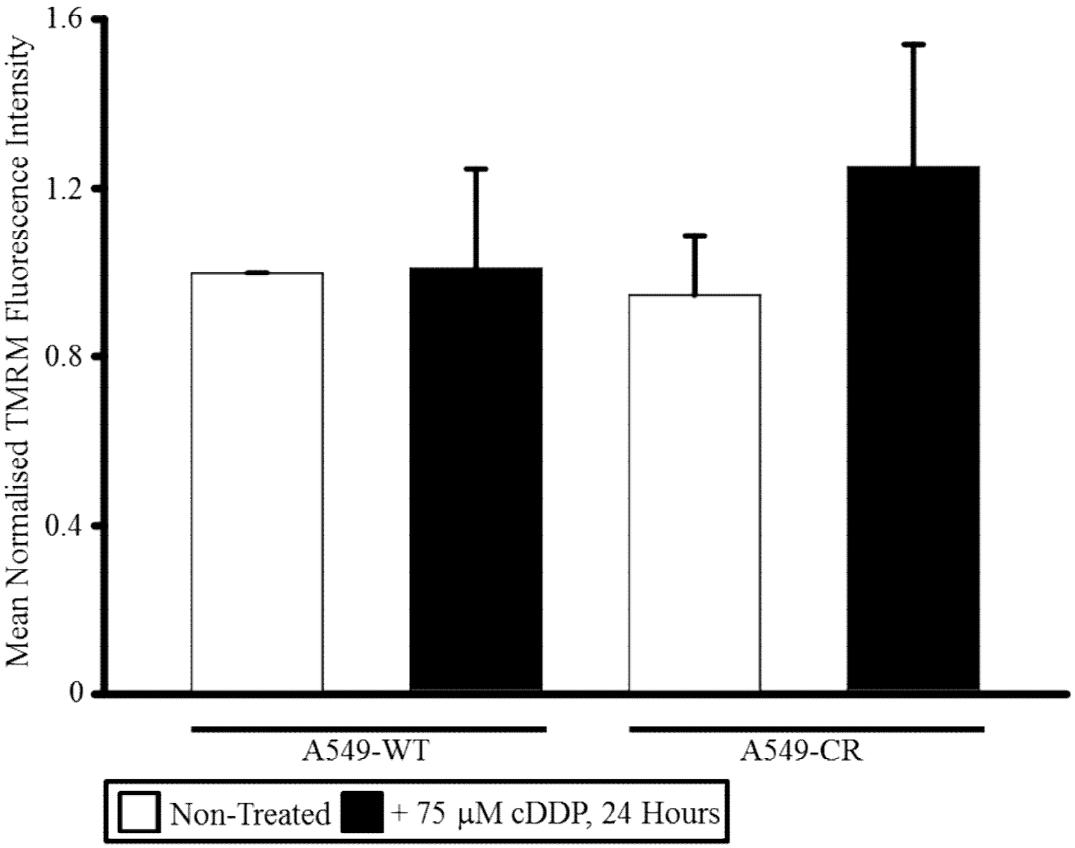

3.3 Mitochondrial Function and cDDP-Sensitivity

Figure 31: ΔΨ does not differ between A549-WT cells and A549-CR cells. A549-WT cells and A549-CR cells were incubated in normal cell culture medium or in normal cell culture medium + 75 µM cDDP for 24 hours**,** and ΔΨ measured as the intensity of fluorescence in maximal confocal projections of cells loaded with 50 nM TMRM. Data were normalised relative to non-treated A549-WT cells and represent the mean of three independent experiments + S.E.M.

3.3 Mitochondrial Function and cDDP-Sensitivity

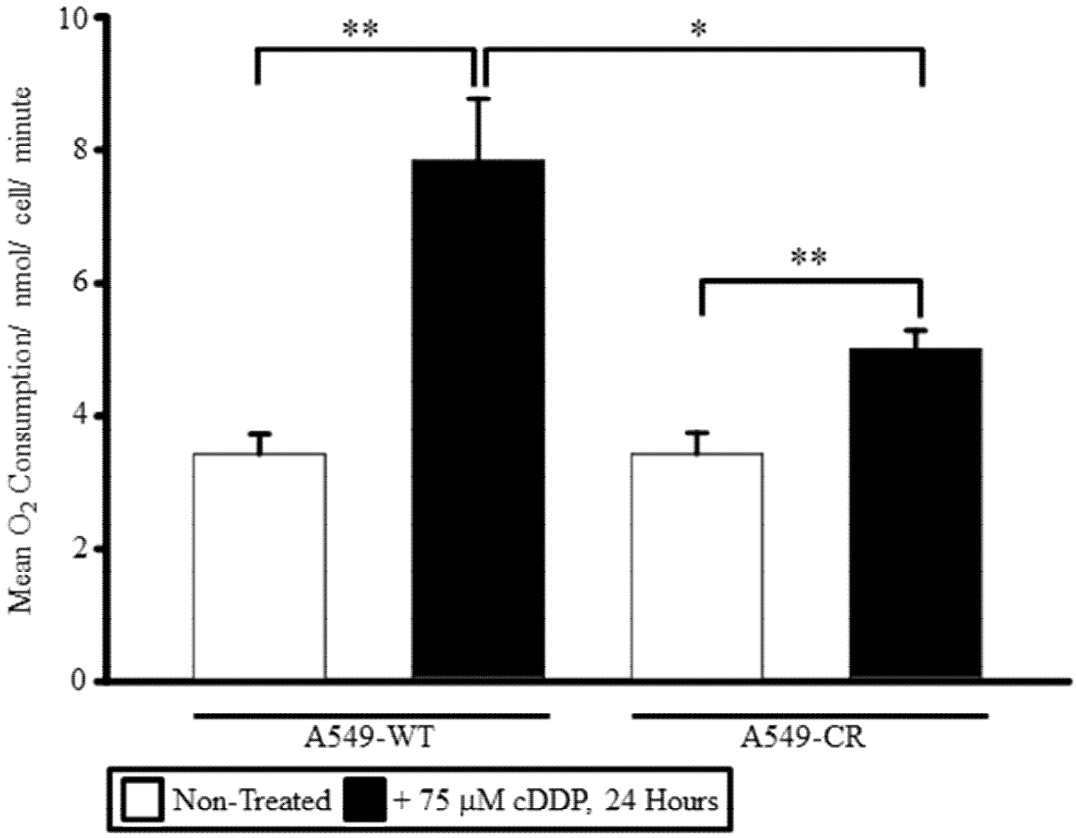

Figure 32: Cellular O_2 consumption is increased in A549-WT cells and A549-CR cells following cDDP treatment. A549-WT and A549-CR cells were cultured in 6 well tissue culture plates for 24 hours in normal cell culture medium or normal cell culture medium + 75 µM cDDP. O_2 consumption was measured using a Clark type electrode at 37 ^{o}C and normalised relative to the number of cells present during the assay. Data represent the mean of three independent experiments + S.E.M. * $p < 0.05$. ** $p < 0.01$.

3.3 Mitochondrial Function and cDDP-Sensitivity

Table 4: The ratio of cellular O_2 consumption due to uncoupled respiration : basal cellular O_2 consumption does not differ between A549-WT cells and A549-CR cells under normal growth conditions or following exposure to cDDP. A549-WT cells and A549-CR cells were incubated in normal cell culture medium or in normal cell culture medium + 75 µM cDDP for 24 hours**.** O_2 consumption was measured using a Clark type electrode at 37 ^{o}C, and O_2 consumption not due to oxidative phosphorylation was measured following the addition of 7 µM oligomycin. Data were normalised relative to the number of cells present during the assay.

	A549-WT		**A549-WT + cDDP**		**A549-CR**		**A549-CR + cDDP**	
	Mean	*S.E.M.*	*Mean*	*S.E.M.*	*Mean*	*S.E.M.*	*Mean*	*S.E.M.*
Basal O_2 Consumption/ nmol/cell/minute	3.43	0.29	7.84	0.92	3.43	0.39	5.00	0.29
Uncoupled O_2 Consumption/ nmol/cell/minute	2.26	0.26	5.70	0.81	1.80	0.24	3.39	0.35
Ratio 'Uncoupled : Basal'	0.71	0.14	0.75	0.10	0.54	0.08	0.68	0.06

3.3 Mitochondrial Function and cDDP-Sensitivity

3.3.3 cDDP Treatment Induces Increased Cellular Oxygen Consumption in A549-WT and A549-CR Cells

A marked difference in the rate of intracellular ROS production was observed between A549-WT and A549-CR exposed to cDDP, thus the functional state of mitochondria in A549-WT and A549-CR cells incubated with 75 µM cDDP for 24 hours was investigated, again measuring the parameters of $\Delta\Psi$ and cellular O_2 consumption. No significant difference was observed in the mean fluorescence signal measured in A549-WT and A549-CR cells loaded with 50 nM TMRM following cDDP treatment, indicating that $\Delta\Psi$ was comparable in both cell types (Figure 32). Likewise, incubation with cDDP did not significantly alter the degree of respiratory uncoupling in either A549-WT cells or A549-CR cells. However, the rate of cellular O_2 consumption was significantly increased in A549-WT cells following incubation with cDDP compared to A549-WT cells not treated with cDDP (7.84 ± 0.92 nmol O_2 / cell / minute vs. 3.43 ± 0.29 nmol O_2 / cell / minute, $p < 0.01$) (Figure 32). A similar, although less pronounced, effect was measured in A549-CR cells in which the rate of cellular O_2 consumption was significantly increased following incubation with cDDP compared to A549-CR cells not treated with cDDP (5.00 ± 0.29 nmol O_2 / cell / minute vs. 3.43 ± 0.31 nmol O_2 / cell / minute, $p < 0.01$) (Figure 32). The rate of cellular O_2 consumption was significantly greater in A549-WT cells incubated with cDDP than in A549-CR cells incubated with cDDP ($p < 0.05$). Treatment with cDDP therefore increased mitochondrial oxidative activity in both A549-WT and A549-CR cells.

3.3.4 cDDP Treatment Increases Maximal Cellular Oxidative Capacity Only in A549-WT Cells

Treatment with cDDP induced a significant increase in basal cellular O_2 consumption in both A549-WT and A549-CR cells. The maximal rate of mitochondrial oxidative activity was also determined in A549-WT and A549-CR cells before and after 24 hours incubation with 75 µM cDDP by measuring cellular O_2 consumption in the presence of 2 µM FCCP. No significant difference was measured in the maximal rate of mitochondrial oxidative activity between A549-WT and A549-CR cells without exposure to cDDP (Figure 33). Treatment with cDDP increased the maximal rate of mitochondrial oxidative activity in A549-WT cells compared to control A549-WT cells not exposed to cDDP (7.58 ± 0.78 nmol O_2 / cell / minute vs. 4.01 ±

0.55 nmol O_2 / cell / minute, $p < 0.01$), however no significant difference was observed in the maximal rate of mitochondrial oxidative activity in A549-CR cells with or without cDDP treatment (Figure 33).

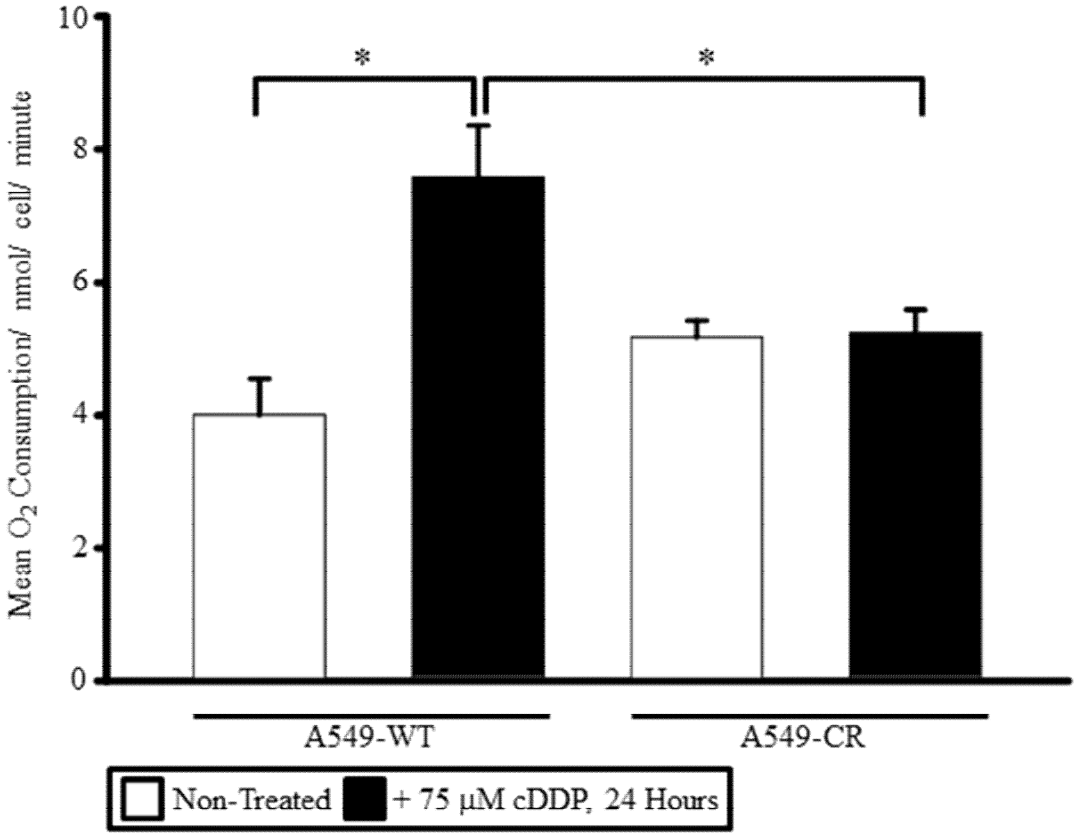

Figure 33: Maximal cellular oxidative capacity is increased in A549-WT cells, but not A549-CR cells, following cDDP treatment. A549-WT cells and A549-CR cells were incubated in normal cell culture medium or in normal cell culture medium + 75 µM cDDP for 24 hours. The maximal cellular oxidative capacity was measured after addition of 2 µM FCCP to uncouple the ETC. O_2 consumption rates were normalised relative to the number of cells present during the assay. Data represent the mean of three independent experiments + S.E.M. * $p < 0.05$.

3.3 Mitochondrial Function and cDDP-Sensitivity

3.3.5 mtDNA Copy Number is Increased Following cDDP Treatment

Comparable cellular O_2 consumption and $\Delta\Psi$ was measured in both A549-WT cells and A549-CR cells, whilst 24 hours incubation with 75 µM cDDP caused a significant increase in cellular O_2 consumption in both cell types. However, this increase was significantly more pronounced in A549-WT cells, and, unlike A549-WT cells, no increase in the total oxidative capacity of A549-CR cells was observed after cDDP treatment. Since the maximal rate of cellular O_2 consumption measured with a Clark-type electrode after addition of FCCP reflects the maximal activity of the mitochondrial respiratory chain, the difference in mitochondrial activity after cDDP treatment, and between the A549-WT and A549-CR cell lines, may be due to differences in the relative expression level of respiratory chain components. As key subunits of the respiratory chain are encoded by the mitochondrial genome, the mtDNA copy number of A549-WT cells and A549-CR cells was determined by RT-qPCR after 24 hours incubation in normal cell culture medium or in normal cell culture medium + 75 µM cDDP. No significant difference in mtDNA copy number was measured between A549-WT cells or A549-CR cells maintained in normal cell culture medium (Figure 34). Following incubation with cDDP, mtDNA copy number was significantly increased by approximately 40% in A549-WT cells ($p < 0.01$) and increased by approximately 60% in A549-CR cells ($p < 0.01$), relative to non-treated A549-WT control cells and non-treated A549-CR control cells respectively (Figure 34). The increase in mtDNA copy number in A549-CR cells was significantly greater than that in A549-WT cells ($p < 0.05$).

3.3 Mitochondrial Function and cDDP-Sensitivity

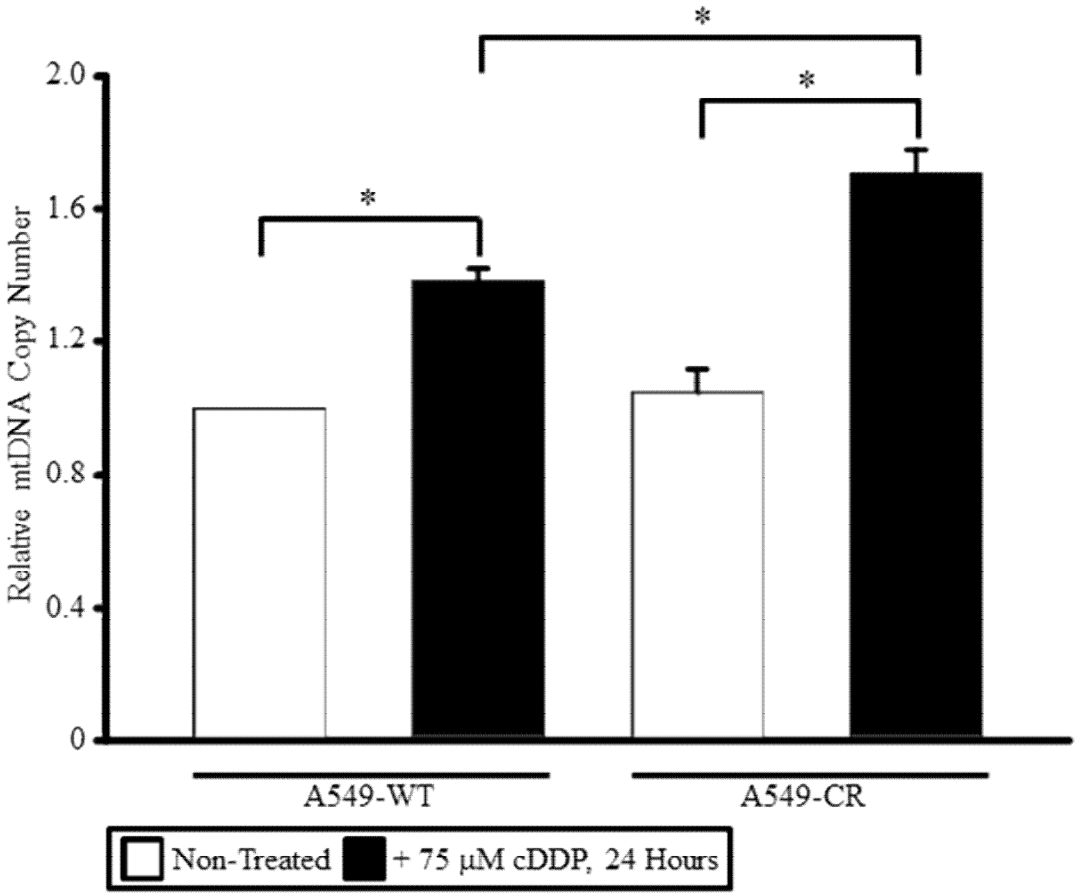

Figure 34: cDDP treatment results in increased mtDNA copy number. A549-WT cells were incubated in normal cell culture medium or in normal cell culture medium + 75 µM cDDP for 24 hours, and mtDNA copy number determined relative to β-actin gene abundance by RT-qPCR. Data were normalised to non-treated A549-WT cells, and represent the mean of seven independent experiments + S.E.M. * $p < 0.05$.

3.3 Mitochondrial Function and cDDP-Sensitivity

3.3.6 Expression of Mitochondrial Respiratory Complex I is Increased in A549-CR Cells Relative to A549-WT Cells

Treatment with cDDP increased the mtDNA copy number in both A549-WT cells and A549-CR cells. This replication of DNA might have been accompanied by increased expression of genes encoding respiratory chain components, and potentially result in increased cellular oxygen consumption following cDDP exposure. To investigate this possibility, the abundance of mitochondrial respiratory complexes was determined by immunoblotting using an antibody cocktail reactive towards single subunits of complex I, complex II, complex III, complex IV and ATP synthase (Figure 35 A). Importantly, each selected subunit is highly labile and rapidly degraded if not assembled into the full complex, thus the abundance of these subunits reflects the abundance of the entire respiratory complex.

A significant increase of approximately 50% in the abundance of respiratory complex I was measured in A549-CR cells relative to A549-WT cells ($p < 0.05$) (Figure 35 B). Notably, a similar strong increasing trend in A549-CR cells in comparison to A549-WT cells was observed in the relative abundance of respiratory complex IV, although this difference was not calculated to be significant ($p = 0.06$). The abundance of respiratory complexes I – IV was not significantly different following 24 hours incubation with 75 µM cDDP in A549-WT cells or A549-CR cells compared to non-treated control A549-WT cells and non-treated control A549-CR cells respectively. Treatment with cDDP resulted in a significant increase of approximately 40% in the abundance of ATP synthase in A549-WT cells relative to non-treated controls, but did not cause changes in ATP synthase abundance in A549-CR cells (Figure 35 B).

3.3 Mitochondrial Function and cDDP-Sensitivity

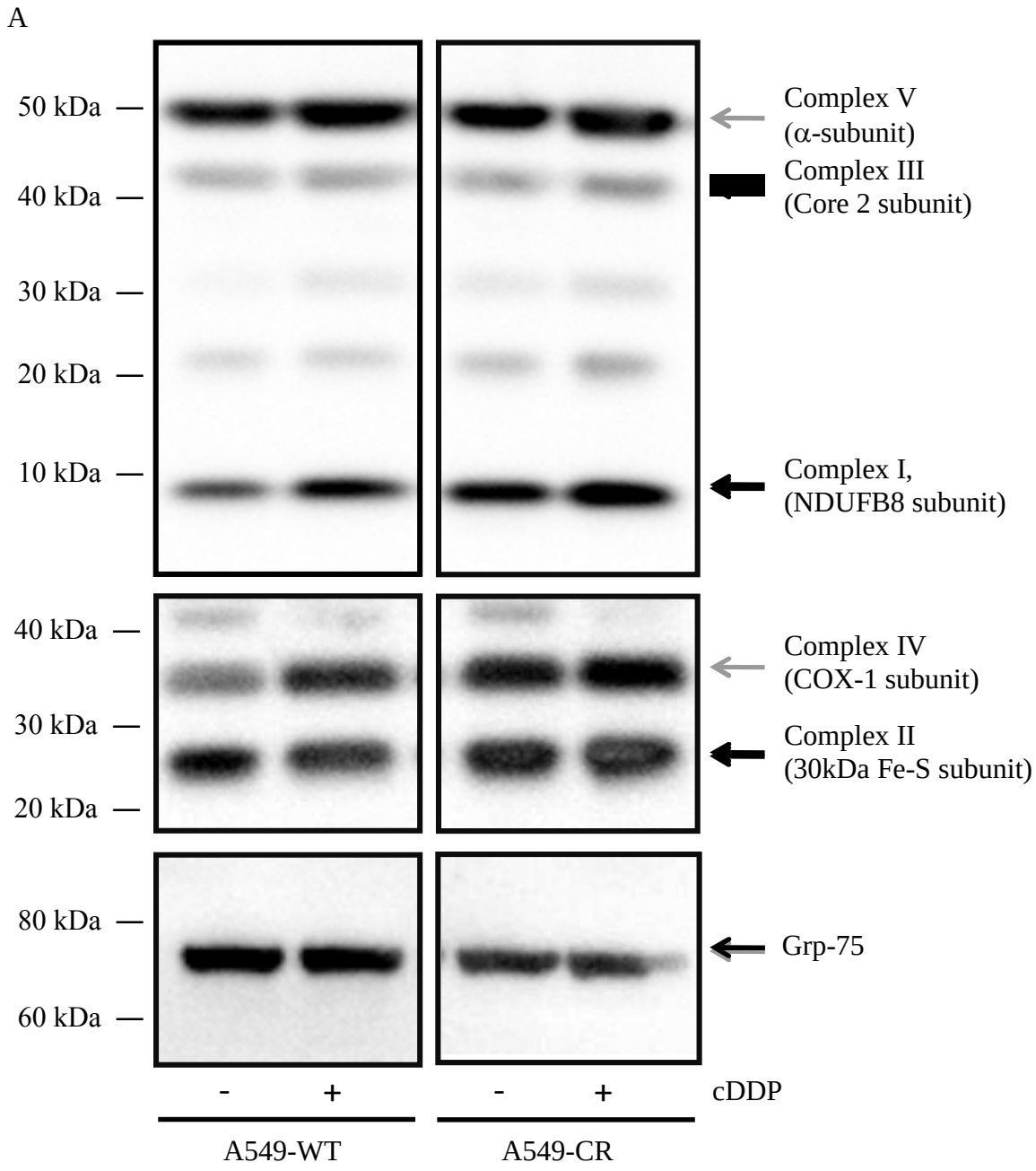

3.3 Mitochondrial Function and cDDP-Sensitivity

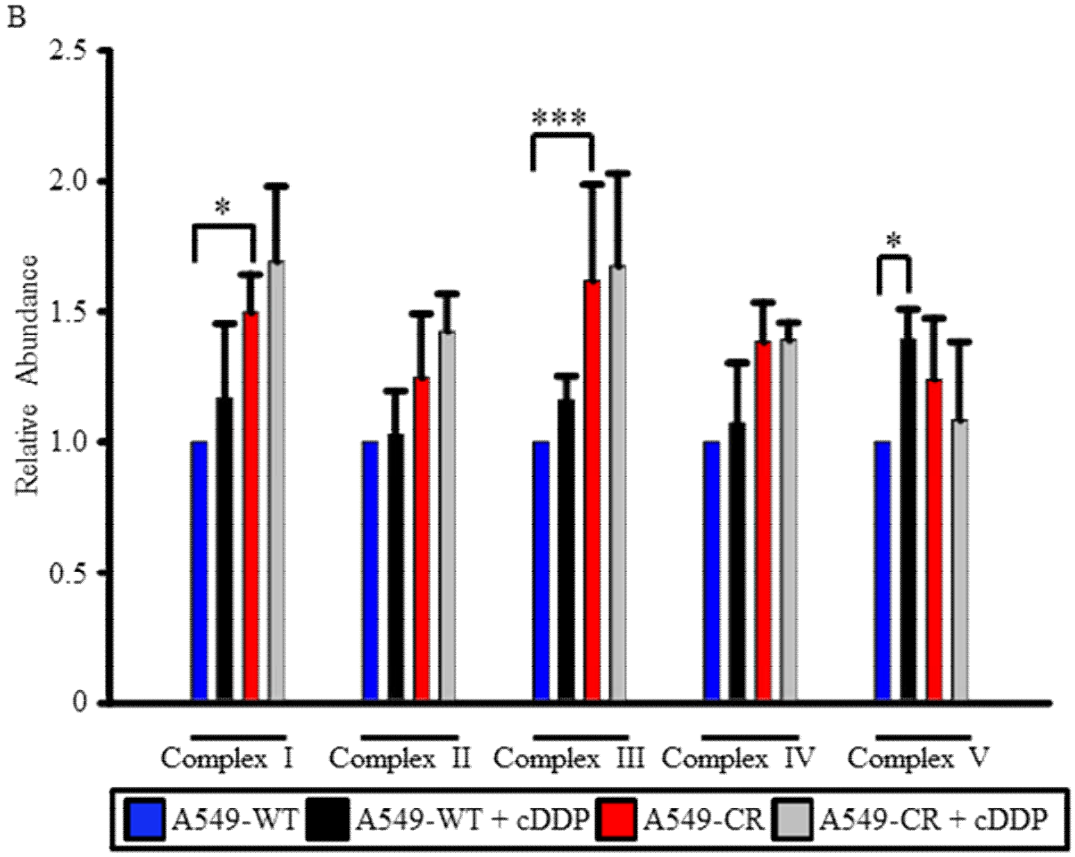

Figure 35: Expression of mitochondrial respiratory complex I is increased in A549-CR cells relative to A549-WT cells. A549-WT cells and A549-CR cells were incubated in normal cell culture medium or normal cell culture medium + 75 µM cDDP for 24 hours, and the relative abundance of mitochondrial respiratory complexes determined by western blot. (A) Representative western blot and (B) quantification for single subunits of mitochondrial respiratory complexes I – IV and ATP synthase, indicative of the abundance of the entire complex. Complex abundance data were normalised relative to non-treated A549-WT cells, and represent the mean of five sets of samples from three independent experiments + S.E.M. * $p < 0.05$. *** $p = 0.06$.

3.3 Mitochondrial Function and cDDP-Sensitivity

3.3.7 Novel Point Mutations are Present in the mtDNA of A549-CR Cells

Although the level expression of mitochondrial respiratory complexes was consistently increased in A549-CR cells compared to the A549-WT cell line, basal mitochondrial function did not differ, and cDDP induced changes in cellular O_2 consumption and maximal oxidative capacity were significantly less prominent in A549-CR cells. Mutations in mtDNA have previously been associated with both tumourigenesis and cancer cell resistance to chemotherapy, and may reduce the activity of the mitochondrial respiratory chain. To determine whether such changes contributed to the differences observed in mitochondrial oxidative activity between A549-WT and A549-CR cells, the mtDNA sequence of both cell types was determined using Mitochip V 2.0 sequencing (Affymetrix). Variation from the revised Cambridge mtDNA Reference Sequence (rCRS) was detected at a total of eighteen points in A549-WT cell mtDNA and 24 points in A549-CR cell mtDNA (Appendix III Table 1). Of these variations: sixteen point mutations were common to both A549-WT and A549-CR mtDNA, representing previously reported SNPs in either the test samples or reference sequence; one previously unreported point mutation was detected in the *MT-ND5* gene of A549-WT cells but not in A549-CR cells; three previously reported SNPs were detected in the D-loop region of A549-CR mtDNA but not A549-WT mtDNA; five previously unreported point mutations, one in the D-loop region and three in the *MT-CYTB* gene, were detected in A549-CR mtDNA but not A549-WT mtDNA, and one previously unreported point mutation was detected in the *MT-ND2* gene of both cell types, existing in heteroplasmy in A549-WT mtDNA and homoplasmy in A549-CR mtDNA. Mitochip sequencing thus identified six previously unreported variations present in A549-CR mtDNA but not A549-WT mtDNA (Table 5).

Sanger sequencing was used to further confirm the six A549-CR mtDNA variants present only in A549-CR cells identified by Mitochip sequencing. D-loop point mutation 225G>T and *MTND2* point mutation 4587T>C were both confirmed as correct. However, each of the four point nucleotides identified as potential novel varients in the *MT-CYTB* gene in A549-CR cells were identical to rCRS in four replicates, indicating potential Mitochip sequencing errors (Table 6). The mtDNA of A549-CR cells therefore contains two previously unreported variations which might affect respiratory chain function which are not present in the mtDNA of A549-WT cells (Figure 36).

3.3 Mitochondrial Function and cDDP-Sensitivity

Table 5: Previously unreported mtDNA point mutations identified by Mitochip sequencing present in A549-CR cells but not present A549-WT cells. A549-WT cells and A549-CR cells were incubated in normal cell culture medium for 24 hours. Sequence analysis of the mtDNA genome was performed using Mitochip V2.0 following PCR amplification of mtDNA as described in '*Methods 2.20*'. Italics = deviation from revised Cambridge reference sequence. * Exists in heteroplasmy.

rCRS Position	Reference	A549-WT	A549-CR	Gene	Gene Product	Amino Acid Change
225	G	G	*T*	D-Loop	N/A	Non-Coding
4587	T	T / *C* *	*C*	MT-ND2	ND2	Phe 40 Leu
15042	G	G	*A*	MT-CYTB	Cyt b	Gly 99 Glu
15352	A	A	*G*	MT-CYTB	Cyt b	Glu 202 Glu
15656	A	A	*G*	MT-CYTB	Cyt b	Ile 1304 Val
15659	C	C	*T*	MT-CYTB	Cyt b	Pro 305 Ser

3.3 Mitochondrial Function and cDDP-Sensitivity

Table 6: Previously unreported mtDNA point mutations identified by Sanger sequencing present in A549-CR cells but not present A549-WT cells. Primer sets specific to the six regions of mtDNA identified by Mitochip sequencing as containing point mutations present in the A549-CR cell line but not the A549-WT cell line were used to amplify these regions through PCR, and sequencing performed as described in '*Methods 2.21*'. Italics = deviation from revised Cambridge reference sequence. * Exists in heteroplasmy.

rCRS Position	Reference	A549-WT	A549-CR	Gene	Gene Product	Amino Acid Change
225	G	G	*T*	D-Loop	N/A	Non-Coding
4587	T	T / *C* *	*C*	MT-ND2	ND2	Phe 40 Leu
15042	G	G	G	MT-CYTB	Cyt b	N/A
15352	A	A	A	MT-CYTB	Cyt b	N/A
15656	A	A	A	MT-CYTB	Cyt b	N/A
15659	C	C	C	MT-CYTB	Cyt b	N/A

3.3 Mitochondrial Function and cDDP-Sensitivity

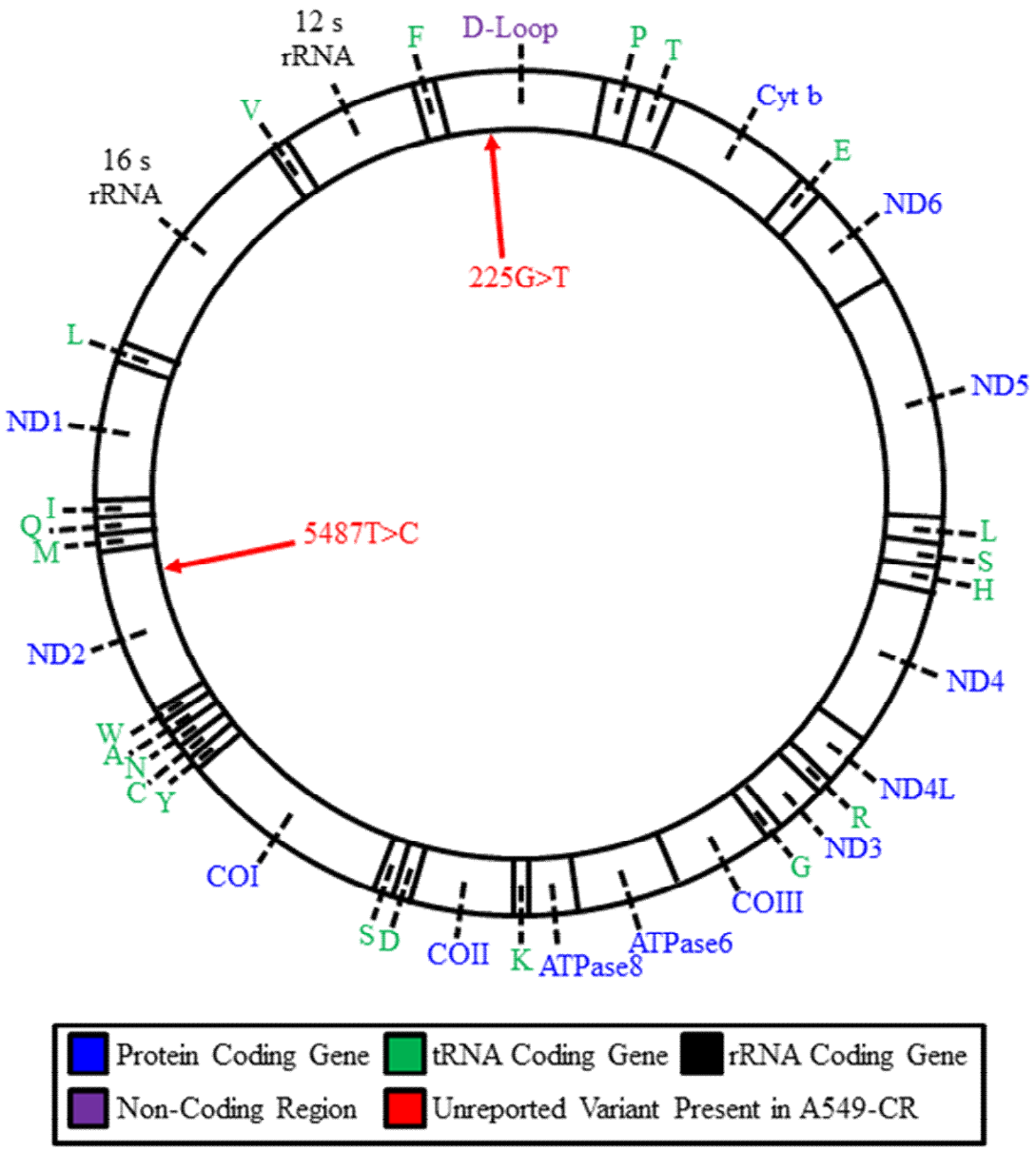

Figure 36: Schematic representation of previously unreported mtDNA point mutations present in A549-CR cells but not present in A549-WT cells. Of six previously unreported mutations as determined by Mitochip sequencing and Sanger sequencing, one mapped to the non-coding D-loop region, one mapped to the *MT-ND2* gene and four mapped to the *MT-CYTB* gene.

3.3 Mitochondrial Function and cDDP-Sensitivity

3.3.8 Rotenone Sensitive Respiratory Complex I Activity is Decreased in A549-CR Cells Relative to A549-WT Cells

Several novel mtDNA mutations which may affect respiratory chain activity were found to be present in A549-CR cells but absent in A549-WT cells. Intruigingly, one previously unreported point mutation was found to be present in the respiratory complex I *MT-ND2* gene in heteroplasmy in A549-WT cells but in homoplasmy in A549-CR cells, whilst the abundance of complex I was increased by approximately 50% in A549-CR cells relative to A549-WT cells. The effects of this mutation were thus investigated by measuring both the rotenone-insensitive and rotenone-sensitive activity of mitochondrial respiratory complex I in A549-WT cells and A549-CR cells.

Rotenone-insensitive complex I activity was measured using MitoSciences Microplate Assay for Human Complex I Activity. This assay measures the rate of increase of absorbance in the assay solution due to reduction of a chemical dye which acts as a H^+ acceptor during NADH oxidation by immunocaptured complex I. The reaction is not dependent upon successful transfer of an electron through the respiratory complex to ubiquinone, thus acts as a measure of only the NADH dehydrogenase type activity of complex I. No significant difference in the rate of increase in absorbance due to dye reduction was observed between A549-WT and A549-CR cells, indicating complex I NADH dehydrogenase activity was not altered (Figure 37). The rate of dye reduction by immunocaptured respiratory complex I isolated from mtDNA deficient A549 Rho-0 cells was less than 20% of that measured in A549-WT cells and A549-CR cells (Figure 37). Thus, no difference exists in the rotenone-insensitive activity of respiratory complex I in A549-WT cells and A549-CR cells.

Rotenone-sensitive complex I activity was measured by calculating the change in the rate of NADH oxidation, measured by absorbance at 340 nm in a spectrophotomter, after addition of rotenone to the assay solution. NADH oxidation in this assay depends upon successful transfer of electrons to Ubq, present in excess, thus acts as a measure of the overall activity of complex I. The difference in the rate of change in absorbance at 340 nm following addition of rotenone was significantly greater in A549-WT cell lysates than that measured in A549-CR cell lysates (3.19 ± 0.46 nmol/ minute/ ml/ µg vs 1.67 ± 0.18 nmol/ minute/ ml/ µg, $p < 0.05$) (Figure 38), indicating that rotenone-sensitive respiratory complex I activity is reduced in A549-CR cells relative to A549-WT cells.

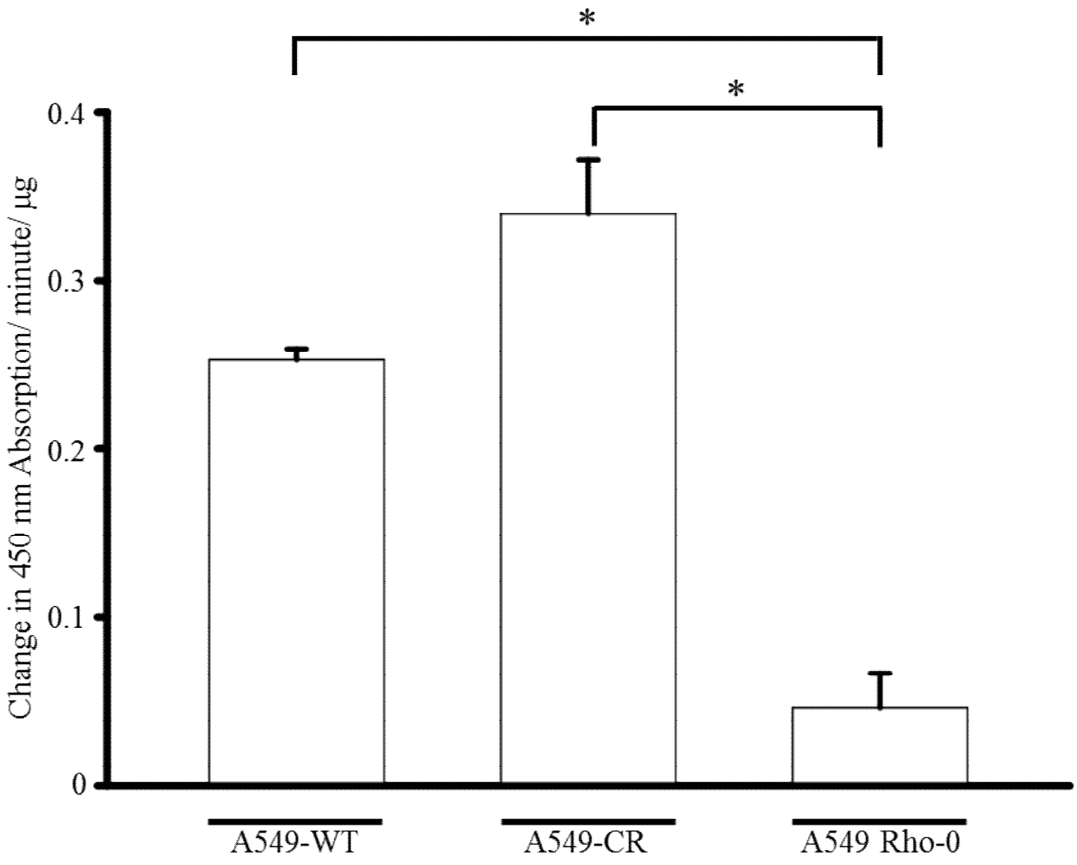

Figure 37: No difference exists in the rotenone-insensitive NADH oxidase activity of respiratory complex I between A549-WT cells and A549-CR cells. A549-WT cells and A549-CR cells were incubated in normal cell culture medium or normal cell culture medium + 75 µM cDDP for 24 hours, and the activity of immunocaptured respiratory complex I determined using MitoSciences Microplate Assay for Human Complex I Activity. The rate of increase in absorbance of the assay solution, dependent upon complex I activity, was monitored for 30 minutes. Data represent the mean of three independent experiments+ S.E.M.

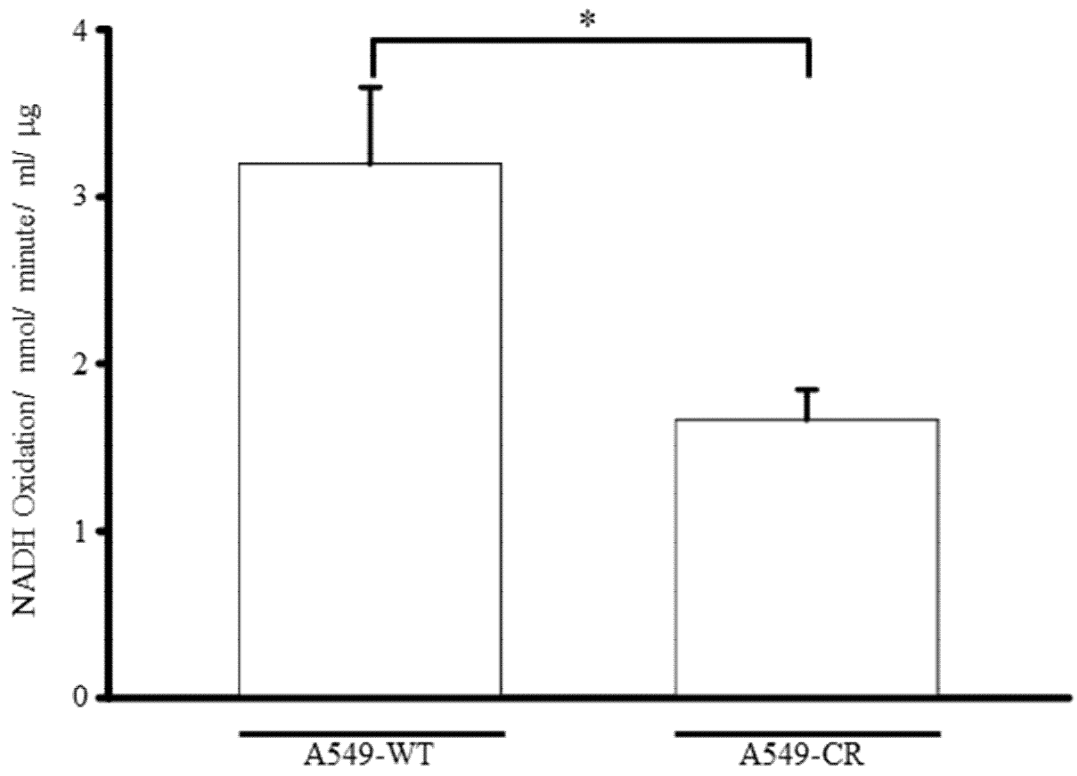

Figure 38: Rotenone-sensitive complex I activity is inhibited in A549-CR cells relative to A549-WT cells. The activity of immunocaptured respiratory complex I determined as described in *'Methods 2.17'* from A549-WT cells and A549-CR cells maintained in normal cell culture medium. The decrease in the rate of NADH oxidation in the presence of excess ubiquinone following addition of rotenone to cell lysates was determined using a spectrophotometer. Data represent the mean of three independent experiments+ S.E.M. * $p < 0.05$.

4. Discussion

4.1 In Vitro Modelling of cDDP Cytotoxicity and Resistance Using A549 Cells

Although cDDP remains a mainstay of chemotherapy regimes, the precise mechanisms which underpin the antineoplastic effects of the drug remain unclear (Siddik, 2003). At the subcellular level, cDDP has been observed to act upon a range of targets, including the nucleus, mitochondria, the ER and plasma membrane channels and transporters (Brozovic et al., 2010; Mandic et al., 2003; Martins et al., 2008; Siddik, 2003). The present study has sought to further current knowledge on the contribution of effects outside of the nucleus to cellular response to cDDP, focussed upon the ER and mitochondria, by identifying functional differences in these organelles between two A549 cell lines with differing cDDP sensitivity, before and after cDDP exposure. The A549 cell line is well characterised and established as an *in vitro* model, derived from a clinically relevant tumour type, for studying both cDDP cytotoxicity and tumour drug resistance (Beleford et al., 2010; Brozovic et al., 2010; Giard et al., 1973; Liu et al., 2008).

The LD_{50} of cDDP over 24 hours drug treatment in A549-WT cells was determined to be 75 µM, whilst A549-CR cells displayed approximately two-fold cDDP resistance at this concentration (Figure 4). Although a drug concentration of 75 µM is significantly greater than clinical estimates of cDDP concentration within tumour cells, approximately 10 µM (Puig et al., 2008), *in vitro* studies of cDDP using cell lines commonly require increased drug concentration, spanning the range 20 µM - 100 µM (Del Bello, Moretti, Gamberucci, & Maellaro, 2007; Dursun et al., 2006; Garrido et al., 2008; Kawai et al., 2006; L. Liu, Xing, & Chen, 2009; Mandic et al., 2003; Splettstoesser et al., 2007). The mean concentration of cDDP used in published studies was recently estimated to be 50 µM (Berndtsson et al., 2007). Use of a drug concentration at the upper end of this range was necessitated by the lack of significant effects on cell survival in either cell type using cDDP concentrations up to and including 20 µM, suggesting a degree of intrinsic resistance in A549-WT cells. A549 cells have previously been reported to show the least sensitivity to cDDP in a panel of lung tumour derived cell lines (J. Chen, Emara, Solomides, Parekh, & Simpkins, 2010) and both results may be considered consistent with the relative resistance to cDDP of NSCLC compared to other tumour types (Stephens & Aigner, 2009). A two-fold level of resistance in A549-CR cells in comparison to A549-WT cells represents a relatively modest change in sensitivity in contrast to some *in vitro* models which may exceed a level of 50 – 100-fold acquired cDDP

resistance, although such modest changes are also reported, and may tally more closely with levels of resistance observed in patients undergoing chemotherapy (Köberle et al., 2010; Siddik, 2003). Treatment of A549-WT cells and A549-CR cells with 75 µM cDDP over a 24 hour period thus provides an appropriate experimental condition, within an accepted concentration range to study cDDP cytotoxicity, at which a clear difference in the response of A549-WT cells and A549-CR cells may be measured.

The cytotoxic effects of cDDP were assessed in this study by measuring the ability of cells under varying drug treatment conditions to exclude the membrane-impermeable fluorescent dye PI, monitoring the loss of plasma membrane integrity associated with necrosis and the latter stages of apoptosis to define a cell as 'live' or 'dead'. It is notable however that such measurements provide only a static indication of the effect of a given drug or treatment on the viability of a cell population at a given time, and do not provide information on long term cellular growth and survival. For example, such methodology does not distinguish between a live cell capable of continued growth and proliferation, a cell in which cell death pathways are delayed but not prevented, a quiescent cell which may resume proliferation and a cell which has lost proliferative ability; in all cases cells will be defined as 'live'. Indeed, combined with the PI exclusion method, the drug concentration(s) required to induce acute apoptosis and/ or prevent further long term cell growth may be identified and compared. Clonogenic survival assays, in which the ability of cells to form proliferating colonies following a period of cDDP exposure is assessed, may therefore be better suited to determine the combined effect of cDDP on A549 cell survival and proliferative potential. Further, such experiments may clarify whether cDDP-resistance in the A549-CR cell line represents delayed cell death or an ability to continue proliferation following cDDP exposure.

4.2 cDDP Induces Caspase-Dependent Apoptosis and Caspase-Independent Cell Death in A549 Cells

Following exposure to cDDP, cell death may occur through multiple routes, including apoptosis and/ or necrosis, dependent upon both the cell type and cDDP concentration under investigation. To determine the mode of cell death induced by the LD_{50} concentration of cDDP used in the present A549 cell model, imaging of both plasma membrane and nuclear morphology was performed at regular intervals throughout the 24 hour drug treatment period on A549-WT cells and A549-CR cells. For both cell lines, the first morphological changes

associated with cell death began to occur approximately six hours after drug addition (Figure 6 D and E). These changes were characterised by decreased cellular volume, a 'rounding' of cellular architecture, irregular plasma membrane structure, condensation and fragmentation of Hoechst-stained nuclei and, in the latter stages, apparent fragmentation of the cell, and as such are consistent with the morphological definition of apoptosis (Galluzzi et al., 2007; Kroemer et al., 2009). *In vitro* treatment with cDDP has previously been widely reported to lead to apoptotic cell death in a range of cell lines, including A549 cells (Del Bello et al., 2007; Alan Eastman, 1999; Kelland, 2007; L. Liu et al., 2008; Mandic et al., 2002; Siddik, 2003), and similar morphological changes in plasma membrane structure in response to cDDP have recently been reported in another lung adenocarcinoma cell line and a human kidney cell line (Liu et al., 2008; Sancho-Martínez, Piedrafita, Cannata-Andía, López-Novoa, & López-Hernández, 2011). Furthermore, whilst the first apoptotic cells appear six hours after cDDP addition, within 12 hours the majority of A549 cells which undergo cell death during the experimental period showed changes in morphology associated with apoptosis. This time-course is again in agreement with previous data from numerous cell models which detected pro-apoptotic signalling, including Bid cleavage and the release of cytochrome *c* and AIF from mitochondria, occurring between six and nine hours post cDDP exposure (L. Liu et al., 2009, 2008; Mandic et al., 2002; Sancho-Martínez et al., 2011). Thus, 75 µM cDDP induces apoptotic cell death in A549-WT cells and A549-CR cells.

Apoptotic cells became evident in both A549-WT cells and A549-CR cells approximately six hours after drug addition. However, by 24 hours post drug addition, apoptotic cells represented a relatively small proportion of A549-CR cells whilst the majority of A549-WT cells showed a degree of morphological changes associated with apoptosis (Figure 6 D and E), in agreement with the difference in cDDP sensitivity measured by PI exclusion (Figure 4). It is notable that apoptotic cells appeared at similar time points in both cell types following cDDP addition, and is indicative of overlapping drug sensitivity. Given that both cell lines represent mixed rather than clonal cell populations, it is possible that a sub-population of A549-CR cells may have undergone selection for continued growth in the presence of low concentrations of cDDP, yet show similar sensitivity to acute apoptosis induced by higher concentrations of cDDP as A549-WT cells. Alternatively, the earliest apoptotic cells may represent those undertaking a cellular process such as DNA replication, which may sensitise the cDDP cytotoxicity and account for the similarities in the initial response to cDDP between the cell lines. It is not clear from the present data whether the cDDP resistant

phenotype of the A549-CR cell line represents insensitivity to the cytotoxic action of the drug or rather a delay in the death process, and would require further cell viability studies at time points beyond 24 hours post drug addition.

The morphology of A549-WT cells following 24 hours of cDDP exposure indicates the majority of cells to be dead or dying (Figure 6 D). As such, cellular measurements taken at this time point may not accurately reflect normal cellular behaviour, as targeting of key regulators of cell metabolism and structure by the apoptotic pathway drastically alters cellular function. Measurements were performed following 24 hours incubation with cDDP as this experimental condition caused loss of plasma membrane integrity measured by PI staining in 50% of A549-WT cells, and a clear two-fold cDDP resistance was observed in A549-CR cells under the same conditions (Figure 4). The reason for the discrepancy in apparent A549-WT cell death at the 24 hour time point measured by FACS analysis or morphological imaging is unknown. It is possible that A549-WT cells enter into the apoptotic pathway by 24 hours, but not all reach the latter stages of apoptosis in which plasma membrane integrity is lost, thus are categorised as 'live' by PI incorporation, or that a proportion of dead cells are lost during cell collection for FACS analysis. The investigation may thus benefit from measurements made at earlier time points following cDDP addition, when an increase in the proportion of PI positive A549 cells may be measured, yet not all cells have undergone changes in cellular structure associated with apoptosis. Indeed, such a methodology may reveal interventions which delay the onset of cDDP-induced apoptosis, and thus may contribute to altered cellular sensitivity to cDDP.

The progression of cells through the stages of the cell cycle is governed by key checkpoints, including those regulated by DNA damage. The efficacy of a given chemotherapy drug in killing cancer cells may vary with the stage of the cell cycle at which a tumour cell is exposed to the drug (Schwartz & Shah, 2005), depending upon its particular mode of action. Such cell cycle specific action necessitates several rounds of administration of chemotherapy in order to eliminate tumour cells which remained in a drug-insensitive phase of the cell cycle during the initial treatment. As an alkylating-like agent, cDDP is considered to be a cell cycle-independent drug, capable of inducing cell death at any stage of the cell cycle (M A Shah & Schwartz, 2001; Siddik, 2003). However, cellular sensitivity to cDDP may vary during the cell cycle, with maximal sensitivity in G1 and declining sensitivity with the onset of S-phase and G2 (Donaldson, Goolsby, & Wahl, 1994; M A Shah & Schwartz, 2001). Cell cycle arrest at G2 may allow for repair of cDDP-DNA adducts and prevent aberrant mitosis, and indeed

abrogation of G2-M phase cell cycle arrest increases the sensitivity of some cell lines to cDDP treatment (Demarcq, Bunch, Creswell, & Eastman, 1994; Siddik, 2003). Cells grown to confluent culture may display a different distribution of the cellular population in the phases of the cell cycle than those at lower density, actively proliferating in the log-phase of cell growth. The initial density of cells during investigation of cDDP-induced apoptosis (Figure 6) may thus have influenced the sensitivity of A549 cells to cDDP treatment, even though cells adopting a mitotic morphology were observed in non-treated cells throughout the 24 hour investigation period (Figure 6C). As such, the investigation of cellular cDDP sensitivity would benefit from being repeated, seeding cells at an initial density which ensures confluence is not reached and the cell culture remains in the log-phase of growth throughout the experimental time period. Furthermore, such data may be extended through synchronising cells at different stages of the cell cycle before cDDP treatment, to investigate whether, and to what degree, the ability of cDDP to induce cell death varies during the cell cycle in the A549 cell line.

Exposure to cDDP prevented cell division in both A549-WT cells and A549-CR cells (Figure 6 and Table 1), consistent with significant accumulation of p53 protein following cDDP treatment in both cell types (Figure 5). This observation matches with previous work linking cDDP treatment, the DNA damage response and cell cycle arrest (reviewed in Siddik, 2003). Although loss of p53 has been linked with both increased sensitivity (Basu & Krishnamurthy, 2010; Fujiwara et al., 1994; Osaki et al., 2000) and increased resistance (R. Brown et al., 1993; Fan et al., 1995; C. L. Johnson, Lu, Huang, & Basu, 2002) of tumour cells to cDDP-induced cell death, the comparable p53 accumulation in A549-WT cells and A549-CR cells, accompanied by significantly reduced cell death in A549-CR cells compared to the A549-WT line, further demonstrates that inhibition of the p53 response is not a pre-requisite for cDDP resistance. It has been suggested that inhibition of tumour cell proliferation by cDDP may represent a major part of its antineoplastic activity (Havelka, Berndtsson, Olofsson, Shoshan, & Linder, 2007; Puig et al., 2008). That cDDP treatment can induce identical cell cycle arrest in both A549 cell lines but differing effects on cell viability suggests the cytotoxic activity and cytostatic activity may, at least in part, be mediated by separate signalling pathways.

The precise signalling pathways involved in cDDP-induced cell death are complex, and may differ between cell models, with conflicting reports upon which effectors are responsible for the death process. To clarify this issue, cell death resulting from cDDP exposure was further investigated in the A549-WT cell line. Activation of caspase enzymes is responsible for the

major morphological changes associated with apoptosis and caspase involvement in cDDP-induced cell death is well reported (Basu & Krishnamurthy, 2010; Del Bello et al., 2007; Dursun et al., 2006; Siddik, 2003), and indeed incubation with the pharmacological pan-caspase inhibitor z-VAD-FMK significantly reduced the percentage of PI positive A549-WT cells measured following cDDP treatment (Figure 7), further confirming cDDP induces caspase-dependent apoptosis in A549-WT cells.

The role of caspase-8 has proved particularly divisive, with evidence accumulated both for (Lacour et al., 2003; Spierings, de Vries, Vellenga, & de Jong, 2003; Toyozumi et al., 2004) and against (Splettstoesser et al., 2007; Vakifahmetoglu, Olsson, Tamm, et al., 2008) a requirement in cDDP-induced apoptosis. Incubation of A549-WT cells with IETD-FMK, a pharmacological inhibitor of caspase-8, did not inhibit the increase in PI positive cells measured after 24 hours incubation with cDDP (Figure 8), thus signalling through caspase-8 does not appear to be involved in this A549 cell model, and confirms previous work by Liu and co-workers who similarly observed that IETD-FMK did not alter A549 cell apoptosis induced by cDDP (Liu et al., 2008).

Whilst inhibition of caspases reduced A549-WT cell death in response to cDDP by approximately 50%, a significant increase in the percentage of PI positive A549-WT cells was still measured following 24 hours drug exposure in comparison to untreated control cells, suggesting that caspase-independent cell death might also occur. Indeed, in other studies pharmacological caspase inhibition has not fully prevented cell death induced by cDDP, and death inhibition may commonly range from 20-50% (Del Bello et al., 2007; L. Liu et al., 2009; Mandic et al., 2002). Notably, pharmacological caspase inhibition in A549 cells by Liu *et al.* delayed cDDP-induced cytochrome *c* release and cell death compared to controls without caspase inhibition up to 16 hours post drug addition, however at later time points cDDP-induced cell death did not differ between these groups, indicating multiple modes of cell death may be in operation (Liu et al., 2008).

Necrotic cell death may result from cDDP treatment in some models, although it has been suggested that this response results mostly from very high, supramaximal cDDP concentrations in the 0.1 – 1 mM range, and a recent report described a switch from apoptotic to necrotic renal cell death with increasing cDDP concentration, with intermediate concentrations eliciting both death modalities in the cell population (Dursun et al., 2006; Mandic et al., 2002; Sancho-Martínez et al., 2011). Interestingly, it has been suggested that

this apoptosis-necrosis switch may occur due to direct inhibition of executioner caspases by cDDP after engagement of the apoptotic machinery (Sancho-Martínez et al., 2011), a situation possibly akin to pharmacological caspase inhibition. Similarly, the p53 status of cells treated with cDDP has been proposed as regulating whether cDDP induces apoptosis or necrosis following mitotic catastrophe (Vakifahmetoglu, Olsson, Tamm, et al., 2008). Thus, under conditions of caspase inhibition, some cells may die through necrosis after initial engagement of the apoptotic machinery. However, the abrupt gain in cellular volume and plasma membrane rupture characteristic of necrosis (Kroemer et al., 2009) was not observed during morphological imaging of A549-WT cells treated with cDDP (Figure 6 D).

Permeability transition of mitochondria may also lead to cell death. Inhibition of the Cyp D component of the mPTP using CsA however increased the cytotoxic effect of cDDP (Figure 10). Such toxic effects of CsA in combination with cDDP have been reported previously, and notably a similar effect was observed using an alternative Cyp D inhibitor, sanglifhrin A (X. Han et al., 2010; Mandic et al., 2002). It is possible that inhibition of the peptidl-prolyl cis-trans isomerise activity of Cyp D may prove deleterious to cell survival in light of protein damage by cDDP, however such reasoning remains no more than hypothesis for further testing.

Recently, a role for the involvement of calpains in mediating cDDP-induced cell death, at least in *in vitro* models, has begun to emerge. Although the exact role of calpains during cell death is not known, activation of these enzymes may in turn activate caspases and/ or cleave key cellular targets including cytoskeletal proteins, causing cell death (Liu et al., 2009). A number of studies have suggested a key role for calpain activation in pro-apoptotic cleavage of Bid, release of pro-apoptotic molecules including AIF from the mitochondria, caspase activation and induction of p73 following cDDP exposure (Al-Bahlani et al., 2011; Del Bello et al., 2007; L. Liu et al., 2009, 2008; Mandic et al., 2002; Splettstoesser et al., 2007). Indeed, Liu *et al* have suggested the calpain-mediated cell death pathway is the predominant means of caspase activation in A549 cells treated with cDDP (Liu et al., 2008). Although in the current investigation changes in $[Ca^{2+}]_{cyt}$ and $[Ca^{2+}]_{ER}$ were not observed in response to cDDP (Figures 26 & 27), this need not preclude a role for calpain activation since multiple mechanisms of activation other than Ca^{2+} exist (Del Bello et al., 2007). However, pharmacological inhibition of calpains using ALLN, an inhibitor of m-calpain, µ-calpain and cathepsins, did not inhibit A549-WT cell death induced by cDDP (Figure 9). The reason for such disparity with previous work is unclear. Dursun and co-workers have suggested that

calpains are important only for necrotic type cell death induced by cDDP (Dursun et al., 2006), whilst in the present study necrotic morphology is not observed. Alternatively, a number of previous studies have used calpeptin, a more specific calpain inhibitor, rather than ALLN to inhibit calpain activation. Whether differences in the mode of enzyme inhibition may impact upon cDDP sensitivity is not known but should be investigated before discounting a role for calpains in this model. Finally, the role of calpains in the present experimental system may be redundant with that of caspases, and thus only apparent under conditions of concomitant caspase inhibition, which may produce an additive inhibition of cDDP induced cell death.

AIF release from mitochondria may result in caspase-independent nuclear condensation and cell death in certain cell types, and several links between AIF release and cDDP sensitivity have been made in recent years (L. Liu et al., 2009; X. Yang, Fraser, Abedini, Bai, & Tsang, 2008). However, AIF release from mitochondria in response to cDDP appears to be dependent upon calpain activation (Liu et al., 2009), and given the lack of alterations in A549-WT cell death under conditions of calpain inhibition (Figure 9), seems unlikely to be a major requirement in the current model.

4.3 Increased ROS Production is Not Required for cDDP-Induced Cell Death in A549 Cells

Treatment with cDDP has been reported to increase the rate of ROS generation in a diverse range of cell types, including both tumour and non-tumour tissues (Berndtsson et al., 2007; Brozovic, Ambriović-Ristov, & Osmak, 2010; Kawai, Nakao, Kunimura, Kohda, & Gemba, 2006; Martins, N. A. G. Santos, Curti, Bianchi, & A. C. Santos, 2008; Santandreu, Roca, & Oliver, 2010). Such increased ROS production may play a role in cell death following cDDP treatment, and under some experimental conditions has been suggested to make a major contribution to cDDP-induced apoptosis (Berndtsson et al., 2007; Brozovic et al., 2010; Havelka et al., 2007). The nature of this contribution is complex and remains unclear, but has been suggested to involve oxidative damage of nuclear DNA, ER stress, mitochondrial oxidative dysfunction, antioxidant depletion, pro-apoptotic activation of mitogen-activated protein kinases and altered plasma membrane composition and fluidity leading to clustering of CD95 (Brozovic & Osmak, 2007; Brozovic et al., 2010; H.-L. Huang et al., 2003; Lacour et al., 2004; Mandic et al., 2003).

4. Discussion

An increased production of $O_2^{\bullet-}$ was measured both in the cytosol and mitochondria of both A549-WT cells and A549-CR cells following 24 hours incubation with cDDP (Figure 12 & Figure 13), in agreement with previous observations of $O_2^{\bullet-}$ production induced by cDDP in colon carcinoma and renal cells (Berndtsson et al., 2007; Kawai et al., 2006). Strikingly, this increase in cellular $O_2^{\bullet-}$ levels was significantly less apparent in A549-CR cells compared to the A549-WT cell line (Figure 12 & Figure 13). Similarly, whilst exposure to cDDP increased the rate of production of H_2O_2 in A549-WT cells, no significant difference was observed in the rate of H_2O_2 production by A549-CR cells following cDDP treatment compared to non-treated control A549-CR cells (Figure 11). The reason for a lack of a significant increase in H_2O_2 production caused by cDDP in A549-CR cells is not clear, but may be related to differences in ROS detoxification by A549-WT cells and A549-CR cells, such as decreased MnSOD activity, or alternatively due to the reduced rate of $O_2^{\bullet-}$ production in A549-CR cells following cDDP treatment compared to the A549-WT cell line.

Given the potential role of ROS production in cDDP cytotoxicity and the disparity in cDDP-induced ROS production between A549-WT cells and A549-CR cells, the contribution of ROS to cell death in this experimental system was investigated through addition of antioxidants to A549-WT cells during the cDDP treatment period. NAC fully prevented any increase in the percentage of PI positive A549-WT cells measured after cDDP treatment compared to control A549-WT cells (Figure 14). However, caution should be exercised in the interpretation of data derived from experiments involving co-incubation of cDDP and NAC. The aquated, reactive form of cDDP forms a nucleophile with high reactivity towards thiol groups, such as that contained in the NAC molecule, thus there exists the possibility of direct binding and inactivation of cDDP by the antioxidant. Although NAC is commonly used in investiagtion of cDDP and ROS generation (Mandic et al., 2003; Park, Choi, Bang, Huh, & Kim, 2002; Tajeddine et al., 2008), where possible alternative antioxidants without prominent thiol groups should be used to reduce the potential of experimental artefacts arising from direct drug detoxification. Accordingly, no protective effect against cDDP cytotoxicity was afforded by incubation of A549-WT cells with TEMPOL (Figure 15) or ascorbic acid (Appendix I Figure 1) during the drug treatment period. Thus, increased ROS production does not appear to be a significant requirement for cDDP-induced cell death in this experimental model. This finding is in contradiction with a number of other studies demonstrating a clear requirement for ROS production in cDDP cytotoxicity (Berndtsson et al., 2007; Brozovic et al., 2010; Kawai et al., 2006; Santandreu et al., 2010), whilst ascorbic

acid abrogated renal toxicity associated with cDDP treatment (Antunes, Darin, & Bianchi, 2000; Fatima, Arivarasu, & Mahmood, 2007; Maliakel, Kagiya, & Nair, 2008). Such differences may be due to cellular differences in the experimental systems and drug concentrations employed.

Since increased ROS production has been suggested to be the causative factor in cDDP-induced CD95 clustering and cell death through the receptor-mediated pathway (H.-L. Huang et al., 2003), that ROS production is not a component required for A549-WT cell death following cDDP treatment further suggests caspase-8 does not play a role in cDDP cytotoxicity in this experimental system.

4.4 cDDP Altered Mitochondrial Function in A549-WT Cells But Not A549-CR Cells

Although cDDP-induced cell death in A549 cells is not dependent upon increased ROS generation, a marked reduction in cellular $O_2^{\bullet -}$ and H_2O_2 production was observed in A549-CR cells following exposure to cDDP in comparison with the A549-WT cell line. Such a difference might be indicative of another altered cellular response to cDDP which itself contributes to modulate cDDP sensitivity, and a secondary effect of which results in diminished ROS generation. A reduction in cellular cDDP uptake resulting in a lesser degree of interference with cellular processes might explain the difference in ROS generation, and indeed all differences between A549-WT cells and A549-CR cells following cDDP exposure. Reduced drug accumulation is a recognised mechanism of tumour cell cDDP resistance (Siddik, 2003), and cannot be excluded without measurement of cDDP uptake kinetics in the two cell lines. However, p53 accumulation (Figure 5) and GSH depletion (Figure 30) caused by cDDP treatment did not differ between A549-WT cells and A549-CR cells, whilst the cDDP-induced increase in mtDNA copy number was significantly greater in A549-CR cells (Figure 34). These observations of similarities in magnitude of the DNA damage response and slight GSH depletion suggest that, rather than representing differences of degree, specific dissimilarities exist in cellular response to cDDP.

GSH represents an important and abundant cellular scavenger of free radicals which might account for the difference in ROS generation measured between A549 cell lines, and GSH overexpression has been linked to tumour cell cDDP resistance (Godwin, 1992; Siddik, 2003), inactivating cDDP through direct reaction. However, no significant difference was

observed in cellular levels of GSH in A549-WT cells and A549-CR cells measured by MCB fluorescence (Figure 30). Further investigations are required to determine whether changes in other cellular antioxidant systems might account for reduced ROS production by A549-CR cells following cDDP treatment.

Recent work has suggested the expression of mitochondrial uncoupling protein-2 (UCP2) may alter the sensitivity of cells to the cytotoxic effects of cDDP (Santandreu et al., 2010). Leukaemia cells resistant to cDDP expressed increased levels of UCP2 and maintained a reduced $\Delta\Psi$ compared to cDDP-sensitive cells, accompanied by reduced ROS production under conditions of cellular stress and resistance to cDDP-induced apoptosis (Harper et al., 2002). However, neither $\Delta\Psi$ (Figure 31) nor the degree of uncoupling of mitochondrial oxidative respiration (Table 4) were significantly different between A549-WT cells and A549-CR cells, both under normal cell growth conditions and following cDDP treatment, indicating increased mitochondrial uncoupling through UCP2 does not account for the difference in ROS production observed.

The mitochondrial electron transport chain is the primary source of $O_2^{\bullet-}$ generation in most cell types (Koopman et al., 2010; Orrenius, 2008), and as such differences in mitochondrial activity and/ or function following cDDP treatment could explain reduced ROS generation in A549-CR cells compared to A549-WT cells. No significant differences were measured in $\Delta\Psi$ (Figure 31), basal cellular O_2 consumption (Figure 32), maximal cellular oxidative capacity (Figure 33), or mtDNA copy number (Figure 34) indicating that under normal cell growth conditions basal mitochondrial function is comparable in A549-WT cells and A549-CR cells. Following cDDP treatment, the basal rate of cellular O_2 consumption increased in both A549 cell lines (Figure 32), consistent with the observed increase in cellular $O_2^{\bullet-}$ production. Notably, the drug induced increase in mitochondrial oxidative activity was significantly greater in A549-WT cells than in the A549-CR cell line, again in agreement with the observed difference in $O_2^{\bullet-}$ production following cDDP exposure. The difference in H_2O_2 production might be explained by differences in the level of $O_2^{\bullet-}$ generation and the superoxide dismustase activities of ROS detoxification systems in the two cell lines. Total cellular oxidative capacity was also significantly increased after the cDDP treatment period in A549-WT cells, but unaltered in A549-CR cells (Figure 33). Thus, cDDP treatment caused an increase in mitochondrial oxidative activity of A549-WT cells, and a significantly less pronounced increase in A549-CR cells, a pattern which strongly correlates with, and may explain, differences in drug-induced ROS production between the two cell lines.

4. Discussion

Differences in the oxidative activity of mitochondria following cDDP treatment are notable, as regulation of mitochondrial respiratory complexes (Lemarie & Grimm, 2011) and electron flux through the ETC is emerging as a key determinant in the induction of apoptosis. Partial depletion or complete loss of ETC components in osteocarcinoma cybrid cells generated using mtDNA donor cells harbouring a range mtDNA mutations resulted in marked resistance to apoptosis via the mitochondrial pathway in response to staurosporine and etoposide (Kwong et al., 2007). Interestingly, the same mutations sensitised cybrid cells to ER stress-induced apoptosis, suggesting the protective effect may depend upon the apoptotic stimulus and signalling pathways activated. In a similar manner, reduced activity of the ETC in human leukaemia cells induced resistance to the microtubule destabilising agent Taxol (Jia et al., 1997). Conversely, increased mitochondrial activity may sensitise cancer cells to cDDP treatment. Pyruvate generated through glycolysis is converted to acetyl-CoA for entry into the TCA cycle by the action of pyruvate dehydrogenase (PDH), the enzymatic activity of which is in turn regulated by pyruvate dehyrogenase kinase (PDK). Decreased conversion of pyruvate to acetyl-CoA is common is tumour cells, and may contribute to the characteristic Warburg effect. Dichloroacetate (DCA), a drug commonly used for treatment of lactic acidosis, effectively inhibits PDK activity, relieving inhibition of PDH, and increases mitochondrial activity by boosting entry of pyruvate into the TCA cycle (Sébastien Bonnet et al., 2007). DCA enhanced the cytotoxic effects of cDDP in HeLa cells (Xie et al., 2011), and a novel fusion drug comprised of cDDP and DCA showed greater activity in inducing apoptosis of cancer cells than either drug alone (Dhar & Lippard, 2009). This fusion drug was further able to restore drug sensitivity to cDDP-resistant ovarian cancer cells. Thus, the functional difference in mitochondria identified between A549-WT cells and A549-CR cells following cDDP treatment may directly contributed to modulating cDDP sensitivity in tumour cells, and warrants further investigation. Restoration of increased ETC activity following cDDP treatment may increase A549-CR cell response to the drug, and provide a rationale for chemotherapy regimes combining cDDP with drugs selectively targeted to boosting mitochondrial function.

Whilst increased activity of the ETC may sensitise cancer cells to the cytotoxic effects of cDDP, the mechanism behind the increase in cellular oxygen consumption observed in A549-WT cells following treatment with cDDP is not clear. Mitochondrial dysfunction and inhibition of mitochondrial respiratory complex activity following cDDP treatment has been demonstrated by a number of studies (Cullen, Yang, Schumaker, & Z. Guo, 2007;

Kruidering, Van de Water, de Heer, Mulder, & Nagelkerke, 1997; H. Ma et al., 2010; Martins, N. A. G. Santos, Curti, Bianchi, & A. C. Santos, 2008; Sancho-Martínez, Piedrafita, Cannata-Andía, López-Novoa, & López-Hernández, 2011; Santandreu et al., 2010). This is the first report of a cDDP-induced increase in cellular O_2 consumption, and as such requires confirmation through an independent method. Why the present observations differ from previous literature is not clear, but may depend upon differences in the genetic background of the model systems and their response to cDDP, or indeed the type of experimental model, non-tumour or tumour tissue, as mitochondrial injury induced by cDDP has been studied as a mechanism of chemotherapy side effects (Cullen et al., 2007). Methodological differences may also play a role, both in the time period following cDDP exposure in which measurements are made, and the measurements of mitochondrial function taken, as a number of studies rely upon measurements of $\Delta\Psi$ and ROS production which depend upon a number of other factors in addition to ETC activity.

Increased mitochondrial oxidative activity has previously been reported following exposure to cytotoxic agents. Genistein, a topioisomerase inhibitor, showed inhibitory effects on the proliferation of MCF-7 breast cancer cells, Jurkat cells and transformed mouse fibroblasts causing cell cycle arrest at the G2/ M phase checkpoint, accompanied by increased mitochiondrial activity as measured by MTT assay (Pagliacci et al., 1993). Treatment with cDDP may also induce significant G2/ M phase arrest (Siddik, 2003), and it is possible that increased mitochondrial enzymatic activity may represent, in certain experimental models, a stress-induced metabolic adaptation. Mitochondrial proliferation as an adaptive response to ETC damage and dysfunction, upregulating the activity of dysfunction mitochondria in order to maintain basal function, might also account for increased cellular O_2 consumption in A549-WT cells following incubation with cDDP, and such responses have been observed in cells following exposure to both radiation and toxic pharmacological agents (Karbowski et al., 2001; Kluza et al., 2004; C.-F. Lee, Liu, Hsieh, & Wei, 2005; Limoli et al., 2003; Mancini et al., 1997; Nugent et al., 2007; Pagliacci et al., 1993; Reipert, Berry, Hughes, Hickman, & Allen, 1995). A link between the DNA damage response and mitochondrial biogenesis has been suggested to occur through ATM-dependent activation of 5'-AMP activated protein kinase (AMPK) (Fu, Wan, Lyu, Liu, & Qi, 2008). Although the maximal cellular oxidative capacity of A549-WT cells was significantly increased following the cDDP treatment period (Figure 33), no changes in the abundance of mitochondrial respiratory complexes were measured in A549-WT cells or A549-CR cells (Figure 35). This finding

suggests that the changes in A549-WT mitochondrial oxidative activity induced by cDDP are not due to a drug-induced increase in mitochondrial proliferation, but may in fact represent a change in regulation or substrate availability. Glucose uptake and the activity of glycolytic enzymes may be inhibited by cDDP (Aull et al., 1979; Rodríguez-Enríquez et al., 2009; R. Zhou et al., 2002), therefore it is conceivable that metabolic shifts may occur to maintain cellular energy production following changes in the activity of metabolic pathways caused by cDDP. Long term adaptations in cells selected for growth in cDDP, through altered enzyme expression levels for example, could account for differences in mitochondrial activity measured after acute cDDP treatment.

4.5 mtDNA Copy Number of A549 Cells was Increased Following cDDP Treatment

Recent work has increasingly recognised mitochondria as clinically relevant target organelles of cDDP chemotherapy, at both the level of protein damage and mtDNA modification (Cullen et al., 2007; Sharma & Edwards, 1983; Tajeddine et al., 2008; Z. Yang et al., 2006). Indeed, cDDP may bind mtDNA with equal affinity as with nuclear DNA, and cDDP-mtDNA adducts may in some cases outnumber cDDP-DNA adducts in the nucleus (Murata, Hibasami, Maekawa, Tagawa, & Nakashima, 1990; Olivero, Chang, Lopez-Larraza, Semino-Mora, & Poirier, 1997; Podratz et al., 2011). Such accumulation may in part be driven by the mitochondrial membrane potential, and adducts may persist due to the lack of a NER pathway in mitochondria, required to remove cDDP adducts from DNA (Murata et al., 1990; Olivero et al., 1997; Singh & Maniccia-Bozzo, 1990). Further, unlike the nuclear genome, mtDNA is not associated with histone proteins, thus may be particularly vulnerable to oxidative and chemical damage.

The mtDNA copy number of both A549-WT cells and A549-CR cells was increased by incubation with cDDP (Figure 36). It is appreciated that cDDP-mtDNA adducts may interfere with the qPCR reaction used to estimate mtDNA copy number in the present investigation. Inhibition of *Taq* polymerase progression by cDDP-mtDNA lesions in a PCR assay has been reported (Garrido et al., 2008), however template DNA for this study was prepared from isolated mitochondria treated with cDDP in the millimolar range, thus its relevance to studies involving treatment of whole cells with lower cDDP concentrations may be questioned. Increased mtDNA replication in A549 cells treated with cDDP should be confirmed through an independent method such as BrdU incorporation assays. The integrity of mtDNA

molecules replicated in the presence of cDDP should also be investigated, as present results do not preclude cycles of abortive mtDNA replication, generating mtDNA fragments including the amplified sequence.

Treatment with cDDP has previously been reported to cause depletion of cellular mtDNA content in cardiac, hepatic and neuronal models (El-Awady, Moustafa, Abo-Elmatty, & Radwan, 2011; Garrido et al., 2008; Podratz et al., 2011). Conversely, separate studies have observed an increase in cellular mtDNA content in colon carcinoma cells and renal and hepatic tissues following cDDP exposure (Gerschenson, Paik, Gaukler, Diwan, & Poirier, 2001; Maniccia-Bozzo, Espiritu, & Singh, 1990; Santandreu et al., 2010). Interestingly, mtDNA content may be increased, decreased or unchanged in different tissues of animal models of cDDP chemotherapy (Gerschenson et al., 2001; Maniccia-Bozzo et al., 1990), suggesting cell specific responses to cDDP may be important in determining this effect.

Conceptually, whilst depletion of mtDNA may be accounted for through direct inhibition of the mtDNA replication process, the mechanism behind an increase in mtDNA copy number caused by cDDP treatment is not immediately obvious. Such an increase may be in agreement with a general drug-induced proliferation of mitochondria, however since cDDP did not cause significant changes in the abundance of mitochondrial respiratory complexes in either cell type (Figure 35), this is unlikely to be the case in this model.

Alternatively, increased mtDNA content might be interpreted as an adaptive response to mtDNA damage. Current knowledge suggests mitochondria lack the capacity to repair bulky cDDP-DNA intrastrand adducts (Singh & Maniccia-Bozzo, 1990), therefore increased replication of mtDNA may represent a means to maintain a pool of undamaged mtDNA above a threshold level required to maintain mitochondrial function. Exposure to low levels of ROS has been demonstrated to lead to an increase of mtDNA copy number in a human osteocarcinoma cell line (C.-F. Lee et al., 2005). In this osteocacinoma model, higher ROS exposure dramatically decreased mtDNA content, thus differences in ROS production by cells treated with cDDP may account for the variable effects of cDDP treatment on mtDNA copy number between cell models. It is tempting to speculate that the significantly greater increase in mtDNA copy number induced by cDDP in A549-CR cells compared to A549-WT cells may be linked to the significantly reduced rate of ROS production in this cell line, and further investigation of the ROS dependence of this effect is justified.

4. Discussion

Should increased mtDNA replication prove to be an adaptive response to mtDNA damage under certain conditions, several clues exist as to the molecular mechanisms driving this effect. Mitochondrial transcription factor A (TFAM) is a transcription factor essential for transcription of mitochondrial genes, but also required for the maintenance and, potentially, replication of mtDNA (Kang, Kim, & Hamasaki, 2007; Larsson et al., 1998). TFAM is a major component of mtDNA nucleoids, and may further act to regulate the mass of cellular mtDNA by binding along the entire genome in a manner akin to the histone proteins of nuclear DNA. In this scenario, mtDNA molecules which do not become associated with TFAM are degraded, and indeed overexpression and knockdown of TFAM correlated with increased and decreased mtDNA copy number respectively (Kang et al., 2007). TFAM is a member of the HMG family of proteins (Parisi & Clayton, 1991), which bind to distorted regions of DNA such as those caused by cDDP. Binding of TFAM to damaged regions of mtDNA has been demonstrated, and specifically translocation of a fraction of p53 to the mitochondrial matrix upon cDDP treatment of colon adenocarcinoma cells enhanced preferential binding of TFAM to cDDP-mtDNA adducts, accompanied by an increase in TFAM expression (Yoshida et al., 2002, 2003). Similar signalling events leading to increased TFAM expression levels in A549 cells following cDDP treatment could account for the observed increase in mtDNA copy number. Finally, it should be noted that the contribution of the cDDP-induced increase in mtDNA content of A549 cells to cell fate requires further investigation, and may equally represent an adaptive response to maintain mtDNA integrity and mitochondrial function, a secondary effect with no contribution to cell fate or may promote cytotoxicity since, for example, increased binding of HMG proteins to cDDP adducts in the nucleus may actually shield these lesions from repair (Siddik, 2003).

4.6 Novel mtDNA Point Mutations Inhibit A549-CR Respiratory Complex I Activity

Mutations of mtDNA, encompassing nucleotide insertion, deletion and substitution, are now well recognised as correlating with the initiation, progression and drug resistant phenotype of human cancers (Chatterjee et al., 2006; H.-C. Lee, Chang, & Chi, 2010; J. Lu, Sharma, & Bai, 2009; S. Mizutani et al., 2009). A review of recent literature estimated that 60% of cancer cells harbour mtDNA point mutations, with approximately 25% of these affecting conserved nucleotides likely to alter mitochondrial function (H.-C. Lee et al., 2010). Mutant mtDNA causing loss of function in ETC components has been shown to correlate with

resistance to apoptosis through the mitochondrial pathway (Kwong et al., 2007), and HeLa cell cybrids generated using mtDNA derived from pancreatic cancer samples showed increased resistance to cDDP-induced apoptosis compared to a cybrid line generated using mtDNA derived from non-tumour pancreatic tissue (S. Mizutani et al., 2009). Resistance to cDDP was similarly observed in HeLa cell cybrids generated using mtDNA derived from the tissue of mitochondrial encephalomyopathy patients, containing point mutations in the *MTATP6* gene (Shidara et al., 2005).

Several previously reported cancer-associated SNPs were found to be present in the mtDNA of both A549-WT cells and A549-CR cells (Appendix III Table 1). In addition, a previously unreported point mutation, 225G>T, was identified in the D-loop region of mtDNA in A549-CR cells, whilst A549-WT mtDNA contained the reference nucleotide (Figure 36, Table 5 & Table 6). Mutations in the D-loop region are commonly observed in cancer cells (H.-C. Lee et al., 2010), and have been associated with poor prognosis in late stage lung cancer patients (Matsuyama et al., 2003). The D-loop has been suggested to act as a binding site for proteins regulating the structure of mtDNA nucleoids (J. He et al., 2007), and ATAD3, a protein known to bind in this region, has recently been suggested to be a factor modulating cDDP sensitivity in lung adenocarcinoma cells (H.-Y. Fang et al., 2010). The potential functional effects of this mutation on both mtDNA nucleoid structure and cDDP sensitivity were not investigated during this study, but may form the basis of further work.

A previously unreported mtDNA point mutation in the *MTND2* gene (4587T>C) was also identified as existing in heteroplasmy at a low level in A549-WT cells, and in homoplasmy in A549-CR cells. The transition from a low level variant in heteroplasmy to homoplasmy suggested a positive selection for the mutation may have occurred during acquisition of cDDP resistance by A549-CR cells, thus the functional consequences of this mutation were further characterised. *MTND2* encodes the ND2 subunit of mitochondrial respiratory complex I, an iron-sulphur protein in the peripheral arm of the complex, from which electrons are transferred to Ubq (Koopman et al., 2010; Nakamaru-Ogiso et al., 2010). The 4587T>C mutation occurs within a protein-coding region, and produces a F40L amino acid substitution.

Relative to A549-WT cells, the rotenone-sensitive activity of respiratory complex I of A549-CR cells, that is, the ability of the isolated complex to reduce NADH with concomitant transfer of electrons through the complex to Ubq, was reduced by approximately 50% (Figure 38). Measurement of the rotenone-insensitive NADH oxidase activity of complex I

(diaphorase type activity), independent of electron transfer to Ubq, revealed no difference in enzyme activity between A549-WT cells and A549-CR cells (Figure 37). These data are consistent with the role of the ND2 subunit in electron transfer through complex I (Koopman et al., 2010; Nakamaru-Ogiso et al., 2010), and strongly suggests that the 4587T>C point mutation present in homoplasmy in A549-CR cells attenuates the function of complex I in this cell line. Mutation of mtDNA genes encoding complex I components has been linked with thyroid cancer (Abu-Amero, Alzahrani, Zou, & Shi, 2005), and intriguingly may occur with greater frequency in cancer cells than mutations in components of other respiratory complexes (J. Lu et al., 2009).

Thus, A549-CR cells contain a point mutation in the *MTND2* mtDNA gene, which is likely the cause of reduced activity of respiratory complex I in this cell line. The present data do not indicate whether this mutation may alter cellular sensitivity to cDDP, or indeed induce general resistance to mitochondria-initiated apoptosis, and generation of cybrid cells using A549-WT cell mtDNA and A549-CR cell mtDNA is required to investigate any pro-survival effects of this mutation, independent of changes in the nuclear genetic background of the cell. Furthermore, homoplasmic mtDNA mutations which alter mitochondrial function have also been shown to promote tumour growth *in vivo*, and HeLa cell cybrid xenografts harbouring mutant mtDNA in nude mice have been shown to have a greater proliferative rate (Shidara et al., 2005) and improved resistance to cDDP chemotherapy-induced apoptosis (S. Mizutani et al., 2009; Shidara et al., 2005).

How mtDNA mutations may modulate cDDP sensitivity also requires further study, however changes in the function of complex I have been linked to the induction of apoptosis (Lemarie & Grimm, 2011). Increased expression of HIF transcription factors correlates with enhanced tumour cell cDDP resistance in a range of tumour types, including NSCLC, hepatocarcinoma and cancers of the head and neck, whilst HIF-1α silencing increased cellular cDDP sensitivity (Hao et al., 2008; Lau et al., 2009; Xianrang Song et al., 2006; Weidemann et al., 2008; Z. F. Yang, Poon, To, Ho, & Fan, 2004; van den Broek et al., 2009). Deficiencies in the ETC might lead to HIF stabilisation, and promote cell survival under cDDP treatment. Interestingly, exogenous expression of ND2 mutants in head and neck cancer cells lead to HIF-1α accumulation and promoted tumour cell growth (S. Zhou et al., 2007). The HIF status of A549-WT cells and A549-CR cells, both under normal growth conditions and following cDDP treatment, should thus form a priority for further investigation. A hypothesis involving HIF stabilisation may be particularly attractive given the role of this transcription factor in

shifting cellular metabolism away from oxidative respiration, and the reduced cellular O_2 consumption of A549-CR cells compared to A549-WT cells following cDDP treatment (Section 4.4). However, HIF stabilisation due to mitochondrial dysfunction may require enhanced ROS production (Majmundar, Wong, & Simon, 2010; S. Zhou et al., 2007), whilst no difference in ROS generation was observed between the two cell lines under normal growth conditions and A549-CR cells produced ROS at a significantly reduced rate compared to A549-WT cells in the presence of cDDP (Figure 11, Figure 12 & Figure 13), thus the true explanation may not be so straightforward.

4.7 Mitochondrial Function is Impaired in A549-CR Cells Only Under Conditions of Cellular Stress

The activity of mitochondrial respiratory complex I was reduced by approximately 50% in A549-CR cells compared to A549-WT cells (Figure 38), likely due to a point mutation in A549-CR cell mtDNA affecting the *MTND2* gene (Figure 36). However, neither $\Delta\Psi$ (Figure 31) nor the basal or maximal oxidative activity of the ETC differed between A549-WT and A549-CR cells under normal growth conditions (Figure 33 & Figure 34). Therefore, A549-CR cells were able to maintain mitochondrial function comparable to that of A549-WT cells in spite of complex I dysfunction. The contribution of the individual respiratory complexes to electron flux along the ETC to O_2 varies in a manner that is both cell type and growth stage specific (Inomoto et al., 1994; Kuznetsov et al., 1997), thus the effect of a change in the activity of a single complex on the activity of the ETC as a whole cannot be simply predicted without knowing the relative contribution of that complex. Similarly, the degree of inhibition of complex activity must surpass a threshold level before functional effects are observed in the rate of O_2 consumption, and again this threshold may vary between complexes and cell type (Davey, Peuchen, & Clark, 1998). Therefore, one potential explanation for the observed similarity in basal mitochondrial function may be that the effect of the mtDNA mutation on complex I activity does not affect the rate of O_2 reduction by the ETC, and the relative contribution of respiratory complexes I-IV in maintaining $\Delta\Psi$ and O_2 reduction may be assessed to confirm or exclude this possibility.

Alternatively, the $\Delta\Psi$ and cellular O_2 consumption data may be interpreted in terms of mitochondrial function being maintained, in spite of altered complex I activity, by specific compensatory mechanisms in A549-CR cells. Indeed, the activity of complex I may prove to

be a rate limiting factor for the ETC in some models (Moreno-Sánchez et al., 2010; Telford, Kilbride, & Davey, 2009). Analysis of the abundance of the respiratory complexes demonstrated that complex I expression is significantly increased in A549-CR cells in comparison to A549-WT cells, whilst a strong increasing trend was noted in the abundance of complex III (Figure 35). This observation may support the notion of a compensatory upregulation of complex I components in A549-CR cells in response to dysfunction and partial inhibition of the activity of the complex. Increased expression of mitochondrial proteins in response to mitochondrial dysfunction caused by mtDNA mutations has been described (A.-M. Joseph, Rungi, Robinson, & Hood, 2004; Wojewoda, Duszyński, & Szczepanowska, 2011), and the exact response may vary with the nature of the defect.

Dysfunction of the ETC may also provide further understanding of the disparity in both basal O_2 consumption and maximal oxidative activity between A549-WT cells and A549-CR cells following incubation with cDDP. It is possible that under normal growth conditions A549-CR cells are functioning at, or close to, the maximal oxidative capacity of mitochondria in this cell line. Such a situation may occur through a fundamental shift away from oxidative metabolism as part of an adaptive response to reduced complex I activity, or may represent the maximal activity for biosynthesis of mitochondria in this cell type. Thus, cDDP-induced changes in cell metabolism leading to an oxidative phenotype, or drug-induced proliferation of mitochondria (Section 4.4) would not alter basal O_2 consumption or maximal oxidative activity of the ETC of A549-CR cells, as observed in this study (Figure 33 & Figure 34). Should this be the case, A549-CR cells should be more sensitive than A549-WT cells to conditions which favour an oxidative phenotype, such as treatment with DCA or provision galactose in place of glucose as the sole sugar in growth medium, the metabolism of which requires oxidative phosphorylation (Gohil et al., 2010). Alternatively, dysfunction of complex I might lead to a decreased contribution of this complex to electron flux through the ETC, thus should cDDP induces changes in the activity of complex I the effect may be less pronounced. Complex I has been suggested as the major source of increased ROS generation in renal cells treated with cDDP (Kruidering et al., 1997), thus cellular adaptation to complex I dysfunction caused by mtDNA mutations may alter cDDP sensitivity.

4. Discussion

4.8 Intracellular Ca^{2+} Signalling is Reduced in A549-CR Cells

The regulation of Ca^{2+} homeostasis is crucial in both the life and death of a cell (Section 1.2.6), and indeed the opposing actions of pro-apoptotic and anti-apoptotic BCL-2 family proteins is in part mediated through changes in cellular Ca^{2+} handling (Palmer et al., 2004; Rong & Distelhorst, 2008). Dampening of intracellular Ca^{2+} release and/ or a reduction in intracellular Ca^{2+} store content, as may occur following overexpression of anti-apoptotic BCL-2 proteins or through the action of pro-survival signalling such as the PI3K/ Akt pathway (Harr & Distelhorst, 2010; Marchi et al., 2008; Rong & Distelhorst, 2008), increases cellular tolerance to apoptotic stimuli. Conversely, prolonged, pathological rises in intracellular Ca^{2+} and/ or increases in intracellular Ca^{2+} store content, as may occur in response to apoptotic stimuli or activation of pro-apoptotic BCL-2 proteins (Harr & Distelhorst, 2010; R Rizzuto et al., 2003; Rong & Distelhorst, 2008), favours cell death, and enhances the apoptogenic potential of the cellular Ca^{2+} store. Rises in intracellular Ca^{2+} have been suggested to form part of the cytotoxic mechanism of cDDP, and indeed a phenotype characterised by reduced intracellular Ca^{2+} content and a reduced propensity for large Ca^{2+} responses has been described in cDDP-resistant cells (Al-Bahlani et al., 2011; Del Bello et al., 2007; Kawai et al., 2006; Liang & Huang, 2000). Further, cDDP-induced ER-stress signalling has been suggested to lead to apoptosis independent of DNA damage (Mandic et al., 2003), and release of ER store Ca^{2+} may be part of this cell death pathway (Chami et al., 2008; Pinton et al., 2008).

The A549 cell line is known to express a number of plasma membrane Ca^{2+} channels, including at least three isoforms of the G-protein linked P2Y receptor, a P2X receptor channel, the L-type voltage dependent Ca^{2+} channel and capacitative Ca^{2+} entry channels, and respond to stimulation with extracellular ATP with a rise in $[Ca^{2+}]_{cyt}$ (Zhao et al., 2000). ATP stimulation evoked a rapid increase in $[Ca^{2+}]_{cyt}$ measured by aequorin in A549-WT cells, however no perceptible changes were measured in A549-CR cells (Figure 17). It is possible that ATP addition caused low amplitude rises in $[Ca^{2+}]_{cyt}$ which were not detected due to the relatively low Ca^{2+} binding affinity of aequorin. Reduced cellular Ca^{2+} response to ATP has previously been reported in cDDP resistant NSCLC cell lines (Schrödl, Oelmez, Edelmann, Huber, & Bergner, 2009). Given the range of plasma membrane Ca^{2+} channels expressed by A549 cells, and that both IP_3Rs and RYRs are present in the ER membrane, reduced Ca^{2+} signalling following ATP stimulation might be equally well explained by modifying any one of a number of signalling pathways, thus the cause of this disparity was further investigated.

4. Discussion

Reduced ER store Ca^{2+} correlates with apoptosis resistance in some experimental models and a decrease in the total releasable intracellular Ca^{2+} pool may explain reduced response to ATP challenge. No significant difference was observed in change in the Fura-2 fluorescence ratio upon depletion of ER Ca^{2+} in nominally 'Ca^{2+} free' buffer (Figure 20), indicating $[Ca^{2+}]_{ER}$ did not differ between the A549 cell lines. Furthermore, no significant difference was observed in the 'FRET-ratio' of an ER-targeted cameleon probe (Figure 26), a direct measurement of the ER Ca^{2+} store content. Thus, inhibition of Ca^{2+} signals in A549-CR cells in response to a physiological agonist is not due to reduced $[Ca^{2+}]_{ER}$.

ATP induces cytosolic Ca^{2+} signals by stimulating the generation of IP_3 through activation of phospholipase C through P2Y receptors, and reduced activation of IP_3Rs upon IP_3 binding could explain the reduced response of A549-CR cells to ATP stimulation. This hypothesis was tested directly using a cell permeable caged IP_3. Uncaging of IP_3 in the cytosol induced a rise in $[Ca^{2+}]_{cyt}$ measured by Fluo-4 in both A549 cell lines, however the peak response was reduced by approximately 50% in A549-CR cells in comparison to A549-WT cells. This reduced response was not due to decreased expression of the receptor, since comparable expression of IP_3R-1 was observed in both A549-WT cells and A549-CR cells (Figure 21), although altered expression of IP_3R-2 or IP_3R-3 cannot be excluded. Thus, the dissimilarity in Ca^{2+} signalling represents a functional difference. Differences in the opening probability of the IP_3R may explain the inhibition of Ca^{2+} release induced by ATP in A549-CR cells, although additional differences in signalling induced by extracellular ATP still might also contribute.

The inhibition of intracellular Ca^{2+} signalling in A549-CR cells extends beyond that evoked by IP_3 releasing ligands such as ATP. Addition of Ca^{2+} to the nominally 'Ca^{2+} free' extracellular buffer solution following depletion of ER Ca^{2+} using Tg caused a rapid rise in $[Ca^{2+}]_{cyt}$ through the SOCE response in A549-WT cells, measured by both Fura-2 (Figure 20) and aequorin (Figure 19). In contrast, the SOCE signal measured by Fura-2 in A549-CR cells was reduced by approximately 50% relative to A549-WT cells (Figure 20), whilst no significant increase in aequorin bioluminescence was observed upon Ca^{2+} addition following ER store depletion (Figure 19). The discrepancy in A549-CR SOCE signalling measured by Fura-2 and aequorin likely relates to the low affinity of aequorin for Ca^{2+}, thus low amplitude Ca^{2+} signals may not be detected using this probe. Such reasoning also explains the lack of cytosolic Ca^{2+} signals caused by Tg treatment, as SERCA inhibition produces a prolonged, low amplitude rise in $[Ca^{2+}]_{cyt}$ due to passive leak of Ca^{2+} from the ER. The differing SOCE

response of A549-WT cells and A549-CR cells was not due to incomplete emptying of the ER Ca^{2+} store, since no significant difference was observed in the Fura-2 signal measured following Tg addition (Figure 20), indicating comparable store depletion in both cell lines. A recent study has linked decreased expression of Orai, the key plasma membrane component of the SOCE response, to resistance to apoptosis induced by multiple stimuli, including cDDP, in a prostate cancer cell line (Flourakis et al., 2010), and influx of Ca^{2+} across the plasma membrane following cDDP treatment has been suggested to mediate cDDP cytotoxicity (Splettstoesser et al., 2007). However, cDDP treatment did not cause depletion of ER Ca^{2+} in either A549-WT cells or A549-CR cells (Figure 26), and chelation of extracellular Ca^{2+} using EGTA failed to alter the percentage of PI positive A549-WT cells measured following cDDP treatment (Figure 24), indicating SOCE and influx of external Ca^{2+} are not modulators of cDDP-sensitivity in this A549 cell model.

4.9 Inhibition of A549-CR IP_3R Ca^{2+} Channel Function Does Not Contribute to cDDP Resistance

A limited and conflicting body of work exists linking the IP_3R to cell fate following exposure to cDDP. Increased IP_3R expression has been reported to correlate with cDDP resistance in NSCLC cell lines, and was linked to a reduced ER store Ca^{2+} content (Schrödl et al., 2009). In contrast, the expression of IP_3R-1 decreased in primary tumour samples following cDDP treatment, and modulation of expression was demonstrated to directly correlate with changes in the cDDP sensitivity of a bladder cancer cell line. An increased level of expression sensitised cells to cDDP, whilst knockdown of expression inhibited apoptosis (Tsunoda et al., 2005). Given the previous data linking IP_3R-1 to cDDP sensitivity, this isoform was selected for further study. Although basal IP_3R expression did not differ between A549-WT cells and A549-CR cells, Ca^{2+} release in response to IP_3 was significantly inhibited in the A549-CR cell line, thus it was hypothesised that IP_3R function rather than absolute expression level may be the factor impacting upon cellular response to cDDP. Indeed, Tsunoda *et al* (Tsunoda et al., 2005) did not provide a mechanism beyond demonstrating that the IP_3R expression level directly correlated with the induction of cell death. Thus, subsequent experimental approaches were directed towards altering IP_3R function by both genetic and pharmacological means.

4. Discussion

Manipulation of the expression of IP_3R-1 through overexpression of an exogenous receptor or knockdown of gene expression may alter the activity of the channel in cellular signalling. The transfection efficiency of a siRNA construct targeted towards IP_3R-1 mRNA proved too low for efficient protein silencing during the course of this investigation (data not shown). Further optimisation of the transfection protocol is thus required to evaluate the effect of IP_3R-1 knockdown in A549-WT cells and A549-CR cells. Alternatively, the DT40 chicken lymphocyte cell line and IP_3R triple knockout DT40 cell line provides an appropriate model to investigate the role of the IP_3R in cDDP cytotoxicity, and transfection of individual IP_3R isoforms in knockout cells may provide information on isoform specific contributions. Since redundancy may exist in the ability of the IP_3R isoforms to induce apoptosis (S. K. Joseph & Hajnóczky, 2007), such an approach may prove most productive.

Overexpression of IP_3R-1 A549-WT cells did not alter the percentage of PI positive cells measured following cDDP exposure, relative to A549-WT cells transfected with a control ER-GFP construct (Figure 22). It is notable that control transfection of ER-GFP in A549-CR cells resulted in significant toxicity. The reason for this effect is unknown, since transfection of the same construct in A549-WT cells did not significantly increase cDDP-induced cytotoxicity, and transfection using different control constructs should be investigated. Should similar toxicity specific to A549-CR cells be observed using unrelated control constructs, differences in the protein translation machinery and ER stress response may be considered and investigated. For the purposes of the present study, the unacceptable level of toxicity in control A549-CR cells prevents interpretation of this data. Although both IP_3R-1 silencing and overexpression studies in A549 cells encountered significant problems, the fact that basal IP_3R-1 expression is comparable in A549-WT cells and A549-CR cells, and that overexpression of IP_3R-1 in A549-WT cells did not induce a significant increase in cDDP sensitivity relative to control A549-WT cells, suggests that the expression level of IP_3R-1 is not a modulator of cDDP sensitivity in A549 cells. However, further investigations are required before a genuine conclusion may be formed. Further extension to include the expression of IP_3R mutants containing a non-functional Ca^{2+} channel domain or mutations within the cytosolic protein binding domain would help delineate which function of the IP_3R may be important in determining cell fate.

Since direct modulation of IP_3R-1 expression in A549 cells proved problematic, the role of Ca^{2+} in cDDP cytotoxicity and the effect of pharmacological inhibition of the IP_3R were assessed to determine whether the inhibition of Ca^{2+} signalling in A549-CR cells contributed

to the reduced cDDP sensitivity. Exposure to cDDP over 24 hours did not cause a significant change in $[Ca^{2+}]_{ER}$ in either A549-WT cells or A549-CR cells, indicating cDDP does not induce perturbations of intracellular Ca^{2+} homeostasis in this A549 cell model, although direct measurement of $[Ca^{2+}]_{cyt}$ at this time point is required for this to be fully determined. Treatment with cDDP has been reported to induce rises in intracellular Ca^{2+} within one hour of drug addition in a range of cell types, including renal cells, colon carcinoma cells and ovarian carcinoma cells (Berndtsson et al., 2007; Kawai et al., 2006; Mandic et al., 2003; Splettstoesser et al., 2007). No significant change in Fura-2 fluorescence was observed in either A549-WT cells or A549-CR cells over a one hour cDDP treatment period (Figure 27), further suggesting cDDP does not cause Ca^{2+} perturbations in A549 cells. The difference from previous reports may suggest that a requirement for rises in $[Ca^{2+}]_{cyt}$ in cDDP-induced cell death may depend upon the cell type under investigation, whether calpain activation is required in the induction of apoptosis, and upon the drug concentrations and intrinsic cDDP sensitivity of the cells to be studied. Indeed, Splettstoesser *et al.* observed a rise in $[Ca^{2+}]_{cyt}$ in an ovarian cancer cell line but not an osteocarcinoma cell line following cDDP treatment (Splettstoesser et al., 2007).

It is notable that a role for cytosolic Ca^{2+} changes in cDDP cytotoxicity has been inferred from a disparate selection of experimental models using very different drug concentrations, ranging from 3 μM to 1 mM (Kawai et al., 2006; Mandic et al., 2003, 2002; Splettstoesser et al., 2007). Furthermore, the means by which intracellular Ca^{2+} was measured varies dramatically, and includes protocols loading cells with non-ratiometric Ca^{2+} indicators without measures to account for potential differences in dye loading, population measurements of Ca^{2+} likely to include both live and apoptotic cells and manual harvesting of cells which may itself directly cause cell damage and $[Ca^{2+}]_{cyt}$ changes (Berndtsson et al., 2007; Del Bello et al., 2007; Kawai et al., 2006; Mandic et al., 2003; Splettstoesser et al., 2007). Perhaps tellingly, Del Bello *et al.* observed changes in $[Ca^{2+}]_{cyt}$ following cDDP treatment only in frankly apoptotic cells (Del Bello et al., 2007). A role for Ca^{2+} changes in mediating cell death following cDDP treatment is increasingly becoming accepted, and indeed may play a role in some models. However, the evidence upon which this hypothesis is based is surprisingly weak, and the literature would benefit from a systematic study of changes in intracellular Ca^{2+} following treatment with a range of cDDP concentrations in several cell types, in which intracellular Ca^{2+} signalling pathways are well characterised, to help clarify the issue.

4. Discussion

The role of Ca^{2+} in the cDDP sensitivity of A549 cells was further investigated by pharmacological chelation of Ca^{2+} during the cDDP treatment period. Chelation of Ca^{2+} in the extracellular medium did not alter the percentage of PI positive A549-WT cells measured following cDDP treatment (Figure 24), suggesting influx of Ca^{2+} across the plasma membrane is not required for cDDP-induced cell death in this cell line, consistent with the lack of observed changes in intracellular Ca^{2+}. Splettstoesser *et al.* suggest such Ca^{2+} influx may be important only in cells in which a fraction of the IP_3R is localised to the plasma membrane; if this is indeed the case it may be predicted that both A549 cell lines in the present investigation lack such a plasma membrane fraction of the receptor.

Incubation with 10 μM BAPTA-AM during treatment with cDDP provided a modest protection against cell death to A549-WT cells (Figure 23), indicating a potential contribution of intracellular Ca^{2+} to the death process. Several studies have suggested that cDDP may cause emptying of intracellular Ca^{2+} stores to induce cell death (Al-Bahlani et al., 2011; Kawai et al., 2006; Liang & Huang, 2000; Mandic et al., 2002). However, no depletion of the ER Ca^{2+} store was observed in A549-WT cells nor in A549-CR cells following cDDP treatment, and whilst in each of these studies $[Ca^{2+}]_{cyt}$ increased within one hour of drug exposure, such an increase did not occur in the current experimental model. It is possible that limited Ca^{2+} transfer may have occurred directly between the ER and mitochondria to potentiate apoptosis, and direct measurement of mitochondrial Ca^{2+} during cDDP treatment may confirm or disprove this. Likewise, a contribution for other intracellular Ca^{2+} storage compartments in cell death, such as the acidic Ca^{2+} stores, may not be ruled out. Under certain circumstances the ER stress response has been shown to play a pro-survival role and abrogate the toxic effects of cDDP (Feng, Zhai, Yang, Jin, & Zhang, 2011; Y. Lin, Wang, Liu, & Chen, 2011; Pagliacci et al., 1993; Podratz et al., 2011; L.-J. Zhang, Li, Yang, Li, & Ji, 2009), whilst a delay in caspase-3 activation was observed in enucleated melanoma cells expressing high levels of Grp78, an ER-stress induced chaperone, following cDDP treatment (Mandic et al., 2003). Since maintenance of $[Ca^{2+}]_{ER}$ is required for proper function of ER resident proteins and the ER protein-folding machinery, it is also possible that depletion of intracellular Ca^{2+} stores induced an ER stress response in A549-WT cells, providing a degree of protection against cDDP-induced cell death.

Finally, the role of Ca^{2+} efflux through the IP_3R in cDDP-induced cell death of A549-WT cells was directly assessed using the pharmacological IP_3R channel blocker 2-APB. Incubation with 2-APB completely inhibited the rise in $[Ca^{2+}]_{cyt}$ observed in A549-WT cells

in response to stimulation with a supramaximal concentration of extracellular ATP (Figure 28). However, incubation with 2-APB during cDDP treatment did not cause a significant change in the percentage of PI positive A549-WT cells measured after 24 hours (Figure 29), indicating that IP_3R Ca^{2+} channel function is not required for the induction of cell death in response to cDDP. This finding is consistent with the previous observation that cDDP does not cause perturbations of intracellular Ca^{2+} in the A549 cell line under the present experimental conditions.

A549-CR cells showed a marked reduction in intracellular Ca^{2+} signalling evoked by ATP stimulation, store Ca^{2+} depletion and direct stimulation of the IP_3R, however this phenotype was not directly linked to cDDP sensitivity in the present investigation, since cell death in A549-WT cells showed little requirement for Ca^{2+} and occurred independently of IP_3R Ca^{2+} channel activity. It is possible that the observed difference in IP_3R function is related to changes in activity independent of its Ca^{2+} channel function. Anti-apoptotic BCL-2 family proteins inhibit Ca^{2+} release from the IP_3R (Rong & Distelhorst, 2008), and increased expression of these proteins may inhibit cell death in response to cDDP in A549-CR cells, accompanied by decreased intracellular Ca^{2+} responses. Overexpression of these regulators however is often associated with a reduction in the $[Ca^{2+}]_{ER}$ (Rong & Distelhorst, 2008), whilst no difference in ER Ca^{2+} was observed between A549-WT cells and A549-CR cells, thus the expression level of these proteins should be determined. Altered protein binding to the cytosolic domain of the IP_3R may also promote cell survival independent of Ca^{2+} signalling. For example, the IP_3R regulates cellular autophagy through interaction with Beclin-1 (Vicencio et al., 2009), and increased autophagy has been associated with increased cellular resistance to apoptosis, including that induced by cDDP (Claerhout et al., 2010; Harhaji-Trajkovic, Vilimanovich, Kravic-Stevovic, Bumbasirevic, & Trajkovic, 2009; O'Donovan, O'Sullivan, & McKenna, 2011; J.-H. Ren et al., 2010). Whilst the interaction between the IP_3R and Beclin-1 does not alter intracellular Ca^{2+} signalling (Vicencio et al., 2009), changes in the population of proteins interacting with the receptor, such as increased binding of BCL-2, might disrupt Beclin-1 binding and enhance cellular autophagy. As such, the level of autophagy should be determined in both A549-WT and A549-CR cells under normal growth conditions and following cDDP treatment, and the effect of pharmacological enhancers and inhibitors of autophagy on cDDP sensitivity investigated.

Alongside protein binding, the activity of the IP_3R is regulated by posttranslational modification, including phosphorylation. Phosphorylation of the receptor by Akt inhibits

opening of the Ca^{2+} channel (Szado et al., 2008), and since Akt overactivation has been strongly linked with cDDP resistance (Basu & Krishnamurthy, 2010), increased phosphorylation by Akt could induce decreased response to IP_3 in a drug resistant cell line. However, Akt activation was significantly reduced in A549-CR cells relative to A549-WT cells (Figure 16) thus regulation of the IP_3R by Akt is unlikely to account for the functional differences observed in the receptor. The IP_3R is also a target for regulation by other cellular kinases. Phosphorylation at serine residues by PKA sensitises the receptor to opening upon IP_3 binding (S. K. Joseph & Hajnóczky, 2007), and reduced PKA activity has been shown to be linked to the cDDP sensitivity of ovarian carcinoma cells (Cvijic & Chin, 1997). A similar change in the activity of PKC, or another enzyme capable of modulating IP_3R function, favouring cell survival may account for the changes measured in Ca^{2+} signalling.

Although the phenotype of reduced intracellular Ca^{2+} signalling does not contribute to modulating the sensitivity of A549 cells to acute apoptosis induced by high concentrations of cDDP, such changes may have been important during the acquisition of cDDP resistance. Exposure to cDDP induces cellular stress, including increased ROS production, ER stress and nutrient withdrawal due inhibition of metabolic processes by cDDP, which may induce cell death with a Ca^{2+} dependent component. Cells treated with cDDP frequently undergo a period of senescence before resistant colonies of cells are established (Puig et al., 2008). Inhibition of large changes in intracellular Ca^{2+} may favour cell survival under these conditions, and thus not contribute to cellular response to cDDP directly, but promote cell survival during the initial stages of acquiring cDDP resistance. If this were to be the case, A549-CR cells may be predicted to show reduced cell death in response to cellular stress such as nutrient starvation, agents which induce ER stress such as tunicamycin and drugs known to induce Ca^{2+} dependent cell death, such as C_2-ceramide (K. Bianchi et al., 2006). An attempt to model such ROS and Ca^{2+} induced cell death was made during this investigation (Section 3.2.5 & Section 4.11). General adaptation to cellular stress during the acquisition of cDDP resistance may indeed partially explain why some cDDP resistant tumour cells are cross-resistant to a diverse range of other chemotherapy drugs.

Interestingly, reduced function of the IP_3R could be linked to the differences observed in mitochondrial function between A549-WT cells and A549-CR cells (Section 3.3). The IP_3R forms part of an interorganelle complex with VDAC on the mitochondrial outer membrane, mediated by chaperone proteins (Szabadkai et al., 2006), which promotes Ca^{2+} transfer between the organelles. It was recently reported that basal Ca^{2+} release from the IP_3R may be

required to maintain mitochondrial function, increasing basal O_2 consumption and inhibiting the induction of autophagy (Cárdenas et al., 2010). Loss of this basal Ca^{2+} release reduced the activity of PDH, reduced cellular O_2 consumption, and lead to a pro-survival autophagy response mediated through AMPK activation. Inhibition of Ca^{2+} release via the IP_3R may form part of cellular adaptation to mitochondrial dysfunction, inhibiting increases in mitochondrial activity and shifting metabolism away from oxidative phosphorylation. Although no depletion of $[Ca^{2+}]_{ER}$ was observed in A549 cells following cDDP treatment, small IP_3R signalling events involving only a small number of channels do not lead to complete store emptying. Thus it is possible that the increase in mitochondrial oxidative activity measured in A549-WT cells after exposure to cDDP (Figure 32 & Figure 33) may be due to an increase in the frequency of small IP_3R signalling events, whilst inhibition of these events in A549-CR cells prevents similar changes in mitochondrial function from occurring. Disruption of complexes coupling the ER and mitochondrial membranes involving the IP_3R may further act to reduce mitochondrial Ca^{2+} uptake and inhibit increases in mitochondrial function. This hypothesis further highlights the need to investigate changes in mitochondrial Ca^{2+} and autophagic flux following cDDP treatment in both A549 cell lines.

4.10 Oxidative Stress Induced Through TMRM Photoactivation Does Not Model Pathophysiological ER-Mitochondria Ca^{2+} Transfer in A549 Cells

Disruption of IP_3R function may alter the efficiency of Ca^{2+} transfer from the ER to mitochondria, and alter the sensitivity of cells to death induced through mitochondrial Ca^{2+} overload (Szabadkai et al., 2006). Since IP_3R function in A549-CR cells was significantly inhibited in comparison with A549-WT cells, pathological Ca^{2+} transfer from the ER to mitochondria was directly examined using a model of laser-induced oxidative stress. Photoexcitation of TMRM generates both $O_2^{\bullet -}$ and $OH^{\bullet -}$ free radicals (Zorov, Filburn, Klotz, Zweier, & Sollott, 2000). In astrocytes (Jacobson & Duchen, 2002) and cardiomyocytes (Hüser & Blatter, 1999) ROS produced in this way have been hypothesised to act directly at the ER to induce Ca^{2+} release and mPT, most likely through oxidising redox-sensitive residues of the IP_3R and/ or RYR. The process leading from mitochondrial ROS to loss of $\Delta\Psi$ is however not well understood, and in other cell types the mitochondrial 'flickering' characteristic of this method seemingly occurs independent of Ca^{2+} and the mPTP (Falchi, Isola, Diana, Putzolu, & Diaz, 2005; O'Reilly, Fogarty, Drummond, Tuft, & Walsh, 2004;

Zorov et al., 2000). The same appears to be true for the A549 cell line, given that mitochondrial depolarisation induced in A549-WT cells proved insensitive to Ca^{2+} chelation using EGTA + BAPTA-AM, EGTA and ER store Ca^{2+} depletion using Tg prior to illumination and Cyp D inhibition by CsA (Figure 25 C). Instead, one might infer depolarisation in A549 cells loaded with TMRM represents Ca^{2+} independent opening of the mPTP and/ or non-specific toxicity through oxidative damage to the respiratory chain. In further support of this scheme, a threshold concentration of TMRM greater than 50 nM is required for loss of $\Delta\Psi$ within the experimental time period (Figure 25 E), possibly indicating a threshold level of required ROS production, and both depolarisation and $\Delta\Psi$ 'flickering' are fully prevented by addition of ascorbic acid to the cell buffer solution (Figure 25 D). TMRM-induced ROS production is therefore not an appropriate model to measure pathological interorganelle Ca^{2+} transfer in A549 cells, which may be more appropriately investigated using mitochondrial Ca^{2+} probes to monitor changes in mitochondrial matrix Ca^{2+} concentration following stimulation of intracellular Ca^{2+} signalling and the addition of drugs known to induce mitochondrial Ca^{2+} overload. It is worth noting that under TMRM illumination, no significant difference existed between A549-WT cells and A549-CR cells in the time at which loss of $\Delta\Psi$ began or the kinetics of depolarisation. Since this process is wholly dependent upon ROS production (Figure 25 D & E), the lack of a significant difference in the sensitivity to depolarisation suggests the ROS sensitivity of the two A549 cell lines is comparable, and that the difference in ROS production measured following cDDP exposure (Figure 11, Figure 12 & Figure 13) may not be due to differences in the expression of cellular antioxidant defences.

5. Summary

5.1 Future Directions

The present study has identified a novel point mutation in the mtDNA encoded *MT-ND2* gene and D-loop region of a cDDP-resistant NSCLC cell line. Whilst the mutation is present as a low level heteroplasmic variant in the parental, cDDP-sensitive A549-WT cell line, cDDP-resistant A549-CR mtDNA is homoplasmic for this change. Mutations in mtDNA correlate both with tumourigenesis and drug resistant phenotypes in cancer cells (A Chatterjee et al., 2006; H.-C. Lee et al., 2010; S. Mizutani et al., 2009), thus the ND2 mutant here identified may directly contribute to the cDDP-resistant phenotype of A549-CR cells. The creation of cybrid cell lines presents the most direct methodology to assess the contribution of mutations in the mtDNA of the A549-CR cell line to reduced drug sensitivity. To determine the role of changes in the mtDNA sequence on the same nuclear genetic background, enucleated A549-WT and A549-CR cells may be used as mtDNA donors to the same mtDNA deficient (ρ_0) cell line, and the ability of cDDP to induce cell death measured in the resulting cybrid cell lines; differences in drug sensitivity may thus be attributed as resulting from mutant mtDNA. Further, cybrid cell lines created using A549-WT nuclear donor cells with A549-CR mtDNA donor cells, and vice versa, may identify the relative importance of novel mtDNA mutations in governing cDDP-resistance in the A549 cell line, demonstrating whether changes in mtDNA play and important role in comparison to adaptations of nuclear DNA.

The transition of the non-synonymous mt5487T>C mutation from a low-level heteroplasmic variant in A549-WT cells to homoplasmy in the non-clonal A549-CR cell population raises the interesting possibility of positive selection for mtDNA molecules harbouring this mutation, either as a direct influence upon cDDP-sensitivity or promoting the adaptation of tumour cells to survival following cDDP treatment. Further evidence for this may be acquired should a similar apparent selection of mutant mtDNA occur if a second population of cDDP-resistant A549 cells were independently derived from the parental A549-WT cell line *in vitro*, and/ or in an *in vivo* animal model, which might be predicted to show a similar genetic drift in mtDNA.

It is unclear at present how changes in mtDNA may influence cellular sensitivity to apoptotic stimuli, and indeed the effect may depend both upon the nature of the mtDNA mutation and the nature of the apoptotic stimulus (Kwong et al., 2007). Should cybrid cells containing

5. Summary

A549-CR mtDNA be found to be resistant to cDDP-induced cell death, it would be of interest to determine whether this resistance extends to other cellular stresses such as nutrient starvation, UV irradiation, platinum-based chemotherapy drugs such as carboplatin and oxaliplatin, ER stress and microtubule destabilising agents. Conversely, homoplasmic mutations in mtDNA might render A549-CR cells more sensitive to agents which promote mitochondrial metabolism or inhibit glycolysis, such as DCA and 2-deoxyglucose respectively.

The homoplasmic mtDNA mutation present in the *MT-ND2* gene of A549-CR mtDNA likely affects the function of the ND2 subunit, since the rotenone-sensitive activity of respiratory complex-I was reduced in this cell line relative to A549-WT cells. As such, the activity of complex-I may be a determinant of cellular sensitivity to cDDP in this cell model. As a pharmacological approach to this question, incubation of A549-WT cells with low, sub-optimal concentrations of rotenone may mimic the reduced electron transfer from complex I to ubiquinone observed in A549-CR cells, and thus may reduce the sensitivity of A549-WT cells to cDDP. Alternatively, creating cybrid cell lines using cells harbouring independent mutations in *MT-ND2* or mtDNA encoded respiratory complex components may determine whether any pro-survival effect mtDNA mutations following cDDP treatment are specific for those affecting complex-I, or indeed those affecting ND2 function. A method for the exogenous expression of wild-type or mutant ND2, by transfecting nuclear-transcribed DNA constructs converted to the nuclear genetic code along with a mitochondrial targeting sequence, has previously been reported (S. Zhou et al., 2007). The same methodology may be employed in the A549 cell line, creating stable clones expressing the Phe40Leu ND2 mutation varying levels, to assess the effect of increasing mutational load on cDDP sensitivity. Similarly, transfection of wild-type ND2 into A549-CR cells may restore drug sensitivity. Finally, *in silico* analysis of mtDNA sequences derived from cDDP-sensitive and cDDP-resistant tumour samples may reveal whether mutations in *MT-ND2* or respiratory complex-I subunits associate with cDDP resistance *in vivo*.

5. Summary

5.2 Summary

The present work used an A549 lung adenocarcinoma cell line model of acquired cDDP resistance to investigate the potential contribution of the ER and mitochondria to modulation of cDDP sensitivity. A549-CR cells were derived through prolonged culture in the presence of a low concentration of cDDP, and show an approximately two-fold level of resistance to cell death relative to the cDDP-sensitive parental A549-WT cell line following exposure to cDDP.

Treatment with cDDP induced caspase-dependent apoptosis in A549-WT cells 6-12 hours post drug exposure, consistent with the known cytotoxic activity of cDDP. Alterations in cell morphology during this time period were consistent with current definitions of apoptosis, whilst loss of cell viability was significantly inhibited by a pharmacological pan-caspase inhibitor. Cell death was not affected by pharmacological inhibition of caspase-8, indicating that the receptor-mediated pathway of apoptosis is not activated by cDDP in A549 cells. A strong induction of p53 and arrest of cellular proliferation was also observed following cDDP exposure, in agreement with cell cycle arrest known to occur in response to cDDP. However, inhibition of caspases did not completely prevent cell death, indicating that multiple cell death pathways may be stimulated in A549-WT cells by cDDP. Although cDDP caused a significant increase in the rate of both mitochondrial and cytosolic ROS production, A549-WT cell death was not dependent on ROS since antioxidant treatment failed to significantly protect cells from cDDP-induced death. In contrast to a growing number of reports, including studies of the A549 cell line, cDDP did not cause perturbations of cellular Ca^{2+} homeostasis, and accordingly pharmacological calpain inhibition in A549-WT cells did not modulate cDDP sensitivity, suggesting these enzymes are not required for cell death in this experimental model.

The ER may induce cell death through both Ca^{2+} dependent and Ca^{2+} independent pathways, and has been linked in some models to cDDP cytotoxicity. Further, perturbation of intracellular Ca^{2+} homeostasis, caused either by emptying of intracellular Ca^{2+} stores or influx of Ca^{2+} across the plasma membrane, and reduced intracellular Ca^{2+} content has been measured in cDDP resistant cells. Whilst no difference in $[Ca^{2+}]_{ER}$ existed between A549-WT cell and A549-CR cells, intracellular Ca^{2+} a physiological ligand or store depletion was significantly reduced in A549-CR cells in comparison to A549-WT cells. This reduced Ca^{2+} signalling phenotype was due in part to inhibition of IP_3R function, since direct stimulation of

the receptor using a caged IP_3 compound lead to significantly greater changes in $[Ca^{2+}]_{cyt}$ in A549-WT cells, and was not caused by a difference in the basal level of expression. However, pharmacological inhibition of the IP_3R in A549-WT cells did not alter cellular sensitivity to cDDP, indicating that IP_3R Ca^{2+} channel function does not impinge upon cellular cDDP sensitivity. Furthermore, chelation of intracellular Ca^{2+} provided only very modest protection to A549-WT cells treated with cDDP, and removal of external Ca^{2+} was without effect, consistent with the lack of changes in intracellular Ca^{2+} homeostasis induced by cDDP and that calpain activation is not required for cell death under these conditions. Thus, changes in intracellular Ca^{2+} and the Ca^{2+} channel function of the IP_3R do not modulate cDDP sensitivity of A549 cells, although the marked differences in IP_3R function warrant further investigation of factors known to regulate channel activity and IP_3R Ca^{2+} channel independent functions as potential extranuclear determinants of cellular response to cDDP.

Exposure to cDDP significantly increased the rate of ROS production in both A549 cell lines, however this increase was significantly attenuated in A549-CR cells. Similarly, cellular O_2 consumption was significantly increased in A549-WT cells but unchanged in A549-CR cells following cDDP treatment, potentially explaining the difference measured in ROS production. Although reduced ROS production did not contribute to the cDDP-resistant phenotype, decreased flux through the electron transport chain may reduce the propensity of cells to undergo apoptosis, thus the mechanism behind the disparity in O_2 consumption was further investiged. A novel point mutation in the *MTND2* gene of mtDNA was identified as present in heteroplasmy in A549-WT cells and homoplasmy in A549-CR cells, and correlated with an approximately 50% reduction in the activity of mitochondrial respiratory complex I. Both mutations in mtDNA and reduced activity of the ETC have been linked to increased tolerance to apoptosis inducing stimuli, thus the contribution of the changes identified in A549-CR cell mitochondrial to altered cDDP sensitivity will be addressed in future investigations through the generation of cybrid cells using A549-WT cells and A549-CR cells. Although the activity of mitochondrial respiratory complex I was significantly reduced in A549-CR cells, basal mitochondrial function did not differ between A459-WT cells and A549-CR cells. Investigation of the ETC revealed a significantly greater abundance of respiratory complex I in A549-CR cells compared to the A549-WT cell line, possibly a compensatory response to respiratory complex dysfunction. Such changes may form part of a mitochondria-nucleus retrograde response, which in turn may promote cell survival and could alter tumour cell drug sensitivity.

5. Summary

In summary, this study has:

- Further clarified the complex pathways by which cDDP may induce cell death in tumour cells.
- Excluded altered intracellular Ca^{2+} homeostasis, inhibition of Ca^{2+} signalling and reduced IP_3R Ca^{2+} channel function as a determinant of cellular cDDP sensitivity in this experimental model.
- Identified for further study key differences in mitochondrial function between A549-WT cells and A549-CR cells. These differences have the potential to directly impact upon tumour cell fate in response to chemotherapy, and require further investigation to determine whether such differences may modulate cDDP sensitivity.

The present investigation has further outlined the complex nature of the cytotoxic action of cDDP. Whilst describing an apoptotic response with kinetics in good correlation with previously published data, dissimilarities in the contributing factors, notably a lack of Ca^{2+} and ROS dependence, have been observed. As such, the work highlights the complex, cell-type specific nature of responses to cDDP, and may help to explain the variation in the responsiveness of different tumour types to cDDP. In better understanding how such responses may vary, novel drug targets to modulate cDDP sensitivity relative to tumour type may be identified.

Finally, two novel point mutations were found in the mtDNA of drug-resistant cells. This is the first report of the non-synonymous mt5487T>C mutation of *MT-ND2*, and an original characterisation of the reduction in complex I activity reduced complex I activity resulting from mutant ND2. The identification of this novel genetic and functional change in a core cellular metabolic protein associated with a drug resistant cell line may further knowledge on the mechanisms of the emerging role of mtDNA variation on cell fate. Changes in mitochondrial and respiratory complex function related to mtDNA mutations may serve to alter the threshold apoptotic stimulation (mitochondrial priming) required for mitochondria to engage the apoptotic pathway (Chonghaile et al., 2011), altering the sensitivity of tumour cells to chemotherapeutic agents. Research in both *in vitro* and tumour xenograft models may reveal the contribution of changes in mitochondrial function to the apoptotic sensitivity of the organelle.

5. Summary

The correlation between functional complex I mutations and chemoresistance may provide a rationale for further investigation of how mutations in respiratory complex I subunits impinge upon the cDDP-sensitivity of tumour cells. The overall activity of mitochondria in A549-CR cells was not altered relative to A549-WT cells, due to compensatory upregulation of complex I subunit expression and assembly. This is likely to represent a novel mitochondria-nucleus signalling mechanism, and demonstrates the ability of cells to alter metabolism to restore normal cellular function following genetic perturbations. Further work into the signalling factors which allow such changes will shed light on the influence of metabolism and mitochondria on the transcriptional profile of the cell. Targeting such adaptive signalling components may provide a mechanism to modulate tumour cell drug sensitivity.

6. References

Abu-Amero, K. K., Alzahrani, A. S., Zou, M., & Shi, Y. (2005). High frequency of somatic mitochondrial DNA mutations in human thyroid carcinomas and complex I respiratory defect in thyroid cancer cell lines. *Oncogene*, *24*(8), 1455-60. doi:10.1038/sj.onc.1208292

Ahmad, S. (2010). Platinum-DNA interactions and subsequent cellular processes controlling sensitivity to anticancer platinum complexes. *Chemistry & biodiversity*, *7*(3), 543-66. doi:10.1002/cbdv.200800340

Al-Bahlani, S., Fraser, M., Wong, A. Y. C., Sayan, B. S., Bergeron, R., Melino, G., & Tsang, B. K. (2011). P73 regulates cisplatin-induced apoptosis in ovarian cancer cells via a calcium/calpain-dependent mechanism. *Oncogene*. Macmillan Publishers Limited. doi:10.1038/onc.2011.134

Alberts, B. (2008a). Molecular biology of the cell: Reference edition (5th ed., pp. 912-916). Garland Science.

Alberts, B. (2008b). Molecular biology of the cell: Reference edition (5th ed., pp. 45-125). Garland Science.

American Type Culture Collection (ATTC). (2010). ATCC: A549. Retrieved August 7, 2010, from http://www.atcc.org/ATCCAdvancedCatalogSearch/ProductDetails/tabid/452/Default.aspx?ATCCNum=CCL-185&Template=cellBiology

Ando, H., Mizutani, A., Kiefer, H., & Tsuzurugi, D. (2006). IRBIT suppresses IP3 receptor activity by competing with IP3 for the common binding site on the IP3 receptor. *Molecular cell*.

Antunes, L. M., Darin, J. D., & Bianchi, M. D. (2000). Protective effects of vitamin c against cisplatin-induced nephrotoxicity and lipid peroxidation in adult rats: a dose-dependent study. *Pharmacological research : the official journal of the Italian Pharmacological Society*, *41*(4), 405-11. doi:10.1006/phrs.1999.0600

Appleton, T. G. (1999). Diammine- and Diamineplatinum Complexes with Non-Sulfur-Containing Amino Acids and Peptides. In B. Lippert (Ed.), *Cisplatin: Chemistry and Biochemistry of a Leading Anticancer Drug* (pp. 363-378). Wiley.

Aull, J., Allen, R., Bapat, A., Daron, H., Friedman, M., & Wilson, J. (1979). The effects of platinum complexes on seven enzymes. *Biochimica et Biophysica Acta (BBA) - Enzymology*, *571*(2), 352-358. doi:10.1016/0005-2744(79)90105-0

Basu, A., & Krishnamurthy, S. (2010). Cellular responses to Cisplatin-induced DNA damage. *Journal of nucleic acids*, *2010*. doi:10.4061/2010/201367

Baughman, J. M., Perocchi, F., Girgis, H. S., Plovanich, M., Belcher-Timme, C. A., Sancak, Y., Bao, X. R., et al. (2011). Integrative genomics identifies MCU as an essential

component of the mitochondrial calcium uniporter. *Nature*, *advance on*. Nature Publishing Group, a division of Macmillan Publishers Limited. All Rights Reserved. doi:10.1038/nature10234

Beleford, D., Rattan, R., Chien, J., & Shridhar, V. (2010). High temperature requirement A3 (HtrA3) promotes etoposide- and cisplatin-induced cytotoxicity in lung cancer cell lines. *The Journal of biological chemistry*, *285*(16), 12011-27. doi:10.1074/jbc.M109.097790

Berndtsson, M., Hägg, M., Panaretakis, T., Havelka, A. M., Shoshan, M. C., & Linder, S. (2007). Acute apoptosis by cisplatin requires induction of reactive oxygen species but is not associated with damage to nuclear DNA. *International journal of cancer. Journal international du cancer*, *120*(1), 175-80. doi:10.1002/ijc.22132

Berridge, M. J., Bootman, M. D., & Roderick, H. L. (2003). Calcium signalling: dynamics, homeostasis and remodelling. *Nature reviews. Molecular cell biology*, *4*(7), 517-29. Nature Publishing Group. doi:10.1038/nrm1155

Berry, D. L., & Baehrecke, E. H. (2007). Growth arrest and autophagy are required for salivary gland cell degradation in Drosophila. *Cell*, *131*(6), 1137-48. doi:10.1016/j.cell.2007.10.048

Bianchi, K., Vandecasteele, G., Carli, C., Romagnoli, A., Szabadkai, G., & Rizzuto, R. (2006). Regulation of Ca2+ signalling and Ca2+-mediated cell death by the transcriptional coactivator PGC-1alpha. *Cell death and differentiation*, *13*(4), 586-96. doi:10.1038/sj.cdd.4401784

Boehning, D., Patterson, R. L., Sedaghat, L., Glebova, N. O., Kurosaki, T., & Snyder, S. H. (2003). Cytochrome c binds to inositol (1,4,5) trisphosphate receptors, amplifying calcium-dependent apoptosis. *Nature cell biology*, *5*(12), 1051-61. Nature Publishing Group. doi:10.1038/ncb1063

Bonnet, Sébastien, Archer, S. L., Allalunis-Turner, J., Haromy, A., Beaulieu, C., Thompson, R., Lee, C. T., et al. (2007). A mitochondria-K+ channel axis is suppressed in cancer and its normalization promotes apoptosis and inhibits cancer growth. *Cancer cell*, *11*(1), 37-51. doi:10.1016/j.ccr.2006.10.020

Borutaite, V., & Brown, G. C. (2007). Mitochondrial regulation of caspase activation by cytochrome oxidase and tetramethylphenylenediamine via cytosolic cytochrome c redox state. *The Journal of biological chemistry*, *282*(43), 31124-30. doi:10.1074/jbc.M700322200

Bosanquet, N., & Sikora, K. (2006). The economics of cancer care (pp. 1-18). Cambridge University Press.

Brini, M., & Carafoli, E. (2009). Calcium pumps in health and disease. *Physiological reviews*, *89*(4), 1341-78. doi:10.1152/physrev.00032.2008

Brini, M., Marsault, R., Bastianutto, C., Alvarez, J., Pozzan, T., & Rizzuto, R. (1995). Transfected aequorin in the measurement of cytosolic Ca2+ concentration ([Ca2+]c). A critical evaluation. *The Journal of biological chemistry*, *270*(17), 9896-903.

6. References

Brown, R., Clugston, C., Edlin, A., Vasey, P., Kaye, S. B., Burns, P., & Vojtěšek, B. (1993). Increased accumulation of p53 protein in cisplatin-resistant ovarian cell lines. *International Journal of Cancer*, *55*(4), 678-684. doi:10.1002/ijc.2910550428

Brozovic, A., & Osmak, M. (2007). Activation of mitogen-activated protein kinases by cisplatin and their role in cisplatin-resistance. *Cancer letters*, *251*(1), 1-16. doi:10.1016/j.canlet.2006.10.007

Brozovic, A., Ambriović-Ristov, A., & Osmak, M. (2010). The relationship between cisplatin-induced reactive oxygen species, glutathione, and BCL-2 and resistance to cisplatin. *Critical reviews in toxicology*, *40*(4), 347-59. doi:10.3109/10408441003601836

Cahalan, M. D. (2009). STIMulating store-operated Ca(2+) entry. *Nature cell biology*, *11*(6), 669-77. Nature Publishing Group. doi:10.1038/ncb0609-669

Cancer Research UK. (2010). CancerStats Key Facts lung cancer and smoking. *Lung Cancer*, (July). Retrieved from http://info.cancerresearchuk.org/cancerstats/types/lung/index.htm?script=true

Cereghetti, G. M., & Scorrano, L. (2006). The many shapes of mitochondrial death. *Oncogene*, *25*(34), 4717-24. doi:10.1038/sj.onc.1209605

Chami, M., Oulès, B., Szabadkai, G., Tacine, R., Rizzuto, R., & Paterlini-Bréchot, P. (2008). Role of SERCA1 truncated isoform in the proapoptotic calcium transfer from ER to mitochondria during ER stress. *Molecular cell*, *32*(5), 641-51. doi:10.1016/j.molcel.2008.11.014

Chatterjee, A, Mambo, E., & Sidransky, D. (2006). Mitochondrial DNA mutations in human cancer. *Oncogene*, *25*(34), 4663-74. doi:10.1038/sj.onc.1209604

Chen, J., Emara, N., Solomides, C., Parekh, H., & Simpkins, H. (2010). Resistance to platinum-based chemotherapy in lung cancer cell lines. *Cancer chemotherapy and pharmacology*, *66*(6), 1103-11. doi:10.1007/s00280-010-1268-2

Chen, R., Valencia, I., Zhong, F., McColl, K. S., Roderick, H. L., Bootman, M. D., Berridge, M. J., et al. (2004). Bcl-2 functionally interacts with inositol 1,4,5-trisphosphate receptors to regulate calcium release from the ER in response to inositol 1,4,5-trisphosphate. *The Journal of cell biology*, *166*(2), 193-203. doi:10.1083/jcb.200309146

Chiesa, A., Rapizzi, E., Tosello, V., Pinton, P., de Virgilio, M., Fogarty, K. E., & Rizzuto, R. (2001). Recombinant aequorin and green fluorescent protein as valuable tools in the study of cell signalling. *The Biochemical journal*, *355*(Pt 1), 1-12.

Chinnadurai, G., Vijayalingam, S., & Rashmi, R. (2008). BIK, the founding member of the BH3-only family proteins: mechanisms of cell death and role in cancer and pathogenic processes. *Oncogene*, *27 Suppl 1*, S20-9. doi:10.1038/onc.2009.40

Chipuk, J. E., Moldoveanu, T., Llambi, F., Parsons, M. J., & Green, D. R. (2010). The BCL-2 family reunion. *Molecular cell*, *37*(3), 299-310. doi:10.1016/j.molcel.2010.01.025

6. References

Chonghaile, T. N., Sarosiek, K. A., Vo, T.-T., Ryan, J. A., Tammareddi, A., Moore, V. D. G., Deng, J., et al. (2011). Pretreatment Mitochondrial Priming Correlates with Clinical Response to Cytotoxic Chemotherapy. *Science (New York, N.Y.), 334*(6059), 1129-33. doi:10.1126/science.1206727

Chowdhury, I., Tharakan, B., & Bhat, G. K. (2008). Caspases - an update. *Comparative biochemistry and physiology. Part B, Biochemistry & molecular biology, 151*(1), 10-27. doi:10.1016/j.cbpb.2008.05.010

Claerhout, S., Verschooten, L., Van Kelst, S., De Vos, R., Proby, C., Agostinis, P., & Garmyn, M. (2010). Concomitant inhibition of AKT and autophagy is required for efficient cisplatin-induced apoptosis of metastatic skin carcinoma. *International journal of cancer. Journal international du cancer*, *127*(12), 2790-803. doi:10.1002/ijc.25300

Cotter, T. G. (2009). Apoptosis and cancer: the genesis of a research field. *Nature reviews. Cancer*, *9*(7), 501-7. doi:10.1038/nrc2663

Csordás, G., Madesh, M., Antonsson, B., & Hajnóczky, G. (2002). tcBid promotes Ca(2+) signal propagation to the mitochondria: control of Ca(2+) permeation through the outer mitochondrial membrane. *The EMBO journal*, *21*(9), 2198-206. doi:10.1093/emboj/21.9.2198

Csordás, G., Renken, C., Várnai, P., Walter, L., Weaver, D., Buttle, K., Balla, T., et al. (2006). Structural and functional features and significance of the physical linkage between ER and mitochondria. *The Journal of cell biology*, *174*(7), 915-21. doi:10.1083/jcb.200604016

Cullen, K. J., Yang, Z., Schumaker, L., & Guo, Z. (2007). Mitochondria as a critical target of the chemotheraputic agent cisplatin in head and neck cancer. *Journal of bioenergetics and biomembranes*, *39*(1), 43-50. Springer New York. doi:10.1007/s10863-006-9059-5

Cvijic, M. E., & Chin, K. V. (1997). Characterization of a cAMP-dependent protein kinase mutant resistant to cisplatin. *International journal of cancer. Journal international du cancer*, *72*(2), 345-50.

Cárdenas, C., Miller, R. A., Smith, I., Bui, T., Molgó, J., Müller, M., Vais, H., et al. (2010). Essential regulation of cell bioenergetics by constitutive InsP3 receptor Ca2+ transfer to mitochondria. *Cell*, *142*(2), 270-83. doi:10.1016/j.cell.2010.06.007

Dasgupta, P., Kinkade, R., Joshi, B., Decook, C., Haura, E., & Chellappan, S. (2006). Nicotine inhibits apoptosis induced by chemotherapeutic drugs by up-regulating XIAP and survivin. *Proceedings of the National Academy of Sciences of the United States of America*, *103*(16), 6332-7. doi:10.1073/pnas.0509313103

Davey, G. P., Peuchen, S., & Clark, J. B. (1998). Energy thresholds in brain mitochondria. Potential involvement in neurodegeneration. *The Journal of biological chemistry*, *273*(21), 12753-7.

6. References

De Stefani, D., Raffaello, A., Teardo, E., Szabò, I., & Rizzuto, R. (2011). A forty-kilodalton protein of the inner membrane is the mitochondrial calcium uniporter. *Nature*. doi:10.1038/nature10230

DeBerardinis, R. J., Lum, J. J., Hatzivassiliou, G., & Thompson, C. B. (2008). The biology of cancer: metabolic reprogramming fuels cell growth and proliferation. *Cell metabolism*, *7*(1), 11-20. doi:10.1016/j.cmet.2007.10.002

DePinho, R. A. (2000). The age of cancer. *Nature*, *408*(6809), 248-54. doi:10.1038/35041694

Debatin, K.-M., & Krammer, P. H. (2004). Death receptors in chemotherapy and cancer. *Oncogene*, *23*(16), 2950-66. Nature Publishing Group. doi:10.1038/sj.onc.1207558

Declercq, W., Van Herreweghe, F., Vanden Berghe, T., & Vandenabeele, P. (2010). Death Receptor-induced Necroptosis. In G. Melino & D. L. Vaux (Eds.), *Cell Death* (pp. 127-135). Wiley-Blackwell.

Degterev, A., Hitomi, J., Germscheid, M., Ch'en, I. L., Korkina, O., Teng, X., Abbott, D., et al. (2008). Identification of RIP1 kinase as a specific cellular target of necrostatins. *Nature chemical biology*, *4*(5), 313-21. doi:10.1038/nchembio.83

Del Bello, B., Moretti, D., Gamberucci, A., & Maellaro, E. (2007). Cross-talk between calpain and caspase-3/-7 in cisplatin-induced apoptosis of melanoma cells: a major role of calpain inhibition in cell death protection and p53 status. *Oncogene*, *26*(19), 2717-26. doi:10.1038/sj.onc.1210079

Demarcq, C., Bunch, R. T., Creswell, D., & Eastman, A. (1994). The role of cell cycle progression in cisplatin-induced apoptosis in Chinese hamster ovary cells. *Cell growth & differentiation : the molecular biology journal of the American Association for Cancer Research*, *5*(9), 983-93. Retrieved from http://www.ncbi.nlm.nih.gov/pubmed/7819136

Deng, J., Carlson, N., Takeyama, K., Dal Cin, P., Shipp, M., & Letai, A. (2007). BH3 profiling identifies three distinct classes of apoptotic blocks to predict response to ABT-737 and conventional chemotherapeutic agents. *Cancer cell*, *12*(2), 171-85. doi:10.1016/j.ccr.2007.07.001

Devogelaere, B., Verbert, L., Parys, J. B., & Missiaen, L. (2008). The complex regulatory function of the ligand-binding domain of the inositol 1, 4, 5-trisphosphate receptor. *Cell calcium*.

Dhar, S., & Lippard, S. J. (2009). Mitaplatin, a potent fusion of cisplatin and the orphan drug dichloroacetate. *Proceedings of the National Academy of Sciences of the United States of America*, *106*(52), 22199-204. doi:10.1073/pnas.0912276106

Doll, R., Peto, R., Boreham, J., & Sutherland, I. (2004). Mortality in relation to smoking: 50 years' observations on male British doctors. *BMJ (Clinical research ed.)*, *328*(7455), 1519. doi:10.1136/bmj.38142.554479.AE

6. References

Doll, R., Peto, R., Boreham, J., & Sutherland, I. (2005). Mortality from cancer in relation to smoking: 50 years observations on British doctors. *British journal of cancer*, *92*(3), 426-9. doi:10.1038/sj.bjc.6602359

Donaldson, K. L., Goolsby, G. L., & Wahl, A. F. (1994). Cytotoxicity of the anticancer agents cisplatin and taxol during cell proliferation and the cell cycle. *International journal of cancer. Journal international du cancer*, *57*(6), 847-55. Retrieved from http://www.ncbi.nlm.nih.gov/pubmed/7911457

Donnelly, A., & Blagg, B. S. J. (2008). Novobiocin and additional inhibitors of the Hsp90 C-terminal nucleotide-binding pocket. *Current medicinal chemistry*, *15*(26), 2702-17.

Duchen, M. R., Verkhratsky, A., & Muallem, S. (2008). Mitochondria and calcium in health and disease. *Cell calcium*, *44*(1), 1-5. doi:10.1016/j.ceca.2008.02.001

Duprez, L., Wirawan, E., Vanden Berghe, T., & Vandenabeele, P. (2009). Major cell death pathways at a glance. *Microbes and infection / Institut Pasteur*, *11*(13), 1050-62. doi:10.1016/j.micinf.2009.08.013

Dursun, B., He, Z., Somerset, H., Oh, D.-J., Faubel, S., & Edelstein, C. L. (2006). Caspases and calpain are independent mediators of cisplatin-induced endothelial cell necrosis. *American journal of physiology. Renal physiology*, *291*(3), F578-87. doi:10.1152/ajprenal.00455.2005

Eastman, Alan. (1999). The Mechanism of Action of Cisplatin: From Adducts to Apoptosis. In B. Lippert (Ed.), *Cisplatin: Chemistry and Biochemistry of a Leading Anticancer Drug* (pp. 111-131). Wiley.

El-Awady, E.-S. E., Moustafa, Y. M., Abo-Elmatty, D. M., & Radwan, A. (2011). Cisplatin-induced cardiotoxicity: Mechanisms and cardioprotective strategies. *European journal of pharmacology*, *650*(1), 335-41. doi:10.1016/j.ejphar.2010.09.085

Esteller, M. (2008). Epigenetics in cancer. *The New England journal of medicine*, *358*(11), 1148-59. doi:10.1056/NEJMra072067

Evan, G. I., Wyllie, A. H., Gilbert, C. S., Littlewood, T. D., Land, H., Brooks, M., Waters, C. M., et al. (1992). Induction of apoptosis in fibroblasts by c-myc protein. *Cell*, *69*(1), 119-28.

Falchi, A. M., Isola, R., Diana, A., Putzolu, M., & Diaz, G. (2005). Characterization of depolarization and repolarization phases of mitochondrial membrane potential fluctuations induced by tetramethylrhodamine methyl ester photoactivation. *The FEBS journal*, *272*(7), 1649-59. doi:10.1111/j.1742-4658.2005.04586.x

Fan, S., Smith, M. L., Rivet, D. J., Duba, D., Zhan, Q., Kohn, K. W., Fornace, A. J., et al. (1995). Disruption of p53 function sensitizes breast cancer MCF-7 cells to cisplatin and pentoxifylline. *Cancer research*, *55*(8), 1649-54.

Fang, H.-Y., Chang, C.-L., Hsu, S.-H., Huang, C.-Y., Chiang, S.-F., Chiou, S.-H., Huang, C.-H., et al. (2010). ATPase family AAA domain-containing 3A is a novel anti-apoptotic

factor in lung adenocarcinoma cells. *Journal of cell science*, *123*(Pt 7), 1171-80. doi:10.1242/jcs.062034

Fatima, S., Arivarasu, N. A., & Mahmood, R. (2007). Vitamin C attenuates cisplatin-induced alterations in renal brush border membrane enzymes and phosphate transport. *Human & experimental toxicology*, *26*(5), 419-26. doi:10.1177/0960327106072389

Feinstein-Rotkopf, Y., & Arama, E. (2009). Can't live without them, can live with them: roles of caspases during vital cellular processes. *Apoptosis : an international journal on programmed cell death*, *14*(8), 980-95. doi:10.1007/s10495-009-0346-6

Feng, R., Zhai, W. L., Yang, H. Y., Jin, H., & Zhang, Q. X. (2011). Induction of ER stress protects gastric cancer cells against apoptosis induced by cisplatin and doxorubicin through activation of p38 MAPK. *Biochemical and biophysical research communications*, *406*(2), 299-304. doi:10.1016/j.bbrc.2011.02.036

Ferlay J, Shin HR, Bray F, Forman D, Mathers C, P. D. (2010). GLOBOCAN 2008, Cancer Incidence and Mortality Worldwide: IARC CancerBase No. 10 [Internet]. *GLOBOCAN 2008*. Retrieved from

Fischer, U., Jänicke, R. U., & Schulze-Osthoff, K. (2003). Many cuts to ruin: a comprehensive update of caspase substrates. *Cell death and differentiation*, *10*(1), 76-100. doi:10.1038/sj.cdd.4401160

Flourakis, M., Lehen'kyi, V., Beck, B., Raphaël, M., Vandenberghe, M., Abeele, F. V., Roudbaraki, M., et al. (2010). Orai1 contributes to the establishment of an apoptosis-resistant phenotype in prostate cancer cells. *Cell death & disease*, *1*(9), e75. doi:10.1038/cddis.2010.52

Frezza, C., & Gottlieb, E. (2009). Mitochondria in cancer: not just innocent bystanders. *Seminars in cancer biology*, *19*(1), 4-11. doi:10.1016/j.semcancer.2008.11.008

Fu, X., Wan, S., Lyu, Y. L., Liu, L. F., & Qi, H. (2008). Etoposide induces ATM-dependent mitochondrial biogenesis through AMPK activation. *PloS one*, *3*(4), e2009. doi:10.1371/journal.pone.0002009

Fuertes, M. A., Alonso, C., & Pérez, J. M. (2003). Biochemical modulation of Cisplatin mechanisms of action: enhancement of antitumor activity and circumvention of drug resistance. *Chemical reviews*, *103*(3), 645-62. American Chemical Society. doi:10.1021/cr020010d

Fujiwara, T., Grimm, E. A., Mukhopadhyay, T., Zhang, W. W., Owen-Schaub, L. B., & Roth, J. A. (1994). Induction of chemosensitivity in human lung cancer cells in vivo by adenovirus-mediated transfer of the wild-type p53 gene. *Cancer research*, *54*(9), 2287-91.

Gallego, M.-A., Joseph, B., Hemström, T. H., Tamiji, S., Mortier, L., Kroemer, G., Formstecher, P., et al. (2004). Apoptosis-inducing factor determines the chemoresistance of non-small-cell lung carcinomas. *Oncogene*, *23*(37), 6282-91. Nature Publishing Group. doi:10.1038/sj.onc.1207835

6. References

Galluzzi, L., Maiuri, M. C., Vitale, I., Zischka, H., Castedo, M., Zitvogel, L., & Kroemer, G. (2007). Cell death modalities: classification and pathophysiological implications. *Cell Death and Differentiation*, *14*(7), 1237-1243. doi:10.1038/sj.cdd.4402148

Gao, G., & Dou, Q. P. (2000). N-terminal cleavage of bax by calpain generates a potent proapoptotic 18-kDa fragment that promotes bcl-2-independent cytochrome C release and apoptotic cell death. *Journal of cellular biochemistry*, *80*(1), 53-72.

Garrido, N., Pérez-Martos, A., Faro, M., Lou-Bonafonte, J. M., Fernández-Silva, P., López-Pérez, M. J., Montoya, J., et al. (2008). Cisplatin-mediated impairment of mitochondrial DNA metabolism inversely correlates with glutathione levels. *The Biochemical journal*, *414*(1), 93-102. doi:10.1042/BJ20071615

Germain, M., Mathai, J. P., McBride, H. M., & Shore, G. C. (2005). Endoplasmic reticulum BIK initiates DRP1-regulated remodelling of mitochondrial cristae during apoptosis. *The EMBO journal*, *24*(8), 1546-56. doi:10.1038/sj.emboj.7600592

Gerschenson, M., Paik, C. Y., Gaukler, E. L., Diwan, B. A., & Poirier, M. C. (2001). Cisplatin exposure induces mitochondrial toxicity in pregnant rats and their fetuses. *Reproductive toxicology (Elmsford, N.Y.)*, *15*(5), 525-31.

Giaccone G. (2000). Clinical Perspectives on Platinum Resistance. *Drugs*, *59*, 9-17. Adis International.

Giard, D., Aaronson, S., & Todaro, G. (1973). In vitro cultivation of human tumors: establishment of cell lines derived from a series of solid tumors. *Journal of the ….*

Godwin, A. K. (1992). High Resistance to Cisplatin in Human Ovarian Cancer Cell Lines is Associated with Marked Increase of Glutathione Synthesis. *Proceedings of the National Academy of Sciences*, *89*(7), 3070-3074. doi:10.1073/pnas.89.7.3070

Gohil, V. M., Sheth, S. A., Nilsson, R., Wojtovich, A. P., Lee, J. H., Perocchi, F., Chen, W., et al. (2010). Nutrient-sensitized screening for drugs that shift energy metabolism from mitochondrial respiration to glycolysis. *Nature biotechnology*, *28*(3), 249-55. doi:10.1038/nbt.1606

Goldschneider, D., & Mehlen, P. (2010). Dependence receptors: a new paradigm in cell signaling and cancer therapy. *Oncogene*, *29*(13), 1865-82. Macmillan Publishers Limited. doi:10.1038/onc.2010.13

Gottlob, K., Majewski, N., Kennedy, S., Kandel, E., Robey, R. B., & Hay, N. (2001). Inhibition of early apoptotic events by Akt/PKB is dependent on the first committed step of glycolysis and mitochondrial hexokinase. *Genes & Development*, *15*(11), 1406-1418. doi:10.1101/gad.889901

Gozuacik, D., & Kimchi, A. (2007). Autophagy and cell death. *Current topics in developmental biology 78* (Vol. 78, pp. 217-45). Elsevier. doi:10.1016/S0070-2153(06)78006-1

6. References

Griffiths, E. J., & Halestrap, A. P. (1993). Protection by Cyclosporin A of ischemia/reperfusion-induced damage in isolated rat hearts. *Journal of molecular and cellular cardiology*, *25*(12), 1461-9. doi:10.1006/jmcc.1993.1162

Guo, W., Zhang, Y., Chen, T., Wang, Y., Xue, J., Zhang, Y., Xiao, W., et al. (2010). Efficacy of RNAi targeting of pyruvate kinase M2 combined with cisplatin in a lung cancer model. *Journal of cancer research and clinical oncology*. doi:10.1007/s00432-010-0860-5

Halestrap, A. P. (2009). What is the mitochondrial permeability transition pore? *Journal of Molecular and Cellular Cardiology*, *46*(6), 821-831. doi:10.1016/j.yjmcc.2009.02.021

Han, X., Yoon, S. H., Ding, Y., Choi, T. G., Choi, W. J., Kim, Y. H., Kim, Y.-J., et al. (2010). Cyclosporin A and sanglifehrin A enhance chemotherapeutic effect of cisplatin in C6 glioma cells. *Oncology reports*, *23*(4), 1053-62.

Hanahan, D., & Weinberg, R. A. (2000). The hallmarks of cancer. *Cell*, *100*(1), 57-70.

Hancock, J. (2010). Cell Signalling. In 3rd (Ed.), (pp. 210-243). Oxford University Press.

Hao, J., Song, X., Song, B., Liu, Y., Wei, L., Wang, X., & Yu, J. (2008). Effects of lentivirus-mediated HIF-1alpha knockdown on hypoxia-related cisplatin resistance and their dependence on p53 status in fibrosarcoma cells. *Cancer gene therapy*, *15*(7), 449-55. doi:10.1038/cgt.2008.4

Harhaji-Trajkovic, L., Vilimanovich, U., Kravic-Stevovic, T., Bumbasirevic, V., & Trajkovic, V. (2009). AMPK-mediated autophagy inhibits apoptosis in cisplatin-treated tumour cells. *Journal of cellular and molecular medicine*, *13*(9B), 3644-54. doi:10.1111/j.1582-4934.2009.00663.x

Harper, M.-E., Antoniou, A., Villalobos-Menuey, E., Russo, A., Trauger, R., Vendemelio, M., George, A., et al. (2002). Characterization of a novel metabolic strategy used by drug-resistant tumor cells. *The FASEB journal : official publication of the Federation of American Societies for Experimental Biology*, *16*(12), 1550-7. doi:10.1096/fj.02-0541com

Harr, M. W., & Distelhorst, C. W. (2010). Apoptosis and autophagy: decoding calcium signals that mediate life or death. *Cold Spring Harbor perspectives in biology*, *2*(10), a005579. doi:10.1101/cshperspect.a005579

Havelka, A. M., Berndtsson, M., Olofsson, M. H., Shoshan, M. C., & Linder, S. (2007). Mechanisms of action of DNA-damaging anticancer drugs in treatment of carcinomas: is acute apoptosis an “off-target” effect? *Mini reviews in medicinal chemistry*, *7*(10), 1035-9.

He, J., Mao, C.-C., Reyes, A., Sembongi, H., Di Re, M., Granycome, C., Clippingdale, A. B., et al. (2007). The AAA+ protein ATAD3 has displacement loop binding properties and is involved in mitochondrial nucleoid organization. *The Journal of cell biology*, *176*(2), 141-6. doi:10.1083/jcb.200609158

6. References

Holzer, A. K., Samimi, G., Katano, K., Naerdemann, W., Lin, X., Safaei, R., & Howell, S. B. (2004). The copper influx transporter human copper transport protein 1 regulates the uptake of cisplatin in human ovarian carcinoma cells. *Molecular pharmacology*, *66*(4), 817-23. doi:10.1124/mol.104.001198

Huang, H.-L., Fang, L.-W., Lu, S.-P., Chou, C.-K., Luh, T.-Y., & Lai, M.-Z. (2003). DNA-damaging reagents induce apoptosis through reactive oxygen species-dependent Fas aggregation. *Oncogene*, *22*(50), 8168-77. doi:10.1038/sj.onc.1206979

Hüser, J., & Blatter, L. A. (1999). Fluctuations in mitochondrial membrane potential caused by repetitive gating of the permeability transition pore. *The Biochemical journal*, *343 Pt 2*, 311-7. Retrieved from http://www.pubmedcentral.nih.gov/articlerender.fcgi?artid=1220555&tool=pmcentrez&rendertype=abstract

Inomoto, T., Tanaka, A., Mori, S., Jin, M. B., Sato, B., Yanabu, N., Tokuka, A., et al. (1994). Changes in the distribution of the control of the mitochondrial oxidative phosphorylation in regenerating rabbit liver. *Biochimica et biophysica acta*, *1188*(3), 311-7.

Ishida, S., Lee, J., Thiele, D. J., & Herskowitz, I. (2002). Uptake of the anticancer drug cisplatin mediated by the copper transporter Ctr1 in yeast and mammals. *Proceedings of the National Academy of Sciences of the United States of America*, *99*(22), 14298-302. doi:10.1073/pnas.162491399

Jacobson, J., & Duchen, M. R. (2002). Mitochondrial oxidative stress and cell death in astrocytes--requirement for stored Ca2+ and sustained opening of the permeability transition pore. *Journal of cell science*, *115*(Pt 6), 1175-88.

Jemal, A., Siegel, R., Xu, J., & Ward, E. (2010). Cancer Statistics, 2010. *CA: a cancer journal for clinicians*, caac.20073-. doi:10.3322/caac.20073

Jha, P. (2009). Avoidable global cancer deaths and total deaths from smoking. *Nature reviews. Cancer*, *9*(9), 655-64. Nature Publishing Group. doi:10.1038/nrc2703

Jia, L., Allen, P. D., Macey, M. G., Grahn, M. F., Newland, A. C., & Kelsey, S. M. (1997). Mitochondrial electron transport chain activity, but not ATP synthesis, is required for drug-induced apoptosis in human leukaemic cells: a possible novel mechanism of regulating drug resistance. *British Journal of Haematology*, *98*(3), 686-698. doi:10.1046/j.1365-2141.1997.2683085.x

Johnson, C. L., Lu, D., Huang, J., & Basu, A. (2002). Regulation of p53 stabilization by DNA damage and protein kinase C. *Molecular cancer therapeutics*, *1*(10), 861-7.

Jones, R. G., & Thompson, C. B. (2009). Tumor suppressors and cell metabolism: a recipe for cancer growth. *Genes & development*, *23*(5), 537-48. doi:10.1101/gad.1756509

Joseph, A.-M., Rungi, A. A., Robinson, B. H., & Hood, D. A. (2004). Compensatory responses of protein import and transcription factor expression in mitochondrial DNA defects. *American journal of physiology. Cell physiology*, *286*(4), C867-75. doi:10.1152/ajpcell.00191.2003

6. References

Joseph, S. K., & Hajnóczky, G. (2007). IP3 receptors in cell survival and apoptosis: Ca2+ release and beyond. *Apoptosis : an international journal on programmed cell death*, *12*(5), 951-68. doi:10.1007/s10495-007-0719-7

Jung, Y., & Lippard, S. J. (2007). Direct cellular responses to platinum-induced DNA damage. *Chemical reviews*, *107*(5), 1387-407. American Chemical Society. doi:10.1021/cr068207j

Kang, D., Kim, S. H., & Hamasaki, N. (2007). Mitochondrial transcription factor A (TFAM): roles in maintenance of mtDNA and cellular functions. *Mitochondrion*, *7*(1-2), 39-44. doi:10.1016/j.mito.2006.11.017

Kar, P., Samanta, K., Shaikh, S., Chowdhury, A., Chakraborti, T., & Chakraborti, S. (2010). Mitochondrial calpain system: an overview. *Archives of biochemistry and biophysics*, *495*(1), 1-7. doi:10.1016/j.abb.2009.12.020

Karbowski, M., Spodnik, J. H., Teranishi, M., Wozniak, M., Nishizawa, Y., Usukura, J., & Wakabayashi, T. (2001). Opposite effects of microtubule-stabilizing and microtubule-destabilizing drugs on biogenesis of mitochondria in mammalian cells. *Journal of cell science*, *114*(Pt 2), 281-91.

Karpova, T. S., Baumann, C. T., He, L., Wu, X., Grammer, A., Lipsky, P., Hager, G. L., et al. (2003). Fluorescence resonance energy transfer from cyan to yellow fluorescent protein detected by acceptor photobleaching using confocal microscopy and a single laser. *Journal of microscopy*, *209*(Pt 1), 56-70. Retrieved from http://www.ncbi.nlm.nih.gov/pubmed/12535185

Kaufmann, S. H., & Vaux, D. L. (2003). Alterations in the apoptotic machinery and their potential role in anticancer drug resistance. *Oncogene*, *22*(47), 7414-30. doi:10.1038/sj.onc.1206945

Kawai, Y., Nakao, T., Kunimura, N., Kohda, Y., & Gemba, M. (2006). Relationship of Intracellular Calcium and Oxygen Radicals to Cisplatin-Related Renal Cell Injury. *Journal of Pharmacological Sciences*, *100*(1), 65-72. doi:10.1254/jphs.FP0050661

Kelland, L. (2007). The resurgence of platinum-based cancer chemotherapy. *Nature reviews. Cancer*, *7*(8), 573-84. Nature Publishing Group. doi:10.1038/nrc2167

Kerr, J. F., Wyllie, A. H., & Currie, A. R. (1972). Apoptosis: a basic biological phenomenon with wide-ranging implications in tissue kinetics. *British journal of cancer*, *26*(4), 239-57.

King, A., & Gottlieb, E. (2009). Glucose metabolism and programmed cell death: an evolutionary and mechanistic perspective. *Current opinion in cell biology*, *21*(6), 885-93. doi:10.1016/j.ceb.2009.09.009

King, R. J. B., & Robins, M. W. (2006a). Cancer Biology (3rd ed., pp. 62-87). Pearson Education.

6. References

King, R. J. B., & Robins, M. W. (2006b). Cancer biology (3rd ed., pp. 230-262). Pearson Education.

Kluza, J., Marchetti, P., Gallego, M.-A., Lancel, S., Fournier, C., Loyens, A., Beauvillain, J.-C., et al. (2004). Mitochondrial proliferation during apoptosis induced by anticancer agents: effects of doxorubicin and mitoxantrone on cancer and cardiac cells. *Oncogene*, *23*(42), 7018-30. doi:10.1038/sj.onc.1207936

Knox, R. J., Friedlos, F., Lydall, D. A., & Roberts, J. J. (1986). Mechanism of Cytotoxicity of Anticancer Platinum Drugs: Evidence That cis-Diamminedichloroplatinum(II) and cis-Diammine-(1,1-cyclobutanedicarboxylato)platinum(II) Differ Only in the Kinetics of Their Interaction with DNA. *Cancer Res.*, *46*(4_Part_2), 1972-1979.

Kobayashi, S., Yamashita, K., Takeoka, T., Ohtsuki, T., Suzuki, Y., Takahashi, R., Yamamoto, K., et al. (2002). Calpain-mediated X-linked inhibitor of apoptosis degradation in neutrophil apoptosis and its impairment in chronic neutrophilic leukemia. *The Journal of biological chemistry*, *277*(37), 33968-77. doi:10.1074/jbc.M203350200

Koopman, W. J. H., Nijtmans, L. G. J., Dieteren, C. E. J., Roestenberg, P., Valsecchi, F., Smeitink, J. A. M., & Willems, P. H. G. M. (2010). Mammalian mitochondrial complex I: biogenesis, regulation, and reactive oxygen species generation. *Antioxidants & redox signaling*, *12*(12), 1431-70. doi:10.1089/ars.2009.2743

Kroemer, G., & Levine, B. (2008). Autophagic cell death: the story of a misnomer. *Nature reviews. Molecular cell biology*, *9*(12), 1004-10. Nature Publishing Group. doi:10.1038/nrm2529

Kroemer, G., & Pouyssegur, J. (2008). Tumor cell metabolism: cancer’s Achilles' heel. *Cancer cell*, *13*(6), 472-82. doi:10.1016/j.ccr.2008.05.005

Kroemer, G., Galluzzi, L., & Brenner, C. (2007). Mitochondrial membrane permeabilization in cell death. *Physiological reviews*, *87*(1), 99-163. doi:10.1152/physrev.00013.2006

Kroemer, G., Galluzzi, L., Vandenabeele, P., Abrams, J., Alnemri, E. S., Baehrecke, E. H., Blagosklonny, M. V., et al. (2009). Classification of cell death: recommendations of the Nomenclature Committee on Cell Death 2009. *Cell death and differentiation*, *16*(1), 3-11. NIH Public Access. doi:10.1038/cdd.2008.150

Kruidering, M., Van de Water, B., de Heer, E., Mulder, G. J., & Nagelkerke, J. F. (1997). Cisplatin-induced nephrotoxicity in porcine proximal tubular cells: mitochondrial dysfunction by inhibition of complexes I to IV of the respiratory chain. *The Journal of pharmacology and experimental therapeutics*, *280*(2), 638-49.

Kubbutat, M. H., & Vousden, K. H. (1997). Proteolytic cleavage of human p53 by calpain: a potential regulator of protein stability. *Molecular and cellular biology*, *17*(1), 460-8.

Kuznetsov, A. V., Winkler, K., Kirches, E., Lins, H., Feistner, H., & Kunz, W. S. (1997). Application of inhibitor titrations for the detection of oxidative phosphorylation defects in saponin-skinned muscle fibers of patients with mitochondrial diseases. *Biochimica et biophysica acta*, *1360*(2), 142-50.

6. References

Kwong, J. Q., Henning, M. S., Starkov, A., & Manfredi, G. (2007). The mitochondrial respiratory chain is a modulator of apoptosis. *The Journal of cell biology*, *179*(6), 1163-77. doi:10.1083/jcb.200704059

Köberle, B., Tomicic, M. T., Usanova, S., & Kaina, B. (2010). Cisplatin resistance: Preclinical findings and clinical implications. *Biochimica et biophysica acta*, *1806*(2), 172-182. Elsevier B.V. doi:10.1016/j.bbcan.2010.07.004

Lacour, S., Hammann, A., Grazide, S., Lagadic-Gossmann, D., Athias, A., Sergent, O., Laurent, G., et al. (2004). Cisplatin-induced CD95 redistribution into membrane lipid rafts of HT29 human colon cancer cells. *Cancer research*, *64*(10), 3593-8. doi:10.1158/0008-5472.CAN-03-2787

Lacour, S., Micheau, O., Hammann, A., Drouineaud, V., Tschopp, J., Solary, E., & Dimanche-Boitrel, M.-T. (2003). Chemotherapy enhances TNF-related apoptosis-inducing ligand DISC assembly in HT29 human colon cancer cells. *Oncogene*, *22*(12), 1807-16. doi:10.1038/sj.onc.1206127

Lamkanfi, M., Festjens, N., Declercq, W., Vanden Berghe, T., & Vandenabeele, P. (2007). Caspases in cell survival, proliferation and differentiation. *Cell death and differentiation*, *14*(1), 44-55. doi:10.1038/sj.cdd.4402047

Larsson, N. G., Wang, J., Wilhelmsson, H., Oldfors, A., Rustin, P., Lewandoski, M., Barsh, G. S., et al. (1998). Mitochondrial transcription factor A is necessary for mtDNA maintenance and embryogenesis in mice. *Nature genetics*, *18*(3), 231-6. doi:10.1038/ng0398-231

Lau, C. K., Yang, Z. F., Ho, D. W., Ng, M. N., Yeoh, G. C. T., Poon, R. T. P., & Fan, S. T. (2009). An Akt/hypoxia-inducible factor-1alpha/platelet-derived growth factor-BB autocrine loop mediates hypoxia-induced chemoresistance in liver cancer cells and tumorigenic hepatic progenitor cells. *Clinical cancer research : an official journal of the American Association for Cancer Research*, *15*(10), 3462-71. doi:10.1158/1078-0432.CCR-08-2127

Lebiedzinska, M., Szabadkai, G., Jones, A. W. E., Duszynski, J., & Wieckowski, M. R. (2009). Interactions between the endoplasmic reticulum, mitochondria, plasma membrane and other subcellular organelles. *The international journal of biochemistry & cell biology*, *41*(10), 1805-16. doi:10.1016/j.biocel.2009.02.017

Lee, C.-F., Liu, C.-Y., Hsieh, R.-H., & Wei, Y.-H. (2005). Oxidative stress-induced depolymerization of microtubules and alteration of mitochondrial mass in human cells. *Annals of the New York Academy of Sciences*, *1042*, 246-54. doi:10.1196/annals.1338.027

Lee, H.-C., Chang, C.-M., & Chi, C.-W. (2010). Somatic mutations of mitochondrial DNA in aging and cancer progression. *Ageing research reviews*. doi:10.1016/j.arr.2010.08.009

Lemarie, A., & Grimm, S. (2011). Mitochondrial respiratory chain complexes: apoptosis sensors mutated in cancer? *Oncogene*, (April), 1-19. Nature Publishing Group. doi:10.1038/onc.2011.167

6. References

Lemasters, J. J., Theruvath, T. P., Zhong, Z., & Nieminen, A.-L. (2009). Mitochondrial calcium and the permeability transition in cell death. *Biochimica et biophysica acta*, *1787*(11), 1395-401. doi:10.1016/j.bbabio.2009.06.009

Liang, X., & Huang, Y. (2000). Intracellular free calcium concentration and cisplatin resistance in human lung adenocarcinoma A549 cells. *Bioscience reports*, *20*(3), 129-38.

Lieber, M., Smith, B., Szakal, A., Nelson-Rees, W., & Todaro, G. (1976). A continuous tumor-cell line from a human lung carcinoma with properties of type II alveolar epithelial cells. *International journal of cancer. Journal international du cancer*, *17*(1), 62-70.

Limoli, C. L., Giedzinski, E., Morgan, W. F., Swarts, S. G., Jones, G. D. D., & Hyun, W. (2003). Persistent oxidative stress in chromosomally unstable cells. *Cancer research*, *63*(12), 3107-11.

Lin, Y., Wang, Z., Liu, L., & Chen, L. (2011). Akt is the downstream target of GRP78 in mediating cisplatin resistance in ER stress-tolerant human lung cancer cells. *Lung cancer (Amsterdam, Netherlands)*, *71*(3), 291-7. doi:10.1016/j.lungcan.2010.06.004

Liu, Lei, Xing, D., & Chen, W. R. (2009). Micro-calpain regulates caspase-dependent and apoptosis inducing factor-mediated caspase-independent apoptotic pathways in cisplatin-induced apoptosis. *International journal of cancer. Journal international du cancer*, *125*(12), 2757-66. doi:10.1002/ijc.24626

Liu, Lei, Xing, D., Chen, W. R., Chen, T., Pei, Y., & Gao, X. (2008). Calpain-mediated pathway dominates cisplatin-induced apoptosis in human lung adenocarcinoma cells as determined by real-time single cell analysis. *International journal of cancer. Journal international du cancer*, *122*(10), 2210-22. doi:10.1002/ijc.23378

Lu, J., Sharma, L. K., & Bai, Y. (2009). Implications of mitochondrial DNA mutations and mitochondrial dysfunction in tumorigenesis. *Cell research*, *19*(7), 802-15. Shanghai Institutes for Biological Sciences, Chinese Academy of Sciences. doi:10.1038/cr.2009.69

Lujambio, A., Ropero, S., Ballestar, E., Fraga, M. F., Cerrato, C., Setién, F., Casado, S., et al. (2007). Genetic unmasking of an epigenetically silenced microRNA in human cancer cells. *Cancer research*, *67*(4), 1424-9. doi:10.1158/0008-5472.CAN-06-4218

Luo, J., Solimini, N. L., & Elledge, S. J. (2009). Principles of cancer therapy: oncogene and non-oncogene addiction. *Cell*, *136*(5), 823-37. doi:10.1016/j.cell.2009.02.024

Ma, H., Jones, K. R., Guo, R., Xu, P., Shen, Y., & Ren, J. (2010). Cisplatin compromises myocardial contractile function and mitochondrial ultrastructure: role of endoplasmic reticulum stress. *Clinical and experimental pharmacology & physiology*, *37*(4), 460-5. doi:10.1111/j.1440-1681.2009.05323.x

Majmundar, A. J., Wong, W. J., & Simon, M. C. (2010). Hypoxia-inducible factors and the response to hypoxic stress. *Molecular cell*, *40*(2), 294-309. Elsevier Inc. doi:10.1016/j.molcel.2010.09.022

6. References

Maliakel, D. M., Kagiya, T. V., & Nair, C. K. K. (2008). Prevention of cisplatin-induced nephrotoxicity by glucosides of ascorbic acid and alpha-tocopherol. *Experimental and toxicologic pathology : official journal of the Gesellschaft für Toxikologische Pathologie*, *60*(6), 521-7. doi:10.1016/j.etp.2008.04.015

Mancini, M., Anderson, B. O., Caldwell, E., Sedghinasab, M., Paty, P. B., & Hockenbery, D. M. (1997). Mitochondrial proliferation and paradoxical membrane depolarization during terminal differentiation and apoptosis in a human colon carcinoma cell line. *The Journal of cell biology*, *138*(2), 449-69.

Mandic, A., Hansson, J., Linder, S., & Shoshan, M. C. (2003). Cisplatin induces endoplasmic reticulum stress and nucleus-independent apoptotic signaling. *The Journal of biological chemistry*, *278*(11), 9100-6. doi:10.1074/jbc.M210284200

Mandic, A., Viktorsson, K., Strandberg, L., Heiden, T., Hansson, J., Linder, S., & Shoshan, M. C. (2002). Calpain-mediated Bid cleavage and calpain-independent Bak modulation: two separate pathways in cisplatin-induced apoptosis. *Molecular and cellular biology*, *22*(9), 3003-13.

Maniccia-Bozzo, E., Espiritu, M. B., & Singh, G. (1990). Differential effects of cisplatin on mouse hepatic and renal mitochondrial DNA. *Molecular and cellular biochemistry*, *94*(1), 83-8.

Marchi, S., Rimessi, A., Giorgi, C., Baldini, C., Ferroni, L., Rizzuto, R., & Pinton, P. (2008). Akt kinase reducing endoplasmic reticulum Ca2+ release protects cells from Ca2+-dependent apoptotic stimuli. *Biochemical and biophysical research communications*, *375*(4), 501-5. doi:10.1016/j.bbrc.2008.07.153

Marks, F., Klingmüller, U., & Müller-Decker, K. (2009). Cellular signal processing: an introduction to the molecular mechanisms of signal transduction (pp. 477-543). Garland Science.

Martins, N. M., Santos, N. A. G., Curti, C., Bianchi, M. L. P., & Santos, A. C. (2008). Cisplatin induces mitochondrial oxidative stress with resultant energetic metabolism impairment, membrane rigidification and apoptosis in rat liver. *Journal of applied toxicology : JAT*, *28*(3), 337-44. doi:10.1002/jat.1284

Mathai, J. P., Germain, M., & Shore, G. C. (2005). BH3-only BIK regulates BAX,BAK-dependent release of Ca2+ from endoplasmic reticulum stores and mitochondrial apoptosis during stress-induced cell death. *The Journal of biological chemistry*, *280*(25), 23829-36. doi:10.1074/jbc.M500800200

Matsuyama, W., Nakagawa, M., Wakimoto, J., Hirotsu, Y., Kawabata, M., & Osame, M. (2003). Mitochondrial DNA mutation correlates with stage progression and prognosis in non-small cell lung cancer. *Human mutation*, *21*(4), 441-3. doi:10.1002/humu.10196

McCormack, J. G., Halestrap, A. P., & Denton, R. M. (1990). Role of calcium ions in regulation of mammalian intramitochondrial metabolism. *Physiological reviews*, *70*(2), 391-425.

6. References

Michelakis, E. D., Webster, L., & Mackey, J. R. (2008). Dichloroacetate (DCA) as a potential metabolic-targeting therapy for cancer. *British journal of cancer*, *99*(7), 989-94. doi:10.1038/sj.bjc.6604554

Mitchell, P. (1961). Coupling of phosphorylation to electron and hydrogen transfer by a chemi-osmotic type of mechanism. *Nature*, *191*, 144-8.

Miyawaki, A., Matheson, J. M., Sayers, L. G., Muto, A., Michikawa, T., Furuichi, T., & Mikoshiba, K. (1999). Expression of green fluorescent protein and inositol 1,4,5-triphosphate receptor in Xenopus laevis oocytes. *Methods in enzymology*, *302*, 225-33. Retrieved from http://www.ncbi.nlm.nih.gov/pubmed/12876775

Mizutani, S., Miyato, Y., Shidara, Y., Asoh, S., Tokunaga, A., Tajiri, T., & Ohta, S. (2009). Mutations in the mitochondrial genome confer resistance of cancer cells to anticancer drugs. *Cancer science*, *100*(9), 1680-7. doi:10.1111/j.1349-7006.2009.01238.x

Montisano, D. F., Cascarano, J., Pickett, C. B., & James, T. W. (1982). Association between mitochondria and rough endoplasmic reticulum in rat liver. *The Anatomical record*, *203*(4), 441-50. doi:10.1002/ar.1092030403

Moreno-Sánchez, R., Saavedra, E., Rodríguez-Enríquez, S., Gallardo-Pérez, J. C., Quezada, H., & Westerhoff, H. V. (2010). Metabolic control analysis indicates a change of strategy in the treatment of cancer. *Mitochondrion*, *10*(6), 626-39. doi:10.1016/j.mito.2010.06.002

Murata, T., Hibasami, H., Maekawa, S., Tagawa, T., & Nakashima, K. (1990). Preferential binding of cisplatin to mitochondrial DNA and suppression of ATP generation in human malignant melanoma cells. *Biochemistry international*, *20*(5), 949-55. Retrieved from http://www.ncbi.nlm.nih.gov/pubmed?term=Preferential binding of cisplatin to mitochondrial DNA and suppression of ATP generation in human malignant melanoma cells

Nakamaru-Ogiso, E., Han, H., Matsuno-Yagi, A., Keinan, E., Sinha, S. C., Yagi, T., & Ohnishi, T. (2010). The ND2 subunit is labeled by a photoaffinity analogue of asimicin, a potent complex I inhibitor. *FEBS letters*, *584*(5), 883-8. Federation of European Biochemical Societies. doi:10.1016/j.febslet.2010.01.004

Nicholls, D. G., & Ferguson, S. J. (2002). *Bioenergetics* (3rd ed., p. 297). Academic Press.

Norberg, E., Gogvadze, V., Ott, M., Horn, M., Uhlén, P., Orrenius, S., & Zhivotovsky, B. (2008). An increase in intracellular Ca2+ is required for the activation of mitochondrial calpain to release AIF during cell death. *Cell death and differentiation*, *15*(12), 1857-64. Macmillan Publishers Limited. doi:10.1038/cdd.2008.123

Norberg, E., Orrenius, S., & Zhivotovsky, B. (2010). Mitochondrial regulation of cell death: processing of apoptosis-inducing factor (AIF). *Biochemical and biophysical research communications*, *396*(1), 95-100. doi:10.1016/j.bbrc.2010.02.163

Nugent, S. M. E., Mothersill, C. E., Seymour, C., McClean, B., Lyng, F. M., & Murphy, J. E. J. (2007). Increased mitochondrial mass in cells with functionally compromised

mitochondria after exposure to both direct gamma radiation and bystander factors. *Radiation research*, *168*(1), 134-42. doi:10.1667/RR0769.1

Olivero, O. A., Chang, P. K., Lopez-Larraza, D. M., Semino-Mora, M. C., & Poirier, M. C. (1997). Preferential formation and decreased removal of cisplatin-DNA adducts in Chinese hamster ovary cell mitochondrial DNA as compared to nuclear DNA. *Mutation research*, *391*(1-2), 79-86.

Orrenius, S. (2008). Reactive Oxygen Species in Mitochondria-Mediated Cell Death. Informa UK Ltd UK.

Orrenius, S., Zhivotovsky, B., & Nicotera, P. (2003). Regulation of cell death: the calcium-apoptosis link. *Nature reviews. Molecular cell biology*, *4*(7), 552-65. Nature Publishing Group. doi:10.1038/nrm1150

Osaki, S., Nakanishi, Y., Takayama, K., Pei, X. H., Ueno, H., & Hara, N. (2000). Alteration of drug chemosensitivity caused by the adenovirus-mediated transfer of the wild-type p53 gene in human lung cancer cells. *Cancer gene therapy*, *7*(2), 300-7. doi:10.1038/sj.cgt.7700096

O'Donovan, T. R., O'Sullivan, G. C., & McKenna, S. L. (2011). Induction of autophagy by drug-resistant esophageal cancer cells promotes their survival and recovery following treatment with chemotherapeutics. *Autophagy*, *7*(5), 509-24.

O'Dwyer, P. J., Stevenson, J. P., & Johnson, S. W. (1999). Clinical Status of Cisplatin, Carboplatin and Other Platinum-Based Antitumor Drugs. In B. Lippert (Ed.), *Cisplatin: Chemistry and Biochemistry of a Leading Anticancer Drug* (pp. 31-72). Wiley.

O'Reilly, C. M., Fogarty, K. E., Drummond, R. M., Tuft, R. A., & Walsh, J. V. (2004). Spontaneous mitochondrial depolarizations are independent of SR Ca2+ release. *American journal of physiology. Cell physiology*, *286*(5), C1139-51. doi:10.1152/ajpcell.00371.2003

Paget, S., & London, W. (2006). Observations from a ploughman. *Cancer*, *573*(April), 2281-2287.

Pagliacci, M. C., Spinozzi, F., Migliorati, G., Fumi, G., Smacchia, M., Grignani, F., Riccardi, C., et al. (1993). Genistein inhibits tumour cell growth in vitro but enhances mitochondrial reduction of tetrazolium salts: a further pitfall in the use of the MTT assay for evaluating cell growth and survival. *European journal of cancer (Oxford, England : 1990)*, *29A*(11), 1573-7.

Palmer, A. E., Jin, C., Reed, J. C., & Tsien, R. Y. (2004). Bcl-2-mediated alterations in endoplasmic reticulum Ca2+ analyzed with an improved genetically encoded fluorescent sensor. *Proceedings of the National Academy of Sciences of the United States of America*, *101*(50), 17404-9. doi:10.1073/pnas.0408030101

Parisi, M. A., & Clayton, D. A. (1991). Similarity of human mitochondrial transcription factor 1 to high mobility group proteins. *Science (New York, N.Y.)*, *252*(5008), 965-9.

6. References

Park, S. A., Choi, K. S., Bang, J. H., Huh, K., & Kim, S. U. (2002). Cisplatin-Induced Apoptotic Cell Death in Mouse Hybrid Neurons Is Blocked by Antioxidants Through Suppression of Cisplatin-Mediated Accumulation of p53 but Not of Fas/Fas Ligand. *Journal of Neurochemistry*, *75*(3), 946-953. doi:10.1046/j.1471-4159.2000.0750946.x

Pastorino, J. G., & Hoek, J. B. (2008). Regulation of hexokinase binding to VDAC. *Journal of bioenergetics and biomembranes*, *40*(3), 171-82. doi:10.1007/s10863-008-9148-8

Pastorino, J. G., Shulga, N., & Hoek, J. B. (2002). Mitochondrial binding of hexokinase II inhibits Bax-induced cytochrome c release and apoptosis. *The Journal of biological chemistry*, *277*(9), 7610-8. doi:10.1074/jbc.M109950200

Patel, S. (2004). NAADP-induced Ca2+ release -- a new signalling pathway. *Biology of the cell / under the auspices of the European Cell Biology Organization*, *96*(1), 19-28. doi:10.1016/j.biolcel.2003.12.001

Perocchi, F., Gohil, V. M., Girgis, H. S., Bao, X. R., McCombs, J. E., Palmer, A. E., & Mootha, V. K. (2010). MICU1 encodes a mitochondrial EF hand protein required for Ca(2+) uptake. *Nature*. doi:10.1038/nature09358

Pinton, P., Giorgi, C., Siviero, R., Zecchini, E., & Rizzuto, R. (2008). Calcium and apoptosis: ER-mitochondria Ca2+ transfer in the control of apoptosis. *Oncogene*, *27*(50), 6407-18. Macmillan Publishers Limited. doi:10.1038/onc.2008.308

Podratz, J. L., Knight, A. M., Ta, L. E., Staff, N. P., Gass, J. M., Genelin, K., Schlattau, A., et al. (2011). Cisplatin induced Mitochondrial DNA damage in dorsal root ganglion neurons. *Neurobiology of disease*, *41*(3), 661-8. doi:10.1016/j.nbd.2010.11.017

Pop, C., & Salvesen, G. S. (2009). Human caspases: activation, specificity, and regulation. *The Journal of biological chemistry*, *284*(33), 21777-81. doi:10.1074/jbc.R800084200

Puig, P.-E., Guilly, M.-N., Bouchot, A., Droin, N., Cathelin, D., Bouyer, F., Favier, L., et al. (2008). Tumor cells can escape DNA-damaging cisplatin through DNA endoreduplication and reversible polyploidy. *Cell biology international*, *32*(9), 1031-43. doi:10.1016/j.cellbi.2008.04.021

Rao, R. V., Castro-Obregon, S., Frankowski, H., Schuler, M., Stoka, V., del Rio, G., Bredesen, D. E., et al. (2002). Coupling endoplasmic reticulum stress to the cell death program. An Apaf-1-independent intrinsic pathway. *The Journal of biological chemistry*, *277*(24), 21836-42. doi:10.1074/jbc.M202726200

Reedijk, J. (1999). Why Does Cisplatin Reach Guanine-N7 with Competing S-Donor Ligands Available in the Cell? *Chemical Reviews*, *99*(9), 2499-2510. American Chemical Society. doi:10.1021/cr980422f

Reipert, S., Berry, J., Hughes, M. F., Hickman, J. A., & Allen, T. D. (1995). Changes of mitochondrial mass in the hemopoietic stem cell line FDCP-mix after treatment with etoposide: a correlative study by multiparameter flow cytometry and confocal and electron microscopy. *Experimental cell research*, *221*(2), 281-8. doi:10.1006/excr.1995.1376

6. References

Ren, J.-H., He, W.-S., Nong, L., Zhu, Q.-Y., Hu, K., Zhang, R.-G., Huang, L.-L., et al. (2010). Acquired cisplatin resistance in human lung adenocarcinoma cells is associated with enhanced autophagy. *Cancer biotherapy & radiopharmaceuticals*, *25*(1), 75-80. doi:10.1089/cbr.2009.0701

Rizzuto, R, Brini, M., Murgia, M., & Pozzan, T. (1993). Microdomains with high Ca2+ close to IP3-sensitive channels that are sensed by neighboring mitochondria. *Science*.

Rizzuto, R, Pinton, P., Carrington, W., Fay, F., & Fogarty, K. (1998). Close contacts with the endoplasmic reticulum as determinants of mitochondrial Ca2+ responses. *Science*.

Rizzuto, R, Pinton, P., Ferrari, D., Chami, M., Szabadkai, G., Magalhães, P. J., Di Virgilio, F., et al. (2003). Calcium and apoptosis: facts and hypotheses. *Oncogene*, *22*(53), 8619-27. Nature Publishing Group. doi:10.1038/sj.onc.1207105

Rodríguez-Enríquez, S., Marín-Hernández, A., Gallardo-Pérez, J. C., Carreño-Fuentes, L., & Moreno-Sánchez, R. (2009). Targeting of cancer energy metabolism. *Molecular nutrition & food research*, *53*(1), 29-48. doi:10.1002/mnfr.200700470

Rong, Y., & Distelhorst, C. W. (2008). Bcl-2 protein family members: versatile regulators of calcium signaling in cell survival and apoptosis. *Annual review of physiology*, *70*, 73-91. Annual Reviews. doi:10.1146/annurev.physiol.70.021507.105852

Rosenberg, B., Van Camp, L., & Krigas, T. (1965). Inhibition of Cell Division in Escherichia coli by Electrolysis Products from a Platinum Electrode. *Nature*, *205*(4972), 698-699. doi:10.1038/205698a0

Ruddon, R. W. (2007a). Cancer Biology (4th ed., pp. 10-12). Oxford University Press.

Ruddon, R. W. (2007b). Cancer Biology (4th ed., pp. 17-55). Oxford University Press.

Ruddon, R. W. (2007c). Cancer Biology (4th ed., pp. 321-362). Oxford University Press.

Safaei, R. (2006). Role of copper transporters in the uptake and efflux of platinum containing drugs. *Cancer letters*, *234*(1), 34-9. doi:10.1016/j.canlet.2005.07.046

Sancho-Martínez, S. M., Piedrafita, F. J., Cannata-Andía, J. B., López-Novoa, J. M., & López-Hernández, F. J. (2011). Necrotic concentrations of cisplatin activate the apoptotic machinery but inhibit effector caspases and interfere with the execution of apoptosis. *Toxicological sciences : an official journal of the Society of Toxicology*, 1-30. doi:10.1093/toxsci/kfr098

Santandreu, F. M., Roca, P., & Oliver, J. (2010). Uncoupling protein-2 knockdown mediates the cytotoxic effects of cisplatin. *Free radical biology & medicine*, *49*(4), 658-66. Elsevier Inc. doi:10.1016/j.freeradbiomed.2010.05.031

Schrödl, K., Oelmez, H., Edelmann, M., Huber, R. M., & Bergner, A. (2009). Altered Ca2+-homeostasis of cisplatin-treated and low level resistant non-small-cell and small-cell lung cancer cells. *Cellular Oncology*, *31*(4), 301-15. doi:10.3233/CLO-2009-0472

6. References

Schwartz, Gary K, & Shah, M. A. (2005). Targeting the cell cycle: a new approach to cancer therapy. *Journal of clinical oncology : official journal of the American Society of Clinical Oncology*, *23*(36), 9408-21. American Society of Clinical Oncology. doi:10.1200/JCO.2005.01.5594

Scorrano, L., Ashiya, M., Buttle, K., Weiler, S., Oakes, S. A., Mannella, C. A., & Korsmeyer, S. J. (2002). A Distinct Pathway Remodels Mitochondrial Cristae and Mobilizes Cytochrome c during Apoptosis. *Developmental Cell*, *2*(1), 55-67. doi:10.1016/S1534-5807(01)00116-2

Shah, M A, & Schwartz, G. K. (2001). Cell cycle-mediated drug resistance: an emerging concept in cancer therapy. *Clinical cancer research : an official journal of the American Association for Cancer Research*, *7*(8), 2168-81. Retrieved from http://www.ncbi.nlm.nih.gov/pubmed/11489790

Sharma, R. P., & Edwards, I. R. (1983). cis-Platinum: subcellular distribution and binding to cytosolic ligands. *Biochemical pharmacology*, *32*(18), 2665-9.

Shaw, R. J., & Cantley, L. C. (2006). Ras, PI(3)K and mTOR signalling controls tumour cell growth. *Nature*, *441*(7092), 424-30. doi:10.1038/nature04869

Shidara, Y., Yamagata, K., Kanamori, T., Nakano, K., Kwong, J. Q., Manfredi, G., Oda, H., et al. (2005). Positive contribution of pathogenic mutations in the mitochondrial genome to the promotion of cancer by prevention from apoptosis. *Cancer research*, *65*(5), 1655-63. doi:10.1158/0008-5472.CAN-04-2012

Shim, H., Dolde, C., Lewis, B. C., Wu, C. S., Dang, G., Jungmann, R. A., Dalla-Favera, R., et al. (1997). c-Myc transactivation of LDH-A: implications for tumor metabolism and growth. *Proceedings of the National Academy of Sciences of the United States of America*, *94*(13), 6658-63.

Shintani, T., & Klionsky, D. J. (2004). Autophagy in health and disease: a double-edged sword. *Science (New York, N.Y.)*, *306*(5698), 990-5. doi:10.1126/science.1099993

Shlomi, T., Benyamini, T., Gottlieb, E., Sharan, R., & Ruppin, E. (2011). Genome-Scale Metabolic Modeling Elucidates the Role of Proliferative Adaptation in Causing the Warburg Effect. (J. A. Papin, Ed.)*PLoS Computational Biology*, *7*(3), e1002018. doi:10.1371/journal.pcbi.1002018

Shore, G. C., & Tata, J. R. (1977). Two fractions of rough endoplasmic reticulum from rat liver. I. Recovery of rapidly sedimenting endoplasmic reticulum in association with mitochondria. *The Journal of cell biology*, *72*(3), 714-25.

Siddik, Z. H. (2003). Cisplatin: mode of cytotoxic action and molecular basis of resistance. *Oncogene*, *22*(47), 7265-79. Nature Publishing Group. doi:10.1038/sj.onc.1206933

Simmen, T., Aslan, J. E., Blagoveshchenskaya, A. D., Thomas, L., Wan, L., Xiang, Y., Feliciangeli, S. F., et al. (2005). PACS-2 controls endoplasmic reticulum-mitochondria communication and Bid-mediated apoptosis. *The EMBO journal*, *24*(4), 717-29. doi:10.1038/sj.emboj.7600559

6. References

Singh, G., & Maniccia-Bozzo, E. (1990). Evidence for lack of mitochondrial DNA repair following cis-dichlorodiammineplatinum treatment. *Cancer chemotherapy and pharmacology*, *26*(2), 97-100.

Song, Xianrang, Liu, X., Chi, W., Liu, Y., Wei, L., Wang, X., & Yu, J. (2006). Hypoxia-induced resistance to cisplatin and doxorubicin in non-small cell lung cancer is inhibited by silencing of HIF-1alpha gene. *Cancer chemotherapy and pharmacology*, *58*(6), 776-84. doi:10.1007/s00280-006-0224-7

Spierings, D. C. J., de Vries, E. G. E., Vellenga, E., & de Jong, S. (2003). Loss of drug-induced activation of the CD95 apoptotic pathway in a cisplatin-resistant testicular germ cell tumor cell line. *Cell death and differentiation*, *10*(7), 808-22. doi:10.1038/sj.cdd.4401248

Splettstoesser, F., Florea, A.-M., & Büsselberg, D. (2007). IP(3) receptor antagonist, 2-APB, attenuates cisplatin induced Ca2+-influx in HeLa-S3 cells and prevents activation of calpain and induction of apoptosis. *British journal of pharmacology*, *151*(8), 1176-86. doi:10.1038/sj.bjp.0707335

Stephens, F. O., & Aigner, K. R. (2009). Basics of Oncology (pp. 87-120). Springer.

Stryer, L., Berg, J. M., & Tymoczko, J. L. (2002). *Biochemistry* (5th ed.). W.H.Freeman & Co Ltd.

Su, H. C., & Lenardo, M. J. (2010). Apoptosis: Inherited Disorders. *Cell Death* (pp. 253-261). Wiley-Blackwell.

Sudarshan, S., Pinto, P. A., Neckers, L., & Linehan, W. M. (2007). Mechanisms of disease: hereditary leiomyomatosis and renal cell cancer--a distinct form of hereditary kidney cancer. *Nature clinical practice. Urology*, *4*(2), 104-10. Nature Publishing Group. doi:10.1038/ncpuro0711

Szabadkai, G., & Duchen, M. R. (2008). Mitochondria: the hub of cellular Ca2+ signaling. *Physiology (Bethesda, Md.)*, *23*, 84-94. doi:10.1152/physiol.00046.2007

Szabadkai, G., Bianchi, K., Várnai, P., De Stefani, D., Wieckowski, M. R., Cavagna, D., Nagy, A. I., et al. (2006). Chaperone-mediated coupling of endoplasmic reticulum and mitochondrial Ca2+ channels. *The Journal of cell biology*, *175*(6), 901-11. doi:10.1083/jcb.200608073

Szado, T., Vanderheyden, V., Parys, J. B., De Smedt, H., Rietdorf, K., Kotelevets, L., Chastre, E., et al. (2008). Phosphorylation of inositol 1,4,5-trisphosphate receptors by protein kinase B/Akt inhibits Ca2+ release and apoptosis. *Proceedings of the National Academy of Sciences of the United States of America*, *105*(7), 2427-32. doi:10.1073/pnas.0711324105

Tait, S. W. G., & Green, D. R. (2008). Caspase-independent cell death: leaving the set without the final cut. *Oncogene*, *27*(50), 6452-61. Macmillan Publishers Limited. doi:10.1038/onc.2008.311

6. References

Tait, S. W. G., & Green, D. R. (2010). Mitochondria and cell death: outer membrane permeabilization and beyond. *Nature reviews. Molecular cell biology*, (August). Nature Publishing Group. doi:10.1038/nrm2952

Tajeddine, N., Galluzzi, L., Kepp, O., Hangen, E., Morselli, E., Senovilla, L., Araujo, N., et al. (2008). Hierarchical involvement of Bak, VDAC1 and Bax in cisplatin-induced cell death. *Oncogene*, *27*(30), 4221-32. Macmillan Publishers Limited. doi:10.1038/onc.2008.63

Telford, J. E., Kilbride, S. M., & Davey, G. P. (2009). Complex I is rate-limiting for oxygen consumption in the nerve terminal. *The Journal of biological chemistry*, *284*(14), 9109-14. doi:10.1074/jbc.M809101200

Tennant, D. A., Durán, R. V., & Gottlieb, E. (2010). Targeting metabolic transformation for cancer therapy. *Nature reviews. Cancer*, *10*(4), 267-77. doi:10.1038/nrc2817

Tennant, D. A., Durán, R. V., Boulahbel, H., & Gottlieb, E. (2009). Metabolic transformation in cancer. *Carcinogenesis*, *30*(8), 1269-80. doi:10.1093/carcin/bgp070

Thorens, B., & Mueckler, M. M. (2009). Glucose transporters in the 21st Century. *American journal of physiology. Endocrinology and metabolism*, *298*(2), E141-145. doi:10.1152/ajpendo.00712.2009

Timmer, J. C., & Salvesen, G. S. (2007). Caspase substrates. *Cell death and differentiation*, *14*(1), 66-72. doi:10.1038/sj.cdd.4402059

Tomiyama, A., Serizawa, S., Tachibana, K., Sakurada, K., Samejima, H., Kuchino, Y., & Kitanaka, C. (2006). Critical role for mitochondrial oxidative phosphorylation in the activation of tumor suppressors Bax and Bak. *Journal of the National Cancer Institute*, *98*(20), 1462-73. doi:10.1093/jnci/djj395

Toyozumi, Y., Arima, N., Izumaru, S., Kato, S., Morimatsu, M., & Nakashima, T. (2004). Loss of caspase-8 activation pathway is a possible mechanism for CDDP resistance in human laryngeal squamous cell carcinoma, HEp-2 cells. *International journal of oncology*, *25*(3), 721-8.

Tsunoda, T., Koga, H., Yokomizo, A., Tatsugami, K., Eto, M., Inokuchi, J., Hirata, A., et al. (2005). Inositol 1,4,5-trisphosphate (IP3) receptor type1 (IP3R1) modulates the acquisition of cisplatin resistance in bladder cancer cell lines. *Oncogene*, *24*(8), 1396-402. doi:10.1038/sj.onc.1208313

Vakifahmetoglu, H., Olsson, M., & Zhivotovsky, B. (2008). Death through a tragedy: mitotic catastrophe. *Cell death and differentiation*, *15*(7), 1153-62. doi:10.1038/cdd.2008.47

Vakifahmetoglu, H., Olsson, M., Tamm, C., Heidari, N., Orrenius, S., & Zhivotovsky, B. (2008). DNA damage induces two distinct modes of cell death in ovarian carcinomas. *Cell death and differentiation*, *15*(3), 555-66. doi:10.1038/sj.cdd.4402286

6. References

Vander Heiden, M. G., Cantley, L. C., & Thompson, C. B. (2009). Understanding the Warburg effect: the metabolic requirements of cell proliferation. *Science (New York, N.Y.), 324*(5930), 1029-33. doi:10.1126/science.1160809

Vaux, D. L., Cory, S., & Adams, J. M. (1988). Bcl-2 gene promotes haemopoietic cell survival and cooperates with c-myc to immortalize pre-B cells. *Nature, 335*(6189), 440-2. doi:10.1038/335440a0

Vicencio, J. M., Ortiz, C., Criollo, A., Jones, A. W. E., Kepp, O., Galluzzi, L., Joza, N., et al. (2009). The inositol 1,4,5-trisphosphate receptor regulates autophagy through its interaction with Beclin 1. *Cell death and differentiation, 16*(7), 1006-17. doi:10.1038/cdd.2009.34

Voet, D., & Voet, J. (2004a). Biochemistry (3rd ed., pp. 549-574). Wiley.

Voet, D., & Voet, J. (2004b). Biochemistry (3rd ed., pp. 797-842). Wiley.

Voet, D., & Voet, J. (2004c). Biochemistry (3rd ed., pp. 626-656). Wiley.

Vousden, K. H., & Ryan, K. M. (2009). P53 and Metabolism. *Nature reviews. Cancer, 9*(10), 691-700. doi:10.1038/nrc2715

Walczak, H., & Krammer, P. H. (2000). The CD95 (APO-1/Fas) and the TRAIL (APO-2L) apoptosis systems. *Experimental cell research, 256*(1), 58-66. doi:10.1006/excr.2000.4840

Wang, D., & Lippard, S. J. (2005). Cellular processing of platinum anticancer drugs. *Nature reviews. Drug discovery, 4*(4), 307-20. doi:10.1038/nrd1691

Warburg, O. (1956). On the origin of cancer cells. *Science*, (123), 309-314.

Watson, M., Barrett, A., Spence, R. A. J., & Twelves, C. (2006). Oncology (2nd ed., pp. 33-54). Oxford University Press.

Weidemann, A., Bernhardt, W. M., Klanke, B., Daniel, C., Buchholz, B., Câmpean, V., Amann, K., et al. (2008). HIF activation protects from acute kidney injury. *Journal of the American Society of Nephrology : JASN, 19*(3), 486-94. doi:10.1681/ASN.2007040419

Wise, D. R., DeBerardinis, R. J., Mancuso, A., Sayed, N., Zhang, X.-Y., Pfeiffer, H. K., Nissim, I., et al. (2008). Myc regulates a transcriptional program that stimulates mitochondrial glutaminolysis and leads to glutamine addiction. *Proceedings of the National Academy of Sciences of the United States of America, 105*(48), 18782-7. doi:10.1073/pnas.0810199105

Wistuba, I., & Gazdar, A. F. (2006). Lung cancer preneoplasia. *Annual review of pathology, 1*, 331-48. Annual Reviews. doi:10.1146/annurev.pathol.1.110304.100103

Wojewoda, M., Duszyński, J., & Szczepanowska, J. (2011). NARP mutation and mtDNA depletion trigger mitochondrial biogenesis which can be modulated by selenite

supplementation. *The international journal of biochemistry & cell biology*, *43*(8), 1178-86. doi:10.1016/j.biocel.2011.04.011

Wolyniec, K., Haupt, S., & Haupt, Y. (2010). P53 and Cell Death. In G. Melino & D. L. Vaux (Eds.), *Cell Death* (pp. 230-239). Wiley-Blackwell.

Wood, D. E., Thomas, A., Devi, L. A., Berman, Y., Beavis, R. C., Reed, J. C., & Newcomb, E. W. (1998). Bax cleavage is mediated by calpain during drug-induced apoptosis. *Oncogene*, *17*(9), 1069-78. doi:10.1038/sj.onc.1202034

World Health Organisation. (2009). WHO | Cancer. World Health Organization. Retrieved August 7, 2010, from http://www.who.int/mediacentre/factsheets/fs297/en/

Xie, J., Wang, B.-S., Yu, D.-H., Lu, Q., Ma, J., Qi, H., Fang, C., et al. (2011). Dichloroacetate shifts the metabolism from glycolysis to glucose oxidation and exhibits synergistic growth inhibition with cisplatin in HeLa cells. *International journal of oncology*, *38*(2), 409-17. doi:10.3892/ijo.2010.851

Xue, H., Zhao, D. M., Suda, T., & Uchida, C. (2000). Store depletion by caffeine/ryanodine activates capacitative Ca2+ entry in nonexcitable A549 cells. *Journal of ….*

Yang, X., Fraser, M., Abedini, M. R., Bai, T., & Tsang, B. K. (2008). Regulation of apoptosis-inducing factor-mediated, cisplatin-induced apoptosis by Akt. *British journal of cancer*, *98*(4), 803-8. doi:10.1038/sj.bjc.6604223

Yang, Z. F., Poon, R. T., To, J., Ho, D. W., & Fan, S. T. (2004). The potential role of hypoxia inducible factor 1alpha in tumor progression after hypoxia and chemotherapy in hepatocellular carcinoma. *Cancer research*, *64*(15), 5496-503. doi:10.1158/0008-5472.CAN-03-3311

Yang, Z., Schumaker, L. M., Egorin, M. J., Zuhowski, E. G., Guo, Z., & Cullen, K. J. (2006). Cisplatin preferentially binds mitochondrial DNA and voltage-dependent anion channel protein in the mitochondrial membrane of head and neck squamous cell carcinoma: possible role in apoptosis. *Clinical cancer research : an official journal of the American Association for Cancer Research*, *12*(19), 5817-25. doi:10.1158/1078-0432.CCR-06-1037

Yip, K. W., & Reed, J. C. (2008). Bcl-2 family proteins and cancer. *Oncogene*, *27*(50), 6398-406. Macmillan Publishers Limited. doi:10.1038/onc.2008.307

Yoshida, Y., Izumi, H., Ise, T., Uramoto, H., Torigoe, T., Ishiguchi, H., Murakami, T., et al. (2002). Human mitochondrial transcription factor A binds preferentially to oxidatively damaged DNA. *Biochemical and biophysical research communications*, *295*(4), 945-51. Retrieved from http://www.ncbi.nlm.nih.gov/pubmed/12127986

Yoshida, Y., Izumi, H., Torigoe, T., Ishiguchi, H., Itoh, H., Kang, D., & Kohno, K. (2003). P53 physically interacts with mitochondrial transcription factor A and differentially regulates binding to damaged DNA. *Cancer research*, *63*(13), 3729-34.

6. References

Youle, R. J., & Strasser, A. (2008). The BCL-2 protein family: opposing activities that mediate cell death. *Nature reviews. Molecular cell biology*, *9*(1), 47-59. doi:10.1038/nrm2308

Zhang, L.-J., Li, Z.-Q., Yang, Y.-P., Li, X.-W., & Ji, J.-F. (2009). Tunicamycin suppresses cisplatin-induced HepG2 cell apoptosis via enhancing p53 protein nuclear export. *Molecular and cellular biochemistry*, *327*(1-2), 171-82. doi:10.1007/s11010-009-0055-z

Zhao, D. M., Xue, H.-H., Chida, K., Suda, T., Oki, Y., Kanai, M., Uchida, C., et al. (2000). Effect of erythromycin on ATP-induced intracellular calcium response in A549 cells. *Am J Physiol Lung Cell Mol Physiol*, *278*(4), L726-736.

Zhivotovsky, B., & Orrenius, S. (2009). The Warburg Effect returns to the cancer stage. *Seminars in cancer biology*, *19*(1), 1-3. doi:10.1016/j.semcancer.2008.12.003

Zhivotovsky, B., & Orrenius, S. (2010). Cell death mechanisms: cross-talk and role in disease. *Experimental cell research*, *316*(8), 1374-83. doi:10.1016/j.yexcr.2010.02.037

Zhou, R., Vander Heiden, M. G., & Rudin, C. M. (2002). Genotoxic exposure is associated with alterations in glucose uptake and metabolism. *Cancer research*, *62*(12), 3515-20.

Zhou, S., Kachhap, S., Sun, W., Wu, G., Chuang, A., Poeta, L., Grumbine, L., et al. (2007). Frequency and phenotypic implications of mitochondrial DNA mutations in human squamous cell cancers of the head and neck. *Proceedings of the National Academy of Sciences of the United States of America*, *104*(18), 7540-5. doi:10.1073/pnas.0610818104

Zorov, D. B., Filburn, C. R., Klotz, L. O., Zweier, J. L., & Sollott, S. J. (2000). Reactive oxygen species (ROS)-induced ROS release: a new phenomenon accompanying induction of the mitochondrial permeability transition in cardiac myocytes. *The Journal of experimental medicine*, *192*(7), 1001-14.

de Brito, O. M., & Scorrano, L. (2008). Mitofusin 2 tethers endoplasmic reticulum to mitochondria. *Nature*, *456*(7222), 605-10. doi:10.1038/nature07534

van den Broek, G. B., Wildeman, M., Rasch, C. R. N., Armstrong, N., Schuuring, E., Begg, A. C., Looijenga, L. H. J., et al. (2009). Molecular markers predict outcome in squamous cell carcinoma of the head and neck after concomitant cisplatin-based chemoradiation. *International journal of cancer. Journal international du cancer*, *124*(11), 2643-50. doi:10.1002/ijc.24254

Appendix I: Ascorbic Acid Does Not Inhibit cDDP Cytotoxicity

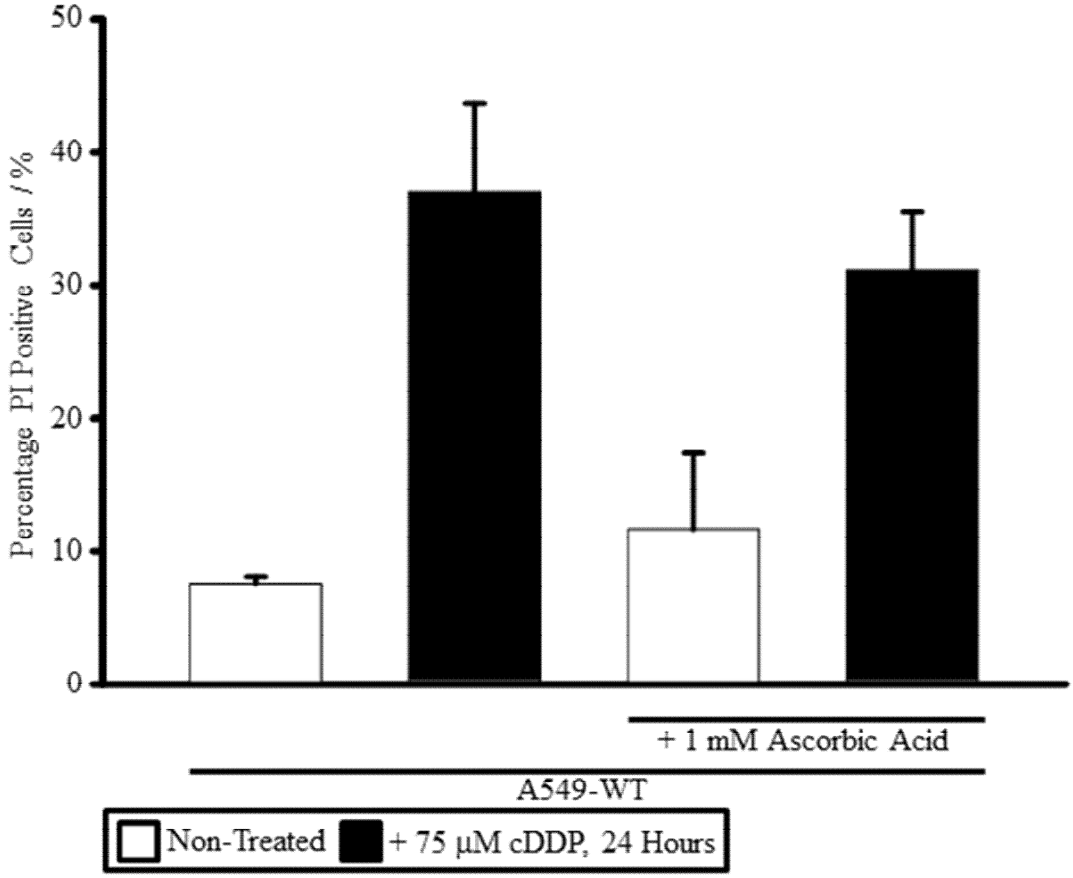

Appendix I Figure 1: Ascorbic acid does not prevent cDDP-induced cytotoxicity in A549-WT cells. A549-WT cells were incubated in normal cell culture medium + 200 1 mM ascorbic acid or in normal cell culture medium + 1 mM ascorbic acid + 75 µM cDDP for 24 hours and cytotoxicity assayed by PI exclusion as outlined in *'Methods 2.4'*. Incubation with 1 mM ascorbic acid was able to fully prevent ROS-induced mitochondrial depolarisation in A549-WT cells under a model of oxidative stress caused by TMRM photoactivation (Figure 25 C), demonstrating the antioxidant properties of ascorbic acid in this cell model. Data represent the mean of three independent experiments + S.E.M. * $p < 0.05$.

Appendix II: IP_3R Stimulation by Caged IP_3 Without Fluo-4 Dye Bleaching Correction

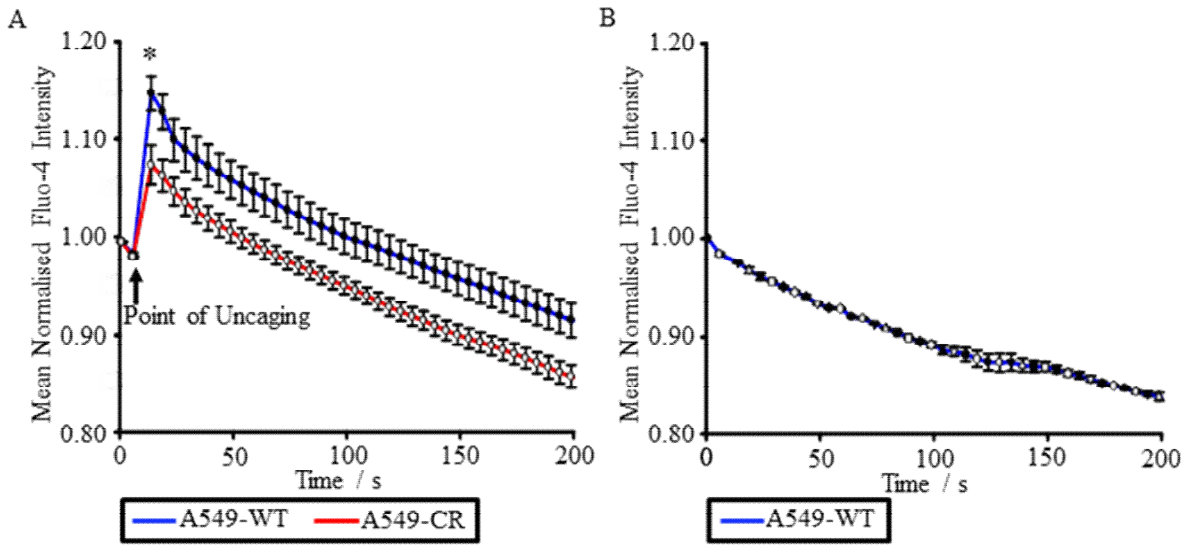

Appendix II Figure 1: IP_3R function is reduced in A549-CR cells relative to A549-WT cells. Cells were loaded with photolabile caged IP_3 and 5 µM Fluo-4-AM, and fluorescence intensity recorded after IP_3 uncaging caused by a period of UV illumination, as described in *'Methods 2.6'*. (A) Mean changes in normalised Fluo-4 fluorescence without dye bleaching correction in A549-WT and A549-CR cells loaded with caged IP_3 following UV illumination. (B) Mean changes in normalised Fluo-4 fluorescence without dye bleaching correction in A549-WT cells loaded with caged IP_3 without the UV illumination period. Traces represent the mean response of a minimum of five coverslips from four independent experiments ± S.E.M. * $p < 0.05$.

Appendix III: Point Mutations of mtDNA Identified in A549-WT Cells and A549-CR Cells by Mitochip Sequencing

Appendix III Table 1: Point mutations present in the mtDNA of A549-WT cells and A549-CR cells identified by Mitochip sequencing. A549-WT cells and A549-CR cells were incubated in normal cell culture medium for 24 hours. Sequence analysis of the mtDNA genome was performed using Mitochip V2.0 following PCR amplification of mtDNA as described in '*Methods 2.20*'. Italics = deviation from revised Cambridge reference sequence. Point mutations highlighted in red represent novel previously unreported nucleotide substitutions. Italics = deviation from reference sequence.* Exists in heteroplasmy.

rCRS Position	Reference	A549-WT	A549-CR	Gene	Gene Product	Amino Acid Change	Type
73	A	*G*	*G*	D-Loop	N/A	Non-Coding	Reference Sequence SNP
225	**G**	**G**	***T***	**D-Loop**	**N/A**	**Non-Coding**	**Unreported Variant**
263	A	*G*	*G*	D-Loop	N/A	Non-Coding	Reference Sequence SNP
750	A	*G*	*G*	MT-RNR1	12 s rRNA	Consensus	Reference Sequence SNP
1438	A	*G*	*G*	MT-RNR1	12 s rRNA	Consensus	Reference Sequence SNP
3992	C	*T*	*T*	MT-ND1	ND1	Thr 229 Met	SNP

4024	A	*G*	*G*	MT-ND2	ND2	Thr 240 Ala	SNP
4587	**T**	**T / *C* ***	***C***	**MT-ND2**	**ND2**	**Phe 40 Leu**	**Unreported Variant**
4769	A	*G*	*G*	MT-ND2	ND2	Met 100 Met	Reference Sequence SNP
5004	T	*C*	*C*	MT-ND2	ND2	Leu 179 Leu	SNP
8269	G	*A*	*A*	MT-CO2	Cox II	Stop 228 Stop	SNP
8860	A	*G*	*G*	MT-ATP6	ATPase 6	Thr 112 Ala	Reference Sequence SNP
9123	G	*A*	*A*	MT-ATP6	ATPase 6	Leu 199 Leu	SNP
10044	A	*G*	*G*	MT-TG	tRNA Gly	Non-coding	SNP
12524	**T**	***C***	**T**	**MT-ND5**	**ND5**	**Ile 163 Thr**	**Unreported Variant**
13105	A	*G*	*G*	MT-ND5	ND5	Ile 257 Val	SNP
14365	C	*T*	*T*	MT-ND6	ND6	Val 103 Val	SNP
14582	A	*G*	*G*	MT-ND6	ND6	Val 31 Ala	SNP
15042	**G**	**G**	***A***	**MT-CYTB**	**Cyt b**	**Gly 99 Glu**	**Unreported Variant**
15326	A	*G*	*G*	MT-CYTB	Cyt b	Thr 194 Ala	Reference Sequence SNP
15352	**A**	**A**	***G***	**MT-CYTB**	**Cyt b**	**Glu 202 Glu**	**Unreported Variant**

Appendix

15656	**A**	**A**	***G***	**MT-CYTB**	**Cyt b**	**Ile 1304 Val**	**Unreported Variant**
15659	**C**	**C**	***T***	**MT-CYTB**	**Cyt b**	**Pro 305 Ser**	**Unreported Variant**
16260	C	C	*T*	D-Loop	N/A	Non-Coding	SNP
16267	C	C	*T*	D-Loop	N/A	Non-Coding	SNP
16268	C	C	*T*	D-Loop	N/A	Non-Coding	SNP

Appendix IV – NAC Inhibits cDDP-Induced H2AX Phosphorylation in A549-WT Cells

A

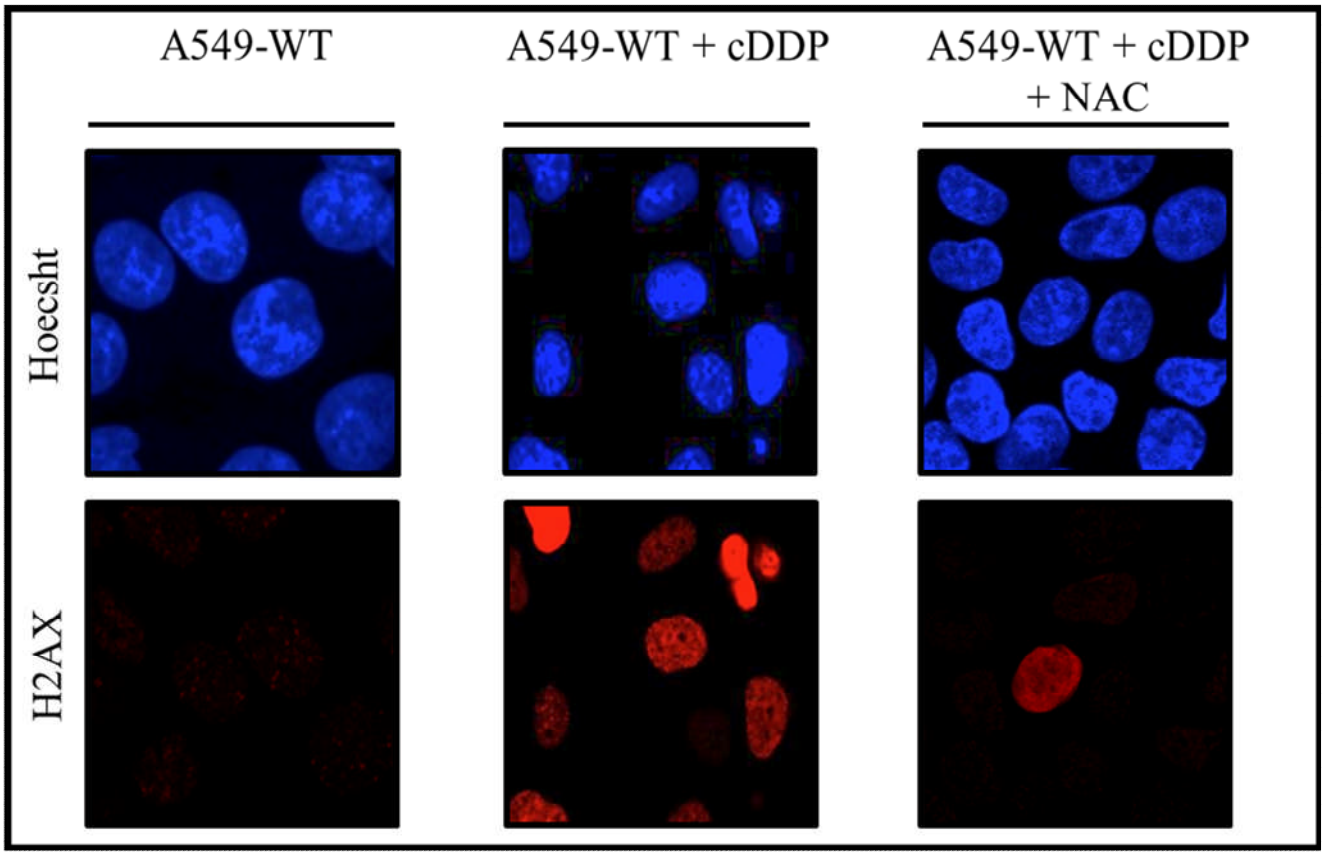

B

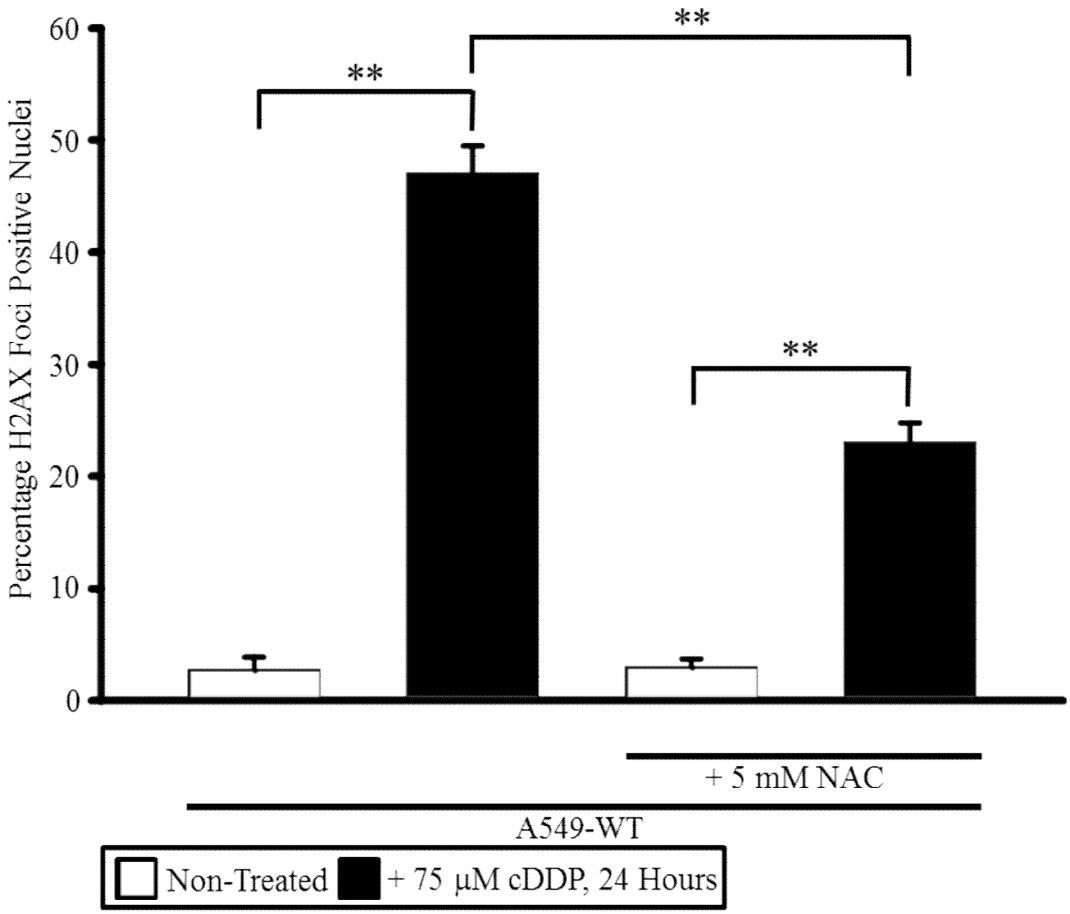

Appendix

Appendix IV Figure 1: NAC Inhibits cDDP-Induced H2AX Phosphorylation in A549-WT Cells. A549-WT cells seeded onto glass coverslips were incubated in normal cell culture medium + 75 µM cDDP or normal cell culture medium + 5 mM NAC + 75 µM cDDP for 24 hours before immunostaining. Briefly, cells were fixed using 4% paraformaldehyde, permeabilised using 0.2% Triton X and blocked with 2% BSA. Cells were incubated with mouse anti-phospho-H2AX primary antibody (Millipore) diluted 1:1000 in PBS + 0.2% BSA at 4 ^{o}C overnight. Coverslips were washed and incubated with goat anti-mouse Alexa 594 conjugated secondary antibody for 45 minutes at room temperature, before three washes with PBS + 1 µg/ ml Hoecsht. Fixed cells were visualised using a confocal microscope. A minimum of 100 randomly selected nuclei were counted under each experimental condition per experiment, and the percentage of phospho-H2AX positive nuclei calculated. (A) Representative images of A549-WT cells incubated in normal cell culture medium, normal cell culture medium + 75 µM NAC or normal cell culture medium + 5 mM NAC + 75µM cDDP for 24 hours before immunostaining. (B) Mean percentage of phosphor-H2AX positive nuclei in A549-WT cells following incubation in 75 µM cDDP in the presence or absence of 5 mM NAC. Data represent the mean of three independent experiments ± S.E.M. ** $p < 0.01$.